Thermomechanical modeling of composite slab joints under fire

Student: S. de Nijs
Studentnumber: 1274201

Supervisors: prof. ir. S.N.M. Wijte
dr. ir. H.H. Hofmeyer
ir. R.A.P. van Herpen

Study load: 45 ECTS
Year of graduation: 2021-2022
Master track: ABP - Structural Engineering and Design

Public information

TU/e

Abstract graduation project Thermomechnical modeling of composite slab joints under fire

The detail of the coupling reinforcement in a composite floor is structural critical, and a temperature increase at this specific location could make the detail even more critical for structural reliability. For this reason, this paper focuses on researching the temperature of the coupling reinforcement in a composite floor caused by fire conditions underneath the floor. Those fire conditions are based on ISO 834. A numerical model of the heat transfer in the composite floor was created to answer the formulated research question, incorporating convection and radiation according to the EN 1992-1-2. This numerical model was verified by a graphical, analytical and Finite Element Method of a simplified model designed for this research. For the research of the numerical model of the composite floor, it was essential to review the temperature of the joint for different widths and depths at various fixed times since it is possible to use the composite floors in different measures for different purposes. By evaluating the results of the Finite Element Method of a composite floor, it became clear that the temperature of the coupling reinforcement does not exceed the temperature in the precast plates. At last, the structural reliability is determined after determining the temperature at different heights and locations in the composite floor. These analyses show that the joint between two precast composite plates is not causing an additional risk for the structural safety of the structure when exposed to fire.

Table of contents

Paper. Thermomechanical modeling of composite slab joints under fire 3
Appendix A. Research question 17
Appendix B. Specific heat of concrete 18
Appendix C. Analytic analysis EN 1992-1-2 20
Appendix D. Analytic analyses Finite difference method 27
i. Exposed surface 27
ii. Internal part 28
iii. Unexposed surface 29
iv. Excel file 29
v. Results 30
Appendix E. Numerical analyses simplified model 34
i. Numerical model 34
ii. Temperature characteristics 35
iii. Results 35
iv. Floor thickness 38
Appendix F. Thermal radiation 40
i. View factor 40
ii. Emission coefficient 44
iii. Simplified radiation model analytical 44
iv. Simplified radiation model numerical 45
Appendix G. Stochastic boundary conditions 47
i. Convection coefficient 47
ii. Mesh configuration 47
iii. Standard fire curve 48
Appendix H. Composite floor at location of the joint 50
i. Numerical model 50
v. Continuous composite floor 51
vi. Composite floor at the location of the joint 51
Appendix I. Reduction of moment capacity 53
i. Precast floor plate 53
ii. Location above the joint 54
Appendix J. Article Cement 55
References 64
List of figures 65

Thermomechanical modeling of composite slab joints under fire

S. de Nijs[1]

[1] Eindhoven University of Technology, Eindhoven, The Netherlands

Abstract

The detail of the coupling reinforcement in a composite floor is structural critical, and a temperature increase at this specific location could make the detail even more critical for structural reliability. For this reason, this paper focuses on researching the temperature of the coupling reinforcement in a composite floor caused by fire conditions underneath the floor. Those fire conditions are based on ISO 834. A numerical model of the heat transfer in the composite floor was created to answer the formulated research question, incorporating convection and radiation according to the EN 1992-1-2. This numerical model was verified by a graphical, analytical and Finite Element Method of a simplified model designed for this research. For the research of the numerical model of the composite floor, it was essential to review the temperature of the joint for different widths and depths at various fixed times since it is possible to use the composite floors in different measures for different purposes. By evaluating the results of the Finite Element Method of a composite floor, it became clear that the temperature of the coupling reinforcement does not exceed the temperature in the precast plates. At last, the structural reliability is determined after determining the temperature at different heights and locations in the composite floor. These analyses show that the joint between two precast composite plates is not causing an additional risk for the structural safety of the structure when exposed to fire.

Keywords: Composite floor, standard fire curve, heat transfer, coupling reinforcement, structural reliability

1. INTRODUCTION

Composite floors consist of precast concrete plates and an in-situ layer on top. It is possible to use the floor with a one-direction span and with a two-direction span. Both ways lead to different load paths over the floors. Therefore, a floor with a two-directional span needs additional coupling reinforcement. Since the partial collapse of the parking garage of Eindhoven Airport on 27 May 2017, the detail of the coupling reinforcement has gotten more attention. Research has shown that the location of the coupling reinforcement above the joint between two precast plates in a two-direction span is structural critical. This detail is critical since the lapping of the coupling reinforcement to the reinforcement in the precast slab could not always resist the forces perpendicular to the joint. [1]

EN 13747 paragraph 4.3.4. gives a design rule about this specific detail according to fire safety. Figure 1 gives an example of how the joint could look.

"The fire resistance of a composite slab made of floor plates without void formers is the same as for a solid slab of identical characteristics. Calculation of the temperatures is carried out without taking into account the joint between floor plates as much as the width b_j is lower than 20 mm, figure 1." [2]

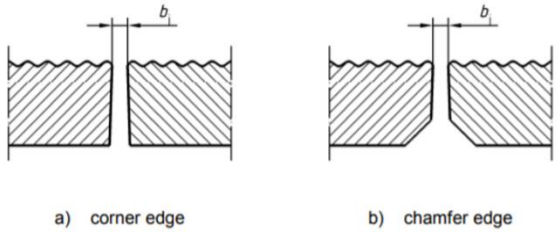

Fig. 1. Examples of current joint profiles with bi. [2]

According to this design rule, it is possible to neglect the heat transfer at the location of the joint between two precast plates. However, it is uncertain whether this design rule applies only for the traditional building method, with a one-direction span, or also for a two-direction span. Since this specific detail of the joint with the coupling reinforcement is critical [1], the question arose if neglecting the joint for heat transfer is not causing an additional risk.

Additionally, a second question arose according to the requirements of the coupling reinforcement in this detail. According to EN 1992-1-1, the coupling reinforcement in the in-situ layer should have a cover to the precast concrete plate. [3] In the Netherlands, this is not common practice. The coupling reinforcement here is located directly on the precast plate. It is questioned whether the design rule in EN 13747 is still valid with this different location of the coupling reinforcement. To verify this design rule, background information about this rule has been searched for in literature and relevant code committees. Unfortunately, no information was found.

This research focuses on the two questions above for a composite floor without void formers using literature study, analytical analyses and Finite Element Method. The research is based on the research question below. In Appendix A, the sub-questions for this research are shown.

What is the behavior under fire conditions at the location of the joint between two precast plates of a composite floor and is this a risk for the safety of the structure?

2. BACKGROUND

During the research, multiple subjects are essential for the final analysis. This chapter discusses the essential subjects: the concept of the composite floor and the critical detail, the principle of fire and heat transfer, and the behavior of concrete and reinforcement steel during a fire.

2.1. Composite floors and the critical detail

A traditional composite floor consists of a precast concrete plate with reinforcement and a concrete topping poured on-site. Those two parts of the slab are connected mainly by lattice girders, which are included in the precast part. By pouring the in-situ concrete, the connection between the two elements is guaranteed by the lattice girders. Additional reinforcement, for instance, coupling reinforcement, is also placed before the in-situ concrete topping is poured.

As already mentioned, a composite slab is used for a one-direction or a two-direction span. A one-direction span is mainly used in buildings

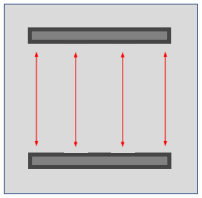

Fig. 2. One-direction span.

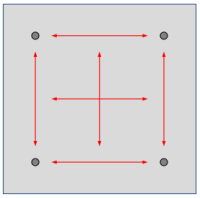

Fig. 3. Two-direction span.

using load-bearing walls, while floors with two-direction spans are used in buildings with columns, figures 2 and 3.

When using a one-direction span, the forces are led into the underneath walls directly. Therefore, the forces are transferred via the plate itself, figure 2. At a two-direction span, the loads are distributed in multiple directions, figure 3. These multiple directions mean that the loads must be transferred perpendicular to the joint since more than two different precast plates may be placed between two columns, see figure 4. The transfer of the load causes internal moments and shear forces in the cross-section at the joint. In order to resist these internal forces, coupling reinforcement is applied perpendicular to the joint. Following EN 13747, the reinforcement is placed at a certain height above the precast floorplate to ensure a concrete cover equal to the bar diameter. [3] However, in the Netherlands, it was common practice in the last decades to place the coupling reinforcement directly on the precast plate without any cover between the precast plate and the reinforcement bar.

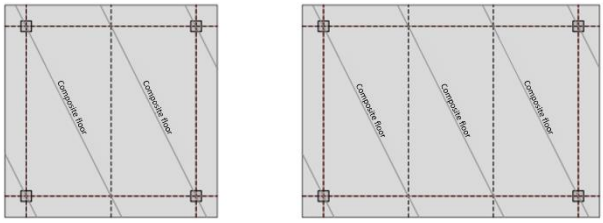

Fig. 4. Examples of possibilities for placing precast concrete plates between two columns. [1]

Due to the internal forces in a two-direction span, a positive moment exists at the cross-section of the joint. This positive moment translates into a tensile force in the coupling reinforcement and a compressive force at the top of the concrete topping. The transfer of this tensile force in the coupling reinforcement into the reinforcement in the precast plate causes a critical detail, figure 5. [1] The moment resistance at the location of the joint is essential to get equilibrium in the system.

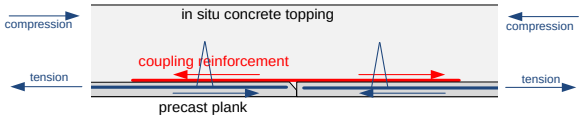

Fig. 5. Critical detail at the location of two precast plates with lattice girders.

According to EN 13747, the influence of the joint on the temperature in the floor is not considered. Therefore, also the temperature in the coupling reinforcement is not considered. However, since this detail of the coupling reinforcement is already critical for structural reliability, it is essential to review the accuracy of this design rule to prevent insufficient resistance during and after a fire.

2.2. Fire

Fire is a phenomenon that arises due to multiple reasons and causes damage and danger. Fire knows three phases: the growing phase, fully-developed fire, and decay. [4] The actual length for each stage depends on different parameters, such as the amount of combustible materials and the dimensions of the fire room. Each fire is different and unpredictable. Therefore, project-specific boundary conditions are necessary for a simulation of the thermal load by a natural fire concept. The standard (ISO 834) fire curve is assumed to be the thermal load in case of fire. This curve is, in most cases, a conservative approach, as a generic, not project-specific approach should be. [5] In a project-specific approach, it is advised to use the natural fire curve.

The standard fire curve is based on a developed fire and presents the phase after the flashover. The flashover is the moment of near-simultaneous ignition of the total fire load in a compartment. The fire resistance is expressed in the number of minutes a structure has sufficient resistance during the standard fire. The temperature increases quickly and stays at the same level during the whole fire. The natural fire curve is a curve based on the actual fire process. It takes longer to reach the maximum temperature, has a higher maximum temperature, and decreases almost directly after this maximum point. This rapid decrease is due to the limited combustible materials. [4] Figure 6 presents the standard fire curve, based on equation 1 [6], and the natural fire curve, based on an example of a natural fire. The natural fire curve has a slow increase in temperature in the beginning. After a while, the flashover takes place, and the temperatures have a quick increase. The temperature raises a peak, and from that point, the cooling phase starts. The combustible materials are burned out, and the temperature starts decreasing. As explained before, the standard fire curve starts after flashover and therefore has an immediate temperature increase. In figure 6, two different curves are shown for the standard fire curve. The continuous line follows the first part of the standard fire curve and then decreases in temperature as soon as the combustible materials are empty. The dotted line, which continues the continuous line, is the standard fire curve. The entire continuous line of the standard fire curves presents the duration of the fire, which is needed to represent the required thermal load of the natural fire curve. By performing this translation, the energy of both curves is equal.

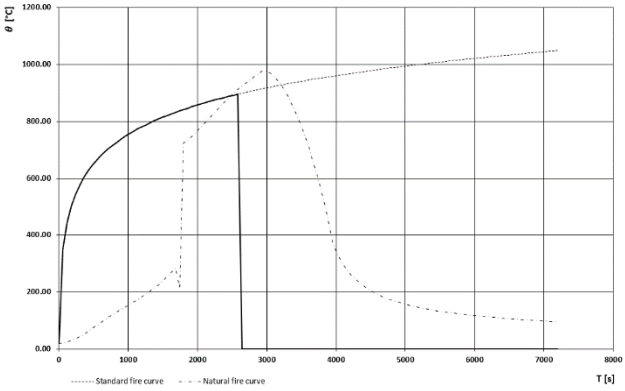

Fig. 6. Standard fire curve and natural fire curve. [5]

Since the EN 1992-1-2 has introduced the standard fire curve, and this research is based on the Eurocode, the standard fire curve is implemented. This curve is expressed with equation 1 and calculates the gas temperature in the compartment where the fire is located. [6]

$$\theta_g = 20 + 345 \cdot log_{10}(8t + 1), \quad (1)$$

In equation 1, θ_g is the gas temperature [in °C] and t the time [in min.].

During the fire, the produced heat spreads through the compartment. This heat is transported in three different ways, namely via convection, conduction, and thermal radiation.

Convection is a way of fluid flow-based heat transfer and is divided into two types: forced and natural convection. If there is pressure to drive the flow, the convection is forced. This pressure is caused by, for instance, wind or a blower. If the flow results from density differences, which is the case if there are temperature differences in a compartment, the convection is called natural. To calculate the convective heat, equation 2 should be used. The equation uses the convective heat transfer coefficient and the temperature difference to calculate the heat transfer rate per unit area per unit time. [7]

$$q = h\left(\theta_f - \theta\right)^n \quad (2)$$

In equation 2, q is the heat transfer per unit area per time [in W/m²] , h is the convection coefficient [in W/m²K], $\theta_f - \theta$ is the difference in temperature between the fire exposure and the concrete surface [in K], and n is the convection power factor.

Conduction is a consequence of higher-temperature molecules interacting and exchanging energy with molecules at a lower temperature. The heat transfer by conduction depends on the thermal conductivity and the differences in temperature in the compartment. The higher the temperatures are, the more interactions between molecules occur. To calculate the conduction, Fourier's law is applied. This law is based on experimental observations and is calculated with equation 3. This

equation calculates the heat flux in a particular direction by multiplying the thermal conductivity and a temperature gradient. [8]

$$q_n'' = -k_n \frac{\partial T}{\partial n} \quad (3)$$

In equation 3, q_n'' is the the heat transfer per unit area per time [in W/m²], k_n is the thermal conductivity in direction n [in W/mK], and $\frac{\partial T}{\partial n}$ is the temperature gradient in direction n.

Thermal radiation is energy transport by electromagnetic waves with wavelengths λ=0,1 till 100 µm. This radiation becomes significantly more important when the temperature of the radiator exceeds 500°C since thermal radiation is proportional to the fourth power of temperature differences. For comparison, conduction and convection are approximately linearly dependent on temperature differences. Other materials absorb electromagnetic waves due to radiation. The amount of waves absorbed by the material depends on the temperature of the material, wavelength, frequency, and wavenumbers. With those characteristics, thermal radiation is calculated by equation 4. [7]

$$q = \upsilon\sigma\left(a\varepsilon_f\theta_f^4 - \varepsilon_s\theta^4\right) \quad (4)$$

In equation 4, q is the the heat transfer per unit area per time [in W/m²], υ is the radiation view factor, σ is the Stefan-Boltz-mann constant [in W/m²K⁴], a the absorptivity of the surface, ε_f and ε_s the emissivity of the fire and the concrete surface, and θ_f and θ the temperatures of the gas and the concrete surface [in K].

Next to the fire load, a building must have a determined fire resistance. During designing, this fire resistance should be taken into account, and it has three primary conditions. Those conditions are called REI and stand for stability (R), integrity (E), and insulation ability (I).

2.3. Concrete and fire

Concrete is a material that does not burn. However, this does not mean that nothing is happening with the concrete during a fire. According to the graph in EN-1992-1-2, figure 7, the temperature of concrete increases over time. [5] The figure is meant for slabs that are exposed to fire at one side. This one side exposure has as a consequence that the surface of the concrete element, on the exposed side, increases the most in temperature. Further inside the slab, the temperature increase becomes less. This lower increase is due to the low thermal conductivity of concrete which decreases when concrete increases in temperature. When the temperature of concrete increases, the characteristics, such as the compressive strength, also changes. When the temperature gets too high, the concrete loses too much strength. This loss of strength also counts for the reinforcement in the concrete floors. Next to the risk of loss of strength, also thermal cracks and spalling of concrete occurs. Those risks are explained in the following paragraphs.

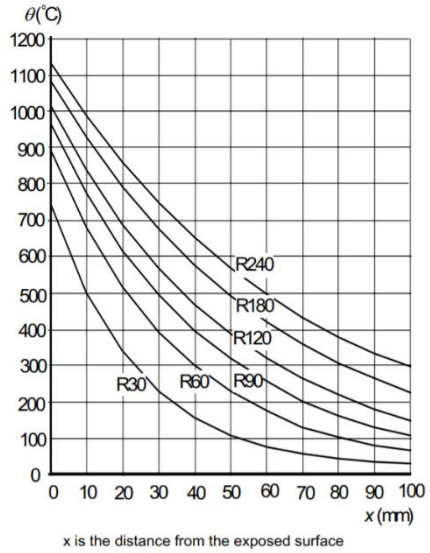

Fig. 7. Temperature profiles for slabs according to the EN-EN 1992-1-2 at *Rx* with *x* is the duriation of the fire. [7]

Due to an increased temperature, thermal cracks may occur. The cracks could have multiple reasons. The first reason is about the expansion coefficient of concrete and reinforcement steel. At low temperatures, concrete and reinforcement steel have an equal thermal expansion coefficient. When the temperature increases, these coefficients become different from each other. The reinforcement steel gets a higher thermal expansion coefficient and, therefore, has an increased thermal expansion compared to concrete. The second reason is a differing thermal expansion between the aggregates and cement paste. This difference also leads to thermal cracking for the same reason explained above. [9]

Another phenomenon that occurs due to the increased temperature of the concrete is spalling. When spalling occurs, parts of the concrete explosively comes off the structure and causes open spaces to the reinforcement. The result of this is that the reinforcement is heating up quicker and therefore loses more strength. In traditional concrete, this mostly happens in the first 20 minutes of the fire. There are multiple theories on how spalling is occurring. Some examples are thermal stress theories, free water and moisture gradients in the concrete, and prestress and compressive stresses. In the research of K.D. Hertz [10] explains that the main reason for spalling is free water and moisture gradients in concrete. From his research also is proven that dry material is not spalling. Concrete has free water in it. This free water evaporates, and steam occurs. This steam partly leaves the concrete at the surface. Due to the pressure this steam causes, the concrete spalls explosively. [10]

Next to explosive spalling, there is sloughing, a different sort of spalling. This spalling type is mainly happening at the edges and, therefore, could be interesting for the behavior of the joint. After spalling, the cover till the reinforcement steel is smaller or even disappears. Therefore the reinforcement increases in temperature quicker. At low temperatures, concrete and reinforcement steel have an equal expansion coefficient. At higher temperatures, reinforcement steel gets an increased expansion coefficient. This increase again leads to more spalling. [9] During further research, cracks and spalling due to the increasing temperature of the concrete are not considered.

During heating, some characteristics of concrete change, namely the density, the specific heat, and the thermal conductivity, which are used to calculate the temperature-dependent characteristics.

The first temperature-dependent characteristic of concrete is density. When the temperature increases, the density of the concrete decreases. The free water in concrete vaporizes between 100 °C and 200 °C. This process causes a decrease in density during the first part of the fire. At a temperature of 250 °C also the chemical bonded water is dehydrating. [9] The following process depends on the kind of aggregates. Between 600 °C and 900 °C, decarbonization of limestone occurs. When using siliceous aggregates, commonly used in the Netherlands, the elements change at 570 °C into crystals leading to decreased density. [11] This decrease also leads to a reduction of compressive strength, which has consequences for the reliability of the structure. According to EN 1992-1-2, the following equations are used for calculating the density during a

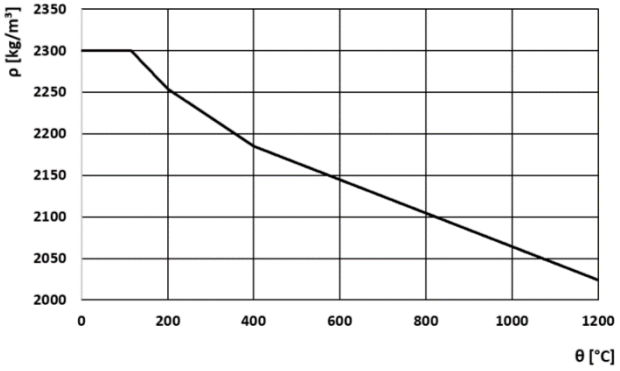

Fig. 8. Density decrease due to temperature change. [7]

fire. For calculations, a density of 2300 kg/m³ should be considered at t = 20°C. [5]

$$\rho(\theta) = \rho(20°) \text{ for } 20°C \leq \theta \leq 115°C \quad (5)$$

$$\rho(\theta) = \rho(20°) \cdot (1 - 0.02(\theta - 115)/85) \text{ for } 115°C \leq \theta \leq 200°C \quad (6)$$

$$\rho(\theta) = \rho(20°) \cdot (0.98 - 0.03(\theta - 200)/200) \text{ for } 200°C \leq \theta \leq 400°C \quad (7)$$

$$\rho(\theta) = \rho(20°) \cdot (0.95 - 0.07(\theta - 400)/800) \text{ for } 400°C \leq \theta \leq 1200°C \quad (8)$$

In equations 5, 6, 7, and 8, ρ is the density [in kg/m³] and θ the temperature [in °C]. In figure 8 the behavior of density due to temperature increase is shown.

The second temperature-dependent concrete property is the specific heat capacity. The specific heat is the energy required to raise the temperature with 1 °C of 1 kg concrete. The specific heat increases due to the difference in water and air amount in the concrete. This increase depends on the type of aggregates and moisture content. [11] According to EN 1992-1-2, the following equations calculate the increase of the specific heat. Depending on the moisture content in the concrete, the specific heat capacity gets a peak value. [5] Figure 9 shows the specific heat capacity of concrete with a moisture content of 1.5%. This percentage is the moisture content assumed to be in the concrete for calculating the heat transfer, explained in section 4. More information about using the equations for concrete with a moisture content of 1.5% is given in Appendix B.

$$C_p(\theta) = 900 \text{ for } 20°C \leq \theta \leq 100°C \quad (9)$$

$$C_p(\theta) = 900 + (\theta - 100) \text{ for } 100°C \leq \theta \leq 200° \quad (10)$$

$$C_p(\theta) = 1000 + (\theta - 200)/2 \text{ for } 200°C \leq \theta \leq 400°C \quad (11)$$

$$C_p(\theta) = 1100 \text{ for } 400°C \leq \theta \leq 1200°C \quad (12)$$

In equations 9, 10, 11, and 12, C_p is the specific heat capacity [in J/(kgK)] and θ the temperature [in °C].

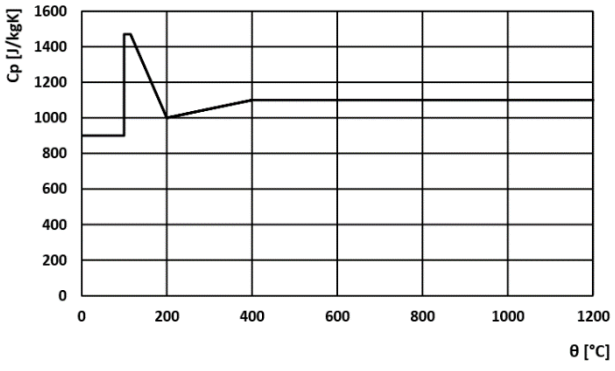

Fig. 9. Specific heat increase due to temperature change based on NEN-EN 1992-1-2. [5]

The last characteristic that changes during heating is thermal conductivity which represents the ability to conduct heat. The higher the thermal conductivity, the sooner the heat transfer takes place. Concrete has a low thermal conductivity compared to, for example, steel, and the conductivity decreases due to heating. The higher the temperature of the concrete gets, the slower the heat transfer takes place. This change is related to the decrease of the density due to the evaporation of the water. Little gaps form in the concrete, which is filled with air. Air has a very low thermal conductivity. [11] According to EN 1992-1-2, the following equations are used for calculating the decrease of thermal conductivity. [5]

$$\lambda_c(\theta) = 2 - 0.2451\,(\theta/100) + 0.0107\,(\theta/100)^2 \text{ for } 20°C \leq \theta \leq 140°C \quad (13)$$

$$\lambda_c(\theta) = -0.02604\,\theta + 5.324 \text{ for } 140°C \leq \theta \leq 160°C \quad (14)$$

$$\lambda_c(\theta) = 1.36 - 0.136(\theta\_c/100) + 0.0057\,(\theta\_c/100)\text{^}2 \text{ for } 140°C \leq \theta \leq 160°C \quad (15)$$

In equations 13, 14, and 15, λ_c is the thermal conductivity [in W/mK] and θ the temperature [in °C]. In figure 10 the behavior of thermal conductivity due to temperature increase is shown.

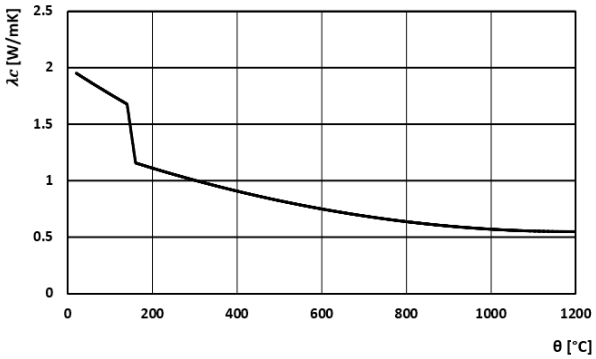

Fig. 10. Thermal conductivity decrease due to temperature change based on EN-EN 1992-1-2. [5]

The three temperature-dependent characteristics which are described above are combined into the thermal diffusivity. By combining density, specific heat, and thermal conductivity, it becomes able to measure the ability of a material to conduct thermal energy relative to its ability to store thermal energy. When the thermal diffusivity becomes higher, the heat transfer goes more rapidly. [12] For concrete, the thermal diffusivity decreases slightly, which means the heat transfer becomes slower with a temperature increase. The expectation is that the difference in speed for the heat transfer is not be noticed since the difference is minimal. Concrete has a thermal diffusivity of $9.44 \cdot 10^{-7}$ at 20 °C and thermal diffusivity of $2.46 \cdot 10^{-7}$ at 1200 °C, figure 11. [11]

$$\alpha = \frac{\lambda}{\rho\, c_p} \quad (16)$$

In equation 16, α is the thermal diffusivity, λ the thermal conductivity [W/mK], ρ the density [kg/m³] and c_p the specific heat [J/(kgK)]. In figure 11 the result of the thermal diffusivity is given.

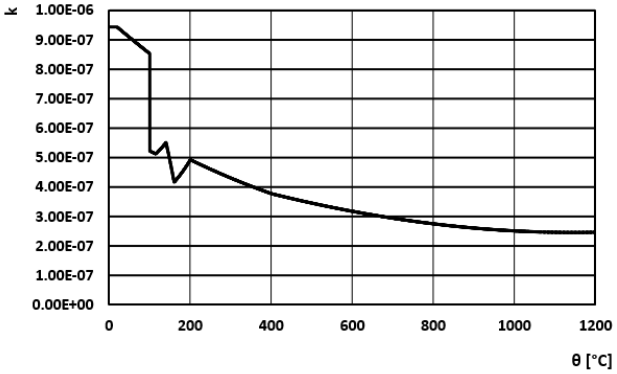

Fig. 11. Thermal diffusity for temperature-dependent characteristics of concrete. [11]

Due to the described characteristics that change due to heating, the compressive and the tensile strength of concrete reduce with increasing temperature. EN 1992-1-2 gives graphs on the reduction of the concrete strength. Depending on the type of aggregates used, the compressive strength decreases over curve one or two. The decrease starts at 100 °C. When the concrete reaches a temperature of 250 °C, the structure of the concrete starts changing. The chemical-connected water vaporizes and causes a brittle material. When reaching 550 °C – 600 °C, the concrete experiences creep. The decrease of strength is due to internal cracks and degradation of cement stone. After the concrete has reached a temperature of 600 °C and higher, the concrete is unable to function at its full structural capacity anymore. Restauration of the affected concrete is necessary. [5] [13] The decrease of compressive strength of concrete is given in figure 12.

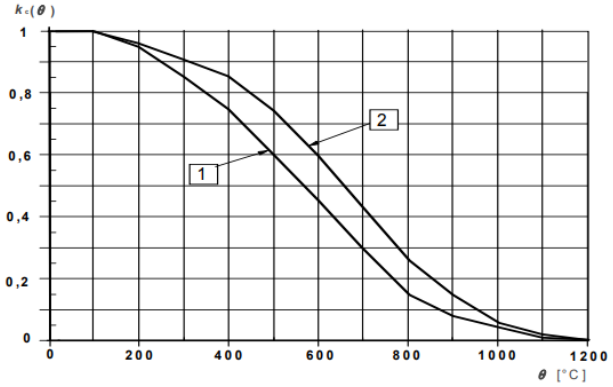

Fig. 12. Decrease of compressive strength of concrete due to temperature change. [5]

Under normal circumstances, the compressive strength is based on the tensile strength in the non-loaded direction. Therefore, there is a relation between the tensile and compressive forces. According to the EN 1992-1-2, the tensile strength of the concrete decreases rapidly in comparison with the compressive strength, figure 12 and figure 13. The tensile strength has a linear decrease from 100% at 100 °C to 0% at 600 °C, figure 13. [5] The decrease of the tensile strength of concrete is quicker than the decrease of the compressive strength of concrete. This difference implies that the relation between compressive strength and tensile strength of concrete during an increase of temperature changes. Unfortunately, no further information about this statement is found in literature.

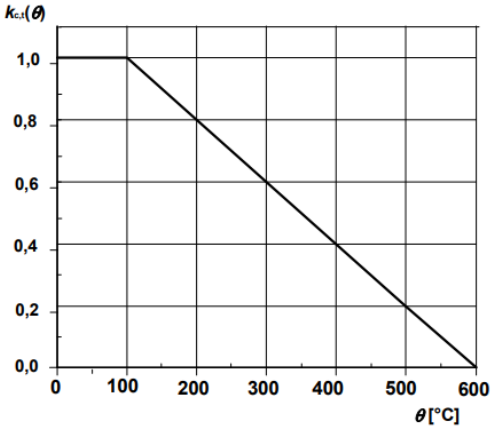

Fig. 13. Decrease of tensile strength of concrete due to temperature change. [5]

Next to the loss of strength of the material, the material deforms due to the temperature increase. Two of the characteristics, which influence this deformation, are thermal expansion and creep. Thermal expansion is the expansion of a material as a unit length of a material when the temperature rises by one degree. Characteristics such as cement type, water content, aggregate type, temperature, and age influence the thermal expansion of concrete. Creep is the time-dependent plastic deformation of the material. Stress level and temperature influence the creep of concrete influenced by fire. [14]

While checking the structural reliability, the shear between the different interfaces of the composite floor must be considered. According to EN 1992-1-1 shear in the interfaces is calculated the same during fire as under normal circumstances. [3]

2.4. Reinforcement steel and fire

Concrete is not the only material that decreases in strength due to heat. In addition, the reinforcement steel decreases in strength, which causes the weakest point in the floor. Figure 14 shows three different types of reinforcement steel and their decrease due to temperature increase. This research is about the traditional composite floor. For that reason, prestressing steel is not considered. Reinforcement steel that is not prestressed loses strength above 350 °C. After this temperature, the characteristic tensile strength decreases linearly from 100% at 350 °C to 10% at 700 °C. [5] Since reinforcement has a lower specific heat capacity which causes a quicker temperature increase than concrete, a concrete cover is crucial for protecting the reinforcement. [15]

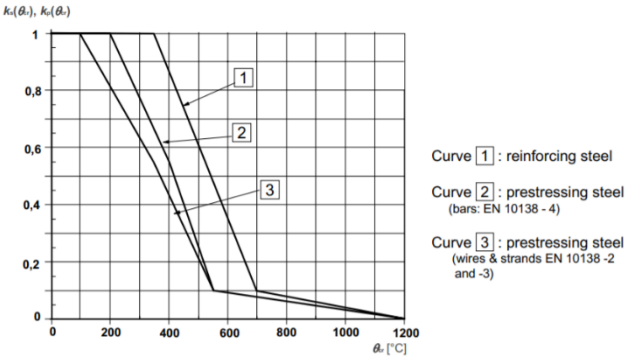

Fig. 14. Decrease of tensile strength of reinforcement due to temperature change. [5]

In a situation without fire, reinforcement steel and concrete affect each other. For example, bonding between the two materials is essential for the final structural behavior of the element. The assumption is that in the case of fire, the materials still affect each other. Literature assumes that the expansion coefficient for steel and concrete is equal until 400 °C, namely between $11.3 \cdot 10^{-6}$ m/m K^{-1} and $13.1 \cdot 10^{-6}$ m/m K^{-1}. [16] [17] This equal expansion coefficient means that the structure changes as one whole. When the temperature increases over 400 °C, the expansion coefficient of steel increases more than the expansion coefficient of concrete. [13] Because of those different expansion coefficients, the materials will expand differently from each other. For example, the reinforcement steel wants to expand more than the concrete, and so the concrete is obstructing the reinforcement steel. This obstruction causes cracks in the concrete at the locations with the highest tension.

For the collaboration between concrete and reinforcement steel anchorage is essential. According to EN 1992-1-2, the anchorage length under fire conditions should be checked by a formula in which the anchorage length under normal conditions is multiplied by the ratio between the partial safety factors of concrete and reinforcement under normal conditions and fire conditions. [5]

2.5 References concrete floors and fire

The previous paragraphs explained the principle of fire and heat transfer, the location of the coupling reinforcement, and the behavior of concrete during a fire. Combining all those elements gives the actual behavior of the concrete floors during a fire. In the past, multiple researches have been performed on this topic. Therefore, this paragraph will show some of the results of this researches. Only researches on full concrete floors are considered.

The first research described monolith concrete floors and their behavior during a fire. [18] The floors are researched using a numerical method. The research assumed a monolith floor in two construction methods. The first is a simply supported concrete floor. The floor is exposed to a fire from below. During the fire, there will be a horizontal and vertical deflection due to the non-linear flexural stiffness in the structure. The second construction method is about rigid supports. When using rigid supports, compressive forces will develop in the slab. Those forces enhance the flexural strength and stiffness of the floor. [18]

A second research is focused on hollow-core slabs. For this research, an analytical analysis is performed. It is mentioned that the behavior of a hollow core slab due to fire is complex. One of the reasons is that decreasing material properties must be taken into account. Another reason is that there is radiation inside the hollow cores. This radiation influences the temperature increase of the floor. For the research, a numerical model is created and used for three different analyses. After validating the numerical model, some of the parameters of mechanical response were investigated, namely aggregates and concrete strength. The research found that mixtures with only siliceous aggregates, compared to only calcareous aggregates, have a more significant loss of strength at an increased temperature and therefore have sooner thermal cracking. The research about concrete strength found that the strength of concrete has almost no influence on thermal behavior.

At last, there is looked for researches about composite floors as used as in this research. Unfortunately, numerical or experimental research, especially on composite floors during a fire, is not found. It is also asked for in fire laboratories, but there was no available experimental research into composite floors. As mentioned before, EN 13747 gives a design rule for fire safety at the location of the joint. In this design rule is referred to EN 13369:2004. This code refers back to EN 1992-1-2. In order to find background information about the determination of the graph from figure 7, the prEN 1992-1-2:2021 is used. [19] This document gives some design rules for calculating the precise values of the graph from figure 7. Those rules were developed after the graph was already used for designing fire safety. The values of the formulated design rules are validated by comparing the results to the existing graphs from EN 1992-1-2. Unfortunately, no additional information is provided on how the graph from figure 7 itself is determined.

3. RESEARCH METHOD

Different steps were taken to answer the research question. For the final answer, a validated numerical model is created to find the temperature of the coupling reinforcement. Before this model is built and used, it is essential to gain knowledge about how the finite element programs, i.e., ABAQUS, works for a heat transfer analysis. For each verification, an introduction, methodology, analyses, and discussion are given.

At first, a verification is made for a simplified model. An analysis based on the graph from the Eurocode is performed for 30, 60, 90, and 120 minutes. The next step is to perform an analytical analysis in which both the equations from the Eurocode as the finite difference method are used. The analysis is performed for 30, 60, 90, and 120 minutes. The results from this analysis are compared to the results of the graphical analyses. The last step in the verification is creating a numerical model to again run the analyses for 30, 60, 90, and 120 minutes. Each result of those fixed times is compared to both the graphical and the analytical analyses. When all the results match, the model yields to reliable results and is useable for complex structures. Only the results of 90 minutes are included in this paper since this is the fire resistance that suits the case study. The case study is explained in chapter 4. The other time steps are researched, so the research is usable in a broader context. Those results are given in appendices belonging to the verification.

The second verification is about thermal radiation at the location of the joint. The amount of thermal radiation that reached the surface depends on the view factor. In the simplified model, the view factor is 1 and is not considered. At the joint, a view factor is essential, and the way of modeling should be changed. Therefore, a simplified thermal radiation model is used to get more familiar with modeling thermal radiation in a finite element program, i.e., ABAQUS.

The simplified concrete floor model combined with the simplified thermal radiation model forms the final model of the critical detail of the composite floor. With this model, the question about the temperature of the coupling reinforcement is answered. With those temperatures, the structural behavior of this location is determined.

4. VERIFICATION

The concrete floor used for this analysis is a floor with a thickness of 200 mm and risk class CC2. The concrete class is C30/37 with an environmental class XC1. The reinforcement in the floor has a cover of 15mm. The Eurocode gives values characteristics of the concrete. Therefore, the emissivity is 0.7 and the moisture content 1.5%. The convection coefficient for exposed concrete is 25 W/m²K according to the EN 1992-1-2. [5] The unexposed concrete surface has a convection coefficient of 9 W/m²K. [19] The exposed surface is the surface that has direct exposure to fire since this surface is in the compartment at the location of the fire. The unexposed surface is at the other side of the structure and not directly exposed to fire. During the analysis, there is no reinforcement present in the model. The reinforcement temperature is determined by assuming that the temperature of the reinforcement is equal to the concrete temperature at that equal depth. Therefore, the concrete is assumed to be intact the whole assumed period and does not spall or crack. All the different analyses are performed with 30, 60, 90, and 120 minutes. Those fixed times are based on the fire safety requirements for buildings. Figure 15 gives an overview of the case study.

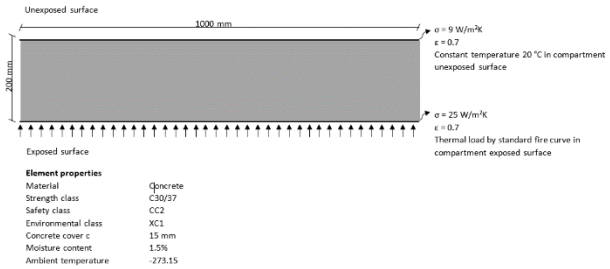

Fig. 15. Casestudy simplified model

4.1 Graphical analysis

EN 1992-1-2, Appendix A gives a graph about the temperature increase in a floor of 200 mm thickness, figure 7. The graph uses the standard fire curve and is only applicable to concrete elements exposed to fire on one side. For the first estimation of the heat transfer through the floor, this graph is used. The results of this analysis are given in table 1. Those temperatures are the basis for the comparison of the results from the analytical and numerical calculations.

Table 1
Temperatures °C in concrete floor according to EN-EN 1992-1-2 [5]

Depth in floor from exposed surface	T [°C] after 30 min.	T [°C] after 60 min.	T [°C] after 90 min.	T [°C] after 120 min.
0 mm	740	890	965	1050
10 mm	500	690	783	835
20 mm	350	520	635	690
30 mm	230	400	512	570
40 mm	160	300	409	460
50 mm	110	240	323	395
60 mm	80	180	252	320
70 mm	50	130	193	255
80 mm	40	100	149	220
90 mm	30	90	119	180

100 mm	20	80	97	160

4.2 Analytical analysis

The analytical analysis is performed with two different methods, using the equations of the Eurocode and the Finite Difference Method. The equations from the Eurocode have some common values which should be used. Since the aim is to use the calculation for a composite slab instead of a monolith concrete floor, the finite difference method is also reviewed. This method uses temperature-dependent characteristics. When the results are equal, the equations of the Eurocode are used. Otherwise, the most accurate method is used.

4.2.1 EN 1992-1-2

The analysis from the Eurocode is an analytical analysis based on the equations of the EN 1992-1-2 for calculating the increased temperature. This Eurocode uses those equations for calculating the graph of figure 7. The analyses use a constant value of k, which represents a combination of values for the thermal conductivity, density, and specific heat characteristics. The results from this analysis should be comparable to those from the graph from the EN 1992-1-2. [5] In Appendix C, more explanation on the equations 17, 18, and 19 is given.

Using the equations of the Eurocode, it is possible to determine the heat transfer through the floor starting from 30 minutes, since R_{fi} is not allowed to be lower than 1800 seconds. No further background information is found on this limitation. The Eurocode assumes a constant value for k, while the values for the density, specific heat, and thermal conductivity change along with the temperature. Each time step after 1800 seconds makes it possible to change the solid value to the specified value according to the temperature. The values are still corresponding to the values of the graph. Remark is that while doing that, the used value for 1800 seconds is much higher than the used values in the next time steps. In Appendix C also the temperatures at 30, 60, and 120 minutes are given.

$$\theta(x, R_{fi}) = \theta_1 + 20 \tag{17}$$

$$\theta_1(x, R_{fi}) = 345 \cdot \log_{10}\left(\frac{7(R_{fi} - \Delta R_{fi})}{60} + 1\right) \cdot \exp\left(-x\sqrt{\frac{0.9k}{R_{fi}}}\right) \tag{18}$$

$$with\ k = \rho\frac{c_p}{\lambda} \tag{19}$$

In equations 17, and 18, θ is the surface temperature [°C], R_{fi} is the duration of the fire [in sec.], ΔR_{fi} is the delay in temperature in the fire compartment and the concrete surface [in sec.]. In equation 19, ρ is the density [in kg/m³], c_p the specific heat [in J/kgK], and λ the thermal conductivity [W/mK].

4.2.2 Finite Difference Method

The second method used for calculating the internal temperature of the floor is the finite difference method. This method uses the temperature-depended values and gives the possibility to calculate the temperature in the floor from each desired starting point. This method divides the floor into three areas: the exposed surface, the inner part, and the unexposed surface. For the inner part, the floor is divided into several layers over the thickness. Using the temperature of the previous time step makes it possible to determine the temperature in the following time step. [19] In this case, the calculation is performed for the exposed surface and the inner part. The assumption is that the unexposed surface has a constant temperature of 20 °C. Therefore, the unexposed surface is not calculated. For more explanation about the equations of the finite difference method, see Appendix D.

Two equations are used to calculate the heat transfer through the floor, and therefore, the increase of temperature over time. Filling in those equations gives the results as mentioned in table 2. In Appendix D also the temperatures at 30, 60, and 120 minutes are given.

$$T_1^{i+1} = T_1^i + \frac{2\cdot\Delta t}{(\rho c_p)_1^i \cdot \Delta x} \cdot \left[q_{net}''^i - \left(\frac{\lambda_1^i + \lambda_2^i}{2}\right) \cdot \left(\frac{T_1^i - T_2^i}{\Delta x}\right)\right] \tag{20}$$

$$T_j^{i+1} = T_j^i + \frac{\Delta t}{(\rho c_p)_1^i \cdot \Delta x^2} \cdot \left[\left(\frac{\lambda_{j-1}^i + \lambda_j^i}{2}\right) \cdot (T_{j-1}^i - T_j^i) - \left(\frac{\lambda_j^i + \lambda_{j+1}^i}{2}\right) \cdot (T_j^i - T_{j+1}^i)\right] \tag{21}$$

In equation 20, T_1^{i+1} is the temperature of the concrete of the exposed surface in the subsequent time step [in K], T_1^i is the temperature of the surface at the present time step [in K], $q_{net}''^i$ is the heat flux [W.m²], and λ_1^i is the thermal conductivity of the present temperature [in W/mK]. In equation 21, T_j^i is the temperature on the inside of the floor [in K], Δt is the time step [in sec.], ρ is the density [in kg/m³], c_p is the specific heat [in J/kgK], Δx is the thickness of the floor layer [in m], and λ_1^i is the thermal conductivity of the present temperature [in W/mK].

In table 2, some minor differences between the graphical and analytical analysis are visible. When comparing the graphical analysis to the analytical analysis with the equations of the Eurocode, it becomes visible that the gotten values are slightly higher. One of the most common reasons is that the equation of the Eurocode is more precise than reading the values of the graph. When comparing the values from the Eurocode and the analytical analysis with the finite difference method, the values are a little bit lower. The closer to the exposed surface, the more the difference increase. The expectation is that those differences are due to the differences in values for the temperature-dependent values. In the beginning, the Eurocode calculates with a value of 660 °C even when the floor has not reached that temperature. In the finite difference method, the expected temperature of the floor is used. Therefore, the expectation is that the finite difference method is a more precise prediction. Another explanation could be that there are some rounding errors in the calculations, leading to differences. The differences between the three different methods are minor. Therefore, the assumption is that the performance of the analytical analysis is yielding to reliable results and that the finite difference method is applicable for complex structures.

4.3 Finite Element Method

The final aim of the numerical analysis is to design a numerical model, which solves the heat transfer in a composite floor. This numerical model aims to verify the correct working of the heat transfer analyses in ABAQUS. Therefore, a numerical model for this simplified situation is designed. The assumption is that when the results of this model are equal to the graphical and analytical analysis results, the model is yielding to reliable results.

The numerical analysis uses the finite element program ABAQUS to build a model for the heat transfer analyses, figure 16. In this model, the floor has a thickness of 200 mm. As a thermal load, the standard fire curve is applied, and the material properties density, specific heat, and thermal conductivity are given as temperature-dependent. The thermal load influences the exposed surface by thermal radiation and convection. For thermal radiation, the unexposed and exposed surface has an emissivity of 0.7. The ambient temperature of the unexposed surface is 20 °C. [5] A heat transfer coefficient of 9 W/m²K for the unexposed surface with an ambient temperature of 20 °C is considered for convection. [18] The convection at the exposed surface has a heat transfer coefficient of 25 W/m²K. [5] Figure 16 gives an overview of the numerical model.

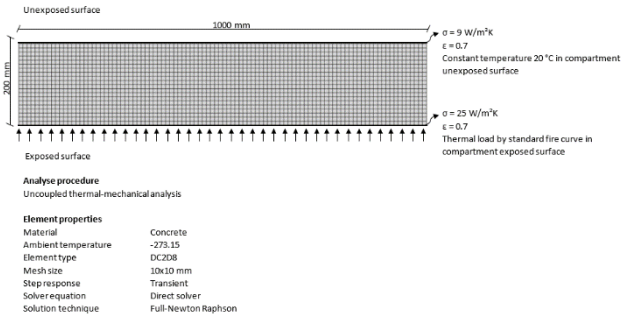

Fig. 16. Model continuous monolith floor

The numerical model is a 2D model using an uncoupled thermal-mechanical analysis. For the simplified model, only the heat transfer is solved. In the heat transfer model, the absolute zero temperature is set to -273.15 and a Stefan-Boltzmann constant of $5.67\cdot10^{-8}$ is used. The setting of the ambient temperature leads to a model which calculates in Celsius

degrees. The concrete parts, which represent the floor, are solid homogeneous and have temperature-dependent characteristics. The next step is designing the mesh for the floor, where the aim is to review the floor in steps of 10 mm thickness. Therefore, the element gets a squared filling with parts of ten-by-ten mm. By using a mesh for a heat transfer analysis with a quadratic geometric order, DC2D8 elements are created. Those elements can only be used in a heat transfer analysis. Using a quadratic geometric order is since the heat transfer in a finite element is not linear.

Furthermore, a heat transfer step is created. The response of this step is transient. Transient means that the research is about the time between the beginning of the fire and the steady-state. For the equation solver, the direct method is used. As a solution technique, the Full-Newton Raphson technique is used. In the step, an incrementation with a maximum allowable temperature change per increment is set at 10 °C. The period of the step changes to the desired period of 1800, 3600, 5400, or 7200 seconds. For applying the thermal load, an amplitude is created. This amplitude is based on the calculated values for the standard fire curve, according to equation 1. This thermal load is applied to the structure at desired locations, using surface radiation and surface film conditions. At last, running the job gives the results as presented in figure 17 and table 2.

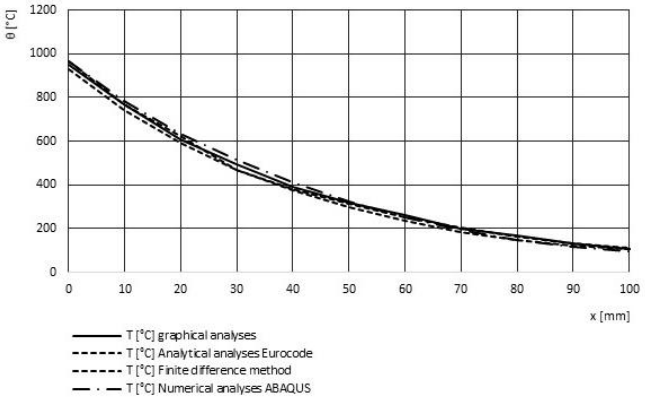

Fig.17. Comparison temperature different analyses

Table 2
Comparison analyses heat transfer through floor at 90 minutes

Depth in the floor from exposed surface	T [°C] Graphical analyses	T [°C] Analytical analyses Eurocode	T [°C] Finite difference method	T [°C] Finite Element Method ABAQUS
0 mm	950	965	930	965
10 mm	770	767	743	783
20 mm	610	625	591	635
30 mm	495	467	470	511
40 mm	390	380	373	409
50 mm	320	312	296	323
60 mm	260	251	234	252
70 mm	200	203	183	192
80 mm	170	165	147	148
90 mm	130	134	123	118
100 mm	105	111	104	96

In the results, some minor differences between the graphical, analytical, and Finite Element Method are visible. The explanation of the difference between the graphical and the analytical analysis is in section 3.2. The difference between the first two analyses and the numerical analysis is that ABAQUS gives a more precise calculation and prediction of reality. In addition, a minor rounding error is possible. The differences are slight. Therefore, the assumption is that the ABAQUS model is yielding to reliable results. The conclusion from this validation is that the analysis is suitable for complicated structures.

The calculation of a monolith concrete floor of 200 mm thickness is verified. The assumption is that this calculation method is also usable for slightly thicker and thinner floors since at least the first 100 mm reaches the same temperatures. The model is adapted to a floor with a thickness of 180 mm en 240 mm to verify this hypothesis. The results in the first 100 mm are equal to the floor with a thickness of 240 mm. Appendix E gives the results of this analysis. Since the results are equal for the different floor thicknesses, the hypothesis is correct. In the first 100 mm of a thinner or thicker floor, the temperature is equal.

4.4 Thermal radiation

Thermal radiation plays a part in the temperature development of the composite floor. Thermal radiation is, as explained before, the energy transport by electromagnetic waves with wavelengths λ=0,1 till 100 µm. For the critical detail at the joint, thermal radiation becomes more important. The previous model assumes that the thermal radiation is all absorbed at the surface since the surface is directly in the compartment. The surface of the joint is not directly in the compartment and, therefore, not absorbing the same amount of thermal radiation. To calculate the amount of thermal radiation which is absorbed, the view factor is used. This factor represents the energy leaving a finite area A_1 arriving at finite area A_2 and is calculated with equation 22. [20]

$$F_{12} = \frac{1}{A_1} \int_{A_1} \int_{A_2} \frac{\cos\theta_1 \cos\theta_2}{\pi r^2} \, dA_2 dA_1 \tag{22}$$

In equation 22, F_{12} is the view factor, A_1 is the finite area with leaving energy [in m²], A_2 is the absorbing finite area [in m²], θ_1 is the angle between the normal axis of the sending area and the visibility line [in °], θ_2 is the angle between the normal axis of the absorbing area and the visibility line [in °], and r is the distance between the areas [in m]. This view factor is different over the height due to the increasing obstruction when looked more into the joint. More information about the calculation of the view factor are given in Appendix F.

The emissivity coefficient for calculating thermal radiation is dependent on the actual amount of electromagnetic waves. The analysis uses the emissivity coefficient as a temperature-independent coefficient. In theory, emissivity is a temperature-dependent characteristic. Multiple resources give an emissivity coefficient for concrete between 0.8 and 0.99 [21] [22] [7], while the Eurocode uses an emissivity coefficient of 0.7. [5] A sensitivity analysis is performed by analyzing the results of the previous model with an emissivity of 0.9 and 0.7. The results with the higher emissivity gave a slightly higher temperature on the inside of the floor, see Appendix F. This difference is because a higher emissivity makes the material more capable of giving heat away and absorbing more heat. Comparing the temperature differences of the different emissivity coefficients shows a slight difference. Since there is no equation to determine the emissivity in a temperature-dependent way, and the difference is slight, the value of the Eurocode is considered as a standard value. The expectation is that this value is gotten by modeling and is an average for the actual changing emissivity coefficient over time.

As explained, radiation plays a different role at the location of the joint than at the other surfaces of the floor. This means that the radiation could be causing different temperatures in this specific area. Before implementing radiation in the numerical model of the composite floor, the method of using radiation in ABAQUS should be verified. Both analytical and Finite Element Method are used.

4.5 Analytical model thermal radiation

To calculate the heat flux between two surfaces in order to be able to verify the numerical model, which is explained later, a simplified model is created, figure 15. This model consists of two surfaces to calculate the thermal radiation transported from one element to another. The surfaces have a constant emission coefficient and a constant temperature. Those temperatures are constant because when the temperature is changing, heat flux is also changing. Since the surfaces are straight against each other, the view factor is 1. The results of the calculation are visible in table 3.

4.6 Numerical model thermal radiation

This numerical model of thermal radiations aims to verify the working of radiation in ABAQUS and implement radiation correctly in the numerical model of the composite floor. If the results are approximately equal to the results of the analytical analyses, it is verified that the method is suitable for using in the numerical model of the composite floor.

The numerical model for the simplified thermal radiation uses the finite element program ABAQUS as a model for heat transfer. The assumptions of the model are the same as in the analytical calculation, figure 18. The model uses two deformable shell elements with a thickness of 5 mm. The thickness is minimal since the wanted information is about the heat flux out of the element. In the analytical analysis, the thickness of the elements is not considered. The mesh used for the elements is DC2D8. The elements are not geometrically connected; however, they are supposed to have a heat transfer to each other. Therefore, the elements are connected by a surface-to-surface interaction. In this interaction, a thermal radiation property is considered in which the emissivity and possible view factor is implemented.

The thermal radiation itself could be modeled in two ways, with surface radiation and cavity radiation. The two options are very close to each other; however, the most considerable difference is in the characteristics of the joint. In this case, and in the model of the composite floor, the joint is open and receives heat from the fire. Since surface radiation is used in situations without a gap or with a closed gap in three-dimensional directions, the option for cavity radiation is more suitable. Both elements have a constant temperature to create the temperature difference, which causes heat transfer. If the temperature difference gets smaller due to the temperature decrease of the surface of 1000 °C and the temperature increase of the surface of 20 °C, the heat flux will decrease. Therefore, the heat flux is taken in an early time step of 0.05 seconds. An overview of the numerical model for simplified radiation can be found in figure 18. The results of the analytical and Finite Element Method about the heat flux are given in table 3. Some additional information is given in Appendix F.

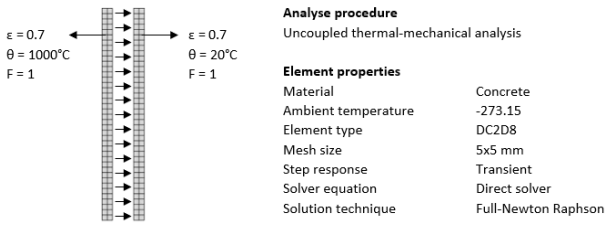

Fig. 18. Model simplified thermal radiation.

Table 3
Analytical and Finite Element Method verification thermal radiation.

Emission coefficient	Analytical analysis [W/m²]	Numerical analysis [W/m²]
0.7	39690	39510
0.3	17010	12717

In the analysis, two emission coefficients are calculated. Using more data minimizes the change of an accidentally false correct answer. The values in the table are approximately equal, and therefore, it is assumed that the performance of the analytical and Finite Element Method is yielding to reliable results. One of the reasons for this difference is that the analytical calculation uses a view factor of 1, while ABAQUS calculates the view factor in the case of an open joint over the whole surface. Therefore the view factor is a little bit lower than one. A second difference between the analytical and numerical model is the ambient temperature. The numerical model considers an ambient temperature, while the analytical analysis only considers the temperatures of the elements. Furthermore, the assumption is that this difference comes from some lost heat transfer through other surfaces than the assumed surface or more accuracy than possible with the analytical calculation. A remarkable difference in outcome is about the difference of the emissivity of 0.3 and 0.7. The assumption is that since the surface is obstructed in radiation due to the emission coefficient of 0.3, more energy is left through the other surfaces. There is no literature found to confirm these assumptions.

4.7 Different assumptions at the location of the joint

In comparison to the continuous floor, some different assumptions should be made to analyse a composite floor with a gap. Those differences led to a slightly different model. Also, some uncertaincies in the numerical model will be explained.

The composite floor model is slightly different in comparison to the monolith floor model when discussing radiation. In 4.6 is verified how radiation is working at an open cavity and, therefore, a constant ambient temperature. In this numerical model, the temperature of the precast plates and the gas in the compartment increase over time. Therefore, the standard fire curve should be implemented in the numerical model at the location of the joint. Unfortunately, it is not possible to model an open cavity while the temperature is increasing over time. Therefore, the cavity should be modeled slightly differently. A possible solution given in the ABAQUS manual is using a closed gap by implementing an external element through which the heat is transferred inside the gap. By modeling this additional element with an emission coefficient of 1, the heat of the standard fire curve is transferred to the joint.

A few uncertaincies in the numerical model are researched before implementing them in the numerical model of the composite floor. The sensitivity analysis in this research is about the lower convection coefficient at the location of the joint. This decreased convection coefficient results from the decreased speed of air and the measure of the whirls at the joint. In the compartment with the fire, the whirls are large, while the whirls at the unexposed surface are smaller. The whirls in the joint are even smaller than at the unexposed surface due to the limited space. Therefore, a decreased convection coefficient must be considered. To gain knowledge about the influences of the convection coefficient at the location of the joint, an additional analysis is performed with three different coefficients, namely 2, 1, and 0.5. The results indicate that the temperature in the in-situ layer above the joint slightly decreases when a convection coefficient of 0.5 is considered. By increasing the coefficient to 2, the temperature above the joint slightly increases. The difference in percentages is that small that the differences are neglectable. At the location of the surfaces of the joint, the differences are also neglectable. The results of the analysis are in Appendix G.

The second sensitivity analysis is about the standard fire curve. The standard fire curve is, in theory, based on two different curves, namely the radiative temperature and the gas temperature. [23] The radiative temperature has a delay compared to the gas temperature due to the lower temperature of the materials of the walls. To gain more knowledge about the difference in using the standard fire curve or the two different curves, an analysis is performed in which the results of the different models are compared. From the results could be concluded that the differences are neglectable. During the analyses of the composite floor, the standard fire curve will be used. The results of the second sensitivity analysis are given in Appendix G.

The last sensitivity analysis is about the joint itself. According to the EN 13747, the joint is neglectable till 20 mm. Therefore, the analyses are performed with steps of 1 mm to gain knowledge about the influence of the joint. Besides the joint width, the joint depth is also essential for the temperature development at the joint. Since the traditional composite floor uses floor plates from 50 mm till 100 mm, those depths are researched in steps of 10 mm.

5 FIRE BEHAVIOR AT CRITICAL DETAIL

In the previous chapter, the validation of the calculation method for the heat transfer through a concrete floor is explained by simplified models. Based on those analyses, it is concluded that the numerical model of ABAQUS yields to reliable results. Therefore, it is concluded that this method is applicable for complicated structures. For this research, this more complicated structure is the composite floor at the location of the critical detail of the coupling reinforcement. The assumption is that the precast plate and the in-situ concrete have a perfect connection and work

as one element during heat transfer. Since the design rule consists of two parts, a numerical model of a continuous composite slab is made to verify this first part of the rule. Besides this model, another numerical model of the composite floor at the location of the coupling reinforcement is build. This chapter discusses both numerical models with their temperature analyses and the structural analyses at the specific location of the coupling reinforcement are discussed.

5.1 Heat response analyses

The heat response analysis is working equally to the heat response analyses of section 4.3. Therefore, no further explanation is given on the model.

Two different numerical models were designed for the composite floor, one continuous model and the model with the critical detail. Those models are necessary since the design rule consists of two parts. The first part is *"The fire resistance of a composite slab of floor plates without void formers is the same for a solid slab of identical characteristics."* By designing a composite floor without a joint loaded with the standard fire curve, the temperatures of this floor type could be found. The results of the analysis have equal temperatures as in the monolith floor, Appendix H. It could be said that this first part of the design rule is validated.

For the second part of the design rule, "*Calculation of the temperatures is carried out without taking into account the joint between floor plates as much as the width b_j is lower than 20 mm"* a numerical model of a composite floor with a joint is designed. For this numerical model, the expectation is that the heat transfer is different from a continuous floor due to two aspects. The first aspect is thermal radiation in the joint, which is explained more in section 4.6. The second aspect is the different convection coefficient at the location of the joint, as explained in section 4.7.

5.2 Numerical model composite floor

The aim of the numerical model of the composite floor is to determine the temperature difference at the location of the joint. Those analyses could locate possible locations which are causing an additional risk to the detail of the coupling reinforcement. Also, those results will be used afterwards to determine the decrease of strength of the concrete and reinforcement steel.

The basics of the model of the composite floor are equal to the numerical model in the simplified situation. In this paragraph, only the differences between the two models are explained. The numerical model of the composite floor consists of two precast plates at the bottom and an in-situ part at the top. All the parts are connected with tie constraints. In comparison to the simplified model, some assumed boundary conditions and the results from the sensitivity analyses are added. At the location of the joint, a convection coefficient of 1 W/m²K is considered. For radiation, an emissivity of 0.7 is applied, which is multiplied by the view factor. The view factor is calculated for each 5 mm joint depth to reach a realistic approach. The thermal load at the joint for convection and radiation is equal to the thermal load of the standard fire curve. An overview of the numerical model of the composite floor with joint is given in figure 19.

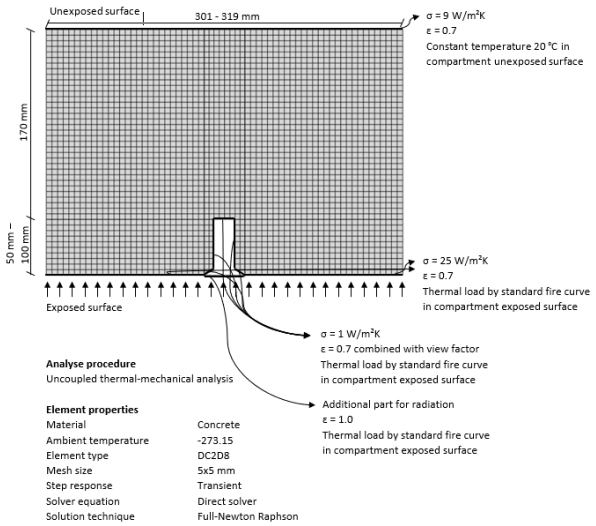

Fig. 19. Model composite floor with joint.

According to the design rule in EN 13747, the heat transfer may be neglected at the joint ranges from 0 mm to 20 mm. The numerical heat transfer analysis is executed for joint widths with a difference of 1 mm to verify this design rule. Furthermore, six different joint heights are researched. All the models are analyzed for the fixed times 30, 60, 90, and 120 minutes. Figure 20 is explaining the different depths in the composite floor which are used for the results of the analyses.

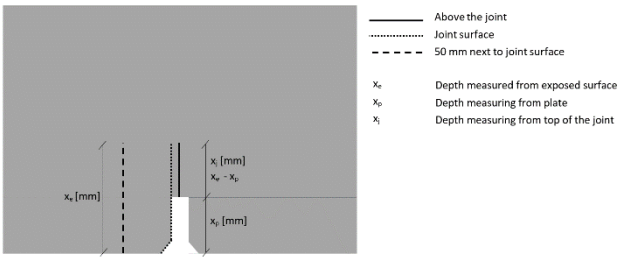

Fig. 20. Explanation depths in the composite floor.

In figure 20, three different depths are shown. The first depth x_e, exposed surface, is the total depth in the floor measured from the exposed surface. The second depth is x_p plate, representing the depth of the precast plate and this precast plate can vary from 50 mm to 100 mm. The third depth x_j, joint, is the depth in the floor measured from the top surface of the joint, and this distance is equal to $x_e - x_p$. The drawn lines implicate the horizontal locations of which the temperatures are measured.

The results of the analyses are given in the following figures. Figure 21 presented the temperatures of the concrete above the joint at different heights in the in-situ layer, combined with the six different joint depths. In this figure, the joint width is a constant of 19 mm at a fixed time of 120 minutes. The temperatures concrete above the joint at other joint widths are presented in Appendix H.

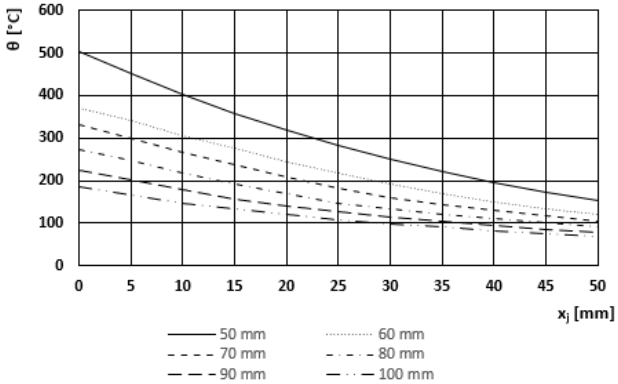

Fig. 21. Temperature of the concrete above the joint at depth x_j measured from the top of the joint after 120 minutes plotted over different joint depths. The joint width is 19 mm.

Figure 22 gives the temperatures of the concrete above the joint at different joint widths with a fixed time of 120 minutes. In this figure, the joint depth, x_p, is a constant of 50 mm. The exact temperatures of the concrete above the joint and the other joint depths are presented in Appendix H.

Based on the results shown in figures 21 and 22, a joint width of 19 mm and a joint depth of 50 mm is reaching the highest temperatures above

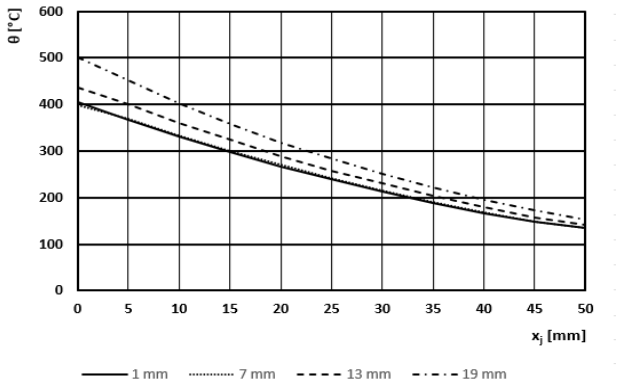

Fig. 22. Temperature of the concrete above the joint at depth x_j measured from the exposed surface after 120 minutes plotted over different joint widths. The joint depth is 50 mm.

the joint. The results can be explained by the used view factors at this specific situation. By increasing the joint depth, the view factors at the top of the joint decrease. The same is applicable for the joint width. By decreasing the width, the view factors at the surface of the joint are also decreasing.

For the last analysis, the normative situation becomes a floor with a joint depth of 50 mm and a joint width of 19 mm. At this moment, the location of the joint is researched. However, there is no guarantee that the floor will fail at the location of the joint. When another part of the floor reaches a higher temperature, the floor probably fail at that location. Therefore, a comparison of the temperatures at the joint surface, in the concrete above the joint and in a section 50 mm sidewards of the joint, is performed. Figure 23 presents the temperature at three different locations in the floor after 120 minutes. The other situations for different joint depths and joint widths are given in Appendix H.

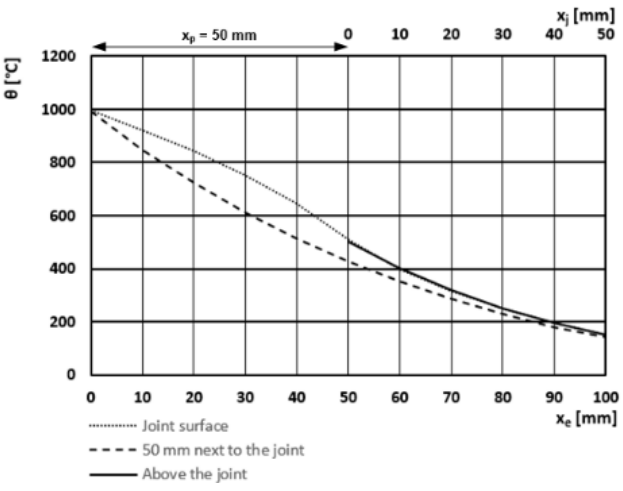

Fig. 23. Temperature of concrete at 120 minutes at three different locations in the floor with joint depth 50 mm and joint width 19 mm.

From the results in figure 23 can be concluded that the joint surface and the concrete above the joint are reaching the same temperature at the same depth. In the precast plate, the temperatures are higher than the temperature above the joint since the floor is directly exposed to radiation and has no view factor. At the location of the joint, the temperature is slightly higher than at the location 50 mm next to the joint. The reason for this temperature difference is due to the additional convection and radiation at this point.

5.3 Structural response analyses

The temperature of concrete will increase due to a temperature increase in the surrounding, which will lead to structural response of the structure. One of those consequences of this increased temperature, concrete will expand. The more the temperature increases, the more the concrete will expand. Since the temperature is the highest at the location of the joint, the assumption is that the most significant deformation is visible at this location.

For the analysis of the deformations, the numerical heat transfer model is used for structural purposes. In order to do so, some changes are made in the model. The calculation method of the numerical model is changed from heat transfer into static analysis. Next, the element type is changed into deformable elements CPE4R, used for analyses with plane strain. The material concrete has gotten some mechanical characteristics. The Young's Modulus is 33000 N/mm² and the Poisson's Ratio 0.2. The expansion coefficient is assumed to be $12 \cdot 10^{-6}$, which is the average from values found during the literature study. [16] Those characteristics are not used as temperature dependent. Furthermore, boundary conditions are added to the mechanical model. Since the model only contains a small part of the floor, both sides of the structure are fully clamped. Only the temperature data from the thermal analysis is applied in this structural simulation, and therefore only the thermal deformation is considered. An

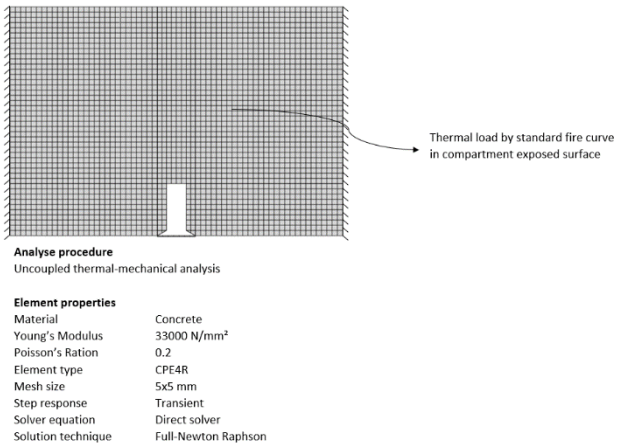

Fig. 24. Model mechanical analysis.

overview of the structural model is given in figure 24.

The deformation of the composite floor is shown in figure 25. This deformation is shown to present the direction of the deformation, but is only analysed on this small part of the floor. The actual amount of deformations in the floor will be different while researching the complete floor. At the location of the joint, the deformation is more significant than at the part of the continuous floor. This deformation is in comparison with the expectation. The precast plates will apply pressure into the in-situ floor due to this deformation, and therefore cause internal forces, such as an increased normal forces at the interface between the precast plate and the in-situ layer.

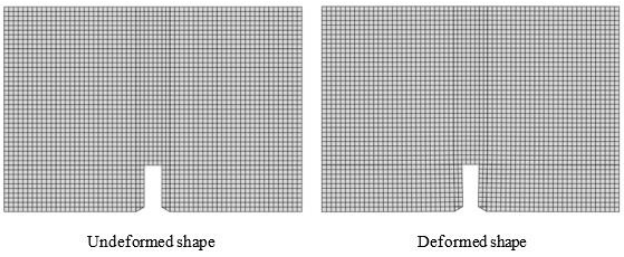

Fig. 25. Undeformed and deformed shape based on thermal loading.

5.4 Structural resistance

Although the normal stresses in the interface increases during the fire, the resistance of the interface is not discussed and require further research. The temperature of reinforcement is considered equal to that of the surrounding concrete. In figure 26 the temperatures of the reinforcement in the precast plate and of the coupling reinforcement are plotted at times 30, 60, 90, and 120 minutes. For the reinforcement in the

precast plate a concrete cover of 20 mm is considered. The coupling reinforcement perpendicular to the joint is placed directly on the precast

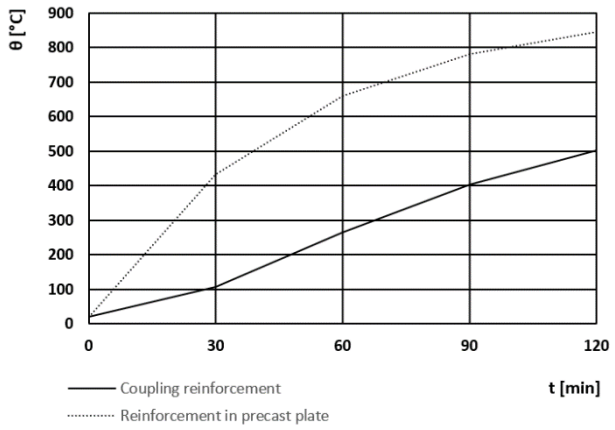

Fig. 26. Temperature at 30, 60, 90, and 120 minutes of the reinforcement in the precast plate with a concrete cover of 20 mm and the coupling reinforcement perpendicular to the joint located directly on the precast plate.

plate. With the temperatures of the reinforcement from the heat transfer analysis, the reduction of the moment capacity due to temperature increase can be calculated.

The strength of concrete and reinforcement decreases due to temperature, and as a consequence the moment capacity decreases. The composite floor has two interesting locations for researching the moment capacity, namely the coupling reinforcement and the reinforcement in the precast plates. The reinforcement of the precast plate is researched in the first and second layers. Therefore, equation 23 is used.

$$M_{Rd} = A_s \cdot f_{yd} \cdot 0.9d \qquad (23)$$

In equation 23, M_{Rd} is the moment capacity [in kNm], A_s is the area of reinforcement [in mm²], f_{yd} is the design strength of reinforcement [N/mm²], and $0.9\ d$ is representing the internal lever arm.

Equation 23 is used for calculating the moment capacity with an ambient temperature. Two changes are implemented to the equation to determine the moment capacity at the moment after the fire. At first, a reduction of the concrete is considered due to the damaged concrete, which has no load-bearing capacity anymore. This concrete reduction is calculated by decreasing the cross-section by removing the concrete, which gets higher than 500 °C. [5] The second change is the calculation value of the reinforcement strength. The reinforcement gets a reduction based on the graph in figure 14 and is multiplied with the f_{yd} of reinforcement steel. Results of the moment capacity are shown in figure 27. In Appendix I the results of the moment capacity of the reinforcement in the precast plates are shown.

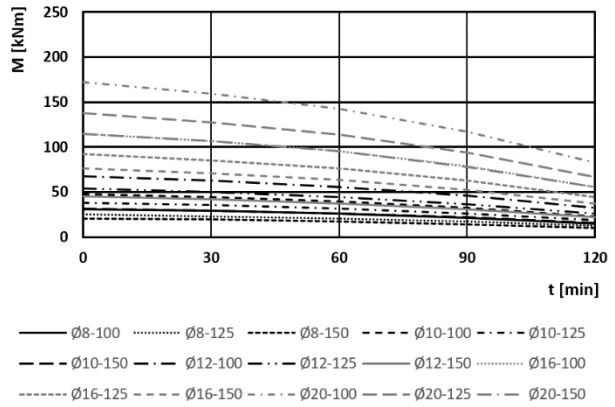

Fig. 27. Decrease moment capacity floor above the joint.

From the results in figure 27 becomes visible that using reinforcement with a higher area is reducing the moment capacity of the cross section more than by using reinforcement with less area. However, the reduction of the moment capacity is less compared to the reduction of moment capacity in the cross section of the precast plate, as described in the Appendix I. Therefore, the joint is not causing an additional risk during a fire.

6 SUMMARY AND CONCLUSION

This research focused on the detail of the coupling reinforcement above a joint of a composite floor. During the performed analyses, some assumed and sensitivity analyses are considered. There are two assumed boundary conditions, namely:

- The material properties density, specific heat, and thermal conductivity. Those material properties are considered as described according to the EN 1992-1-2. No further literature study on the origin of the formulas is performed.
- According to the EN 1992-1-2, the influence of the reinforcement on the temperature field can be neglected. Therefore, no research is performed into the heat transfer between the concrete with increased temperature into the reinforcement embedded in this concrete. The assumption is that the temperature of the reinforcement is equal to the exact location of the concrete.

For the uncertaincies in the numerical model, multiple qualitative sensitivity analyses are performed. The results of those analyses are used in the numerical model of the composite floor.

- The mesh in the numerical model is practically chosen. By choosing this practical mesh, it became simpler to analyze the results of the Finite Element Method. A sensitivity analysis is performed with a mesh twice as large and twice as small to confirm the used mesh size. Those analyses show similar results, and therefore the assumption is that the mesh is usable.
- The standard fire curve is based on two different curves, the radiative temperature and the gas temperature. Those two curves combined form the standard fire curve. Compared to the gas temperature curve, the radiative curve has a delay. A sensitivity analysis is performed to exclude the possibility that this delay causes a different heat transfer. In this sensitivity analysis, analysis with the standard fire curve and the two apart curves are compared. Those analyses gave approximately the same results. Therefore, it is a safe assumption to use the standard fire curve to analyze the composite floor.
- The emission coefficient given by the EN 1992-1-2 is 0.7, while other researchers use an emission coefficient between 0.8 and 0.99. For the sensitivity study, analyses are performed with both emission coefficients of 0.7 and 0.9. The differences between the results were neglectable, and therefore the value of the EN 1992-1-2 is used.
- No literature is found about the use of the convection coefficient at the location of the joint. Since the whirls are smaller at the location of the joint, the convection coefficient will be smaller than at the exposed and unexposed surface. Analyses were made in which a convection coefficient of 0.5, 1, and 2 are compared. The differences between the results are neglectable.

Based on performed research with the assumed boundary conditions and results from the sensitivity analyses, the answer to the research question "*What is the behavior under fire conditions at the location of the joint between two precast plates of a composite floor and is this a risk for the safety of the structure?"* is as followed.

Fire is causing a thermal load on the composite floor. At the location of the joint between two precast plates, an additional thermal load is located on the composite floors due to radiation and convection at those surfaces. All those thermal loads are causing a temperature increase on the inside of the concrete floor. Since the location of the joint has a higher

thermal load, the temperature increases more at this location compared to other parts of the floor. This temperature increase is also the case at the location of the coupling reinforcement. However, the thermal load at the location of the joint has only a slight influence on the temperature increase of the concrete around the joint. Therefore, the temperature at the location of the coupling reinforcement is smaller than the temperature of the reinforcement in the precast plates. This temperature leads to a more substantial reduction of the strength of the reinforcement in the precast plates. Therefore, the reinforcement in the precast plate will probably fail sooner than the structure at the location of the coupling reinforcement. In this research reinforcement with the same diameter for both the precast plate and the coupling reinforcement is considered. For that reason, the presence of a joint between two precast plates in a composite floor, in case of fire is not causing an additional risk to the structural reliability of the composite floor as far as the moment resistance of the cross section above the joint is considered. The conclusion is that the design rule of EN 13747 is applicable for composite floors with a two-directional span. The design rule is also usable when different from requirements, but according to Dutch practice in recent years, the coupling reinforcement is placed directly on the precast floor plates without a concrete cover.

7 RECOMMENDATIONS

Based on this research, two recommendations are formulated to gain more knowledge about this problem and verify the conclusion above.

- This research is performed based on the standard fire curve, ISO 834. Using this fire curve gives a controversial calculation since the fire is not extinguished in this curve. A more realistic calculation method uses the natural fire curve in a project-specific situation to research the temperature increase of the coupling reinforcement in that situation.
- This research is not considering the interface, which is relevant for the transfer of the tension force from the coupling reinforcement to the reinforcement in the precast plate, between the precast concrete and the in-situ layer. To gain knowledge about the actual structural reliability of the composite floor, research into this topic should be performed.

REFERENCES

[1] S. N. M. Wijte, „Rapport 9780-1-0 Voorstellen vooren achtergronden bij rekenregels van beoordeling van bestaande bouw.," Adviesbureau ir. J.G. Hageman B.V., Rijswijk, 20 mei 2019.

[2] „EN 13747:200+A2:2010, IDT, Precast concrete products - Floor plates for floor systems," CEN, 2010.

[3] „EN 1992-1-1:2004+AC:2008+AC:2010, Design of concrete structures - Part 1-1: General rules and rules for buildings," CEN, 2016.

[4] S. E. Magnusson en S. Thelandersson, „Temperature - Time Curves of Complete Process of Fire Development," *Bulletin of Division of Structural Mechanics and Concrete Construction,* nr. 16, 1970.

[5] „EN 1992-1-2 Design of concrete structures - Part 1-2: General rules- Structural fire design," NEN, 2005.

[6] „EN 1991-1-2:2002, Eurocode 1: Actions on structures - Part 1-2: General actions - Actions on structures exposed to fire," CEN/TC 250, 2002.

[7] D. Di Capua en A. R. Mari, „Nonlinear analysis of reinforced concrete cross-sections exposed to fire," *Fire Safety Journal,* vol. 42, pp. 139-149, 2007.

[8] A. Bejan en A. D. Kraus, Heat transfer handbook, Hoboken, New Jersey: John Wiley & Sons, Inc., 2003.

[9] B. Georgali en P. Tsakiridis, „Microstructure of fire-damaged concrete. A case study," *Cement & Concrete Composites,* vol. 27, nr. 2005, pp. 255-259.

[10] K. Hertz, „Limits of spalling of fire-exposed concrete," *Fire Safety Journal,* vol. 2003, nr. 38, pp. 103-116, 2002.

[11] J. Zehfuß, F. Robert, J. Spille en R. N. Razafinjato, „Evaluation of Eurocode 2 approaches for thermal conductivity of concrete in case of fire," *Civil Engineering Design,* vol. 2, pp. 58-71, 2020.

[12] Z. Zhang, „Effect of Temperature on Rock Fracture," *Rock Fracture and Blasting,* 2016.

[13] S. Iffat en S. Bose, „A Review on Concrete Structures in Fire," *International Journal of Civil, Environmental, Structural, Construction and Architectural Engineering,* 2016.

[14] V. Kodur, „Properties of Concrete at Elevated Temperatures," Department of Civil and Environmental Engineering, Michigan State University, 2014.

[15] K. Xiang, G.-h. Wang en Y.-c. Pan, „Thermal properties and heat transfer in concrete filled steel tube reinforced concrete columns exposed to fire," in *7th Internation Conference on Intelligent Computation Technology and Automation*, Changsha, China, 2014.

[16] T. Uygunoğlu en I. B. Topçu, „Thermal expansion of self-consolidating normal and lightweight aggregate concrete at elevated temperure," *Construction and Building Materials,* vol. 23, pp. 3063 - 3069, 2009.

[17] F. Aydin, „Experimental investigation of thermal expansion and concrete strength effects of FRP bars behavior embedded in concrete," *Construction and Building Materials,* vol. 163, pp. 1 - 8, 2018.

[18] W. Borgogno, P. Bischof, J. Burridge, S. Carrascón, F. Ehrlich, N. Forsen, H. Ganz, M. Hallgren, R. J. McNamee, J. F. Jensen, J. Reiners, F. Robert, J. Zehfuß, P. Bamonte en T. Lennon, „Background document for prEN 1992-1-2:2021," CEN TC250/SC2/WG1/SC2.T2, 2021.

[19] A. Lazouski, „Influence of sustained stress and heating conditions on the occurence of fire-induced concrete spalling," University of Edinburgh, 2017-2019.

[20] M. R. Vujičić, N. P. Lavery en S. G. Brown, „View factor calculation using the Monte Carlo method and numerical sensitivity," *Communications in numerical methods in engineering,* vol. 22, pp. 197-203, 2006.

[21] A. Saetta, R. Scotta en R. Vitaliani, „Stress Analysis of Concrete Structures Subjected To Variable Thermal Loads," *Journal of Structural Engineering,* vol. 121, pp. 446-457, 1995.

[22] T. Ficker, „Measurement of emissivity in student laboratories," *European Journal of Physics,* vol. 41, p. 22, 2020.

LIST OF FIGURES

Fig. 1. Examples of current joint profiles with bi. [2]
Fig. 2. One-direction span.
Fig. 3. Two-direction span.
Fig. 4. Examples of possibilities for placing precast concrete plates between two columns. [1]
Fig. 5. Critical detail at the location of two precast plates with lattice girders.
Fig. 6. Standard fire curve and natural fire curve. [5]

Fig. 7. Temperature profiles for slabs according to the EN-EN 1992-1-2 at Rx with x is the duriation of the fire. [7]
Fig. 8. Density decrease due to temperature change. [7]
Fig. 9. Specific heat increase due to temperature change based on NEN-EN 1992-1-2. [5]
Fig. 10. Thermal conductivity decrease due to temperature change based on EN-EN 1992-1-2. [5]
Fig. 11. Thermal diffusity for temperature-dependent characteristics of concrete. [11]
Fig. 12. Decrease of compressive strength of concrete due to temperature change. [5]
Fig. 13. Decrease of tensile strength of concrete due to temperature change. [5]
Fig. 14. Decrease of tensile strength of reinforcement due to temperature change. [5]
Fig. 15. Casestudy simplified model
Fig. 16. Model continuous monolith floor
Fig.17. Comparison temperature different analyses
Fig. 18. Model simplified thermal radiation.
Fig. 19. Model composite floor with joint.
Fig. 20. Explanation depths in the composite floor.
Fig. 21. Temperature of the concrete above the joint at depth x_j measured from the top of the joint after 120 minutes plotted over different joint depths. The joint width is 19 mm.
Fig. 22. Temperature of the concrete above the joint at depth x_j measured from the exposed surface after 120 minutes plotted over different joint widths. The joint depth is 50 mm.
Fig. 23. Temperature of concrete at 120 minutes at three different locations in the floor with joint depth 50 mm and joint width 19 mm.
Fig. 24. Model mechanical analysis.
Fig. 25. Undeformed and deformed shape based on thermal loading.
Fig. 26. Temperature at 30, 60, 90, and 120 minutes of the reinforcement in the precast plate with a concrete cover of 20 mm and the coupling reinforcement perpendicular to the joint located directly on the precast plate.
Fig. 27. Decrease moment capacity floor above the joint.

Appendix A. Research question

Each research is based on a research question. For this research, the research question is as follows:

What is the behavior under fire at the location of the joint between two precast plates of a composite floor and is this a risk for the safety of the structure?

For answering this research question, sub-questions are set. Those sub-questions are answered by a literature study and a case study with analytical analyses and numerical analyses. For the numerical analyses, models for both thermodynamic and thermomechanical calculations are created. After answering the sub-questions, the answers to the sub-questions are used to answer the research question. The answers to the sub-questions are not given directly under the question but are implemented in the paper.

- *How can the physical behavior of a reinforced concrete structure in case it is exposed to fire be determined?*
- *What is the difference in temperature development at the location of the joint in comparison to a continuous composite slab?*
- *What is the risk of the fire for the structural behavior of the composite slab?*

Appendix B. Specific heat of concrete

The specific heat is the energy required to raise the temperature with 1°C of 1kg concrete. Appendix A of NEN-EN 1992-1-2 gives formulas to calculate the specific heat for concrete. [1] Concrete with a moisture content of 1.5% gives a peak value in the specific heat. The standard formulas are based on the moisture content of 0%, formulas 4, 5, 6, and 7.

$c_p(\theta) = 900$	*for 20 °C ≤ θ ≤ 100 °C*	(B1)
$c_p(\theta) = 900 + (\theta - 100)$	*for 100 °C ≤ θ ≤ 200 °C*	(B2)
$c_p(\theta) = 1000 + (\theta - 200)/2$	*for 200 °C ≤ θ ≤ 400 °C*	(B3)
$c_p(\theta) = 1100$	*for 400 °C ≤ θ ≤ 1200 °C*	(B4)

C_p Specific heat of concrete [J/(kgK)]
θ Temperature of the concrete [°C]

In the equations, the first value is 900 J/kgK, the peak value for moisture content of 0%. The peak values for 1.5% and 3.0% are given in figure 1. These peak values can be used for designing the formulas for calculating the specific heat increase at divergent moisture contents.

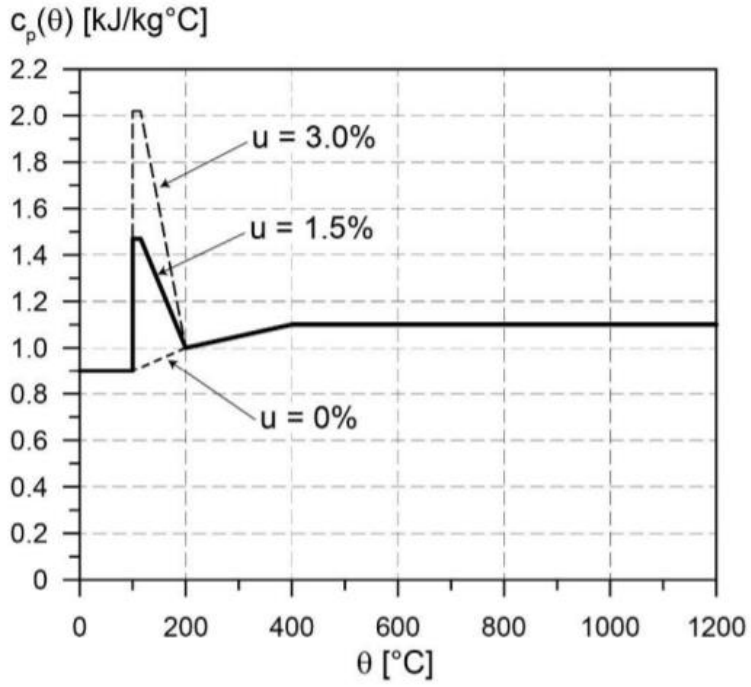

Fig. B4. Peak values for Cp for 0%, 1.5% and 3% moisture content.

Since the EN1992-1-2 is for the heat transfer assuming concrete with a moisture content of 1.5%, this value will be elaborated. At this moisture content, the peak value is 1470 J/kgK from 100 °C to 115 °C. After 115 °C, the temperature has a linear decrease until it reaches the same specific heat as 0% moisture content at 200°C. During the decrease, each degree of the peak value will be different.

For calculating the peak value in the domain of 115 °C till 200 °C, a linear equation is composed. The basics of this equation are $y = ax + b$. Since there are two coordinates, the angle of inclination a can be

calculated with $\frac{y_2-y_1}{x_2-x_1}$. After filling in the value for *a* in the fundamental equation in combination with the coordinates, value *b* can be calculated.

Table B4
Coordinates linear equation

X coordinates	Y coordinates
115	1470
200	1000

$$\frac{y_2-y_1}{x_2-x_1} = \frac{1000-1470}{200-115} = -5.53$$

$$y = ax + b$$
$$1470 = -5.53 \cdot 115 + b$$
$$b = 2105.88$$

The equation for the linear decrease of peak values of moisture content 1.5% becomes:

$$y = -5.53x + 2105.88 \quad \text{(B5)}$$

With formula 8, the specific heat of concrete with a moisture content of 1.5% can be calculated by using the following equations:

$$c_p(\theta) = 900 \quad \textit{for } 20\ ^\circ C \le \theta \le 100\ ^\circ C \quad \text{(B6)}$$
$$c_p(\theta) = 1470 \quad \textit{for } 100\ ^\circ C \le \theta \le 115\ ^\circ C \quad \text{(B7)}$$
$$c_p(\theta) = -5.53\theta + 2105.88 \quad \textit{for } 115\ ^\circ C \le \theta \le 200\ ^\circ C \quad \text{(B8)}$$
$$c_p(\theta) = 1000 + (\theta - 200)/2 \quad \textit{for } 200\ ^\circ C \le \theta \le 400\ ^\circ C \quad \text{(B9)}$$
$$c_p(\theta) = 1100 \quad \textit{for } 400\ ^\circ C \le \theta \le 1200\ ^\circ C \quad \text{(B10)}$$

Appendix C. Analytic analysis EN 1992-1-2

The EN 1992-1-2 is giving a graph in which temperatures inside a concrete floor which are exposed to fire at one side are shown. [1] In this appendix more information about the background of the graph is given.

The formulas of the graph are used for an analytical analysis. The boundary conditions which are used for the graph and the analytical analyses are:

- The emissivity related to the concrete surface is 0.7;
- The thermal conductivity of concrete calculated with the given formulas in EN 1992-1-2 section 3.3.3;
- The specific heat of concrete with a moisture content of 1.5% calculated with the given formulas in EN 1992-1-2 section 3.3.2;
- The density of concrete of concrete calculated with the given formulas in EN 1992-1-2 section 3.3.2;
- The convection coefficient is 25 W/m²K.

For calculating the temperature in the layers, formulas 18 and 19 are used.

$$\theta(x, R_{fi}) = \theta_1(x, R_{fi}) + 20 \quad \text{(C1)}$$

$$\theta_1(x, R_{fi}) = 345\, log\left(\frac{7(R_{fi} - \Delta R_{fi})}{60} + 1\right) \cdot exp\left(-x\sqrt{\frac{0.9k}{R_{fi}}}\right) \quad \text{(C2)}$$

R_{fi}	Duration of the standard fire [s], Rfi ≥ 1800 s
x	Distance from the exposed surface [m]
$\Delta R_{fi} = 720\ s$	Delay between the temperature in the fire compartment and the concrete surface temperature as an approximation for the effects of convection and radiation [s]
$k = \rho \cdot \frac{c_p}{\lambda} = 3.3 \cdot 10^6$	Value of k is coming from a back-calibration to fit the temperature curves

Applying the formulas and the characteristics from the EN 1992-1-2 leads to the temperatures as shown in table C1. The graphical and analytical results are compared to each other in figures C1, C2, C3, and C4.

Table C1
Comparison temperatures °C of graphical analyses and analytical analyses Eurocode

	30 minutes		60 minutes		90 minutes		120 minutes	
Depth x in the floor measured from exposed surface	Graphical analysis [°C]	Analytical analysis [°C]	Graphical analysis [°C]	Analytical analysis [°C]	Graphical analysis [°C]	Analytical analysis [°C]	Graphical analysis [°C]	Analytical analysis [°C]
0mm	740	726	890	872	950	945	1050	1030
10mm	500	484	690	654	770	747	835	811
20mm	350	322	520	491	610	591	690	662

30mm	230	215	400	368	495	467	570	540
40mm	160	143	300	276	390	370	460	441
50mm	110	95	240	207	320	292	390	360
60mm	80	63	180	156	260	231	320	294
70mm	50	42	130	117	200	183	255	240
80mm	40	28	100	88	170	145	220	196
90mm	30	19	90	66	130	114	175	160
100mm	20	13	80	49	105	91	150	130

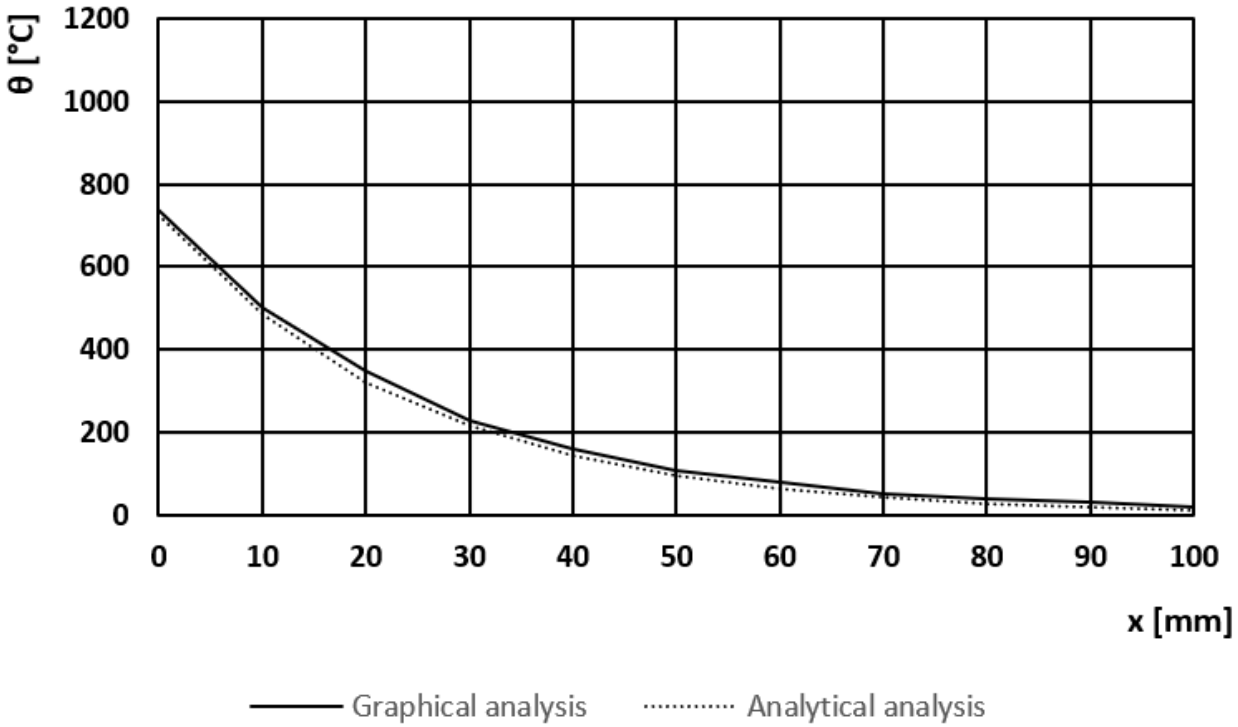

Fig. C1. Comparison temperatures in floor with EN 1992-1-2 graphical and analytical approach, 30 minutes

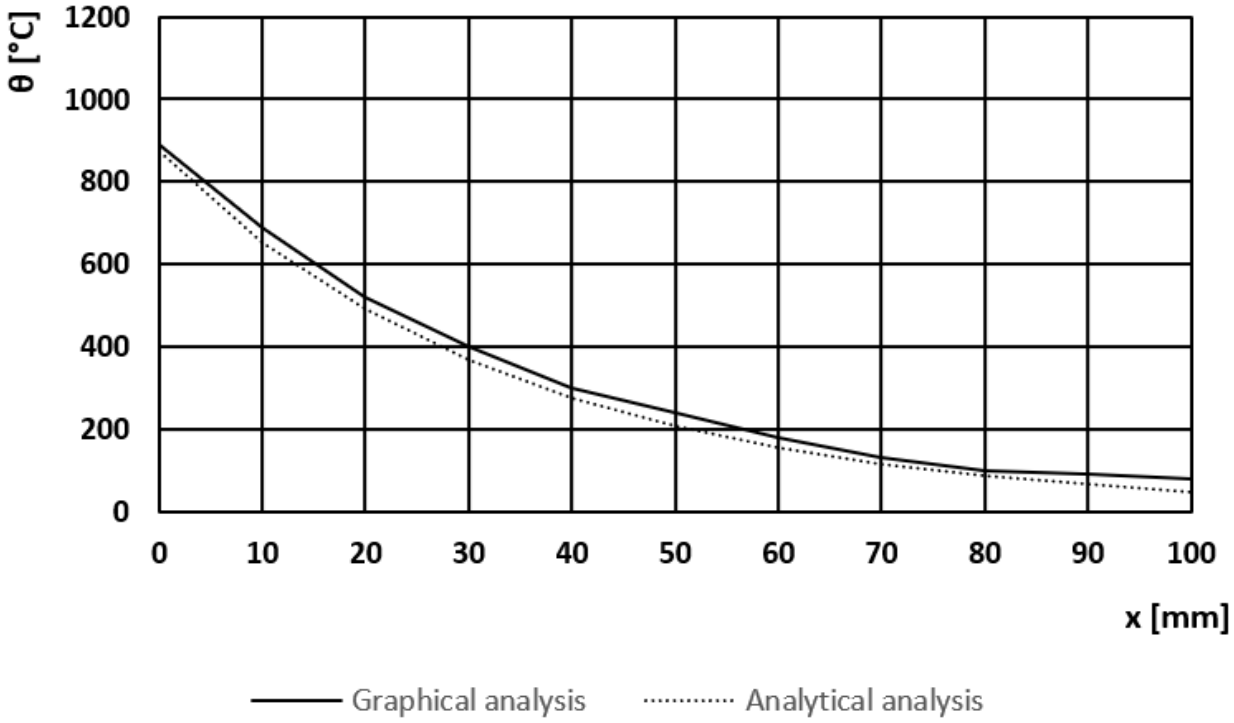

Fig. C2. Comparison temperatures in floor with EN 1992-1-2 graphical and analytical approach, 60 minutes

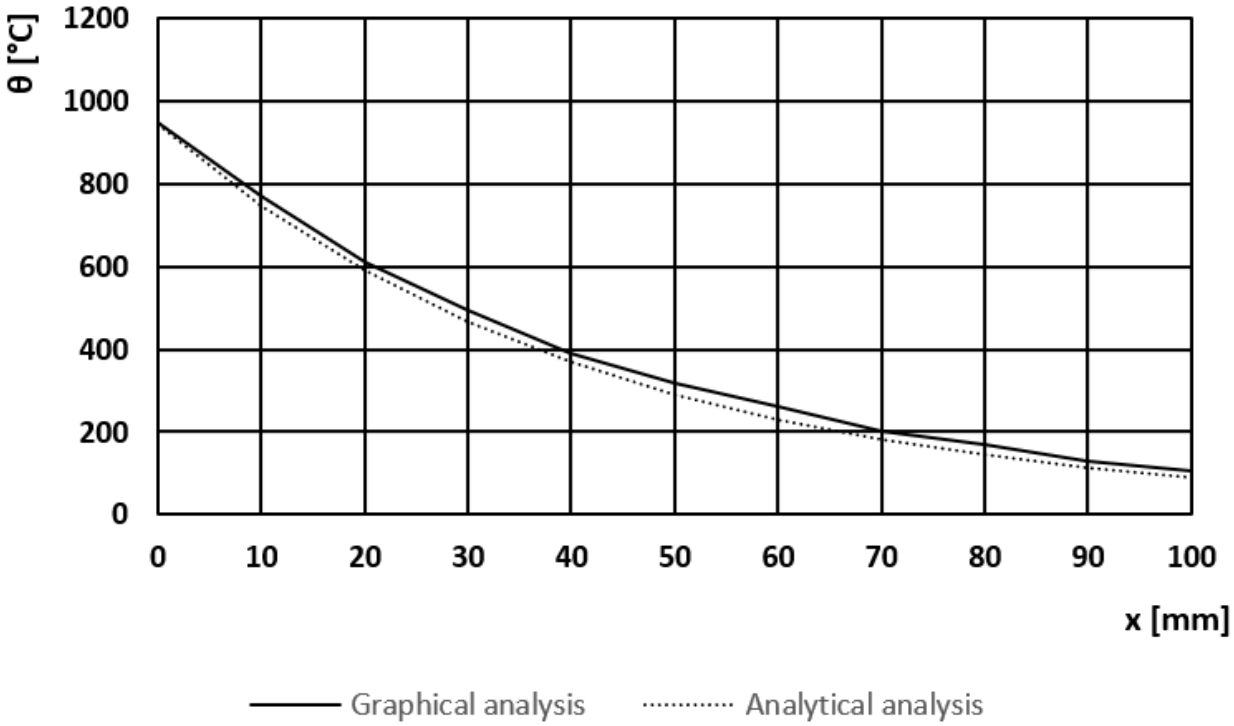

Fig. C3. Comparison temperatures in floor with EN 1992-1-2 graphical and analytical approach, 90 minutes

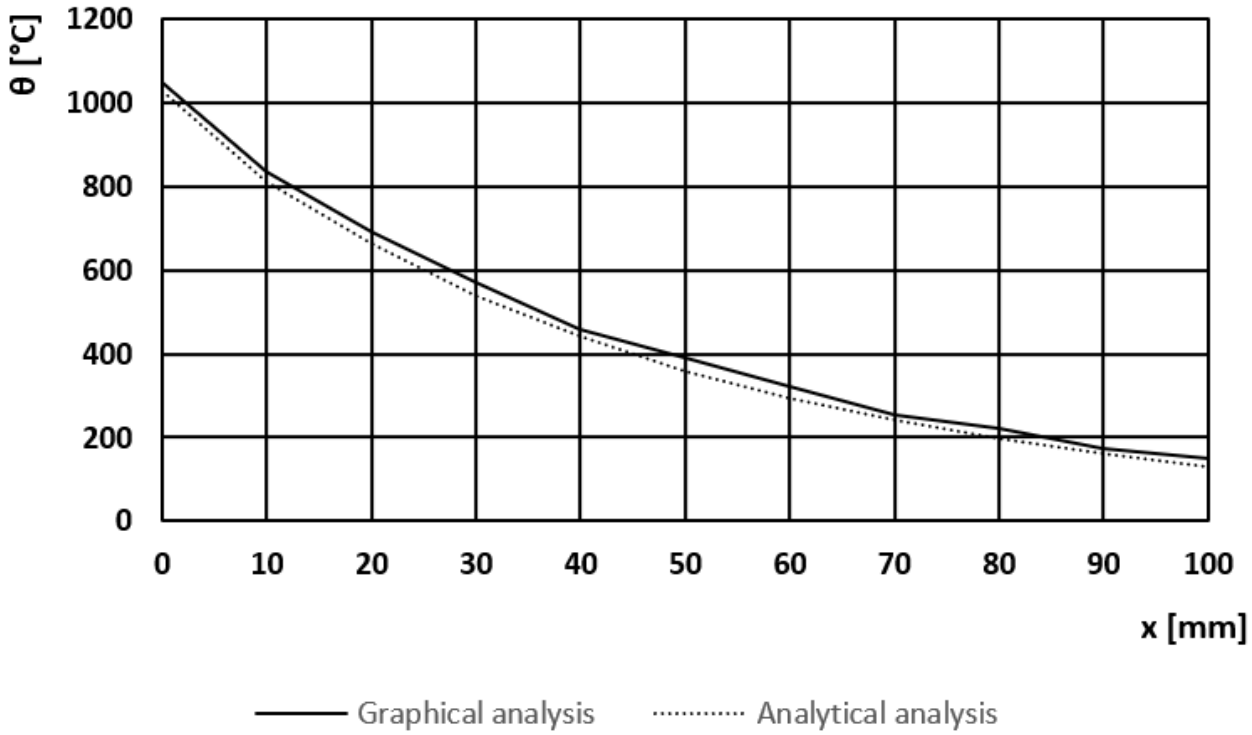

Fig. C4. Comparison temperatures in floor with EN 1992-1-2 graphical and analytical approach, 120 minutes

In figure C1, C2, C3, and C4, the values of the graphical and the analytical analyses based on the EN 1992-1-2 are compared. The outcomes are close to each other and the differences could therefore be neglected. One aspect should be mentioned. In the formulas of the EN 1992-1-2, the characteristics of concrete at specific temperatures are not implemented in the calculation. The values which are used to get the value of k correspond to 659.6 °C. To make a more precise calculation of the temperature in the concrete floor, the formula is filled in again. This time the temperature-depended values are implemented. The results of this analyses are shown in table C2. The figures C5, C6, and C7 show the comparison between the graphical analysis, the

Table C2
Comparison temperatures in floor with Eurocode graph and analytical approach

	30 minutes			60 minutes		
Depth x in the floor measured from exposed surface	Graphical analysis [°C]	Analytical analysis, Temperature-independent k [°C]	Analytical analysis, Temperature-dependent k [°C]	Graphical analysis [°C]	Analytical analysis, Temperature-independent k [°C]	Analytical analysis, Temperature-dependent k [°C]
0mm	740	726	-	890	872	872
10mm	500	484	-	690	654	668
20mm	350	322	-	520	491	534
30mm	230	215	-	400	368	441
40mm	160	143	-	300	276	367
50mm	110	95	-	240	207	371
60mm	80	63	-	180	156	320
70mm	50	42	-	130	117	275
80mm	40	28	-	100	88	235
90mm	30	19	-	90	66	-
100mm	20	13	-	80	49	-

	90 minutes			120 minutes		
Depth x in the floor measured from exposed surface	Graphical analysis [°C]	Analytical analysis, Temperature-independent k [°C]	Analytical analysis, Temperature-dependent k [°C]	Graphical analysis [°C]	Analytical analysis, Temperature-independent k [°C]	Analytical analysis, Temperature-dependent k [°C]
0mm	950	945	945	1050	1030	1030
10mm	770	747	747	835	811	806
20mm	610	591	605	690	662	667
30mm	495	467	497	570	540	562
40mm	390	370	415	460	441	477
50mm	320	292	337	390	360	415
60mm	260	231	287	320	294	361
70mm	200	183	244	255	240	315
80mm	170	145	209	220	196	276
90mm	130	114	-	175	160	-
100mm	105	91	-	150	130	-

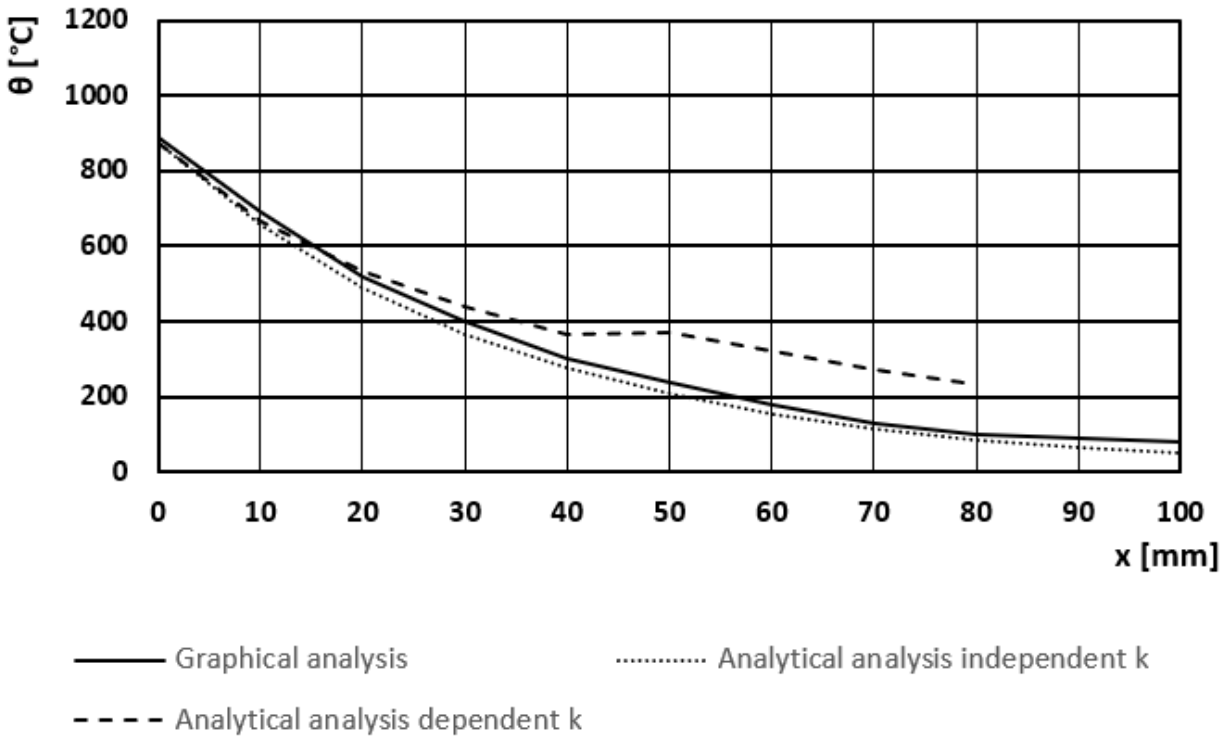

Fig. C5. Comparison temperatures in floor with EN 1992-1-2 graphical, and analytical approach for different settings of k, 60 minutes

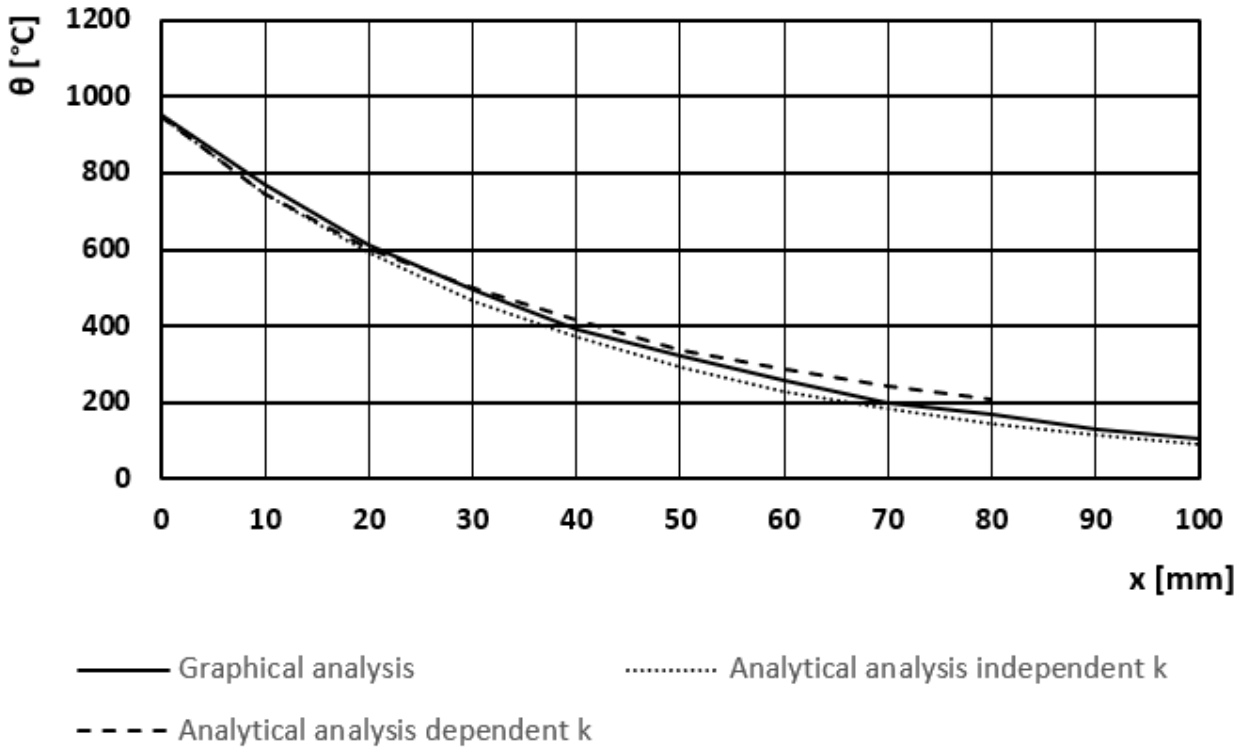

Fig. C6. Comparison temperatures in floor with EN 1992-1-2 graphical, and analytical approach for different settings of k, 90 minutes

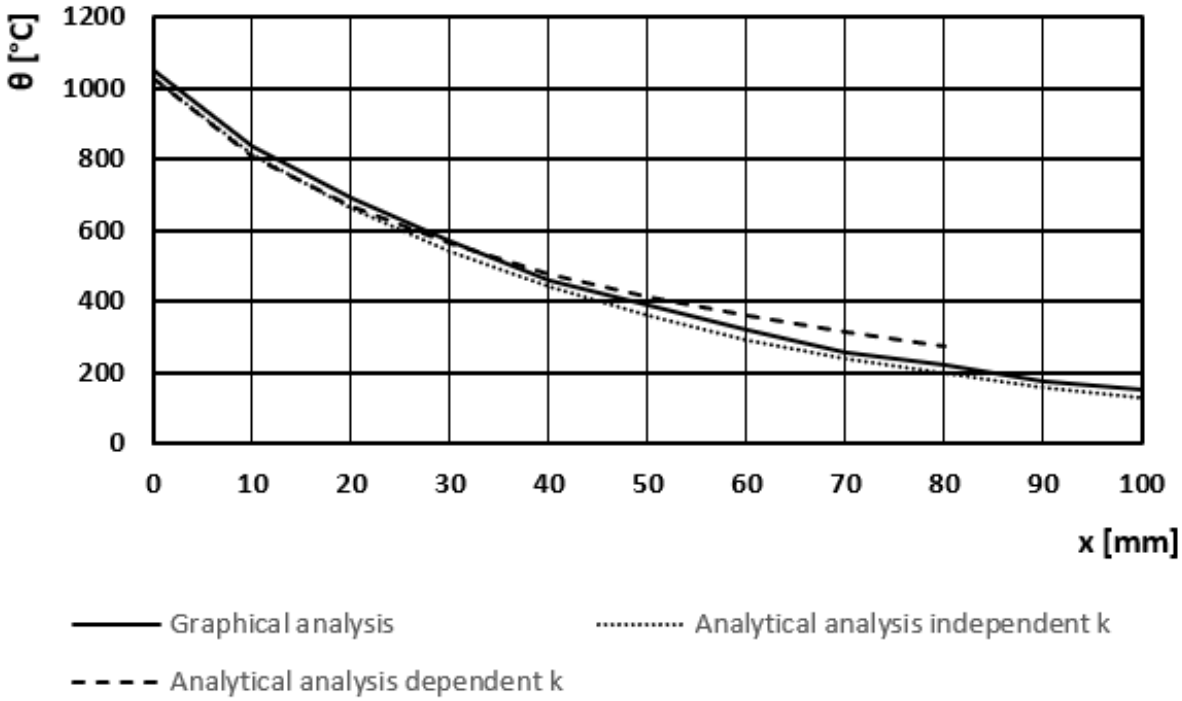

Fig. C7. Comparison temperatures in floor with EN 1992-1-2 graphical, and analytical approach for different settings of k, 120 minutes

The results of the analyses about using an independent or dependent value of k have shown some remarkable aspects. At first, there are no values for the calculation of 30 minutes. The EN 1992-1-2 is giving a restriction in the formula which makes it impossible to calculate the temperature before 30 minutes. Therefore, the results with an independent and dependent k will be equal. The second aspect is about the analyses of the dependent k which ends at 80 mm. The results for 90 mm and 100 mm are unreliable. The floor will have a higher temperature at 90 minutes then at 120 minutes. Since this is impossible, those results are not considered in the comparison. The last aspect that must be mentioned is the divergence in the results between using an independent k and a dependent k. Figure C5 shown a large difference at further depth. At figure C6 and C7 is shown that the results are approximately equal to the other two analyses. At the surface the results are slightly lower and at more depth the results are increased compared to the other analyses. Even while the results match at most of the depths, one thing should be questioned. For the analyses with the dependent k the constant value of k is used at the start of 30 minutes. This could led into a too high temperature at the beginning of the analyses. Due to those remarks on the formula and results, it should be questioned if it is possible to use a temperature dependent k in the formulas of the EN 1992-1-2. In further research another analytical analysis will be performed in which the temperature-dependent characteristics of concrete are assumed.

Appendix D. Analytic analyses Finite difference method

A finite difference model assumes the heat flow as a one-dimensional phenomenon. The whole surface is, during the analysis, exposed to the same heating, and therefore a uniform load is created. The principle of the calculation method can be explained as follows. The analyses element is divided into three parts, the exposed surface, the internal part, and the unexposed surface, figure D1. The internal layer is divided into multiple layers across the thickness. For each of those layers, the temperature can be calculated. The finite difference method uses the temperatures from the current time step to calculate the temperature in the following time step.

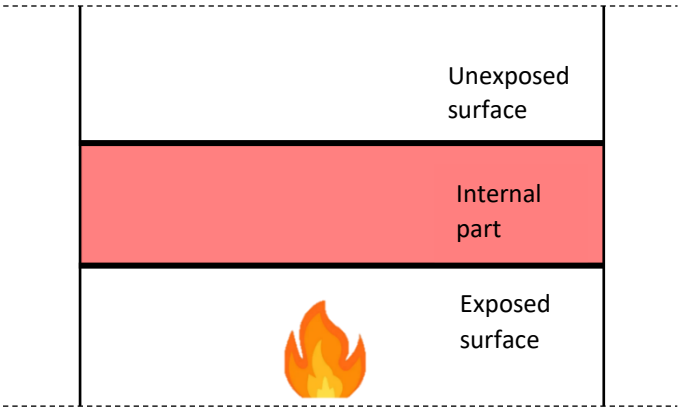

Fig. D1. Dividing area around the analyzing element

i. Exposed surface

The assumed fire will be in the compartment below the concrete floor. Therefore, the surface of the floor in this compartment is the exposed surface. According to the paper Influence of sustained stress and heating conditions on the occurrence of fire-induced concrete spalling [2], the temperature of the exposed surface over time can be calculated with equation D1.

$$T_1^{i+1} = T_1^i + \frac{2 \cdot \Delta t}{(\rho c_p)_1^i \cdot \Delta x} \cdot \left[q_{net}''^i - \left(\frac{\lambda_1^i + \lambda_2^i}{2}\right) \cdot \left(\frac{T_1^i - T_2^i}{\Delta x}\right)\right] \quad \text{(D1)}$$

T_1^{i+1}	Temperature of concrete at the node of the exposed surface in the subsequent time step [K]
T_1	Temperature of concrete at the node of the exposed surface in the present time step [K]
Δt	Time step [s]
ρ	Density of concrete at present temperature [kg/m³]
c_p	Specific heat of concrete at present temperature [J/kg K]
Δx	Size of a layer [m]
$q_{net}''^i$	Net heat flux to the concrete specimen [W/m²]
$\lambda_{1,2}^i$	Thermal conductivity of concrete at nodes 1 and 2 at present temperature [W/m K]

Using equation D1, the temperature in the next step is calculated by using the information of the previous time step.

Some components of equation D1 are unknown. Most of the components can be calculated by using the EN 1992-1-2. [1] The net heat flux is not mentioned in the EN 1992-1-2 and is calculated with formula D2. [3] Equation D3 has also some unknowns, namely the temperature of the gas and the surface temperature.

Net heat flux

The net heat flux is the heat transfer between two elements or from a gas to an element. Both radiation and convection are included in this calculation and can be calculated with the equation D2.

$$q''_{net} = \varepsilon\sigma\left(T_g^4 - T_s^4\right) + h_c(T_g - T_s) \quad \text{(D224)}$$

q''_{net}	Net heat flux to the concrete specimen [W/m²]
ε	Emissivity of hot gasses
σ	Stefan-Boltzmann constant $5{,}67 \cdot 10^{-8}$ [W/m²K⁴]
T_g	Temperature of the hot gasses [K]
T_s	Surface temperature of a concrete specimen [K]
h_c	Convective heat transfer coefficient [W/m²K]

In EN 1992-1-2 appendix A, the values for the emissivity and convective heat transfer are given. Therefore, the emissivity ε must be taken as 0.7 and the convective heat transfer coefficient h_c must be taken as 25 W/m²K.

Gas temperature

The gas temperature is the temperature of the air in the compartment. Without a fire, the gas temperature is set at 20 °C. The gas temperature of the air in the compartment during a fire based on a standard fire can be calculated with the equation D3. [3]

$$\Theta_g = 20 + 345 \cdot log_{10}(8t + 1) \quad \text{(D3)}$$

Θ_g	Gas temperature [°C]
t	Time [min]

Surface temperature

The last unknown variable is the surface temperature. The surface temperature is related to the net heat flux. The increase of the surface temperature is as follows. At t=0, the gas temperature and the surface temperature are 20 °C. Then at t=1, the gas temperature will rise, but the surface is still 20 °C. In t=2, the gas temperature rises further, and the gas temperature from t=1 affects the surface temperature. With the net heat flux, the following surface temperature can be calculated. This process will repeat till the temperature at the desired time step is found.

ii. Internal part

During the calculation for the internal part, the floor must be divided into layers. In this calculation, the layers have a thickness of 10 mm, figure D2. This dimension is chosen since the graph of EN 1992-1-2 uses layers of 10 mm. Using equal dimensions creates a clear comparison. The calculation of the inner nodes the uses formula D4. [4]

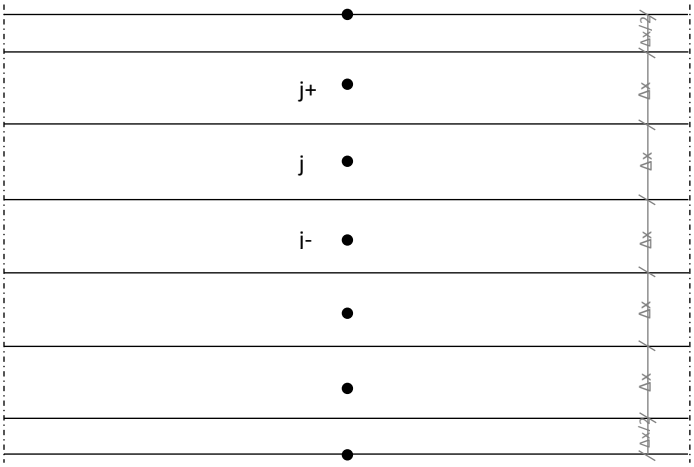

Fig. D2. Dividing internal part in layers

$$T_j^{i+1} = T_j^i + \frac{\Delta t}{(\rho c_p)_1^i \cdot \Delta x^2} \cdot \left[\left(\frac{\lambda_{j-1}^i + \lambda_j^i}{2} \right) \cdot (T_{j-1}^i - T_j^i) - \left(\frac{\lambda_j^i + \lambda_{j+1}^i}{2} \right) \cdot (T_j^i - T_{j+1}^i) \right] \quad \text{(D425)}$$

T_j^{i+1} Temperature of concrete at the node j in the subsequent time step [K]

$T_{j-1,j,j+1}^i$ Temperature of concrete at the nodes j-1, j and j+1 in the present time step [K]

$\lambda_{j-1,j,j+1}^i$ Thermal conductivity of concrete at nodes j-1, j and j+1 at present temperature [W/mK]

iii. Unexposed surface

The final part of the floor is the unexposed surface, the surface of the floor that is not in the fire compartment. The assumption is that the temperature increase is not reaching the top of the floor. Therefore, a standard room temperature of 20°C will be taken into account.

iv. Excel file

With formulas D1 and D4, the temperature inside the floor is calculated for every second of 7200 seconds. For this calculation, an Excel file is used. This file exists out of:

- Surface temperature
- Density
- Specific heat
- Net heat flux
- Thermal conductivity
- Internal temperature

Surface temperature

In figure D3, the calculation of the surface temperature is shown by using formula D1. The temperature is calculated in Kelvin and afterward transferred to Celsius degree. Since the temperature changes every

SOM =C7199+((2*$N$2)/((E7199*F7199)*$N$3))*('4. Net heat flux'!H7201-(((G7199+$J$3)/2)*((C7199-$K$2)/$N$3)))

	A	B	C	D	E	F	G	H	I	J	K	L	M	N	O
1	**Surface temperature**														
2									*t = 0*	20	293.15		*dt*	1	sec
3									*k*	1.95141			*dx*	0.05	m
4									*p*	2300					
5									*Cp*	900					
6															
7	**Secondes**	**Minutes**	**T_s (K)**	**T_s (°C)**	**ρ**	**c_p**	**k**								
8	1	0.016667	293.1606541	20	2300	900	1.9511672								
9	2	0.033333	293.1810251	20	2300	900	1.9511672								
7192	7185	119.75	1251.641948	979	2068.5567	1100	0.574969								
7193	7186	119.7667	1251.665214	979	2068.5567	1100	0.574969								
7194	7187	119.7833	1251.688477	979	2068.5567	1100	0.574969								
7195	7188	119.8	1251.711734	979	2068.5366	1100	0.5749446								
7196	7189	119.8167	1251.734992	979	2068.5366	1100	0.5749446								
7197	7190	119.8333	1251.758245	979	2068.5366	1100	0.5749446								
7198	7191	119.85	1251.781494	979	2068.5366	1100	0.5749446								
7199	7192	119.8667	1251.804738	979	2068.5165	1100	0.5749202								
7200	7193	119.8833	$K$2)/$N$3)))	979	2068.5165	1100	0.5749202								
7201	7194	119.9	1251.851222	979	2068.5165	1100	0.5749202								
7202	7195	119.9167	1251.874457	979	2068.5165	1100	0.5749202								
7203	7196	119.9333	1251.897688	979	2068.5165	1100	0.5749202								
7204	7197	119.95	1251.920914	979	2068.4964	1100	0.5748958								
7205	7198	119.9667	1251.94414	979	2068.4964	1100	0.5748958								
7206	7199	119.9833	1251.967362	979	2068.4964	1100	0.5748958								
7207	7200	120	1251.990579	979	2068.4964	1100	0.5748958								
7208															

Fig. D3. Example of calculation surface temperature with Finite difference method

second, the density, specific heat, and thermal conductivity are also changing. To ensure a realistic temperature at the surface, the characteristics are calculated for each second.

Density, specific heat and thermal conductivity

Density, specific heat, and thermal conductivity are temperature-dependent characteristics considered in the heat transfer calculation. The NEN-EN1992-1-2 formulas gives calculating for those characteristics in different time ranges. [1] Since this range is going till 1200 °C, the calculation is also executed till 1200 °C.

Net heat flux

The temperature development in the floor depends on the net heat flux, calculated by equation D2. The calculation uses the gas temperature at the current time step combined with the surface temperature from the previous time step. The net heat flux depends on convective heat and radiation. Figure D4 shows which time steps are used.

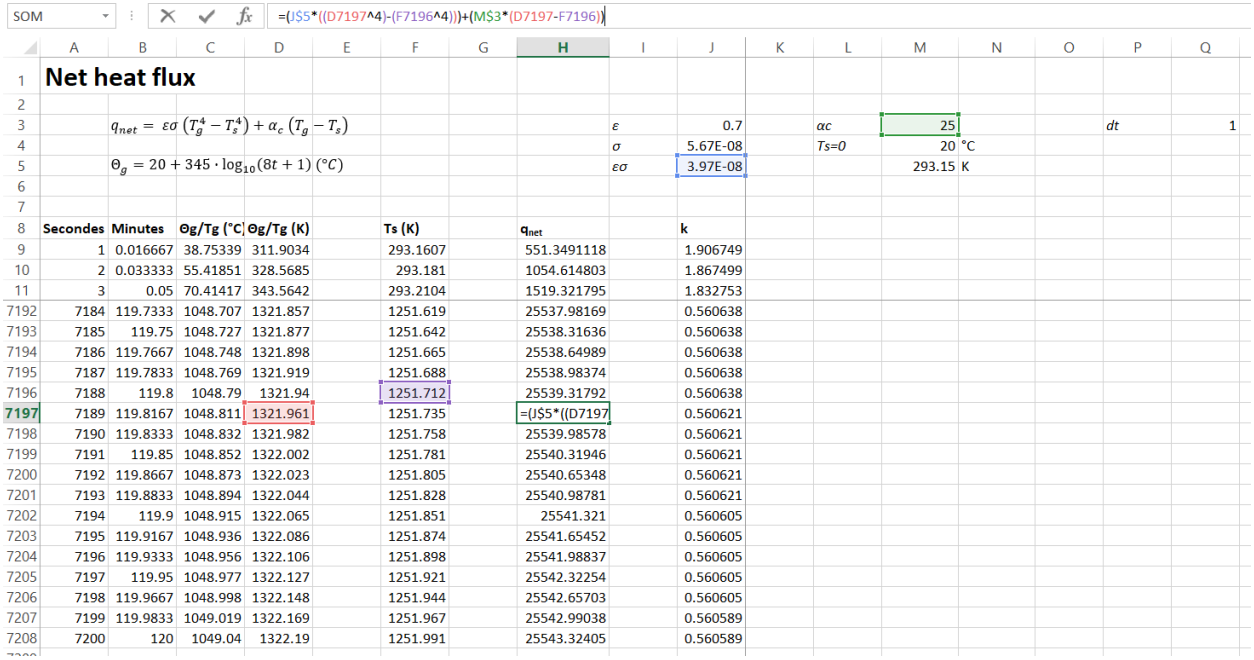

SOM | =(J$5*((D7197^4)-(F7196^4)))+(M$3*(D7197-F7196))

Net heat flux

$q_{net} = \varepsilon\sigma\left(T_g^4 - T_s^4\right) + \alpha_c\left(T_g - T_s\right)$

$\Theta_g = 20 + 345 \cdot \log_{10}(8t + 1)\ (°C)$

	A	B	C	D	E	F	G	H	I	J	K	L	M	N	O	P	Q
3									ε	0.7		αc	25			dt	1
4									σ	5.67E-08		Ts=0	20 °C				
5									εσ	3.97E-08			293.15 K				
8	Secondes	Minutes	Θg/Tg (°C)	Θg/Tg (K)		Ts (K)		q_{net}		k							
9	1	0.016667	38.75339	311.9034		293.1607		551.3491118		1.906749							
10	2	0.033333	55.41851	328.5685		293.181		1054.614803		1.867499							
11	3	0.05	70.41417	343.5642		293.2104		1519.321795		1.832753							
7192	7184	119.7333	1048.707	1321.857		1251.619		25537.98169		0.560638							
7193	7185	119.75	1048.727	1321.877		1251.642		25538.31636		0.560638							
7194	7186	119.7667	1048.748	1321.898		1251.665		25538.64989		0.560638							
7195	7187	119.7833	1048.769	1321.919		1251.688		25538.98374		0.560638							
7196	7188	119.8	1048.79	1321.94		1251.712		25539.31792		0.560638							
7197	7189	119.8167	1048.811	1321.961		1251.735		=(J$5*((D7197		0.560621							
7198	7190	119.8333	1048.832	1321.982		1251.758		25539.98578		0.560621							
7199	7191	119.85	1048.852	1322.002		1251.781		25540.31946		0.560621							
7200	7192	119.8667	1048.873	1322.023		1251.805		25540.65348		0.560621							
7201	7193	119.8833	1048.894	1322.044		1251.828		25540.98781		0.560621							
7202	7194	119.9	1048.915	1322.065		1251.851		25541.321		0.560605							
7203	7195	119.9167	1048.936	1322.086		1251.874		25541.65452		0.560605							
7204	7196	119.9333	1048.956	1322.106		1251.898		25541.98837		0.560605							
7205	7197	119.95	1048.977	1322.127		1251.921		25542.32254		0.560605							
7206	7198	119.9667	1048.998	1322.148		1251.944		25542.65703		0.560605							
7207	7199	119.9833	1049.019	1322.169		1251.967		25542.99038		0.560589							
7208	7200	120	1049.04	1322.19		1251.991		25543.32405		0.560589							

Fig. D4. Example of calculation net heat flux

Internal temperature

With those different values, the temperature of the internal layers can be calculated with equation D4. In figure D5, an overview is given on which characteristic is using which time step.

v. Results

In table D1, the comparison between the analytical calculation of the Eurocode and the analytical calculation of the Finite Difference method is shown. The comparison is executed for 30, 60, 90, and 120 minutes. The results of the analytical analyses are compared to the values from the graphical analysis.

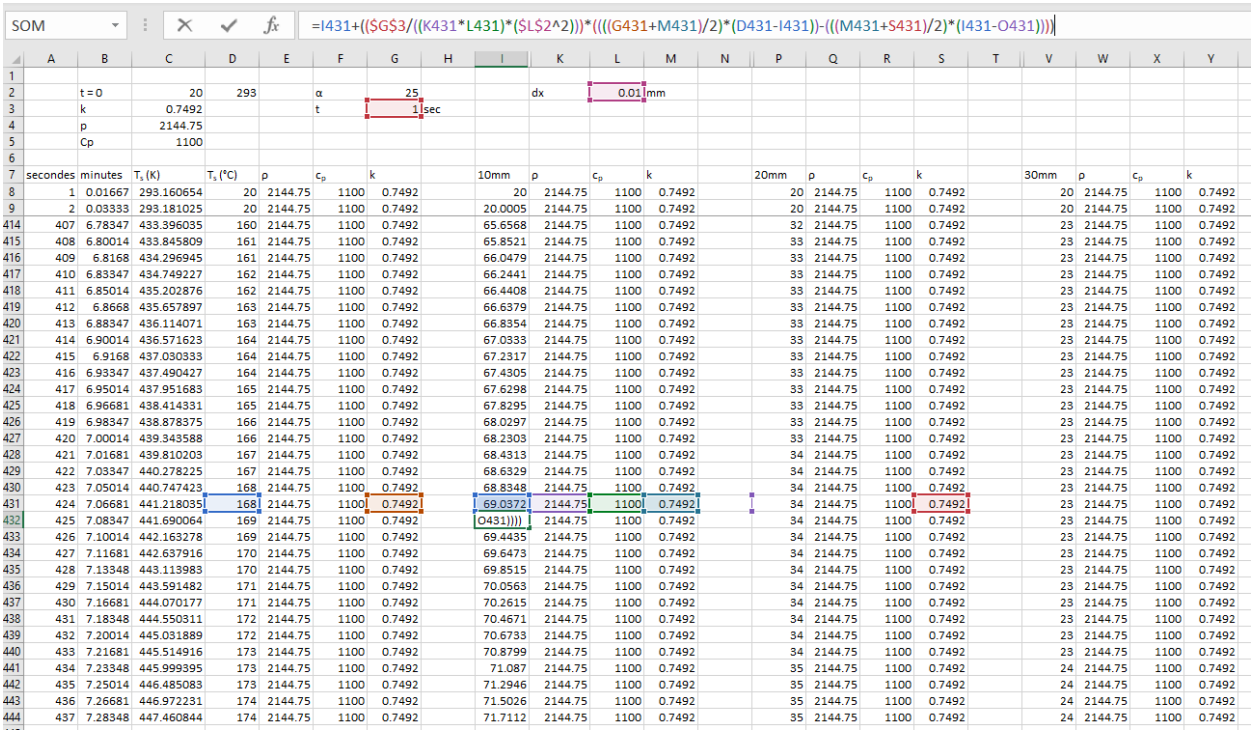

Fig. D5. Example of calculation of the temperature of an internal with Finite difference method

Table D1

Comparison analytical calculation of Eurocode and Finite difference method at fixed times

	30 minutes			60 minutes		
Depth x in the floor measured from exposed surface	Graphical analysis [°C]	Analytical analysis, Eurocode [°C]	Analytical analysis, Finite Difference Method [°C]	Graphical analysis [°C]	Analytical analysis, Eurocode [°C]	Analytical analysis, Finite Difference Method [°C]
0mm	740	726	708	890	872	859
10mm	500	484	456	690	654	648
20mm	350	322	295	520	491	488
30mm	230	215	189	400	368	366
40mm	160	143	130	300	276	274
50mm	110	95	98	240	207	204
60mm	80	63	75	180	156	154
70mm	50	42	58	130	117	123
80mm	40	28	46	100	88	101
90mm	30	19	37	90	66	84
100mm	20	13	31	80	49	70

	90 minutes			120 minutes		
Depth x in the floor measured from exposed surface	Graphical analysis [°C]	Analytical analysis, Eurocode [°C]	Analytical analysis, Finite Difference Method [°C]	Graphical analysis [°C]	Analytical analysis, Eurocode [°C]	Analytical analysis, Finite Difference Method [°C]
0mm	950	945	930	1050	1030	979
10mm	770	747	743	835	811	807
20mm	610	591	591	690	662	662
30mm	495	467	470	570	540	543
40mm	390	370	373	460	441	446
50mm	320	292	296	390	360	365
60mm	260	231	234	320	294	299

70mm	200	183	183	255	240	244
80mm	170	145	147	220	196	198
90mm	130	114	123	175	160	160
100mm	105	91	104	150	130	134

Based on the results from table D1, calculating with the finite difference method gives results that come close to the values from the EN 1992-1-2. Since the finite difference method considers more parameters, the assumption is that the results are also more realistic. Therefore, this method is more suitable for calculating more complicated structures than the formula of then 1992-1-2. Therefore, the other analyses will use the finite difference method.

As explained in Appendix C, EN 1992-1-2 uses temperature-independent values for density, specific heat, and thermal conductivity. To gain knowledge about the difference in calculating the finite difference method with and without temperature dependency, the analysis is performed with a temperature-independent value for density, specific heat, and thermal conductivity. The results are shown in table D2.

Table D5
Comparison Finite difference method with temperature-dependent and temperature-independent characteristics at fixed times

	30 minutes			60 minutes		
Depth x in the floor measured from exposed surface	Graphical analysis [°C]	Analytical analysis, temperature-dependent [°C]	Analytical analysis, Temperature-independent [°C]	Graphical analysis [°C]	Analytical analysis, temperature-dependent [°C]	Analytical analysis, Temperature-independent [°C]
0mm	740	708	708	890	859	859
10mm	500	456	465	690	648	676
20mm	350	295	287	520	488	515
30mm	230	189	169	400	366	380
40mm	160	130	98	300	274	272
50mm	110	98	58	240	204	190
60mm	80	75	38	180	154	89
70mm	50	58	28	130	123	62
80mm	40	46	23	100	101	44
90mm	30	37	21	90	84	34
100mm	20	31	20	80	70	27

	90 minutes			120 minutes		
Depth x in the floor measured from exposed surface	Graphical analysis [°C]	Analytical analysis, temperature-dependent [°C]	Analytical analysis, Temperature-independent [°C]	Graphical analysis [°C]	Analytical analysis, temperature-dependent [°C]	Analytical analysis, Temperature-independent [°C]
0mm	950	930	930	1050	979	979
10mm	770	743	774	835	807	839
20mm	610	591	631	690	662	708
30mm	495	470	504	570	543	589
40mm	390	373	394	460	446	483
50mm	320	296	303	390	365	390
60mm	260	234	228	320	299	310
70mm	200	183	170	255	244	244
80mm	170	147	125	220	198	190
90mm	130	123	92	175	160	146
100mm	105	104	68	150	134	112

The results of table D2 show that by using temperature-independent characteristics, the temperature at the surface of the floor increases more in comparison to using temperature-dependent characteristics. At the inside of the floor, the temperature decreases faster and is also decreased compared to the analysis with temperature dependency. The method with the smallest differences to the graphical analysis will be used, which is the finite difference method with temperature-dependent characteristics.

Appendix E. Numerical analyses simplified model

For the final part of validating the numerical model, a numerical model of the simplified method is created. This numerical model is made in the finite element program ABAQUS by using a heat transfer model. The concrete is modeled with both temperature-dependent and temperature-independent characteristics to gain knowledge about the influence. For the independent-temperature characteristics, the values of the EN 1992-1-2 are taken into account. [1]

i. Numerical model

The EN 1992-1-2 gives a graph with temperatures at different depths in a monolith floor of 200 mm exposed at one surface. The numerical model can be verified by creating a numerical model for this continuous floor, which can be compared to both the graphical and analytical analyses. If the results match, the numerical model can be used for more complicated structures.

For this verifying model, a 2D uncouples thermal-mechanical analysis is performed. The structure in the numerical model consists of one continuous concrete part with a thickness of 200 mm. The absolute zero temperature of the model is -273.15, which is used to let the model calculate in Celsius degree, and the Stefan-Boltzmann constant is set at $5.67 \cdot 10^{-8}$. All the parts are modeled as concrete with temperature-dependent density, specific heat, and conductivity characteristics. Those characteristics are based on the equations from EN 1992-1-2 and are calculated in Celsius degrees. To implement this material to the parts, the parts have given solid elements. The final step for modeling the concrete parts is by defining a mesh. The mesh has a grid of 10x10 mm. By choosing those measures, the comparison between the numerical model and the other analyses is clear. The mesh is modeled for heat transfer and has a quadratic geometric order. Therefore the element type becomes DC2D8 which is only used for heat transfer models.

After finishing the concrete parts, the other elements of the model are modeled. A heat transfer step is created. The step is transient and has fixed periods of 30, 60, 90, and 120 minutes. The step has a maximum allowable temperature change per increment of 10°C and the maximum allowable emissivity change per increment of 0.1. As a thermal load, the standard fire curve is implemented in the numerical model. This thermal load is the boundary condition for the heat and is placed at the exposed surface of the floor. This boundary condition is made using an amplitude with tabular values and is calculated from the equation for the standard fire curve according to EN 1992-1-2. [1]

Furthermore, some instances are used for the thermal characteristics radiation and convection of concrete. Above the floor is the unexposed surface. At this location is no thermal loading. According to the EN 1992-1-2, the convection factor is 9 W/m²K, and the emissivity is 0.7. The assumption is that the compartment above the floor is 20°C, this temperature is set as ambient. *Below the floor* is the exposed surface since the fire is in that compartment. According to the EN 1992-1-2, the convection factor is 25 W/m²K, and the emissivity is 0.7. The instances at the exposed surfaces are loaded with the thermal load of the standard fire curve. In the instances, the sink amplitude should be set to 1, since this value vary the sink temperature with time. This variation means that the sink amplitude will be multiplied by the sink temperature of the amplitude of the standard fire curve. After those steps, a job is created, and the model can be used.

ii. Temperature characteristics

As mentioned before, the numerical analysis is performed with temperature-dependent and temperature-independent characteristics.

Table E1
Comparison between the numerical analyses with temperature-dependent and temperature-independent values for the characteristics

	30 minutes			60 minutes		
Depth x in the floor measured from exposed surface	Graphical analysis [°C]	Numerical analysis, temperature-dependent [°C]	Numerical analysis, Temperature-independent [°C]	Graphical analysis [°C]	Numerical analysis, temperature-dependent [°C]	Numerical analysis, Temperature-independent [°C]
0mm	740	737	758	890	888	897
10mm	500	505	519	690	687	704
20mm	350	337	332	520	528	535
30mm	230	214	198	400	401	393
40mm	160	139	111	300	300	279
50mm	110	95	58	240	219	191
60mm	80	66	29	180	158	127
70mm	50	46	13	130	118	81
80mm	40	32	6	100	91	50
90mm	30	22	2	90	71	30
100mm	20	15	1	80	55	17

	90 minutes			120 minutes		
Depth x in the floor measured from exposed surface	Graphical analysis [°C]	Numerical analysis, temperature-dependent [°C]	Numerical analysis, Temperature-independent [°C]	Graphical analysis [°C]	Numerical analysis, temperature-dependent [°C]	Numerical analysis, Temperature-independent [°C]
0mm	950	965	970	1050	990	994
10mm	770	783	803	835	834	856
20mm	610	635	651	690	701	723
30mm	495	511	516	570	585	600
40mm	390	409	400	460	486	488
50mm	320	323	303	390	400	390
60mm	260	252	224	320	327	307
70mm	200	192	162	255	264	236
80mm	170	148	114	220	211	179
90mm	130	118	79	175	166	133
100mm	105	96	53	150	134	98

From the results in table E1, it can be concluded that the numerical analyses with temperature-dependent characteristics give the most accurate results according to the graphical analysis. The temperature-independent analyses give more accurate results at the bottom of the floor but have more deviation at the inside of the floor. Therefore, the following analyses will be performed with temperature-dependent characteristics.

iii. Results

After analyzing the temperature-dependent and temperature-independent values of the numerical model of the simplification in accordance to the graphical analysis, the results should be compared to the analytical analysis as well. Table E2 is giving this comparison. In the figures E1, E2, E3, and E4 the comparison is also in a graph.

Table E2
Comparison between the graphical, numerical, and numerical analyses for the simplified structure

	30 minutes			60 minutes		
Depth x in the floor	Graphical analysis [°C]	Analytical analysis [°C]	Numerical analysis [°C]	Graphical analysis [°C]	Analytical analysis [°C]	Numerical analysis [°C]
0mm	740	708	737	890	859	888
10mm	500	456	505	690	648	687
20mm	350	295	337	520	488	528
30mm	230	189	214	400	366	401
40mm	160	130	139	300	274	300
50mm	110	98	95	240	204	219
60mm	80	75	66	180	154	158
70mm	50	58	46	130	123	118
80mm	40	46	32	100	101	91
90mm	30	37	22	90	84	71
100mm	20	31	15	80	70	55

	90 minutes			120 minutes		
Depth x in the floor	Graphical analysis [°C]	Analytical analysis [°C]	Numerical analysis [°C]	Graphical analysis [°C]	Analytical analysis [°C]	Numerical analysis [°C]
0mm	950	930	965	1050	979	990
10mm	770	743	783	835	807	834
20mm	610	591	635	690	662	701
30mm	495	470	511	570	543	585
40mm	390	373	409	460	446	486
50mm	320	296	323	390	365	400
60mm	260	234	252	320	299	327
70mm	200	183	192	255	244	264
80mm	170	147	148	220	198	211
90mm	130	123	118	175	160	166
100mm	105	104	96	150	134	134

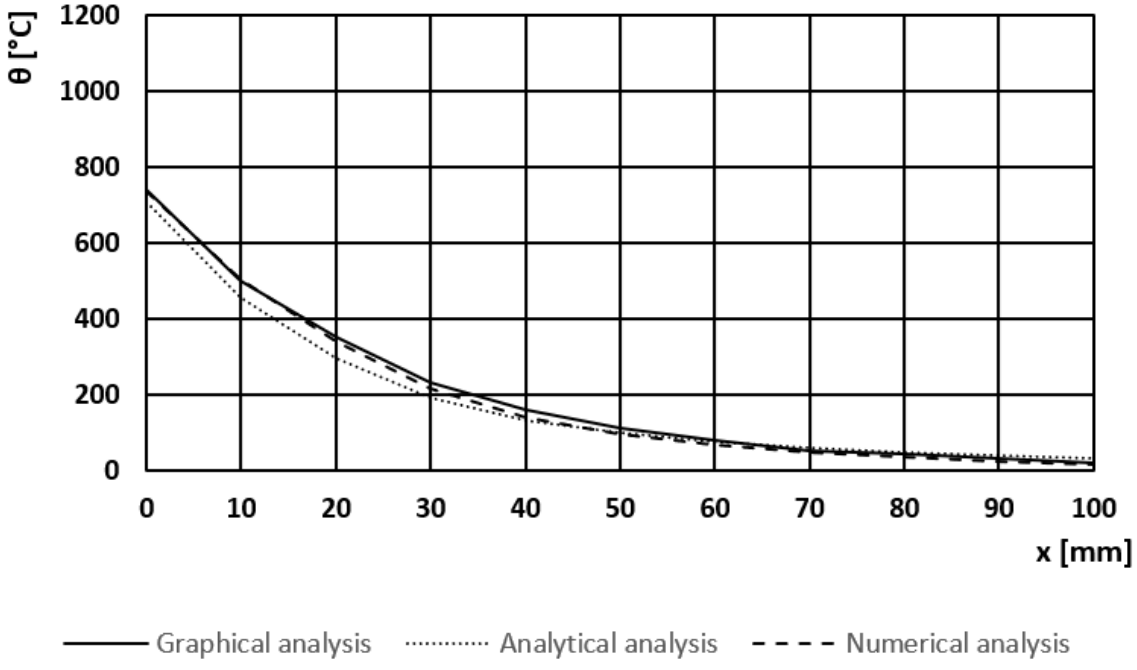

Fig. E1. Comparison between graphical, analytical, and numerical analysis for the simplified structure at 30 minutes.

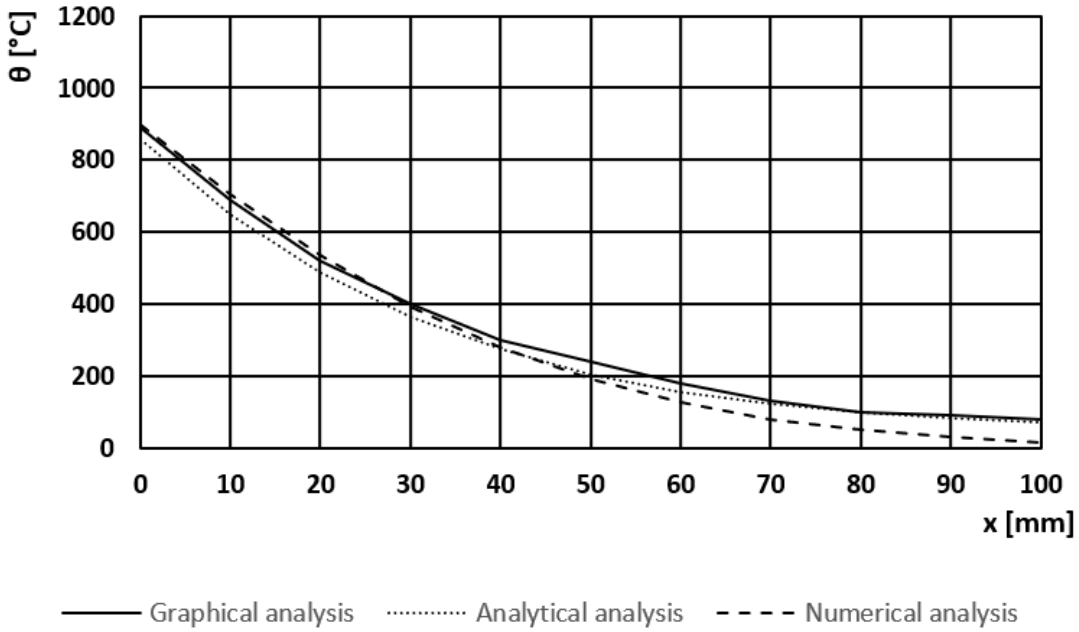

Fig. E2. Comparison between graphical, analytical, and numerical analysis for the simplified structure at 60 minutes.

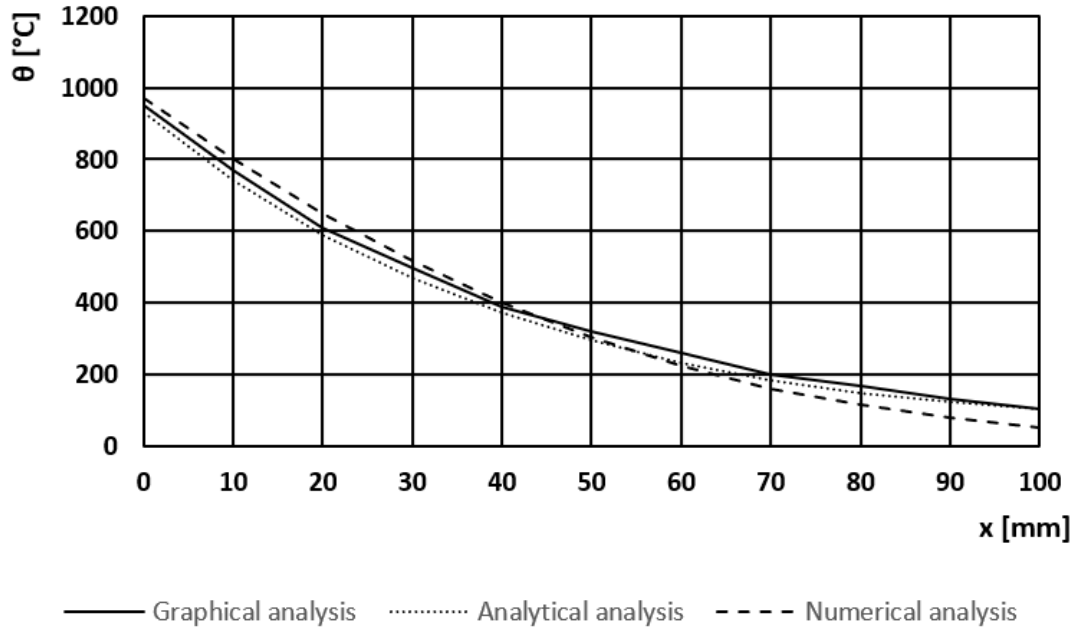

Fig. E3. Comparison between graphical, analytical, and numerical analysis for the simplified structure at 90 minutes

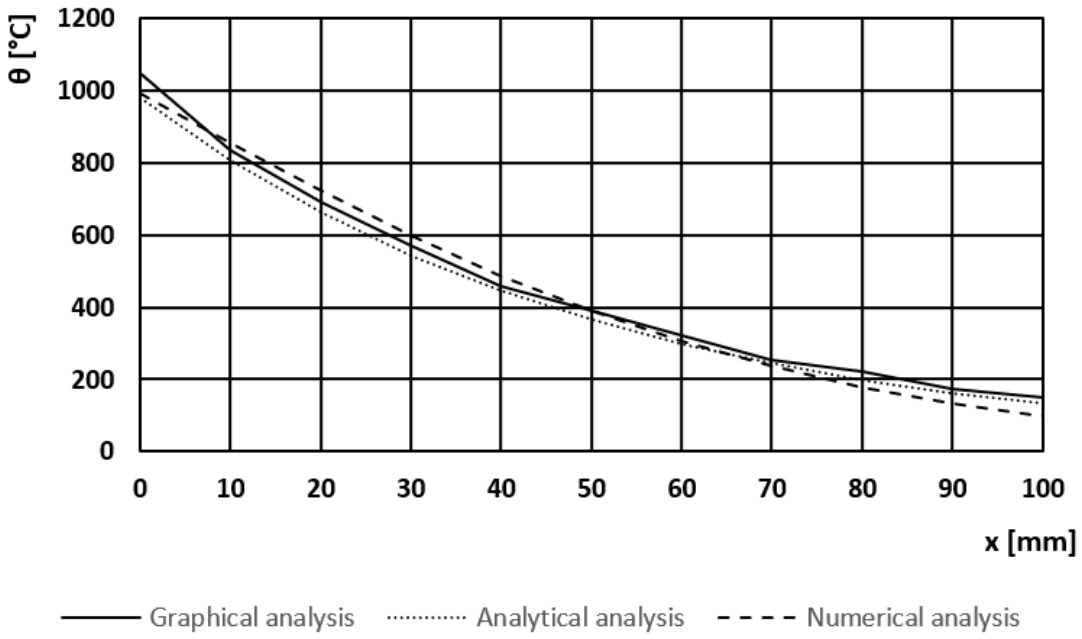

Fig.E4. Comparison between graphical, analytical, and numerical analysis for the simplified structure at 120 minutes

The results of three analyses are comparable to each other. Therefore, the assumption is that the numerical model of the simplified situation is useable for more complicated structures.

iv. Floor thickness

In the EN 1992-1-2, a floor of a thickness of 200 mm is used for the graph about heat transfer. Since a floor can be thinner or thicker, the question arises if this analysis is also applicable to floors with slightly different thicknesses. Therefore the analysis is performed with floors with thicknesses of 180 mm and 240 mm. Those results are compared to the results of a floor with a thickness of 200 mm. The results are shown in table E3.

Table E3
Comparison temperatures for different floor thicknesses after 90 minutes

Depth x in the floor measured from exposed surface	Concrete floor 180mm [°C]	Concrete floor 200mm [°C]	Concrete floor 240mm [°C]
0mm	965	965	965
10mm	783	783	783
20mm	635	635	635
30mm	512	512	512
40mm	409	409	409
50mm	324	323	323
60mm	253	252	251
70mm	194	193	192
80mm	150	149	148
90mm	120	119	118
100mm	98	97	96

The comparison results in table E3 show that the first 100 mm of each floor reaches the same temperature after 90 minutes. Therefore, the calculation method of the EN 1992-1-2 for heat transfer through the floor at a one surface exposure is also applicable for floors with a different thickness of 200mm.

Appendix F. Thermal radiation

At the composite floor with a joint, the thermal radiation is different from the thermal radiation at the exposed surface. This difference is due to the view factor. Another simplified model is created and explained in this appendix to verify the correct use of a finite difference model while using thermal radiation..

i. View factor

At the location of the joint, the concrete is not exposed directly to the fire. Nevertheless, there is heat transport at the inside of the joint. The amount of radiation at the joint depends on the view factor. The concrete obstructs the endless view to the compartment and, therefore, the endless radiation waves. The view factor is determined by calculating the angle from the specific point to the end of the joint. The joint has three locations for which the view factor should be calculated: the straight surface at the precast plates, the straight surface of the in-situ layer, and the diagonal parts at the bottom of the joint. Since the view factor will be implemented later in combination with the emission coefficient, the calculated view factors are multiplied with an emission coefficient of 0.7.

Straight surface at the precast plate

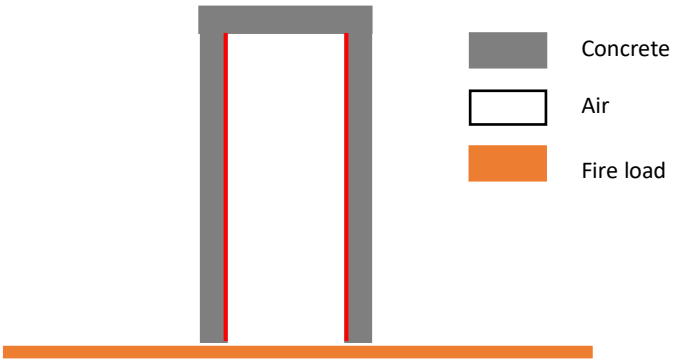

Fig. F1. Location of calculated view factor at the straight surface at the precast plate

For calculating the view factor at the straight surface at the precast plate, the red area in figure F1 is used. In the compartment underneath the joint a fire with a thermal load is present based on the standard fire load. The view factor is determined by calculating the angles of the sightline between the researched point and the obstruction. In figure F2, this calculation is drawn. The results of the view factor, including the emission coefficient, are shown in table F1.

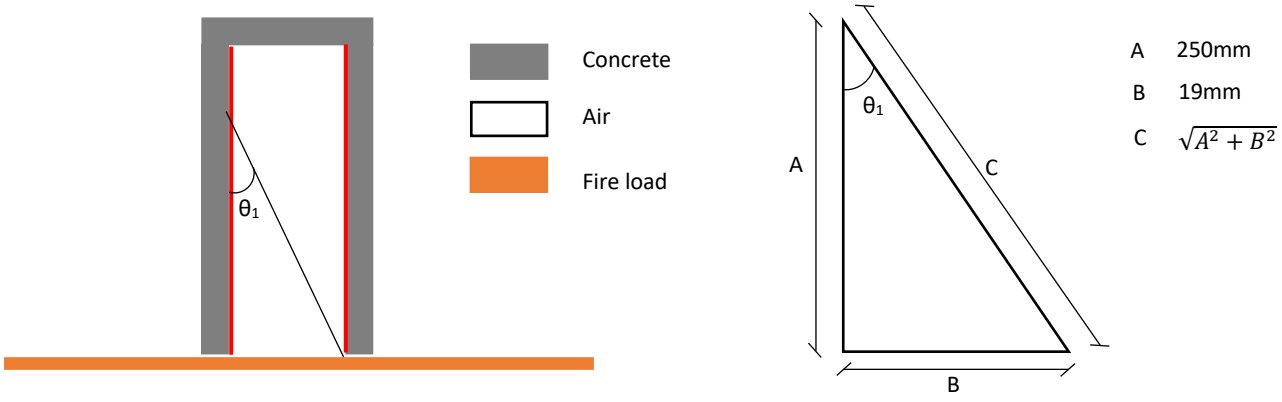

Fig. F2. Calculation method of the view factor at the straight surface at the precast plate

Table F1
View factor combined with the emission coefficient 0.7 for straight parts of the joint

Depth in the joint	1mm	2mm	3mm	4mm	5mm	6mm	7mm	8mm	9mm
0-5mm	0.13	0.18	0.21	0.24	0.25	0.27	0.28	0.28	0.29
5-10mm	0.03	0.06	0.08	0.11	0.13	0.15	0.16	0.18	0.19
10-15mm	0.02	0.03	0.05	0.07	0.08	0.10	0.11	0.12	0.14
15-20mm	0.01	0.02	0.04	0.05	0.06	0.07	0.08	0.09	0.10
20-25mm	0.01	0.02	0.03	0.04	0.05	0.06	0.07	0.07	0.08
25-30mm	0.01	0.01	0.02	0.03	0.04	0.05	0.05	0.06	0.07
30-35mm	0.01	0.01	0.02	0.03	0.03	0.04	0.05	0.05	0.06
35-40mm	0.01	0.01	0.02	0.02	0.03	0.03	0.04	0.05	0.05
40-45mm	0.01	0.01	0.02	0.02	0.03	0.03	0.04	0.04	0.05
45-50mm	0.00	0.01	0.01	0.02	0.02	0.03	0.03	0.04	0.04
50-55mm	0.00	0.01	0.01	0.02	0.02	0.03	0.03	0.03	0.04
55-60mm	0.00	0.01	0.01	0.02	0.02	0.02	0.03	0.03	0.03
60-65mm	0.00	0.01	0.01	0.01	0.02	0.02	0.02	0.03	0.03
65-70mm	0.00	0.01	0.01	0.01	0.02	0.02	0.02	0.03	0.03
70-75mm	0.00	0.01	0.01	0.01	0.02	0.02	0.02	0.02	0.03
75-80mm	0.00	0.01	0.01	0.01	0.01	0.02	0.02	0.02	0.03
80-85mm	0.00	0.01	0.01	0.01	0.01	0.02	0.02	0.02	0.02
85-90mm	0.00	0.01	0.01	0.01	0.01	0.02	0.02	0.02	0.02
90-95mm	0.00	0.00	0.01	0.01	0.01	0.01	0.02	0.02	0.02
95-100mm	0.00	0.00	0.01	0.01	0.01	0.01	0.02	0.02	0.02

Depth in the joint	10mm	11mm	12mm	13mm	14mm	15mm	16mm	17mm	18mm	19mm
0-5mm	0.30	0.30	0.31	0.31	0.31	0.31	0.32	0.32	0.32	0.32
5-10mm	0.20	0.21	0.22	0.23	0.24	0.24	0.25	0.25	0.26	0.26
10-15mm	0.15	0.16	0.17	0.18	0.18	0.19	0.20	0.21	0.21	0.22
15-20mm	0.11	0.12	0.13	0.14	0.15	0.16	0.16	0.17	0.18	0.18
20-25mm	0.09	0.10	0.11	0.11	0.12	0.13	0.14	0.14	0.15	0.15
25-30mm	0.08	0.08	0.09	0.10	0.10	0.11	0.12	0.12	0.13	0.13
30-35mm	0.07	0.07	0.08	0.08	0.09	0.10	0.10	0.11	0.11	0.12
35-40mm	0.06	0.06	0.07	0.07	0.08	0.08	0.09	0.09	0.10	0.10
40-45mm	0.05	0.06	0.06	0.07	0.07	0.07	0.08	0.08	0.09	0.09
45-50mm	0.05	0.05	0.05	0.06	0.06	0.07	0.07	0.08	0.08	0.08
50-55mm	0.04	0.05	0.05	0.05	0.06	0.06	0.07	0.07	0.07	0.08
55-60mm	0.04	0.04	0.05	0.05	0.05	0.06	0.06	0.06	0.07	0.07
60-65mm	0.04	0.04	0.04	0.05	0.05	0.05	0.06	0.06	0.06	0.07
65-70mm	0.03	0.04	0.04	0.04	0.05	0.05	0.05	0.05	0.06	0.06
70-75mm	0.03	0.03	0.04	0.04	0.04	0.05	0.05	0.05	0.05	0.06
75-80mm	0.03	0.03	0.04	0.04	0.04	0.04	0.05	0.05	0.05	0.05
80-85mm	0.03	0.03	0.03	0.03	0.04	0.04	0.04	0.05	0.05	0.05
85-90mm	0.03	0.03	0.03	0.03	0.04	0.04	0.04	0.04	0.04	0.05
90-95mm	0.02	0.03	0.03	0.03	0.03	0.04	0.04	0.04	0.04	0.04
95-100mm	0.02	0.02	0.03	0.03	0.03	0.03	0.04	0.04	0.04	0.04

Diagonal parts at the bottom of the joint

Composite floors have a diagonal part at the side of the floor due to the formwork for producing the plates. The view factor at the location of the diagonal is slightly higher. The measurement of the diagonal parts is performed from a sample of the University of Technology Eindhoven, figure F3. The assumption is that these measures are the same for all kinds of thicknesses of the precast floors. The calculation method is performed in the same way as for the straight surface at the precast plate, figures F4 and F5. The results of the calculation, multiplied by the emission coefficient are given in table F2.

Fig. F3. Measurement of the diagonals at a composite floor

The precast plate in figure F3 has a thickness of 50 mm. Measuring without diagonal part, the floor has a thickness of approximately 45mm. The total length of the diagonal part is 10 mm. Those dimensions will be used by calculating the view factor and modeling this part.

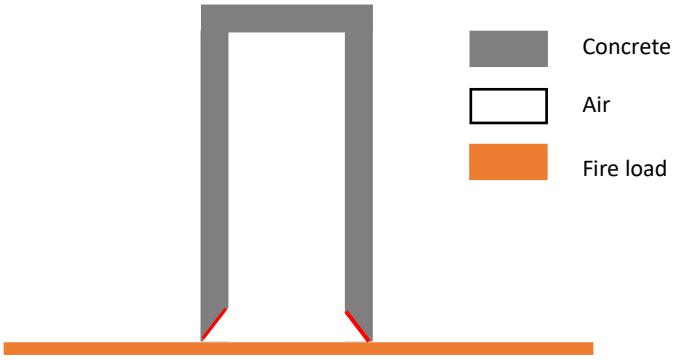

Fig. F4. Location of calculated view factor at the diagonal parts at the bottom of the joint

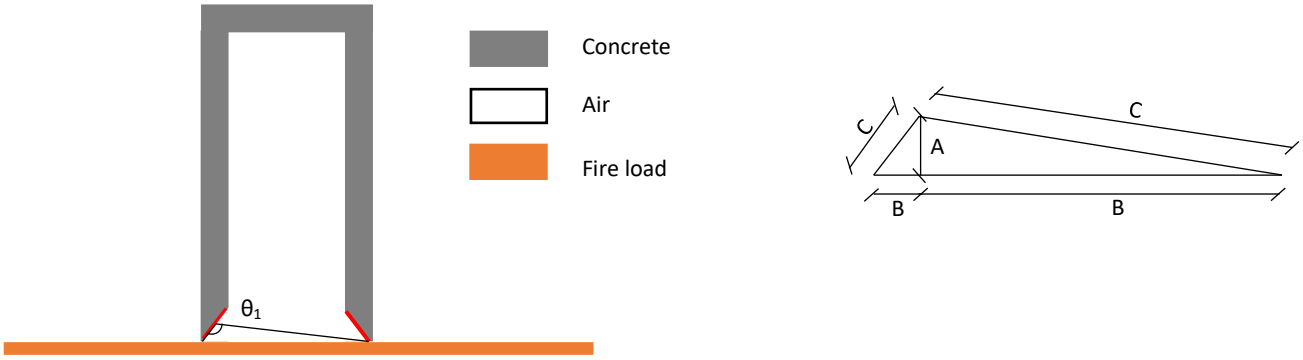

Fig. F5. Calculation method of the view factor at the diagonal parts at the bottom of the joint

Table F2
View factor combined with the emission coefficient 0.7 for diagonal parts of the joint

Depth in the joint	1mm	2mm	3mm	4mm	5mm	6mm	7mm	8mm	9mm
0-5mm	0.56	0.56	0.56	0.57	0.57	0.57	0.57	0.57	0.57
5-10mm	0.51	0.51	0.52	0.52	0.53	0.53	0.53	0.54	0.54

Depth in the joint	10mm	11mm	12mm	13mm	14mm	15mm	16mm	17mm	18mm	19mm
0-5mm	0.57	0.57	0.57	0.57	0.57	0.57	0.57	0.57	0.57	0.57
5-10mm	0.54	0.54	0.54	0.55	0.55	0.55	0.55	0.55	0.55	0.55

Straight surface of the in-situ layer

The in-situ concrete at the top of the joint is also adsorbing radiation, limited due to the view factor. Calculating θ_1 will be done as explained at the other two locations, figure F6. For this part, the view factor will be calculated in the middle of the element, point 2 in figure F6. Points 1 and 3 are assumed to be the same as the view factor at the surface of the precast plate. An average of those three points is considered. The results of the values are given in table F3.

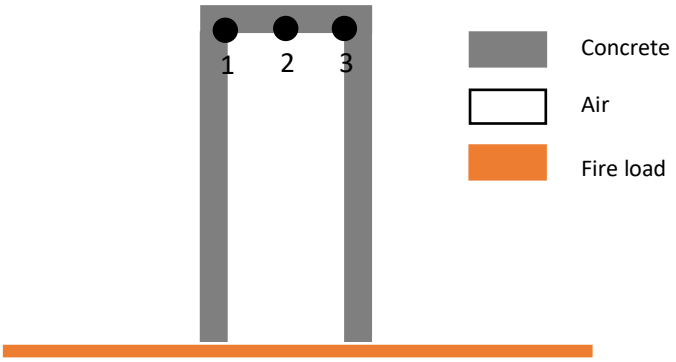

Fig. F6. Location of calculated view factor at the straight part of the in-situ layer

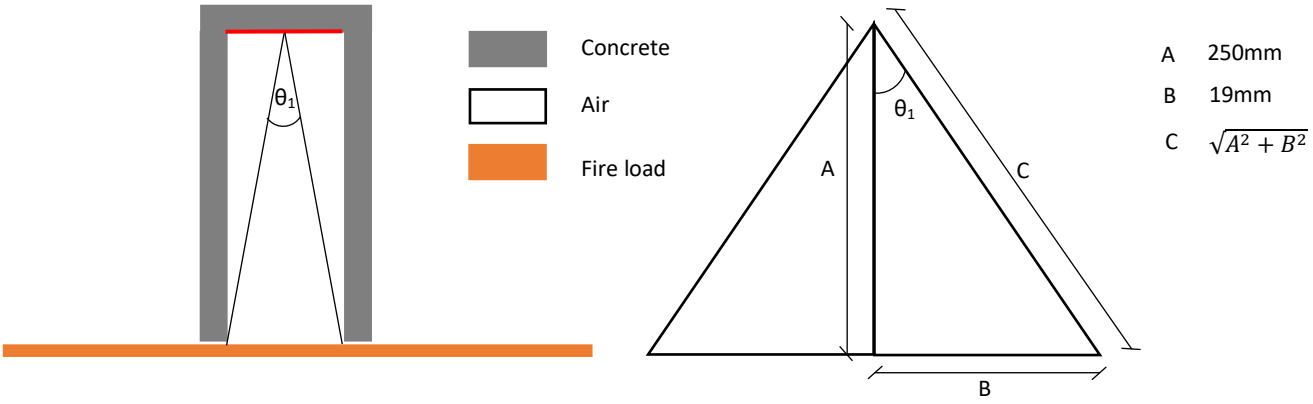

Fig. F7. Calculation method of the view factor at the straight surface of the in-situ layer

Table F3
View factor in-situ concrete at the top of the joint combined with the emission coefficient 0.7

Depth in the joint	1mm	2mm	3mm	4mm	5mm	6mm	7mm	8mm	9mm
50mm	0.03	0.04	0.04	0.04	0.05	0.06	0.06	0.06	0.06
60mm	0.03	0.03	0.04	0.04	0.04	0.04	0.05	0.05	0.06
70mm	0.02	0.03	0.03	0.04	0.04	0.04	0.04	0.04	0.05
80mm	0.02	0.02	0.02	0.03	0.03	0.03	0.04	0.04	0.04
90mm	0.01	0.02	0.02	0.02	0.03	0.03	0.04	0.04	0.04
100mm	0.01	0.02	0.02	0.02	0.03	0.03	0.03	0.04	0.04

Depth in the joint	10mm	11mm	12mm	13mm	14mm	15mm	16mm	17mm	18mm	19mm
50mm	0.07	0.07	0.08	0.08	0.08	0.09	0.09	0.10	0.11	0.11
60mm	0.06	0.06	0.06	0.07	0.08	0.08	0.08	0.08	0.09	0.09
70mm	0.05	0.06	0.06	0.06	0.06	0.06	0.07	0.07	0.08	0.08
80mm	0.04	0.04	0.05	0.05	0.06	0.06	0.06	0.06	0.06	0.07
90mm	0.04	0.04	0.04	0.05	0.05	0.05	0.06	0.06	0.06	0.06
100mm	0.04	0.04	0.04	0.04	0.05	0.05	0.05	0.05	0.06	0.06

ii. Emission coefficient

According to EN 1992-1-2, an emission coefficient is used of 0.7. [1] However, multiple researches give other emission coefficients for concrete. Those coefficients are between 0.8 and 0.99. [5] [6] [7] To learn about the different influences of the emission coefficient, a numerical analysis is performed for emission coefficients of 0.7 and 0.8. The results can be found in table F4.

Table F4
Comparison numerical analyses with different emissivity coefficients after 90 minutes

Depth x_e in the floor measured from exposed surface	Graph [°C]	Numerical analyses emissivity 0.7 [°C]	Numerical analyses emissivity 0.9 [°C]
0mm	950	965	974
10mm	770	783	792
20mm	610	635	643
30mm	495	512	519
40mm	390	409	415
50mm	320	323	329
60mm	260	251	257
70mm	200	192	197
80mm	170	148	152
90mm	130	118	121
100mm	105	96	98

Based on the results of table F4, using an emission coefficients of 0.7 and 0.9 has not much influence on the heat transfer in the concrete floor. The temperatures at 0.9 are slightly higher, which can be explained since the emission coefficient of 0.9 is more capable of absorbing heat than an emission coefficient of 0.7. Since the difference are minor, the other analyses will be performed with 0.7. By using this emission coefficient, the calculation uses more characteristics of the EN 1992-1-2.

iii. Simplified radiation model analytical

As mentioned before, thermal radiation is a part of heat transfer. Thermal radiation can be directly from the fire and from another element that is heated due to the thermal load. At the location of the joint in the

composite floor, only radiation directly from the fire is assumed. The assumption is that the radiation from the sides of the precast concrete plates next to the joint are equal and do not influence each other.

In the situation of a continuous floor, thermal radiation will affect the temperature of the floor differently at the location of the joint. An obstruction at the location of the joint prevents some radiation from reaching the concrete surface. This paragraph will discuss amount of radiation on the surface in the joint will be calculated with an analytical calculation.

The joint is modeled as two concrete plates with the same emission coefficient and a view factor of 1. The concrete plates have a constant temperature as mentioned in figure F7, equations F1 and F2 show the calculation method for the thermal radiation. To prevent a false positive answer, the analysis is performed for both an emission coefficient of 0.3 and 0.7. The results of those analyses can be found in table F5.

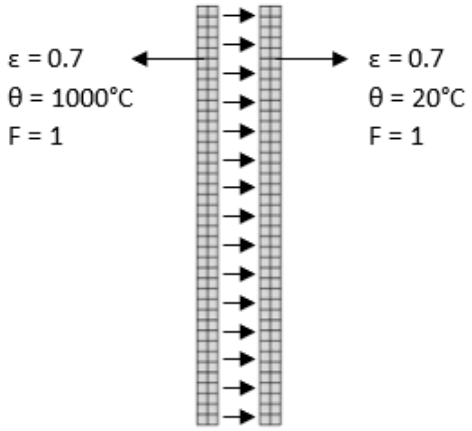

Analyse procedure

Uncoupled thermal-mechanical analysis

Element properties

Material	Concrete
Ambient temperature	-273.15
Element type	DC2D8
Mesh size	5x5 mm
Step response	Transient
Solver equation	Direct solver
Solution technique	Full-Newton Raphson

Fig. F8. Overview model thermal radiation

$$\frac{1}{\varepsilon_{res}} = \frac{1}{\varepsilon_1} + \frac{1}{\varepsilon_2} - 1 \qquad \text{(E1)}$$

$$E = \varepsilon_{res}\sigma(T_1^4 - T_2^4) \qquad \text{(E2)}$$

iv. Simplified radiation model numerical

To verify the results from the analytical calculation, a numerical model for heat transfer is created. Two elements are modeled as concrete surfaces with the same emission coefficient and a constant temperature. The concrete has temperature-dependent characteristics. The mesh of the two parts is 5x5 mm, and the element type is DC2D8. This element type is used for heat transfer calculations. The model has an absolute zero temperature of -273.15, and the Stefan-Boltzmann constant is set on $5.67 \cdot 10^{-8}$. Using an absolute zero temperature of -273.15, the analysis is performed in Celsius degrees. Figure F7 gives an overview of the model.

For this analysis, a heat transfer step is created with a maximum allowed time step of 10 °C. The parts are not connected. However, they must interact with each other. Therefore the instance surface-to-surface is used. In this instance, thermal radiation can be specified. The thermal load of this analysis is described

by the constant temperatures, which are implemented into the model. The final step was to create a job for running the analysis. Table F5 shows the results.

Table F5
Comparison heat flux analytical and numerical analyses with different emissivity coefficients

Emission coefficient	Analytical analysis [W/m²]	Numerical analysis [W/m²]
0.7	39690	39510
0.3	17010	12717

In the results of table F5, it should be noticed that there are some differences. Those differences come from different aspects. The first one is the view factor. In the analytical analysis, a view factor of 1 is considered. A more specific view factor is calculated in the numerical analysis, which is slightly less than 1. Therefore the results of the numerical analysis will be a little lower due to this reason. Another reason is that there is probably also some heat transfer which is leaving through the other surfaces. The analytical assumes that the heat flux is only present at the calculated surface. This reason could explain the differences between 0.7 and 0.3. When an emission coefficient of 0.3 is used, the heat transfer, is obstructed more than at an emission coefficient of 0.7. More heat transfer will go through the other surfaces, and the heat flux at the calculated surface gets less than at an emission coefficient of 0.7. Based on those assumptions, it is concluded that modeling thermal radiation with this method can be used at the location of the gap.

Appendix G. Stochastic boundary conditions

Some differences occur between the continuous floor and the joint location, some differences occur due to changing local situations, which are called from now on stochastic boundary conditions. Sensitivity analyses are performed for this boundary conditions. In this chapter, those stochastic boundary conditions are explained and researched.

i. Convection coefficient

The first stochastic boundary condition is the convection coefficient. The convection coefficient at the continuous surfaces is given in EN 1992-1-2. [1] This coefficient is not applicable at the joint location since the speed of air and measures of the whirls are different here. Due to the limited air, the whirls inside the joint will be smaller than in the compartment with fire. Next to this, the limited space also prevents from significant temperature differences inside the joint, which means a lower speed of air. This speed of air is usually affected by the temperature differences in space.

Since there is no value given for the convection coefficient at the location of the joint, multiple analyses are performed to get more information about the differences in temperature at three locations in the floor. Those locations are above the floor, along the surface of the joint, and 50 mm next to the floor. The results of those analyses can be found in table G1.

Table G1
Comparison temperature at different convection coefficients

Depth x_j in the floor above joint	Numerical analyses convection coefficient Joint surface [°C]			Depth x in the floor from exposed surface	Numerical analyses convection coefficient Joint surface [°C]			Numerical analyses convection coefficient 50 mm next to joint surface [°C]		
	0.5	1	2		0.5	1	2	0.5	1	2
0 mm	368	375	388	0 mm	961	962	963	967	967	967
5 mm	328	334	344	10 mm	840	842	846	791	792	793
10 mm	289	294	302	20 mm	740	744	752	647	648	649
15 mm	253	257	264	30 mm	633	638	649	527	527	529
20 mm	220	223	229	40 mm	519	525	537	423	425	427
25 mm	190	193	198	50 mm	385	391	403	337	338	341
30 mm	163	166	170	60 mm	290	294	302	264	265	268
35 mm	143	145	148	70 mm	219	222	228	203	204	206
40 mm	128	129	131	80 mm	163	165	170	154	155	156
45 mm	114	115	117	90 mm	127	129	131	123	123	124
50 mm	102	103	105	100 mm	102	103	105	99	100	101

Using different coefficients for convection, a higher coefficient gives a slightly higher temperature. The higher or deeper the concrete, the more the temperatures will get the same as other coefficients. When calculating the differences in percentages, the differences are minor. For this reason, the assumption is that no further research is needed on this topic.

ii. Mesh configuration

The mesh is in the beginning practical chosen as 5x5 mm. To confirm this mesh size, a sensitivity analysis is performed. In this mesh configuration, the aim is to get the same results in different mesh types. By choosing the mesh sizes that will be researched, it is essential to ensure that the meshes fit in each other. Therefore, the size of the practical mesh of 5x5 mm is multiplied by 2 and divided by 2.

Table G2
Comparison temperature at different mesh configurations

Depth x_j in the floor above joint	Numerical analyses meshes [°C]		
	10x10 mm	5x5 mm	2.5x2.5 mm
0 mm	376	375	374
5 mm	-	334	333
10 mm	297	294	293
15 mm	-	257	256
20 mm	225	223	223
25 mm	-	193	192
30 mm	167	166	165
35 mm	-	145	144
40 mm	129	129	128
45 mm	-	115	115
50 mm	104	103	103

The results in table G2 show that the difference in temperature between the analyses can be neglected. Therefore, it is concluded that the mesh size is fine enough to reach the correct temperature. No further research is performed.

iii. Standard fire curve

The standard fire curve, which can be calculated by the formula from 1992-1-2, is based on two different curves. Those curves are the gas temperature and the radiative temperature. Those curves are based on the environment in the furnace. The radiative temperature has a delay in the furnace, and the gas temperature is set so that the gas temperature and radiative temperature reach the temperature of the standard fire curve. Sensitivity research is performed to get information about the possibility of differences in results by using the standard fire curve or the two different curves. The results of this analysis are given in tables G3 and G4.

Table G3
Comparison temperature in the composite floor at different fire curves, standard fire curve

Depth x_j in the floor above joint	Numerical analyses Above the joint [°C]				Depth x in the floor from exposed surface	Numerical analyses Joint surface [°C]				Numerical analyses 50 mm next to joint surface [°C]			
	30 min.	60 min.	90 min.	120 min.		30 min.	60 min.	90 min.	120 min.	30 min.	60 min.	90 min.	120 min.
0 mm	94	234	365	460	0 mm	728	889	968	993	738	890	967	992
5 mm	82	205	328	420	10 mm	565	767	867	911	508	695	793	847
10 mm	70	174	291	380	20 mm	417	648	770	833	341	539	650	720
15 mm	59	147	255	341	30 mm	292	525	661	741	220	413	529	608
20 mm	49	128	222	304	40 mm	189	403	542	632	138	311	427	509
25 mm	41	112	192	271	50 mm	108	263	393	486	95	229	340	423
30 mm	34	98	165	241	60 mm	71	178	293	381	67	163	227	347
35 mm	29	96	144	213	70 mm	49	129	222	304	47	122	205	282
40 mm	24	75	128	188	80 mm	34	98	165	240	32	94	154	225
45 mm	20	66	115	165	90 mm	24	95	128	188	22	73	123	117
50 mm	16	58	103	146	100 mm	16	58	109	146	15	57	99	141

Table G4
Comparison temperature in the composite floor at different fire curves, curves of the furnace

Depth x_j in the floor above joint	Numerical analyses Above the joint [°C]				Depth x in the floor from exposed surface	Numerical analyses Joint surface [°C]				Numerical analyses 50 mm next to joint surface [°C]			
	30 min.	60 min.	90 min.	120 min.		30 min.	60 min.	90 min.	120 min.	30 min.	60 min.	90 min.	120 min.
0 mm	84	220	354		0 mm	694	876	960		713	880	961	
5 mm	73	192	318		10 mm	524	751	857		480	682	786	
10 mm	62	163	281		20 mm	379	630	759		316	526	641	
15 mm	52	139	246		30 mm	259	507	649		198	400	520	
20 mm	43	122	213		40 mm	164	386	531		126	300	418	
25 mm	36	10	184		50 mm	96	249	382		86	218	332	
30 mm	30	93	178		60 mm	63	166	283		60	153	259	
35 mm	25	81	139		70 mm	44	122	213		52	109	198	
40 mm	20	71	124		80 mm	30	93	157		29	89	149	
45 mm	17	62	111		90 mm	20	71	124		20	69	119	
50 mm	14	55	99		100 mm	14	55	99		13	53	96	

Tables G3 and G4 show results with a minor deviation based on percentages. The curve of the furnace temperature has no values for 120 minutes, since the used values for these temperatures are not provided above 90 minutes. Based on the results in tables G3 and G4, it is concluded that the standard fire curve can be used for a realistic analysis of the composite floor.

Appendix H. Composite floor at location of the joint

Combining all the assumed and stochastic boundary conditions with the numerical model of the simplified situation, the analysis for the composite floor at the location of the joint can be performed. This appendix explains the numerical model and some additional researched which are performed. The results of the analyses can be found in Excel file. Results heat transfer analyses composite floor at location of the joint.

i. Numerical model

The numerical model consists of 14 elements forming two precast floor plates and a connecting in-situ concrete layer on top. Modeling with smaller parts makes it possible to create a continuous mesh since the elements have the same mesh width.

The numerical analysis is an uncoupled thermal-mechanical analysis. The elements in the model are 2D Planar and created with a shell element. Since the research focuses on the joint in the composite floor, only this detail is modeled with a minor part of the composite floor. The length of the continuous floor is based on a previous model, which has a length of 1000 mm. After approximately 100 mm, the temperature in the floor is no longer influenced by the joint. Therefore, this model is chosen for two precast plates of 150 mm, so the temperature is no longer influenced at the end of the model. For the elements, concrete is modeled with temperature-dependent characteristics. By setting the ambient temperature of the model to -273.15, all the temperature values can be used as Celsius degrees. Also, the Stefan-Boltzmann constant is implemented and set on $5.67 \cdot 10^{-8}$.

The next part is to design the meshes. Each concrete part has a mesh which are all equal to each other. The meshes are placed in the family heat transfer with a standard element library and quadratic geometric order. The geometric order is quadratic since the differential formula for heat transfer is $\frac{\partial^2 T}{\partial x^2} = \frac{1}{\alpha} \cdot \frac{\partial T}{\partial t}$ with $\alpha = \frac{\lambda}{\rho c}$. Using these settings, the floor becomes a DC2D4 element, a 4-node linear heat transfer quadrilateral. The mesh is designed practically to read off the temperatures the desired location. Therefore the mesh is 5x5 mm. Another reason for choosing a fine mesh is for the view factor. With a finer mesh, more view factors can be implemented.

After finishing the parts, tie constraints are used to connect the elements which should be connected. Then a step is created for a heat transfer model. The step is transient and runs for 30, 60, 90, and 120 minutes. In the step, the maximum allowable temperature change per increment is set at 10°C, and the maximum allowable emissivity change per increment is 0.1.

Now that the basic elements are implemented into the model, interactions are created based on a boundary condition for the thermal load. This thermal load is based on the fire curve and is implemented by an amplitude. This amplitude is used for the radiation and convection at the exposed surface and the location of the joint. At the unexposed surface, the temperature is 20°C. As mentioned before, the interactions are working on three different locations, unexposed surface, exposed surface, and at the location of the joint. At the location of the *unexposed surface* is no thermal load. According to the EN 1992-1-2, the convection factor is 9 W/m²K, and the emissivity can be taken as 0.7. [1] The assumption is that the compartment above the floor has an ambient temperature of 20°C. At the location of the *exposed surface*, the thermal load is coming from the standard fire curve. According to the EN 1992-1-2, the convection factor is 25 W/m²K, and the emissivity is 0.7 at this location. [1] As described before, the

standard fire curve is implemented at the conductivity and radiation at the exposed surface. Because the temperature is coming from the amplitude, the sink temperature must be set at 1. The sink amplitude will give the variation of the sink temperature with time. So actually, the sink amplitude will be multiplied by the sink temperature. *At the location of the join,* convection and radiation are also present, but less than at the exposed surface. This decrease is due to the view factor and the low airspeed. Therefore, the emissivity coefficient of 0.7 is multiplied by the view factor, and the convection coefficient is 1 W/m²K.

At the location of the joint cavity radiation is used to model radiation. To set desired thermal load at the location of the joint, the gab should be closed for the simulation. A small part is placed below the joint at which surface radiation is implemented to ensure that the joint gets the same temperature as the compartment. This little part also has the same mesh and section assignment as the other parts. The emissivity coefficient of the external part is one to ensure that all the thermal load is going through the element. In this cavity radiation, the view factor is implemented. The finite element program ABAQUS can calculate the view factor by itself, but all the view factors become one due to the closed gap. By multiplying the calculated view factor by the emission coefficient, the view factor can be implemented in the analysis.

After finishing the model, a job is created for running the model.

v. Continuous composite floor

The different numerical analyses will partly answer the research question, which is based on the design rule of En 13747. The first part of this rule is about a continuous composite floor: *The fire resistance of a composite slab made of floor plates without void formers is the same as for a solid slab of identical characteristics.* To verify this part of the rule, a heat transfer analysis is performed of a continuous composite floor and compared to the monolith floor of the validation method. The results are given in table H1.

Table H1
Comparison temperature at continuous monolith and composite floor

Depth x_j in the floor above joint	Numerical analysis Monolith floor [°C]	Numerical analysis Composite continuous floor [°C]
0 mm	918	918
10 mm	737	737
20 mm	591	591
30 mm	470	471
40 mm	371	371
50 mm	290	290
60 mm	223	223
70 mm	168	168
80 mm	130	131
90 mm	105	105
100 mm	85	85

Table H2 shows that the heat transfer in a continuous composite slab is equal to the heat transfer of a monolith floor. Therefore the conclusion is that the first part of the design rule, *"The fire resistance of a composite slab of floor plates without void formers is the same for a solid slab of identical characteristics.",* is correct.

vi. Composite floor at the location of the joint

For the second part of the design rule, *Calculation of the temperature is carried out without taking into account the joint between floor plates as much as the width b_j is lower than 20 mm;* a model of a composite

slab with a joint is created. Before running to complete analysis, one uncertainty should be researched. Due to the construction of the precast composite floor plates, a small part at the bottom of the floor is divergent. A tiny diagonal part is located here. This small part leads to increased view factors, and therefore a probably increased temperature in the composite floor at the location of the joint. Tables H2 and H3 show the different temperatures of a composite floor with and without the small diagonal part.

Table H6
Comparison analyses heat transfer without diagonal part

Depth x_j in the floor above joint	Numerical analyses Above the joint [°C]				Depth x in the floor from exposed surface	Numerical analyses Joint surface [°C]				Numerical analyses 50 mm next to joint surface [°C]			
	30 min.	60 min.	90 min.	120 min.		30 min.	60 min.	90 min.	120 min.	30 min.	60 min.	90 min.	120 min.
0 mm	100	243	375	470	0 mm	753	890	962	985	738	890	968	992
5 mm	86	211	334	425	10 mm	569	750	842	886	509	694	796	845
10 mm	73	179	294	382	20 mm	417	630	744	807	342	538	654	716
15 mm	61	151	257	341	30 mm	291	509	638	716	221	412	534	604
20 mm	51	130	223	304	40 mm	188	392	525	613	140	311	431	506
25 mm	43	114	193	271	50 mm	111	264	391	483	96	229	344	420
30 mm	36	100	166	241	60 mm	74	180	294	381	68	163	270	345
35 mm	30	87	145	213	70 mm	51	130	222	303	47	123	208	280
40 mm	25	77	129	189	80 mm	36	99	165	240	33	95	157	224
45 mm	20	67	115	165	90 mm	25	76	129	187	23	73	124	177
50 mm	17	59	103	147	100 mm*	17	59	103	147	16	57	101	141

Table H3
Comparison analyses heat transfer with diagonal part

Depth x_j in the floor above joint	Numerical analyses Above the joint [°C]				Depth x in the floor from exposed surface	Numerical analyses Joint surface [°C]				Numerical analyses 50 mm next to joint surface [°C]			
	30 min.	60 min.	90 min.	120 min.		30 min.	60 min.	90 min.	120 min.	30 min.	60 min.	90 min.	120 min.
0 mm	106	264	403	502	0 mm	818	896	973	997	378	890	967	993
5 mm	91	227	356	451	10 mm	584	782	878	921	509	696	795	849
10 mm	76	191	311	403	20 mm	432	661	782	844	342	541	652	723
15 mm	64	159	271	359	30 mm	304	538	674	753	221	415	532	612
20 mm	53	135	235	319	40 mm	199	416	557	647	140	314	430	514
25 mm	44	118	202	284	50 mm	116	282	416	511	96	232	344	427
30 mm	37	103	174	251	60 mm	77	192	310	400	68	165	270	352
35 mm	30	90	150	222	70 mm	53	135	233	318	47	124	208	286
40 mm	25	79	133	196	80 mm	37	102	173	250	33	96	157	229
45 mm	21	69	119	172	90 mm	25	78	132	195	23	74	125	181
50 mm	17	61	106	152	100 mm*	17	60	106	151	16	58	101	143

The results of tables H2 and H3 conclude that the temperatures of a composite floor with a slight deviation at the bottom of the precast composite floor plates are slightly larger. Therefore, analyses of the composite floor with different joints will be calculated with the model, including the diagonal part at the precast plate. All the results of the analyses can be found in the Excel file. Results heat transfer analyses composite floor at the location of the joint.

Appendix I. Reduction of moment capacity

After the analysis of the heat transfer through the composite floor, the structural behavior of the composite floor is determined. This determination is done by calculating the general reduction of moment capacity of the composite floor at the precast plate and the location of the coupling reinforcement. In this appendix, the calculation is elaborated.

i. Precast floor plate

An increased temperature is causing that the strength of concrete and reinforcement steel is decreasing. Therefore, the moment capacity of the structure will decrease. The actual amount of capacity loss is due to the temperature inside the floor. In this paragraph, the reduction of the moment capacity is considered in the precast plate. Since this calculation is not based on a specific situation, multiple diameters are researched.

Before calculating the reduction of the moment capacity, some assumptions about the structure are made. Those are as follows:

Environment class	XC1
Safety class	CC2
Concrete class	C30/37
Reinforcement	S235

At first the moment capacity without fire is calculated to have a comparison to the moment capacity with a reduction. Therefore, equations I1 and I2 are used. The results can be found in the Excel file Reduction momentcapacity composite floor.

$$M_{rd} = A_s \cdot f_{yd} \cdot (0.9d) \quad \text{(I1)}$$

$$d = h - c - \phi h_w - \frac{1}{2}\phi b_w \quad \text{(I2)}$$

For calculating the reduction of the moment capacity, both the values for concrete and reinforcement steel should be decreased. The decrease of concrete will be calculated by the 500°C isotherm method from EN 1992-1-2. [1] This method decreases the concrete area by removing all the concrete which is warmer than 500°C. In the case of a precast plate of 50mm with a joint of 19mm, the floor thickness at 30 minutes will decrease with 15mm. For decreasing the strength of reinforcement, the graph from EN 1992-1-2 will be used again, figure I1. This will lead to an adjusted formulas of I1 and I2 as mentioned in I3 and I4.

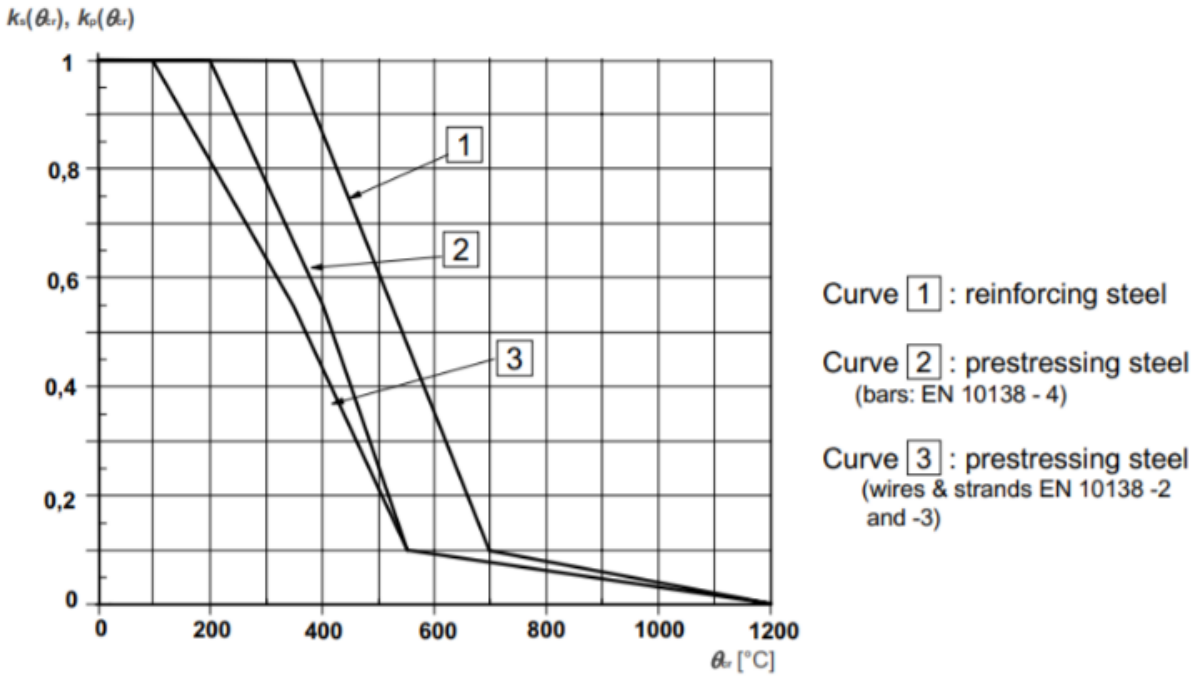

Fig. G1. Decrease of tensile strength of reinforcement due to temperature change [1]

$$M_{rd} = A_s \cdot f_{yd} \cdot k_s \cdot (0.9d) \quad \text{(I3)}$$

$$d = h - Iso500 - c - \phi h_w - \frac{1}{2}\phi b_w \quad \text{(I4)}$$

ii. Location above the joint

The same calculation is performed for the location above the joint as is done for the precast plate. For each 5 mm the momentcapacity is calculated. The results can be found the Excel file Reduction momentcapacity composite floor.

Appendix J. Article Cement

Titel
De invloed van brand op de bezwijkkans van de koppelwapening in een breedplaatvloer

Subtitel
Onderzoek naar temperatuurontwikkeling ter plaatse van de koppelwapening in een breedplaatvloer ten gevolge van brand

Auteurs

Sue Ellen de Nijs	TU Eindhoven
Prof. Ir. Simon Wijte	TU Eindhoven, fac Bouwkunde / Adviesbureau ir. J.G. Hageman
Ir. Ruud van Herpen	TU Eindhoven, fac Bouwkunde / Peutz BV
Dr. Ir. Hèrm Hofmeyer	TU Eindhoven, fac Bouwkunde

Inleiding
Wanneer de temperatuur van beton en betonstaal bij een brand toeneemt, neemt de sterkte van deze materialen af. De dekking op het betonstaal is mede bepalend voor de snelheid waarmee de temperatuur in het betonstaal toeneemt. Een beperkte dekking op de koppelwapening bij breedplaatvloeren kan een negatieve invloed hebben op draagkracht van die vloeren in brandomstandigheden. NEN-EN 13747 beschrijft in een ontwerpregel dat voor de brandveiligheid van breedplaten de koppelwapening ter plaatse van de voeg tussen twee breedplaten niet hoeft te worden beschouwd. [8] De vraag is of dit juist is en zo ja of dit ook geldt als de koppelwapening zonder specifieke dekking is aangebracht?

Body
Bij een in twee richtingen overspannende breedplaat bevindt zich ter plaatse van de voeg tussen twee breedplaatvloeren koppelwapening loodrecht over de voeg waarvan de constructieve kwaliteit mede bepalend is voor de capaciteit van de vloer. Dit is weergegeven in een detail zoals in figuur 1. [9] Meer informatie over dit detail kan teruggevonden worden in het artikel Nieuw stappenplan voor beoordeling breedplaatvloeren van Jacques Linssen, 22 mei 2019.

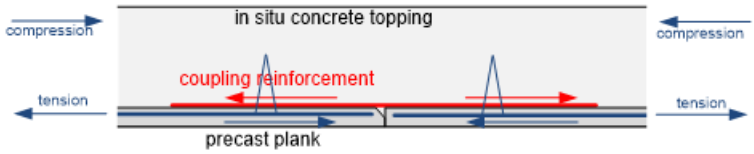

Figuur 1. Detail koppelwapening in breedplaatvloer *[9]*

Naast de feit dat de constructieve veiligheid van dit detail al nader onderzocht is, is het ook van belang om de brandveiligheid hiervan te beschouwen. De NEN-EN 13747 artikel 4.3.4 geeft hiervoor een rekenregel voor de bepaling van brandveiligheid in dit kritieke detail.

"The fire resistance of a composite slab made of floor plates without void formers is the same as for a solid slab of identical characteristics. Calculation of the temperatures is carried out without taking into account the joint between floor plates as much as the width b_j is lower than 20 mm." [8]

In de norm staat niet aangegeven of deze rekenregel geldt voor enkel eenzijdige of ook voor tweezijdige overspanningen. Bovendien staat er in de NEN-EN 1992-1-1 beschreven dat de koppelwapening met een bepaalde dekking geplaatst moet worden. [10] In Nederland werd deze dekking echter vaak niet toegepast en werd de koppelwapening direct op de breedplaat geplaatst. Het betonstaal is zodoende minder beschermd tegen opwarming bij brand. De vraag is of dit een extra risico oplevert voor de constructieve veiligheid.

Brand

Brand is een verschijnsel wat op meerdere manieren kan ontstaan en schade en gevaar kan veroorzaken. Een brand is onvoorspelbaar en afhankelijk van brandstofkenmerken en gebouwkenmerken. Wanneer in de brandontwikkeling met deze projectspecifieke kenmerken rekening wordt gehouden spreken we van een natuurlijke brand. Daardoor bezit elk brandcompartiment een eigen brandscenario met een eigen thermische belasting. Daardoor is de bezwijkkans van een bouwkundige constructie, zoals een vloerconstructie, in een brandcompartiment anders. Leveranciers van dergelijke constructies testen daarom volgens de standaard brandkromme (ISO 834) met een klassificering volgens EN 13501-2, waardoor de constructie generiek toepasbaar is.

Een standaard brandkromme kan worden beschouwd als een volledig ontwikkelde brand zonder ontwikkel- en dooffase. Deze brandkromme kan berekend worden met behulp van NEN-EN 1992-1-2. [11] Beide krommes zijn voor een willekeurig brandcompartiment weergegeven in figuur 2. In figuur 2 is ook zichtbaar tot op welk punt gerekend moet worden met de standaard brandkromme om tot eenzelfde cumulatieve interne gasenergie als met de specifieke natuurlijke brand te komen. Dit is in de standaard brandkromme aangegeven met de dikkere zwarte lijn. Het gaat in figuur 2 dus om de vergelijking van de gastemperaturen in het brandcompartiment ten gevolge van een standaard brand en een natuurlijke brand. De effecten van de lokale brand (ontwikkelfase) ten gevolge van een lokale vlam zijn niet beschouwd.

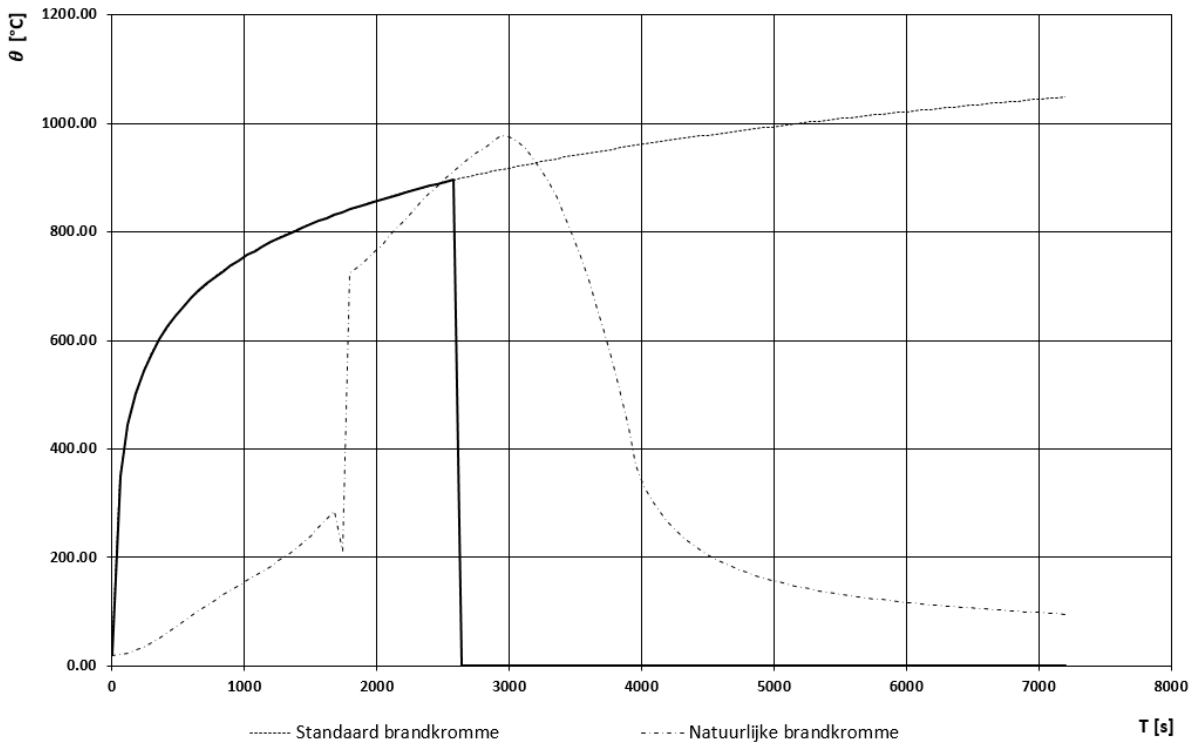

Figuur 2. Gas temperatuur volgens de standaard brandkromme en een voorbeeld van een natuurlijke brandkromme

De warmte die ontstaat bij brand kan zich via drie manieren verspreiden; geleiding, convectie en straling. Bij geleiding geven de moleculen met hogere temperaturen energie af aan moleculen met lagere temperaturen. Hoe groter het verschil in de temperaturen is, hoe groter de warmteafgifte zal zijn. [12] Convectie is gebaseerd op het verspreiden van warmte door de stroming van gas (lucht), ontstaan door een verschil in dichtheid in de ruimte. [6] Bij straling wordt de warmte verspreid door elektromagnetische golven in het infrarode gebied. [6]

Beton en brand
Het is bekend dat de materiaaleigenschappen van zowel beton als van betonstaal in sterkte afnemen bij een temperatuur stijging. Deze reductie heeft te maken met het veranderen van drie belangrijke eigenschappen; dichtheid, soortelijke warmte en thermische geleiding. Samen vormen deze eigenschappen de thermische diffusie. De eigenschappen worden als volgt beïnvloed door temperatuur. [11]

De dichtheid van het beton neemt af naar mate het beton warmer wordt. Dit heeft te maken met het zowel vrije als chemisch gebonden water, wat verdampt en luchtbellen in het beton veroorzaakt. Daarnaast wordt ook de dichtheid van het toeslagmateriaal lager, wat zicht vertaald in een beton met een lagere dichtheid.

Bovendien zal gedurende de opwarming van beton de soortelijke warmte (benodigde energie om 1 kg materiaal 1 ° op te laten warmen) toenemen en in het begin zelfs een piek vertonen. Deze piek is afhankelijk van het vochtgehalte in het beton en heeft te maken met de benodigde energie om water op te warmen. Dus hoe hoger het vochtgehalte, des te hoger is de piek van de soortelijke warmte.

De laatste eigenschap is thermische geleiding, wat staat voor de hoeveelheid warmte die een materiaal kan geleiden. Hoe hoger de thermische geleiding, hoe sneller een materiaal opwarmt. Beton heeft, bijvoorbeeld in vergelijking met staal of water, een lage thermische geleiding. Naar mate het water in het beton afneemt, neemt ook de geleidingscoëfficiënt van het beton verder af.

Dan zijn er nog twee andere verschijnselen welke invloed kunnen hebben op de opwarming van de koppelwapening, namelijk spatten en thermische scheuren. Bij deze verschijnselen komt de het betonstaal bloot te liggen en zal de koppelwapening gemakkelijker warmte opnemen. In dit onderzoek naar de opwarming van de koppelwapening is het spatten en thermisch scheuren van beton niet beschouwd.

Door al deze veranderende eigenschappen, veranderen de druk- en treksterkte van zowel het beton als het betonstaal. De druk- en treksterkte van beton begint met afnemen vanaf 100 °C. Vanaf een temperatuur hoger dan 600 °C is het beton dusdanig beschadigd dat het niet meer hersteld kan worden en zelfs niet meer in staat enige trekkracht op te nemen.

De sterkte van het betonstaal begint met afnemen vanaf een temperatuur van 350 °C. Als het betonstaal 700 °C is, heeft het staal nog 10% van de initiële treksterkte over. Een lagere soortelijke warmte van staal zorgt ervoor dat het betonstaal sneller opwarmt. Omdat het staal verantwoordelijk is voor het opnemen van de trekkrachten, is het van belang dat het beschermd wordt tegen opwarming door het aanbrengen van een betondekking. Als ter plaatse van de voeg tussen twee breedplaten de dekking op de koppelwapening minder is, zou dit bij een brandsituatie tot ongewenste reductie van de constructieve eigenschappen kunnen leiden. Daarom is rekenkundig onderzoek uitgevoerd naar het temperatuursverloop ter plaatse van de voeg tussen twee breedplaten in het geval van brand.

Onderzoeksmethode
Voor het onderzoek naar het temperatuursverloop wordt vanwege de specifieke geometrie ter plaatse van de voeg, gebruik gemaakt van een eindige elementen model. Voor een verificatie van het model is gebruik gemaakt van een versimpelde situatie welke is geanalyseerd met de grafische analyse volgens de Eurocode, een analytische berekening en een numeriek model. De uitkomsten van deze analyses worden vergeleken met elkaar. Daarnaast is voor de processen waarvoor geen eenvoudige analytische beschouwing mogelijk is, zoals bij stralingsoverdracht, de invloed van de spreiding van diverse variabelen op de resultaten van de analyse beoordeeld.

Vergelijkend onderzoek
Voordat een temperatuur analyse uitgevoerd kan worden voor de breedplaatvloer ten gevolge van een brand, wordt een versimpelde situatie gebruikt om een vergelijkende berekening te maken. Door deze versimpelde situatie te vergelijken met de rekenmethode uit de NEN-EN 1992-1-2 en de 'finite difference method' kan bekeken worden of het eindige elementen model een gelijkwaardige uitkomt geeft en daarmee een realistische weergave van de werkelijkheid.

De grafische analyse wordt uitgevoerd met behulp van de grafiek van de NEN-EN 1992-1-2. [11] Deze grafiek is bedoeld voor vloeren van 200 mm dik welke aan één zijde blootgesteld wordt aan brand, zie figuur 3. Door de temperatuur op de verschillende diktes in de vloer op diverse tijdstippen af te lezen, wordt het uitgangspunt van het vergelijkingsproces gevormd, zie tabel 1.

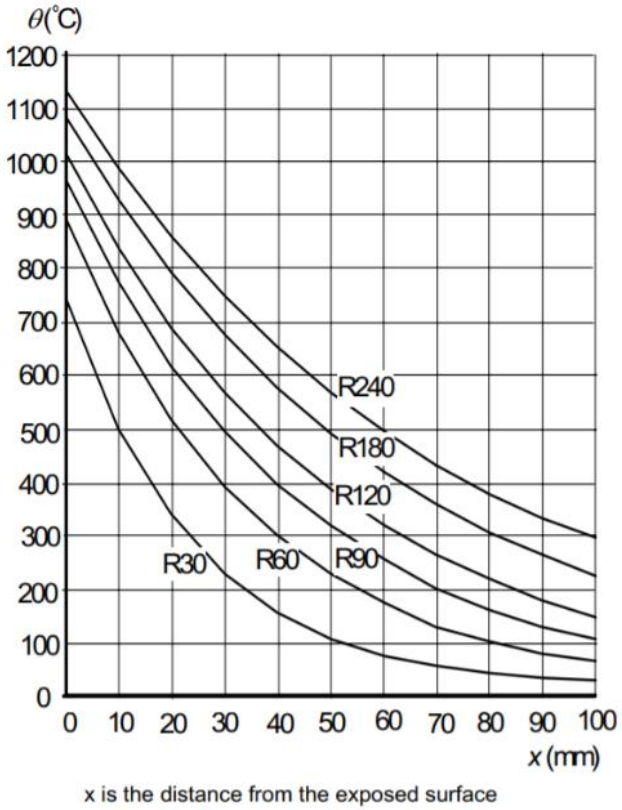

Figuur 3. Grafiek temperatuur toename in een beton vloer van 200 mm dik met *Rx* is de tijdsduur van de brand *[1]*

De analytische berekening bestaat uit twee onderdelen. Als eerste is gebruik gemaakt van de formules uit de Eurocode behorende bij de grafiek uit figuur 3. Met deze formules kan de temperatuur op diepte x in een vloer op een specifiek tijdstip bepaald worden. Deze waarden komen overeen met de waarden van de grafiek, zie ook tabel 1. Hierbij is geconstateerd dat de formules van de Eurocode voor de temperatuur veranderende eigenschappen dichtheid, soortelijke warmte en geleiding, één constante waarde aanhoudt welke overeenkomstig is met de eigenschappen van beton van 660 °C. Bovendien is het niet mogelijk om met deze formule de temperatuur van de vloer onder de 30 minuten te bepalen. Om deze reden is ook een analytische rekenmethode beschouwd waarin meer details beschouwd kunnen worden. Hiervoor is de 'finite difference method' gekozen. [2] Met deze methode wordt de temperatuur voor een volgende tijdstap berekend met behulp van de temperatuur in de huidige tijdstap. Voor deze tijdstappen kan iedere gewenste grootte aangenomen worden. Daarnaast wordt er in iedere tijdstap rekening gehouden met de karakteristieken van het beton op die bepaalde temperatuur. De resultaten van deze methode zijn ook opgenomen in tabel 1.

Tabel 1. Vergelijking temperaturen in de vloer bij verschillende analyses na 120 minuten

Diepte x in vloer vanaf oppervlakte	T [°C] Grafische analyse	T [°C] Analytische methode Eurocode	T [°C] Finite difference method	T [°C] Numerieke analyse ABAQUS
0 mm	1050	1030	979	990
10 mm	835	811	807	834
20 mm	690	662	662	701
30 mm	570	540	543	585
40 mm	460	441	446	486
50 mm	390	360	365	400
60 mm	320	294	299	327
70 mm	255	240	244	264
80 mm	220	196	198	211
90 mm	175	160	160	166
100 mm	150	130	134	134

Uit tabel 1 blijkt dat de resultaten van de drie beschreven methoden goed overeenkomen. Er is sprake van beperkte verschillen tussen de diverse resultaten. Aan de oppervlakte van het beton geeft de 'finite difference method' lagere waarden, wat het gevolg is van de gebruikte temperatuur afhankelijke eigenschappen het beton.

De laatste gemaakte vergelijking is uitgevoerd met een numerieke analyse. Voor deze analyse is een model gemaakt in het eindig elementen programma ABAQUS, zie figuur 4. Door gebruik te maken van een thermodynamisch model, is het mogelijk om het temperatuursverloop in de vloer te bepalen. Hierbij zijn voor de convectie coefficient en de emissie coefficient de waardes uit de NEN EN 1992-1-2 gebruikt. [11] In de analyse worden de temperatuurafhankelijke eigenschappen van beton meegenomen. De temperaturen op de onderzijde van de vloer worden bepaald door de standaard brandkromme en aan de bovenzijde wordt een constante temperatuur van 20 graden Celsius aangehouden. Door de absolute nul temperatuur in ABAQUS op -273.15 te zetten, kan er gerekend worden in graden Celsius. Voor de beton elementen wordt een elementennet van 10x10 mm toegepast met elementen DC2D8 welke enkel gebruikt kunnen worden in een thermodynamisch model. In de analyse wordt de berekening transient opgelost. De resultaten welke hieruit volgen liggen bij 30, 60, 90 en 120 minuten in de buurt van de temperaturen bij de drie hiervoor beschreven methoden. Een voorbeeld van de resultaten is te zien in figuur 5.

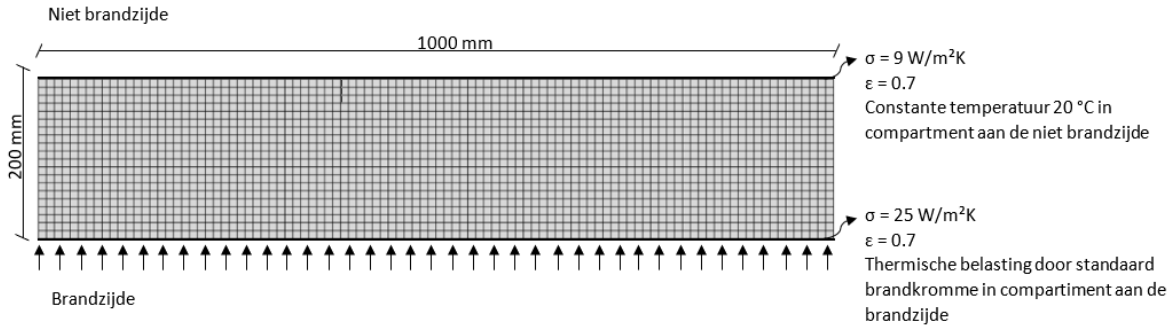

Analyse procedure
Niet gekoppelde thermische-mechanische analuyse

Element eigenschappen

Materiaal	Beton
Absolute nul temperatuur	-273.15
Type elementennet	DC2D8
Afmeting elementennet	10x10 mm
Step response	Transient
Solver equation	Direct solver
Oplossingsmethode	Full-Newton Raphson

Figuur 4. Model doorgaande monoliet betonvloer

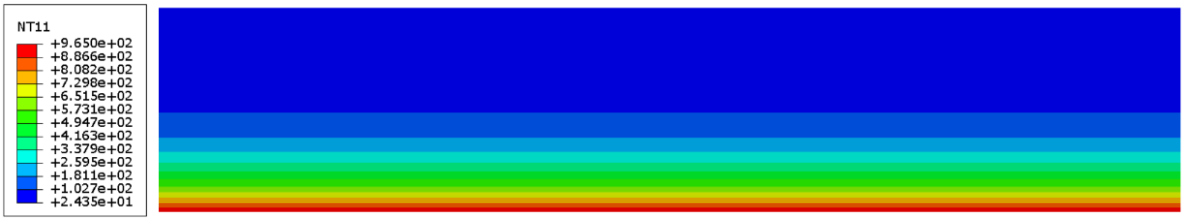

Figuur 5. Uitvoer ABAQUS model doorgaande monoliet betonvloer na 120 minuten

De resultaten van de numerieke analyses komen dermate overeen met de eerder besproken analyses, dat gesteld kan worden dat het gebruikte numerieke model gevalideerd is. Daarom is de verwachting dat dit model voor de beschouwde temperatuursoverdrachtmechanismen gebruikt kan worden voor complexere constructies.

Aandachtspunten

In het verificatie onderzoek is gekeken naar een monoliet vloer, echter is het doel de gevolgen te onderzoeken van een brand ter plaatse van de voeg tussen twee breedplaatvloeren. Om dit onderzoek goed uit te voeren, moet er gekeken worden naar de verschillen tussen deze twee situaties. Hierbij komen aandachtspunten naar voren bij twee overdrachtmechanismen, namelijk straling en convectie. Deze worden ten opzichte van de vlakke vloer extra opgelegd ter plaatse van de voeg. Uit de Eurocode kunnen de constante waardes voor convectie en straling overgenomen worden voor de onderzijde van de plaat. Echter geeft de Eurocode geen waardes welke gebruikt kunnen worden ter plaatse van de voeg.

Straling kan op twee manieren invloed hebben in de voeg, door zowel de straling van de plaat zelf als door brand aan de onderzijde van de plaat. De verwachting is dat de straling van de plaat gedurende de brand gelijk is aan beide zijdes van de voeg en daarom geen temperatuurverhoging veroorzaakt. De straling door brand aan de onderzijde van de plaat heeft wel invloed. Hierbij speelt de zichtfactor een belangrijke rol. Deze bepaald hoeveel straling op het te ontvangen vlak valt. Op het moment dat het ontvangende vlak en het zendende vlak tegenover elkaar staan kan aangenomen worden dat de zichtfactor 1 is. Zodra er een belemmering is tussen deze vlakken, zal de zichtfactor kleiner en de straling groter worden. Dit laatste is het geval ter plaatse van de voeg.

Voor de convectie is de luchtsnelheid in de voeg belangrijk. Door de aanwezigheid van brand en de hierdoor grote temperatuurverschillen onder de vloer zijn de luchtsnelheid en de wervelingen van de lucht hoger. De aanname is dat ter plaatse van de voeg wervelingen erg klein zijn door de beperkte ruimte en dat de temperatuurverschillen daardoor relatief laag zijn. Om deze reden wordt er in de voeg een lagere convectiecoefficient toegepast. In het onderzoek is er voor deze convectiecoefficient een aanname gemaakt. Met behulp van een gevoeligheidsanalyse voor dit aandachtspunt is gebleken dat verschillende convectiecoëfficiënten in de analyse een zeer beperkt effect hebben op het temperatuurverschil.

Naast deze twee aandachtspunten zijn er ook een sensitiviteitsanalyses uitgevoerd op de fijnheid van het gehanteerde elementennet, de standaard brandkromme en de emissie coëfficiënt. Op basis van deze analyses zijn uitgangspunten voor in het numerieke model voor de breedplaatvloer bepaald.

Voor het bepalen van de temperatuurontwikkeling ter plaatse van de voeg tussen twee breedplaten in een breedplaatvloer, is een numeriek model op dezelfde basis opgesteld als voor het vergelijkend onderzoek. In dit model is de voeg tussen twee breedplaatvloeren meegenomen. In deze analyse is de vloer onderzocht op basis een variërende voegbreedte van 1 mm tot 19 mm in stapjes van 1 mm. De breedplaatdikte is gevarieerd tussen 50 mm en 100 mm. Uit de analyses zijn de volgende resultaten gekomen.

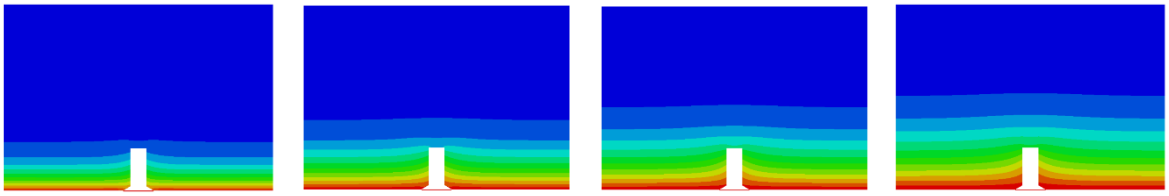

Figuur 6. Voorbeeld temperatuurontwikkeling in de breedplaatvloer op t=30, t=60, t=90 en t=120 minuten

In figuur 6 is het temperatuurverloop zichtbaar in de breedplaatvloeren op 30, 60, 90 en 120 minuten. Hieruit blijkt dat de onderzijde van de breedplaatvloer de hoogste temperatuur bereikt. Daarnaast is te zien dat de temperatuur rondom de voeg hoger is dan bijvoorbeeld op 50 mm van de voeg af. Dit heeft de maken met de straling en convectie in de voeg. Dit temperatuurverloop kan teruggevonden worden in

meerdere analyses met verschillende voegbreedtes en breedplaatdiktes. Echter is er wel een verschil in de temperatuursontwikkeling van de verschillende breedplaatvloeren. Naar mate de breedplaat dunner wordt, of de voegbreedte groter, neemt het verschil in temperatuur van het beton op de locatie van de voeg sneller toe dan de temperatuur van het beton op een afstand van 50 mm naast de voeg. Hieruit kan geconcludeerd worden dat een breedplaatvloer met een voegbreedte van 19 mm en een breedplaatdiepte van 50 mm de hoogste temperatuurontwikkeling geeft. Deze gecombineerde situatie geeft de maatgevende temperatuur op de locatie boven de voeg en wordt verder gebruikt voor de analyse van het temperatuurverloop op diverse locaties in het beton.
In de breedplaatvloer wordt de temperatuur geanalyseerd op drie locaties. Deze locaties zijn uitgewerkt in figuur 7 en de analyse van de temperaturen op deze locaties wordt gegeven in figuur 8.

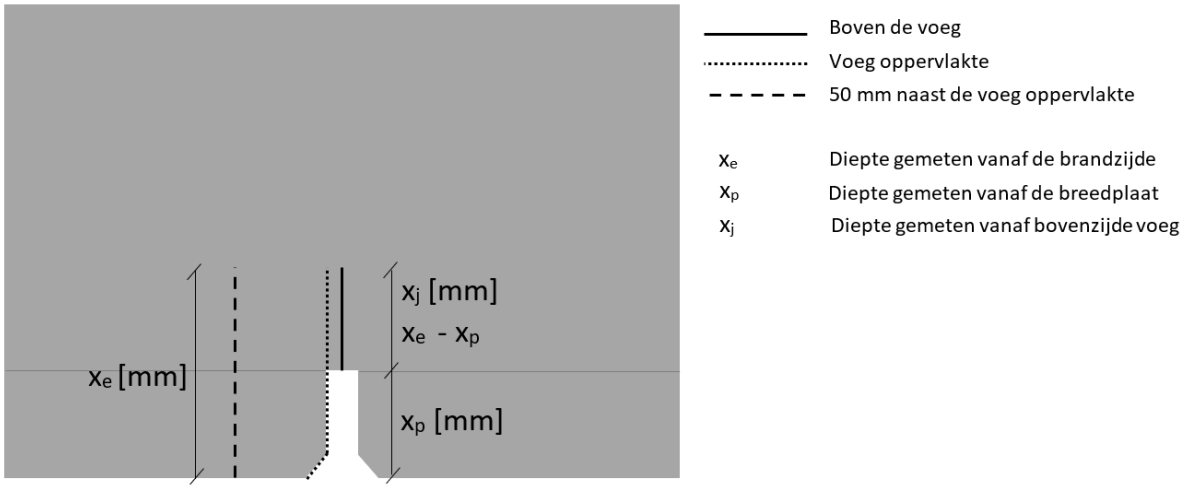

Figuur 7. Omschrijving diverse geanalyseerde locaties in de betonvloer

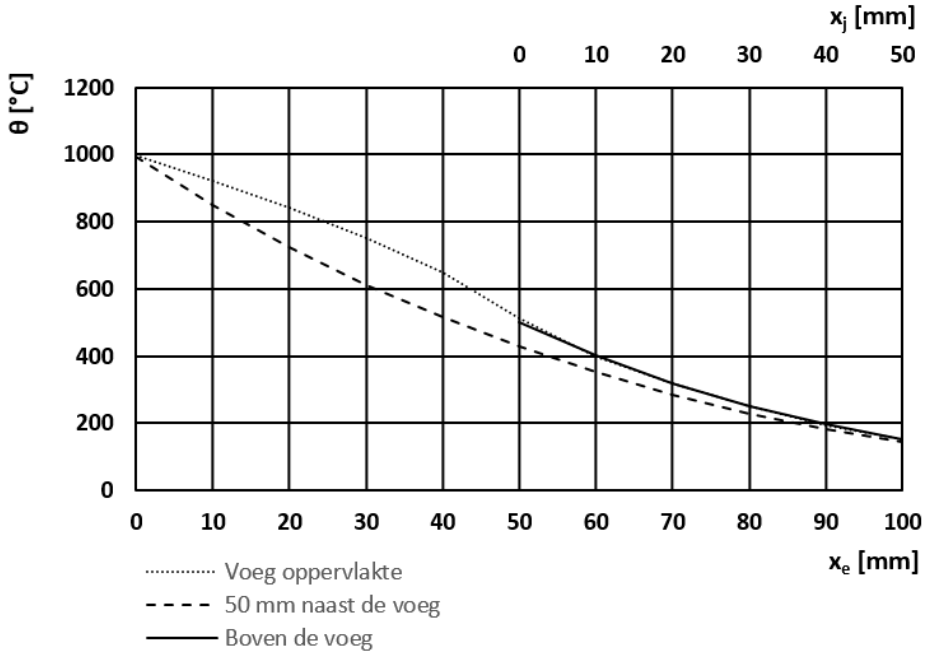

Figuur 8. Temperatuur van het beton na 120 minuten op drie verschillende locaties in de vloer met een voeg van 50 mm diep en 19 mm breed.

In de figuur 8 zijn de drie locaties van figuur 7 geplot na een brand van 120 minuten. Hierin komt nogmaals naar voren dat het beton ter plaatse van de voeg de hoogste temperatuur bereikt. Op basis van de analyse van het temperatuurverloop kan geconcludeerd worden dat de temperatuur van het beton boven de voeg lager blijft dan de temperatuur van de breedplaat. Hierdoor zal het beton van de breedplaat meer afnemen in zowel druk- als treksterkte. Bovendien wordt er aangenomen dat het betonstaal in het beton, dezelfde temperatuur aanneemt als het beton op die locatie. Dit heeft als gevolg dat het betonstaal in de breedplaat warmer zal worden en meer sterkte verliest dan de koppelwapening welke zich boven de voeg bevindt.

Om te bepalen hoeveel het betonstaal in sterkte afneemt, kan de momentcapaciteit berekend worden met een gereduceerde drukzone. Voor deze gereduceerde drukzone wordt het beton met een hogere temperatuur dan 500 graden Celsius buiten beschouwing gelaten. De afname van de sterkte van het betonstaal wordt opgenomen in de f_{yd}. Op basis van de gereduceerde drukzone en sterkte van de wapening wordt bepaald dat de momentcapaciteit van de vloer ter plaatse van de breedplaatvloer meer afneemt dan op de locatie boven de voeg. Hierbij wordt aangenomen dat er in de breedplaat en boven de voeg hetzelfde formaat betonstaal wordt toegepast. Bijvoorbeeld bij het gebruik van wapening Ø12, na een brand van 30 minuten, zal de momentcapaciteit in de doorsnede boven de naad met 9.9% zijn afgenomen en de momentcapaciteit in de doorsnede van de breedplaatvloer met 23.1%. Doordat de breedplaat in deze situatie een procentueel grotere afname in momentcapaciteit heeft, zal deze locatie als eerste bezwijken.

Daarnaast treedt er vervorming op in de breedplaatvloer ten gevolge de temperatuur toename in de breedplaatvloer. De breedplaatvloer wil uitzetten. Bij een grotere temperatuur toename, is de verwachting dat een grotere vervorming zal optreden. Om deze reden zal de onderzijde van de breedplaat verder uitzetten dan de bovenzijde van de vloer. Doordat de vervorming van de onderzijde van de plaat belemmerd wordt, zal deze kromtrekken. Met behulp van de uitvoer van het thermisch model in ABAQUS is een mechanisch model in ABAQUS opgezet om een idee van de vervormingen te krijgen. Deze vervormingen zijn in figuur 9 gevisualiseerd. De verwachting is dat door de kromtrekking de breedplaten in de druklaag duwen. Hierdoor ontstaan extra normaaldrukspanningen in de vloer ter plaatse van het aansluitvlak tussen de breedplaat en de druklaag. In dit onderzoek is geen verder onderzoek uitgevoerd naar de extra normaaldrukspanningen en om deze reden kan er geen verdere uitspraak worden gedaan over de gevolgen van de sterkte voor de breedplaatvloer door deze spanningen.

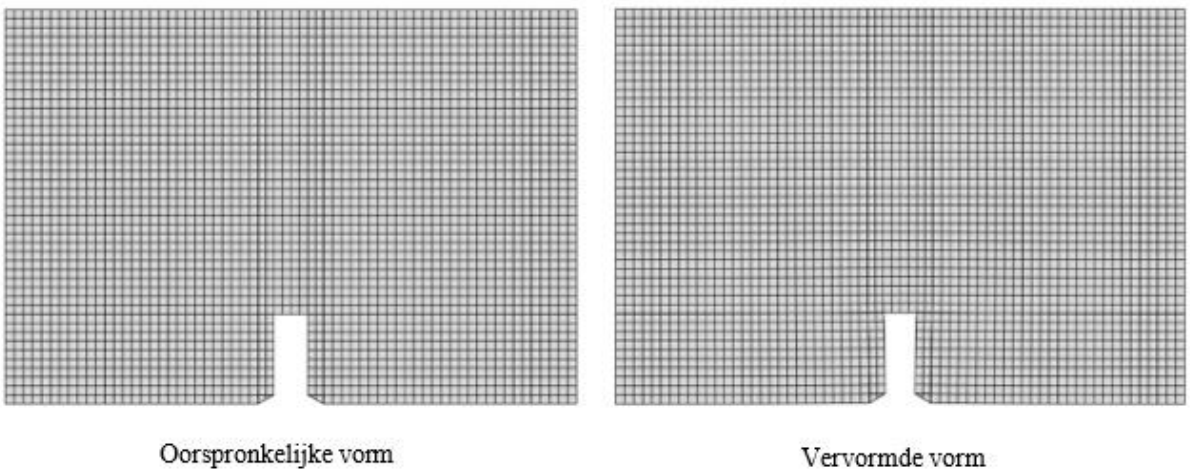

Figuur 9. Indicatie vervorming breedplaatvloer

Slotwoord
Het hiervoor beschreven onderzoek is gebaseerd op waardes uit de NEN-EN 1992-1-2. Het numerieke model dat gegenereerd is, heeft een aanname op de locatie van de voeg voor de convectie coefficient welke onderzocht is met een gevoeligheidsanalyse. In de analyse naar de toenemende temperatuur van de breedplaatvloer zijn de verschijnselen spatten en thermisch scheuren niet opgenomen.

Op basis van het onderzoek naar het temperatuurverloop in een breedplaatvloer ten gevolge van brand kan geconcludeerd worden dat de ontwerpregel in de NEN-EN 13747 juist is. Een onjuiste uitvoering van de breedplaatvloer ter plaatse van de voeg leidt niet tot een meer kritische situatie van de koppelwapening bij brand. In dit onderzoek is de verdere constructieve beschouwing van de breedplaatvloer na een brand niet meegenomen. Ook is er de mogelijkheid dat resultaten voor specifieke situaties met het gebruik van een natuurlijke brandkromme afwijkend zijn. De reden hiervan is dat er in dit onderzoek enkel gebruik is gemaakt van een thermische belasting door gastemperaturen en de lokale brandhaard buiten beschouwing is gelaten.

References

[1] "EN 1992-1-2 Design of concrete structures - Part 1-2: General rules- Structural fire design," NEN, 2005.

[2] A. Lazouski, "Influence of sustained stress and heating conditions on the occurence of fire-induced concrete spalling," University of Edinburgh, 2017-2019.

[3] J. Zehfuß, F. Robert, J. Spille and R. N. Razafinjato, "Evaluation of Eurocode 2 approaches for thermal conductivity of concrete in case of fire," Ernst & Sohn, 2020.

[4] A. Levesque, "Fire Performance of Reinforced Concrete Slabs," 2006.

[5] A. Saetta, R. Scotta and R. Vitaliani, "Stress Analysis of Concrete Structures Subjected To Variable Thermal Loads," *Journal of Structural Engineering,* vol. 121, pp. 446-457, 1995.

[6] D. Di Capua and A. R. Mari, "Nonlinear analysis of reinforced concrete cross-sections exposed to fire," *Fire Safety Journal,* vol. 42, pp. 139-149, 2007.

[7] T. Ficker, "Measurement of emissivity in student laboratories," *European Journal of Physics,* vol. 41, p. 22, 2020.

[8] "NEN-EN 13747:2005+A2:2010, Vooraf vervaardigde betonproducten - Breedplaatvloeren," CEN, 2010.

[9] S. N. M. Wijte, "Rapport 9780-1-0 Voorstellen vooren achtergronden bij rekenregels van beoordeling van bestaande bouw.," Adviesbureau ir. J.G. Hageman B.V., Rijswijk, 20 mei 2019.

[10] "NEN-EN 1992-1-1:2004+AC:2008+AC:2010, Ontwerp en berekening van betonconstructies - Deel 1-1: Algemene regels voor gebouwen," CEN, 2016.

[11] "NEN-EN 1992-1-2 Ontwerp en berekening van betonconstructies - Deel 1-2: Algemene regels - Ontwerp en berekening van constructies bij brand," NEN, 2005.

[12] A. Bejan and A. D. Kraus, Heat transfer handbook, Hoboken, New Jersey: John Wiley & Sons, Inc., 2003.

List of figures

Fig. B5. Peak values for Cp for 0%, 1.5% and 3% moisture content.

Fig. C1. Comparison temperatures in floor with EN 1992-1-2 graphical and analytical approach, 30 minutes
Fig. C2. Comparison temperatures in floor with EN 1992-1-2 graphical and analytical approach, 60 minutes
Fig. C3. Comparison temperatures in floor with EN 1992-1-2 graphical and analytical approach, 90 minutes
Fig. C4. Comparison temperatures in floor with EN 1992-1-2 graphical and analytical approach, 120 minutes
Fig. C5. Comparison temperatures in floor with EN 1992-1-2 graphical, and analytical approach for different settings of k, 60 minutes
Fig. C6. Comparison temperatures in floor with EN 1992-1-2 graphical, and analytical approach for different settings of k, 90 minutes
Fig. C7. Comparison temperatures in floor with EN 1992-1-2 graphical, and analytical approach for different settings of k, 120 minutes

Fig. D1. Dividing area around the analyzing element
Fig. D2. Dividing internal part in layers.
Fig. D3. Example of calculation surface temperature with Finite difference method
Fig. D4. Example of calculation net heat flux
Fig. D5. Example of calculation of the temperature of an internal with Finite difference method

Fig. E1. Comparison between graphical, analytical, and numerical analysis for the simplified structure at 30 minutes.
Fig. E2. Comparison between graphical, analytical, and numerical analysis for the simplified structure at 60 minutes
Fig. E3. Comparison between graphical, analytical, and numerical analysis for the simplified structure at 90 minutes
Fig.E4. Comparison between graphical, analytical, and numerical analysis for the simplified structure at 120 minutes

Fig. F1. Location of calculated view factor at the straight surface at the precast plate
Fig. F2. Calculation method of the view factor at the straight surface at the precast plate
Fig. F3. Measurement of the diagonals at a composite floor
Fig. F4. Location of calculated view factor at the diagonal parts at the bottom of the joint
Fig. F5. Calculation method of the view factor at the diagonal parts at the bottom of the joint
Fig. F6. Location of calculated view factor at the straight part of the in-situ layer
Fig. F7. Calculation method of the view factor at the straight surface of the in-situ layer
Fig. F8. Overview model thermal radiation

Fig. I1. Decrease of tensile strength of reinforcement due to temperature change [1]

Figuur 4. Detail koppelwapening in breedplaatvloer *[9]*
Figuur 5. Gas temperatuur volgens de standaard brandkromme en een voorbeeld van een natuurlijke brandkromme

Figuur 6. Grafiek temperatuur toename in een beton vloer van 200 mm dik met *Rx* is de tijdsduur van de brand *[1]*
Figuur 4. Model doorgaande monoliet betonvloer
Figuur 5. Uitvoer ABAQUS model doorgaande monoliet betonvloer na 120 minuten
Figuur 6. Voorbeeld temperatuurontwikkeling in de breedplaatvloer op t=30, t=60, t=90 en t=120 minuten
Figuur 7. Omschrijving diverse geanalyseerde locaties in de betonvloer
Figuur 8. Temperatuur van het beton na 120 minuten op drie verschillende locaties in de vloer met een voeg van 50 mm diep en 19 mm breed.
Figuur 9. Indicatie vervorming breedplaatvloer

Excel file Results heat transfer analyses composite floor at the location of the joint

Temperatures above the joint, joint width 1 mm

Temperature concrete above the joint after 30 minutes at different joint depts and joint width of 1 mm [°C]						
x_j [mm]	**Joint depth [mm]**					
	50	60	70	80	90	100
0	93	67	49	37	29	22
5	78	56	41	30	21	17
10	65	47	34	25	17	14
15	54	39	28	20	14	11
20	45	32	23	17	10	9
25	38	27	19	14	9	7
30	31	22	16	11	7	6
35	26	18	13	9	6	5
40	22	15	10	7	5	4
45	18	12	8	6	4	3
50	15	10	7	5	3	2

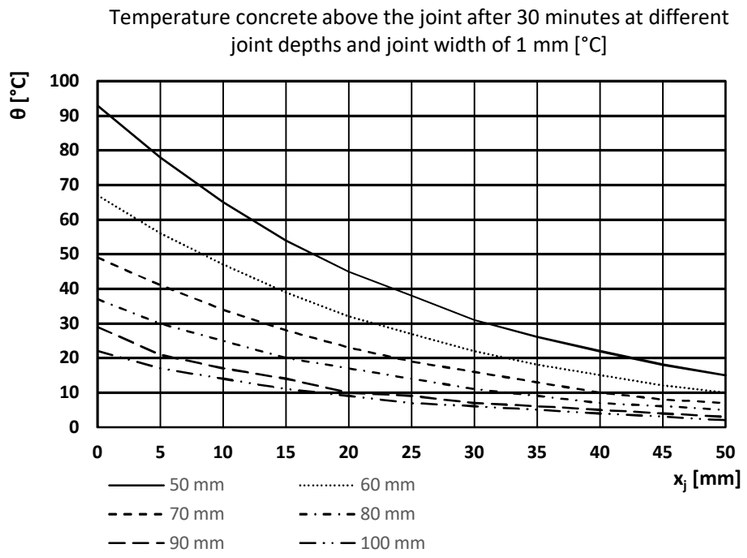

Temperature concrete above the joint after 60 minutes at different joint depts and joint width of 1 mm [°C]						
x_j [mm]	**Joint depth [mm]**					
	50	60	70	80	90	100
0	220	159	122	97	72	63
5	187	137	107	85	68	55
10	156	120	94	74	59	48
15	135	105	82	65	50	42
20	118	92	72	57	44	37
25	104	81	64	50	39	32
30	91	71	56	44	34	28
35	80	63	49	39	29	25
40	70	55	43	34	26	22
45	62	49	38	30	23	19
50	55	43	34	26	20	16

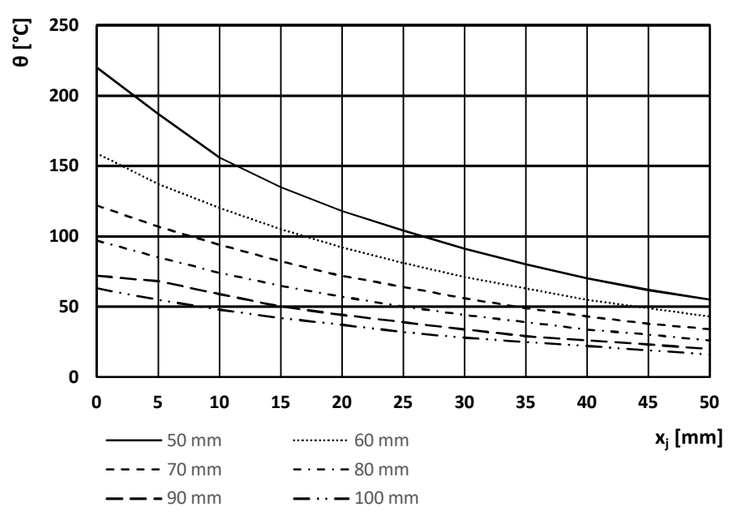

Temperature concrete above the joint after 90 minutes at different joint depts and joint width of 1 mm [°C]						
x_j [mm]	**Joint depth [mm]**					
	50	60	70	80	90	100
0	327	258	201	155	127	105
5	290	227	175	137	110	94
10	255	198	151	123	98	84
15	224	171	135	110	88	75
20	195	149	121	99	80	68
25	169	133	108	89	72	61
30	147	119	97	80	64	55
35	132	107	88	72	58	49
40	118	96	79	65	52	45
45	106	87	71	59	46	40
50	96	78	64	53	43	36

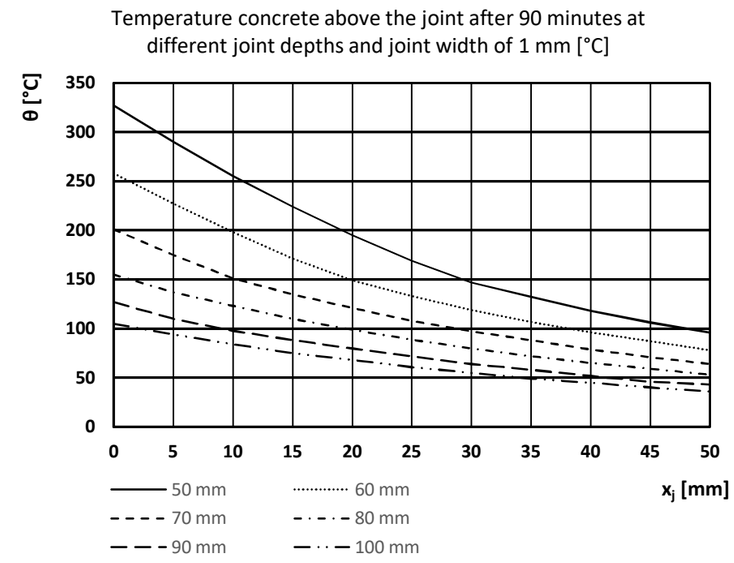

Temperature concrete above the joint after 120 minutes at different joint depts and joint width of 1 mm [°C]						
x_j [mm]	**Joint depth [mm]**					
	50	60	70	80	90	100
0	405	334	274	222	170	145
5	368	301	245	197	151	131
10	331	270	218	174	136	119
15	298	241	193	153	124	108
20	267	215	171	138	113	98
25	239	191	151	126	103	90
30	213	169	136	115	94	82
35	189	149	124	104	86	75
40	167	135	113	95	79	68
45	148	123	103	87	71	63
50	135	113	95	80	62	57

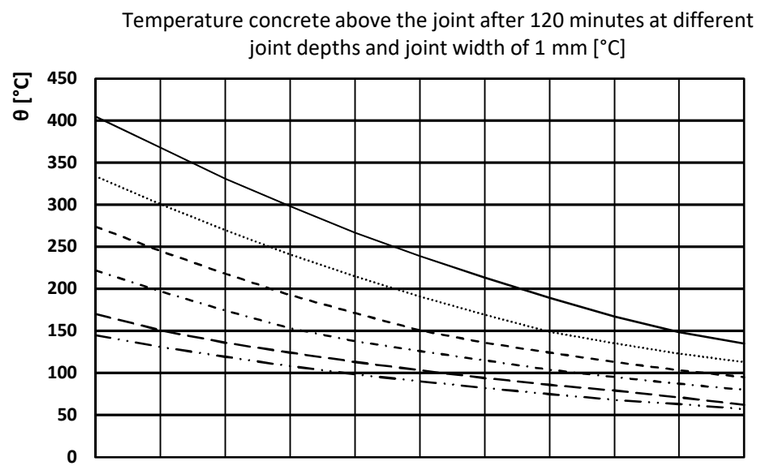

Temperatures above the joint, joint width 2 mm

Temperature concrete above the joint after 30 minutes at different joint depts and joint width of 2 mm [°C]						
x_j [mm]	**Joint depth [mm]**					
	50	60	70	80	90	100
0	92	66	48	36	28	21
5	78	56	41	30	21	17
10	65	47	34	25	17	14
15	54	39	28	20	14	11
20	45	32	23	17	10	9
25	38	27	19	14	9	7
30	32	23	17	12	8	7
35	26	18	13	9	6	5
40	22	15	10	7	5	4
45	18	12	8	6	4	3
50	15	10	7	5	3	2

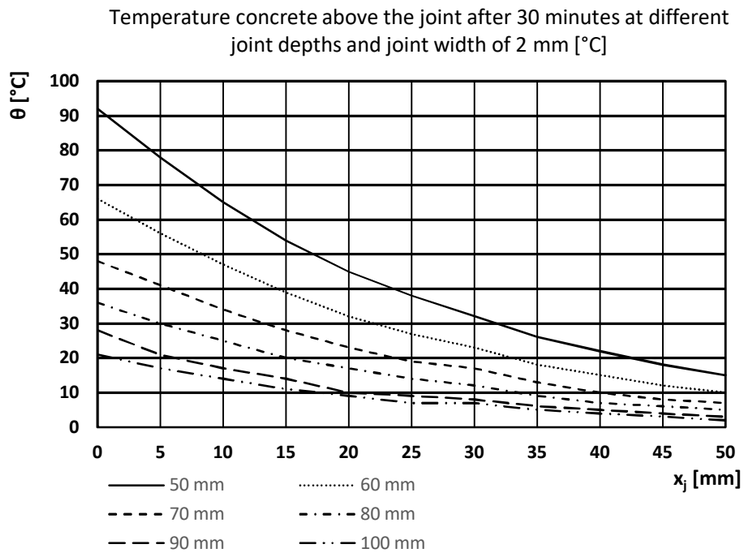

Temperature concrete above the joint after 60 minutes at different joint depts and joint width of 2 mm [°C]						
x_j [mm]	**Joint depth [mm]**					
	50	60	70	80	90	100
0	218	157	120	95	70	61
5	187	137	107	85	68	55
10	157	121	93	75	59	49
15	135	105	82	65	50	42
20	118	92	72	57	44	37
25	104	81	64	50	39	32
30	91	71	56	44	34	28
35	80	63	49	39	29	25
40	71	56	44	35	27	23
45	62	49	38	30	23	19
50	55	43	34	26	20	16

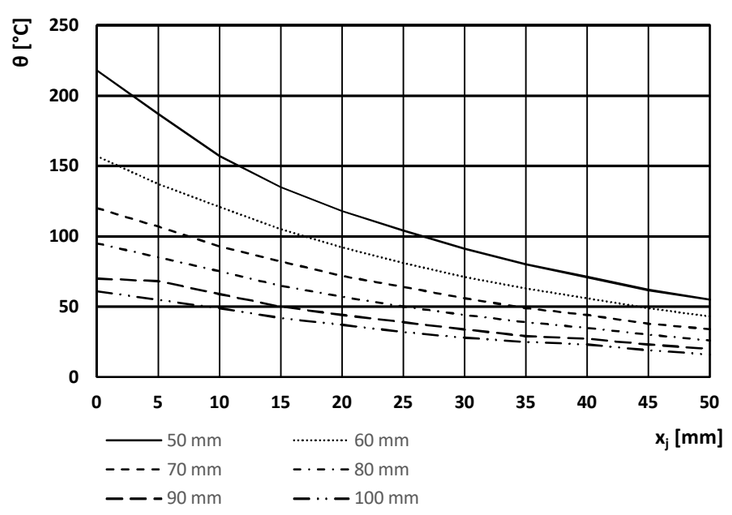

Temperature concrete above the joint after 90 minutes at different joint depts and joint width of 2 mm [°C]						
x_j [mm]	**Joint depth [mm]**					
	50	60	70	80	90	100
0	325	256	199	153	125	103
5	291	228	176	138	111	95
10	257	200	153	125	100	86
15	225	172	136	111	89	76
20	196	150	122	100	81	69
25	170	134	109	90	73	62
30	148	120	98	81	65	56
35	132	107	88	72	58	49
40	119	97	80	66	53	46
45	107	88	72	60	47	41
50	96	78	64	53	43	36

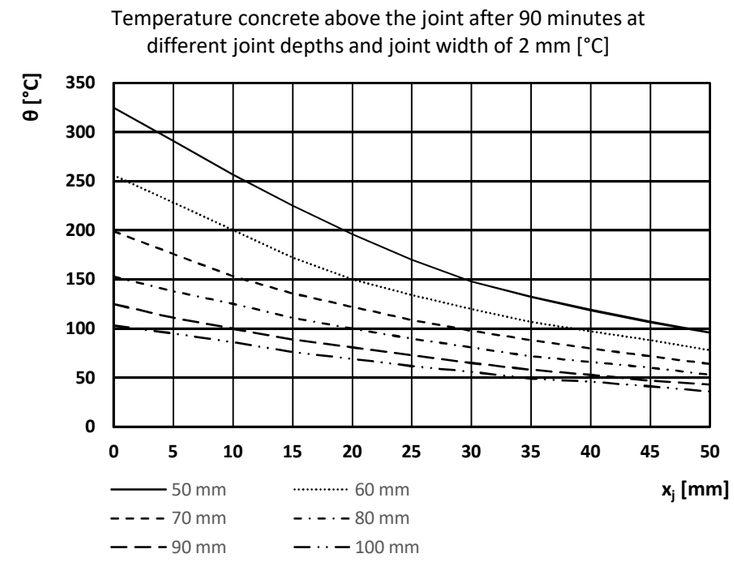

Temperature concrete above the joint after 120 minutes at different joint depts and joint width of 2 mm [°C]						
x_j [mm]	**Joint depth [mm]**					
	50	60	70	80	90	100
0	404	333	273	221	169	144
5	369	302	246	198	152	132
10	333	272	220	176	138	121
15	300	243	195	155	126	110
20	269	217	173	140	114	100
25	241	193	152	128	105	92
30	214	170	137	116	95	83
35	190	150	125	105	87	76
40	168	136	114	96	80	69
45	149	124	104	88	72	64
50	136	114	96	81	63	58

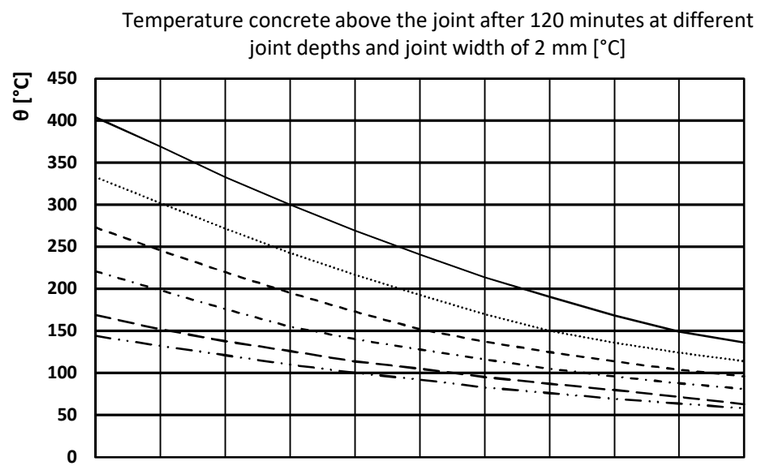

Temperatures above the joint, joint width 3 mm

Temperature concrete above the joint after 30 minutes at different joint depts and joint width of 3 mm [°C]						
x_j [mm]	Joint depth [mm]					
	50	60	70	80	90	100
0	90	64	46	34	26	19
5	77	55	40	29	20	16
10	65	47	34	25	17	14
15	54	39	28	20	14	11
20	45	32	23	17	10	9
25	38	27	19	14	9	7
30	32	23	17	12	8	7
35	26	18	13	9	6	5
40	22	15	10	7	5	4
45	18	12	8	6	4	3
50	15	10	7	5	3	2

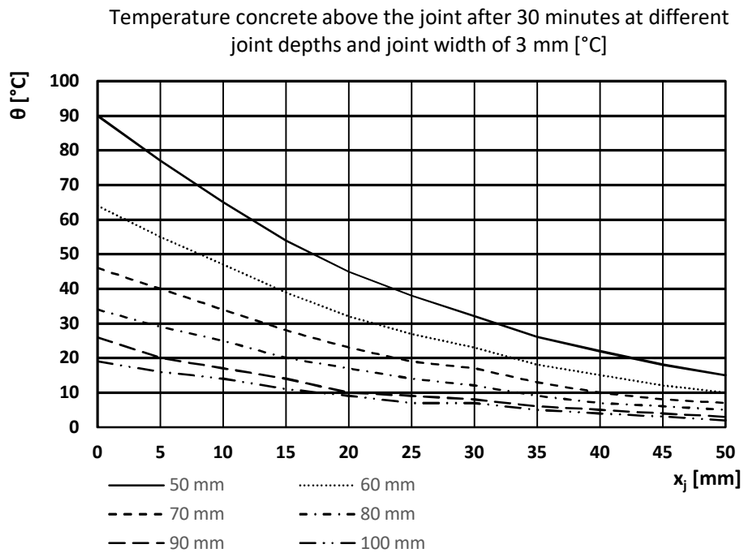

Temperature concrete above the joint after 60 minutes at different joint depts and joint width of 3 mm [°C]						
x_j [mm]	Joint depth [mm]					
	50	60	70	80	90	100
0	213	152	115	90	65	56
5	186	136	106	84	67	56
10	156	120	94	74	58	48
15	135	105	82	65	50	42
20	118	92	72	57	44	37
25	104	81	64	50	39	32
30	91	71	56	44	34	28
35	80	63	49	39	29	25
40	71	56	44	35	27	23
45	62	49	38	30	23	19
50	55	43	34	26	20	16

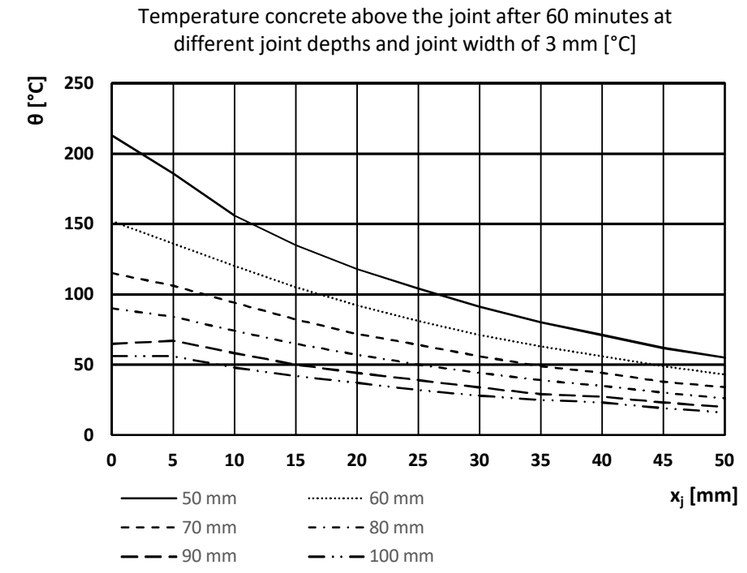

Temperature concrete above the joint after 90 minutes at different joint depts and joint width of 3 mm [°C]						
x_j [mm]	Joint depth [mm]					
	50	60	70	80	90	100
0	321	252	195	149	121	99
5	291	228	176	138	111	95
10	256	199	152	125	99	85
15	225	172	136	111	89	76
20	196	151	122	100	81	69
25	170	134	109	90	73	62
30	148	120	98	81	65	56
35	132	107	88	72	58	49
40	119	97	80	66	53	46
45	107	88	72	60	47	41
50	96	78	64	53	43	36

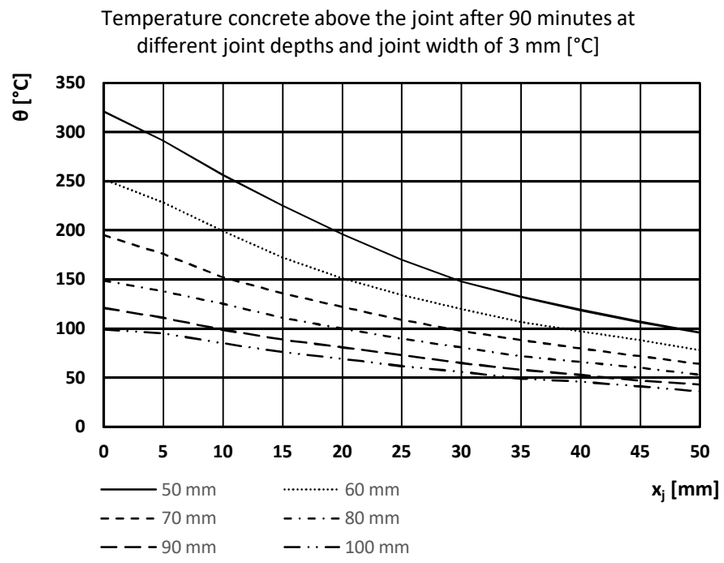

Temperature concrete above the joint after 120 minutes at different joint depts and joint width of 3 mm [°C]						
x_j [mm]	Joint depth [mm]					
	50	60	70	80	90	100
0	400	329	269	217	165	140
5	369	302	246	198	152	132
10	333	272	220	176	138	121
15	300	243	195	155	126	110
20	269	217	173	140	114	100
25	241	193	152	128	105	92
30	215	171	138	117	96	84
35	191	151	126	106	88	77
40	169	137	115	97	81	70
45	150	125	105	89	73	65
50	136	114	96	81	63	58

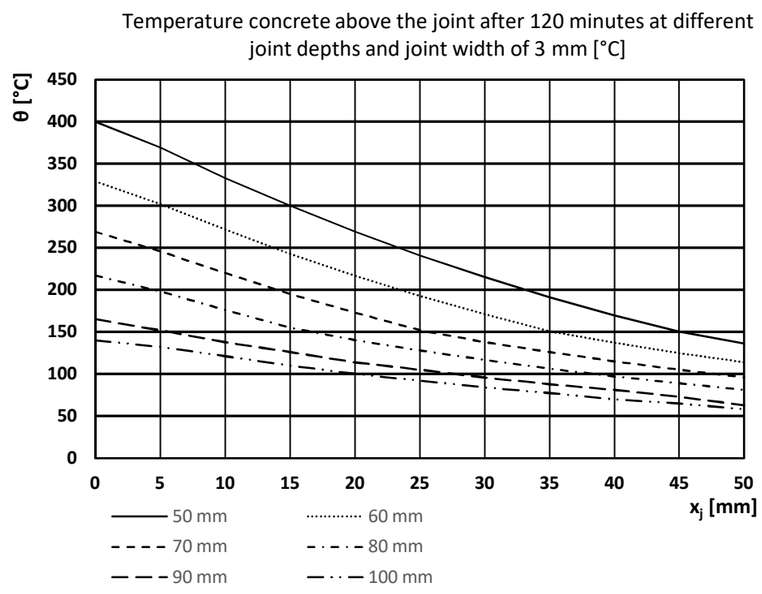

Temperatures above the joint, joint width 4 mm

Temperature concrete above the joint after 30 minutes at different joint depts and joint width of 4 mm [°C]						
x_j [mm]	**Joint depth [mm]**					
	50	60	70	80	90	100
0	84	65	48	36	20	22
5	74	56	41	30	17	18
10	62	47	34	25	14	14
15	52	39	28	21	12	12
20	44	33	24	17	9	9
25	36	27	19	14	7	8
30	30	22	16	11	6	6
35	25	19	13	9	5	5
40	21	15	11	7	4	4
45	17	12	9	6	3	3
50	14	10	7	5	2	3

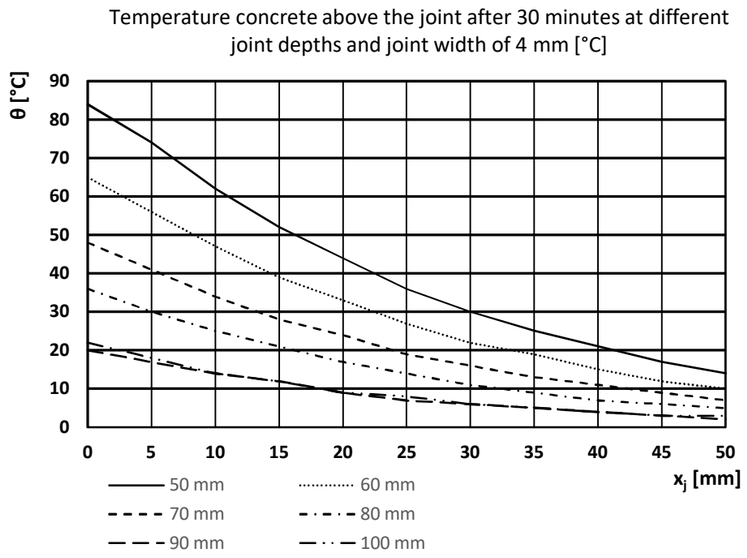

Temperature concrete above the joint after 60 minutes at different joint depts and joint width of 4 mm [°C]						
x_j [mm]	**Joint depth [mm]**					
	50	60	70	80	90	100
0	204	156	120	95	66	62
5	180	138	108	85	61	55
10	152	121	95	75	54	48
15	132	106	83	66	47	42
20	116	93	73	58	42	37
25	102	82	64	51	37	32
30	89	72	57	45	32	29
35	79	63	50	39	28	25
40	69	56	44	35	25	22
45	61	49	39	30	22	19
50	54	43	34	27	19	17

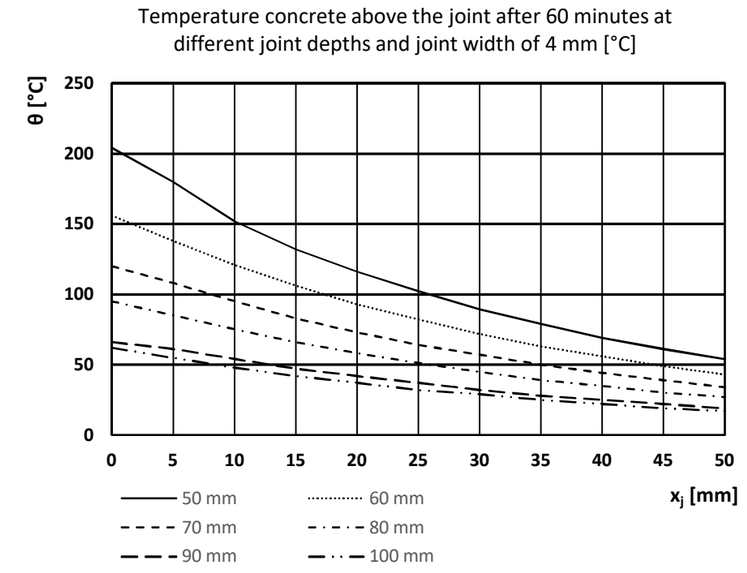

Temperature concrete above the joint after 90 minutes at different joint depts and joint width of 4 mm [°C]						
x_j [mm]	**Joint depth [mm]**					
	50	60	70	80	90	100
0	313	256	199	153	113	104
5	285	230	177	139	105	95
10	251	201	153	124	95	85
15	221	174	136	112	85	76
20	192	151	122	100	77	69
25	167	134	110	90	70	62
30	146	120	98	81	63	56
35	131	108	89	73	57	50
40	117	97	80	66	51	45
45	106	88	72	59	46	41
50	95	79	65	54	42	37

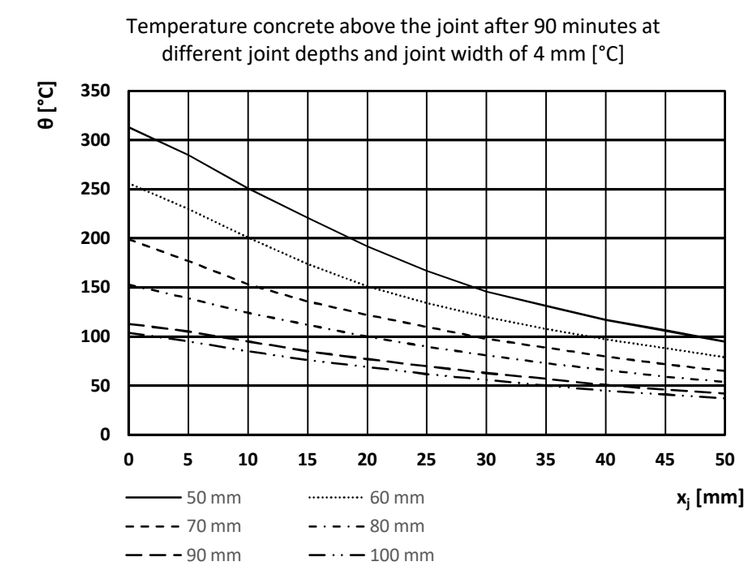

Temperature concrete above the joint after 120 minutes at different joint depts and joint width of 4 mm [°C]						
x_j [mm]	**Joint depth [mm]**					
	50	60	70	80	90	100
0	394	334	273	221	159	144
5	364	306	249	200	147	133
10	329	275	222	177	134	121
15	296	246	197	156	122	110
20	266	219	174	140	111	100
25	238	194	153	127	102	91
30	212	171	138	116	93	83
35	188	151	126	106	85	76
40	166	137	115	96	78	69
45	148	125	105	88	71	63
50	134	114	95	81	65	58

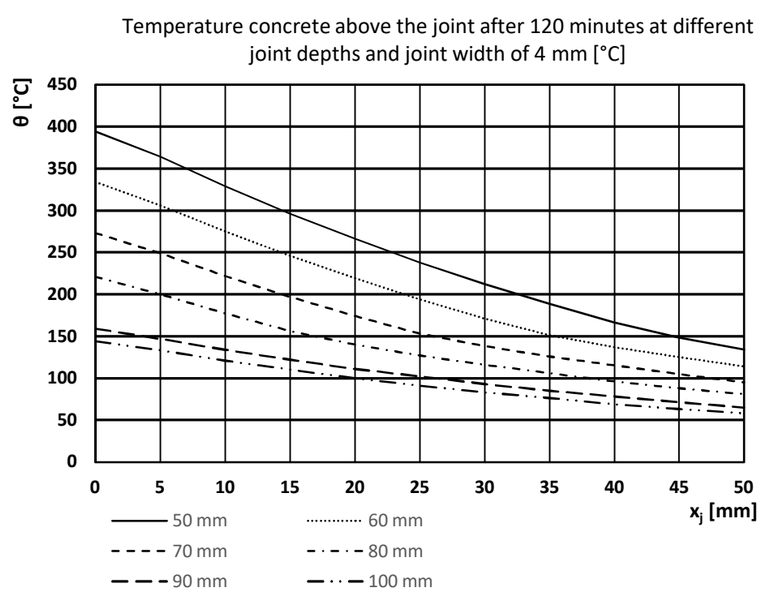

Temperatures above the joint, joint width 5 mm

Temperature concrete above the joint after 30 minutes at different joint depts and joint width of 5 mm [°C]						
x_j [mm]	Joint depth [mm]					
	50	60	70	80	90	100
0	89	65	49	37	28	22
5	78	57	42	31	24	18
10	66	47	35	26	19	15
15	55	40	29	21	16	12
20	46	33	24	17	13	10
25	38	27	20	14	11	8
30	32	23	16	12	8	6
35	27	19	13	9	7	5
40	22	15	11	8	5	4
45	18	12	9	6	4	3
50	15	10	7	5	3	3

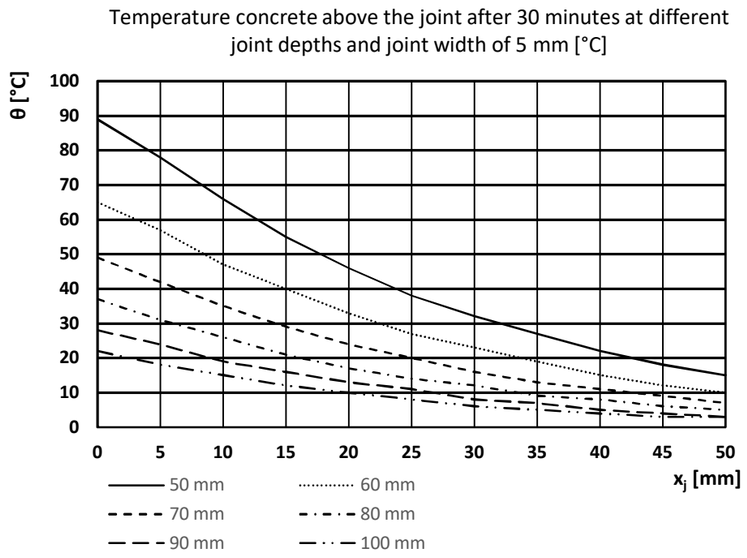

Temperature concrete above the joint after 60 minutes at different joint depts and joint width of 5 mm [°C]						
x_j [mm]	Joint depth [mm]					
	50	60	70	80	90	100
0	214	156	122	96	78	63
5	189	139	109	87	70	56
10	159	122	96	76	61	49
15	137	107	84	67	54	43
20	120	93	74	59	47	38
25	105	82	65	52	41	33
30	92	72	57	45	36	29
35	81	64	50	40	32	26
40	71	56	44	35	28	22
45	63	49	39	31	24	19
50	56	43	34	27	21	17

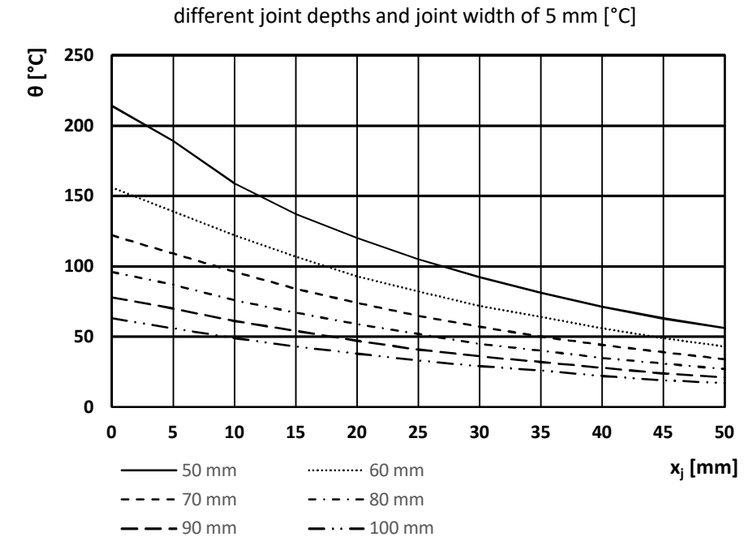

Temperature concrete above the joint after 90 minutes at different joint depts and joint width of 5 mm [°C]						
x_j [mm]	Joint depth [mm]					
	50	60	70	80	90	100
0	325	257	203	156	127	106
5	296	232	181	141	116	97
10	261	202	156	126	104	87
15	229	175	138	113	93	78
20	200	152	123	101	84	70
25	173	135	111	91	75	73
30	150	121	99	82	68	57
35	134	109	89	74	61	51
40	120	98	80	66	55	46
45	108	88	72	60	50	41
50	97	79	65	54	45	37

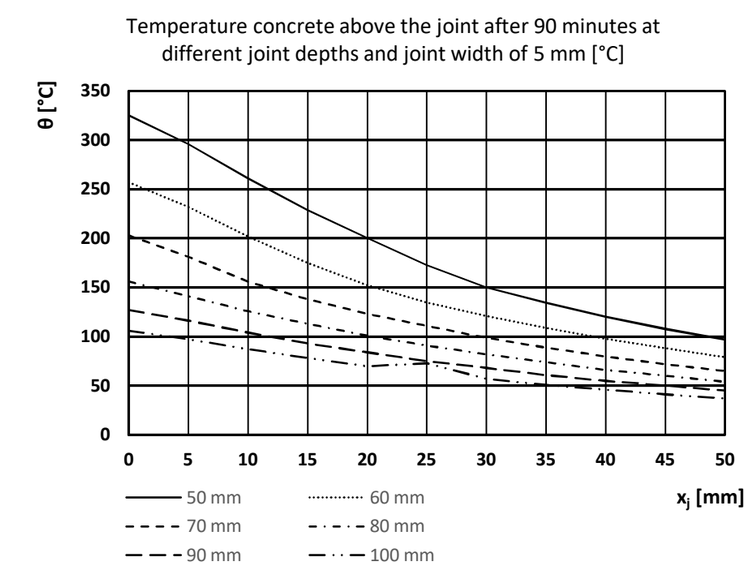

Temperature concrete above the joint after 120 minutes at different joint depts and joint width of 5 mm [°C]						
x_j [mm]	Joint depth [mm]					
	50	60	70	80	90	100
0	407	336	277	225	182	147
5	376	309	253	205	164	135
10	340	277	225	181	145	123
15	306	248	200	159	132	111
20	274	220	176	142	120	101
25	245	195	155	129	109	92
30	218	173	140	117	100	84
35	194	152	127	107	90	77
40	171	138	116	98	83	70
45	151	125	105	89	75	64
50	137	114	96	81	69	59

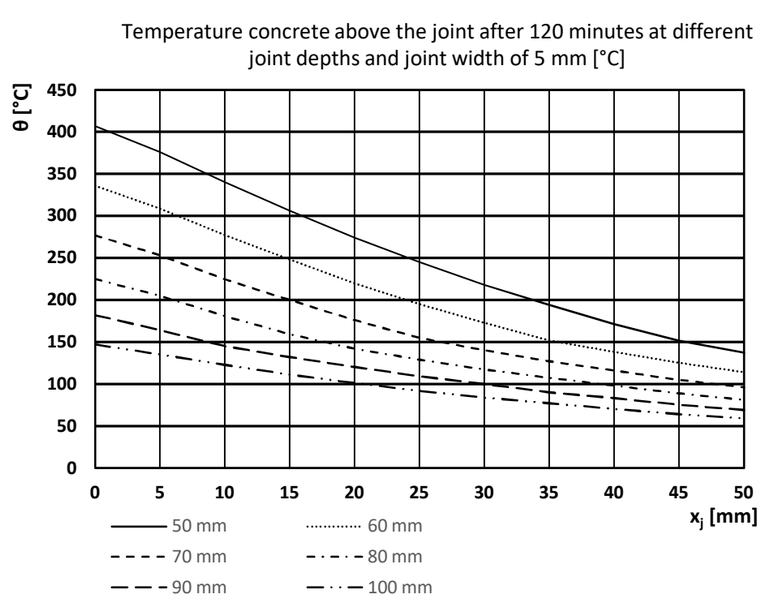

Temperatures above the joint, joint width 6 mm

Temperature concrete above the joint after 30 minutes at different joint depts and joint width of 6 mm [°C]						
x_j [mm]	**Joint depth [mm]**					
	50	60	70	80	90	100
0	83	65	48	36	28	22
5	74	57	42	31	24	19
10	62	47	35	26	20	15
15	52	40	29	21	16	12
20	44	33	24	18	13	10
25	37	27	20	14	11	8
30	30	23	16	12	9	6
35	25	19	13	9	7	5
40	21	15	11	8	6	4
45	17	13	9	6	4	3
50	14	10	7	5	4	3

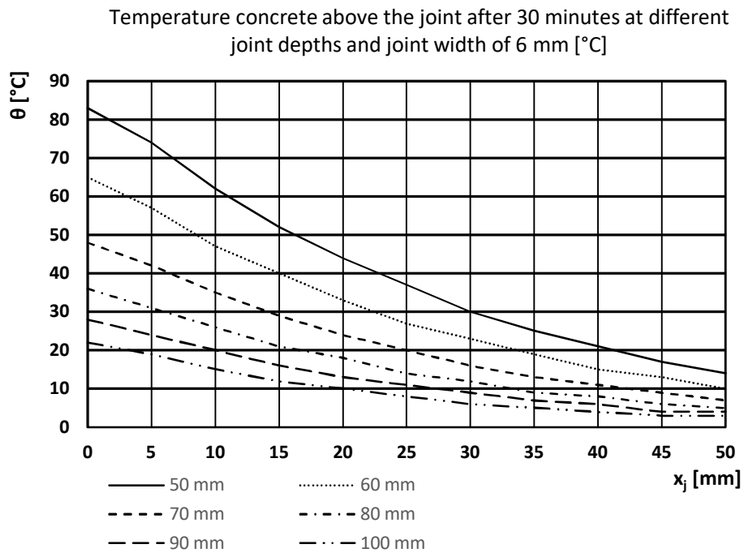

Temperature concrete above the joint after 60 minutes at different joint depts and joint width of 6 mm [°C]						
x_j [mm]	**Joint depth [mm]**					
	50	60	70	80	90	100
0	205	155	121	96	78	63
5	181	139	109	87	70	57
10	153	122	96	76	61	50
15	133	107	84	67	54	44
20	117	94	74	59	47	38
25	102	82	65	52	42	33
30	90	72	57	46	37	29
35	79	64	50	40	32	26
40	70	56	44	35	28	22
45	61	49	39	31	25	20
50	54	43	34	27	22	17

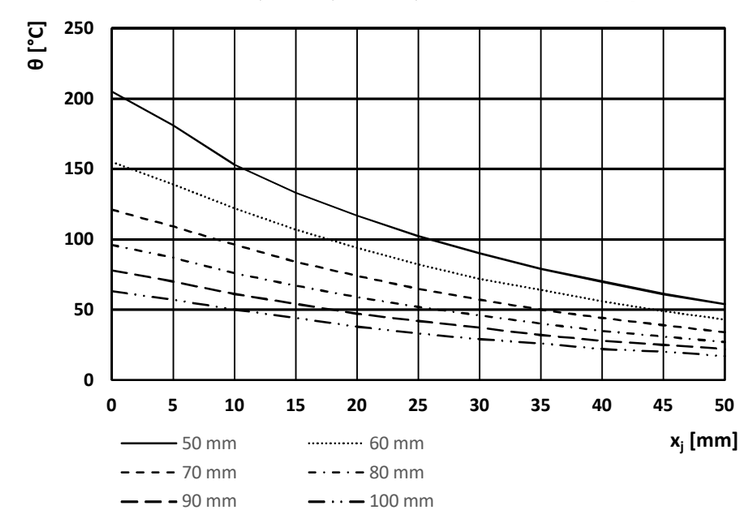

Temperature concrete above the joint after 90 minutes at different joint depts and joint width of 6 mm [°C]						
x_j [mm]	**Joint depth [mm]**					
	50	60	70	80	90	100
0	316	257	201	155	127	106
5	288	232	180	141	117	97
10	255	203	156	126	105	87
15	223	176	138	113	94	78
20	195	152	124	102	84	70
25	169	135	111	91	76	63
30	147	121	100	82	68	57
35	132	109	90	84	61	51
40	118	98	81	67	55	46
45	106	88	73	60	50	41
50	96	79	65	54	45	37

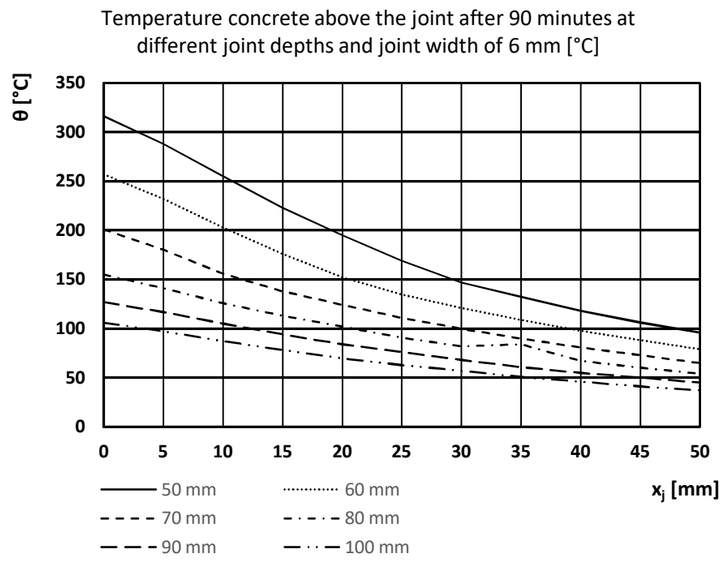

Temperature concrete above the joint after 120 minutes at different joint depts and joint width of 6 mm [°C]						
x_j [mm]	**Joint depth [mm]**					
	50	60	70	80	90	100
0	399	336	276	224	182	147
5	369	310	253	205	165	136
10	333	278	226	181	146	123
15	300	249	200	159	132	112
20	269	221	177	142	120	102
25	241	196	165	129	109	93
30	214	173	140	118	100	84
35	190	153	127	108	91	77
40	168	138	116	98	83	70
45	149	126	106	89	76	64
50	135	115	96	82	69	59

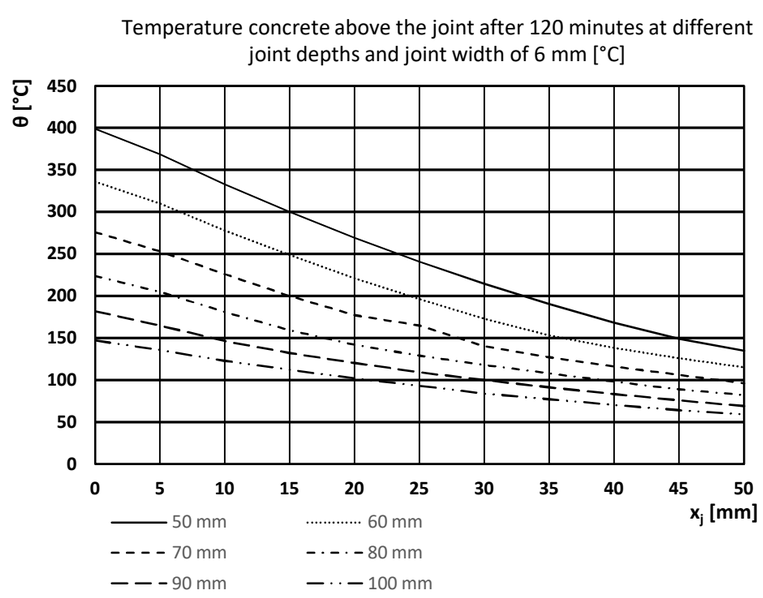

Temperatures above the joint, joint width 7 mm

Temperature concrete above the joint after 30 minutes at different joint depts and joint width of 7 mm [°C]						
x_j [mm]	**Joint depth [mm]**					
	50	60	70	80	90	100
0	82	65	48	37	29	23
5	73	57	42	32	24	19
10	62	48	35	26	20	16
15	52	40	29	22	16	13
20	44	33	24	18	13	10
25	37	28	20	15	11	8
30	31	23	16	12	9	7
35	25	18	13	10	7	5
40	21	15	11	8	6	4
45	17	13	9	6	5	3
50	14	10	7	5	4	3

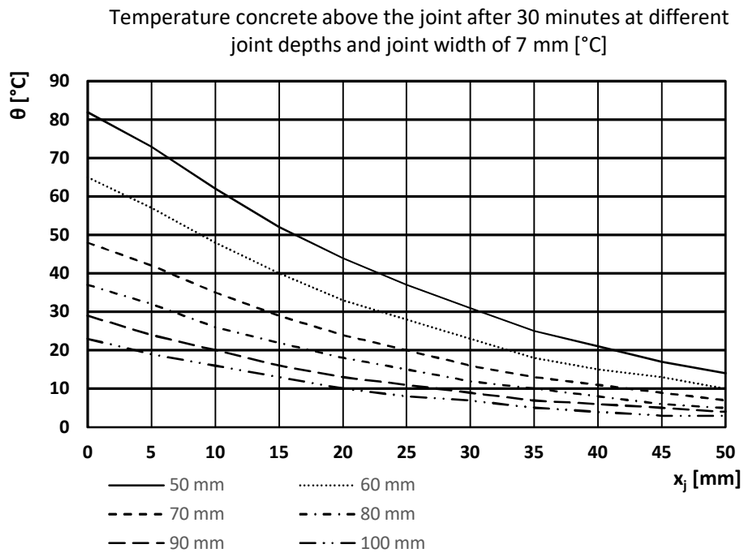

Temperature concrete above the joint after 60 minutes at different joint depts and joint width of 7 mm [°C]						
x_j [mm]	**Joint depth [mm]**					
	50	60	70	80	90	100
0	203	156	120	96	78	64
5	181	140	109	87	70	57
10	153	122	96	77	62	50
15	133	107	84	67	54	44
20	117	94	74	59	48	39
25	103	83	65	52	42	34
30	90	73	57	46	37	30
35	79	64	51	40	32	26
40	70	56	44	35	28	23
45	62	50	39	31	25	20
50	54	44	34	27	22	17

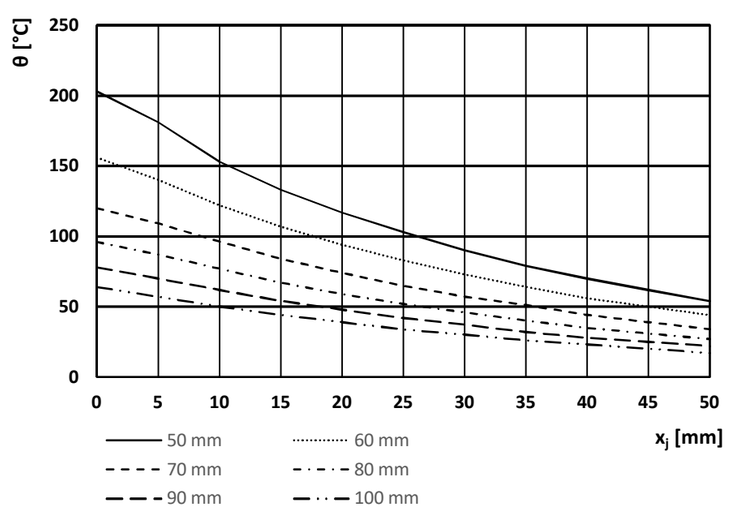

Temperature concrete above the joint after 90 minutes at different joint depts and joint width of 7 mm [°C]						
x_j [mm]	**Joint depth [mm]**					
	50	60	70	80	90	100
0	315	258	201	156	128	106
5	289	234	181	142	118	98
10	255	205	156	127	105	88
15	224	177	138	114	95	79
20	195	153	124	102	85	71
25	169	136	111	92	76	64
30	147	122	100	82	69	57
35	132	110	90	74	62	52
40	118	98	81	67	56	46
45	106	89	73	60	50	42
50	96	80	66	54	45	38

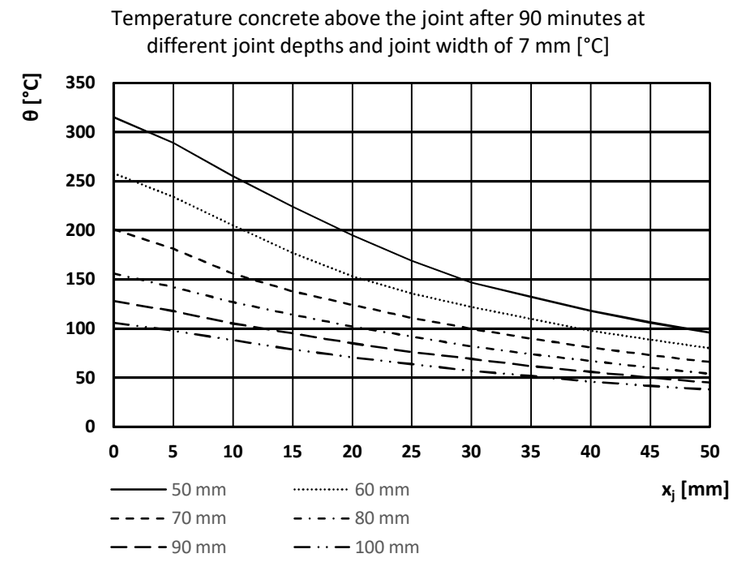

Temperature concrete above the joint after 120 minutes at different joint depts and joint width of 7 mm [°C]						
x_j [mm]	**Joint depth [mm]**					
	50	60	70	80	90	100
0	399	338	276	226	183	148
5	370	312	254	206	166	137
10	334	280	227	182	147	124
15	301	251	201	161	133	113
20	270	223	178	143	121	103
25	242	198	156	130	110	93
30	215	175	140	118	100	78
35	191	154	128	108	91	71
40	169	139	116	98	83	65
45	149	126	106	90	74	59
50	135	115	97	82	70	54

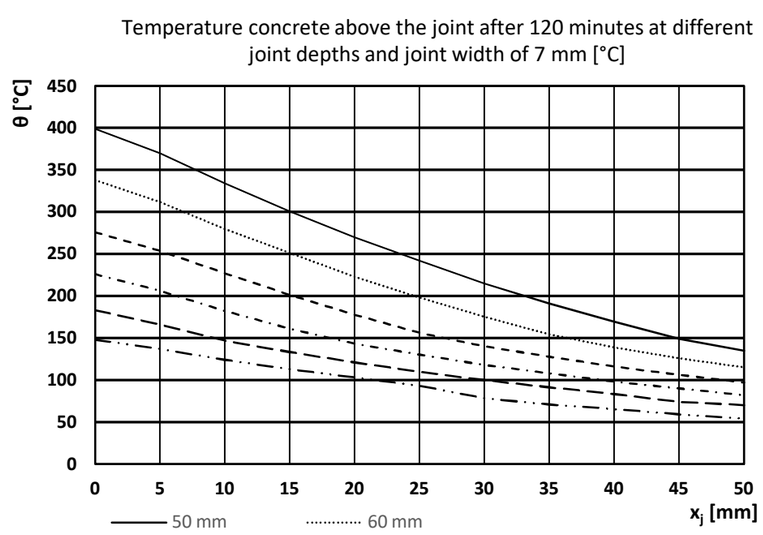

Temperatures above the joint, joint width 8 mm

Temperature concrete above the joint after 30 minutes at different joint depts and joint width of 8 mm [°C]						
x_j [mm]	Joint depth [mm]					
	50	60	70	80	90	100
0	88	64	48	37	29	23
5	77	56	42	32	25	20
10	66	48	35	26	20	16
15	55	40	29	22	17	13
20	46	33	24	18	14	11
25	39	28	20	15	11	9
30	32	23	17	12	9	7
35	27	19	14	10	7	6
40	22	16	11	8	6	4
45	18	13	9	6	5	4
50	15	10	7	5	4	3

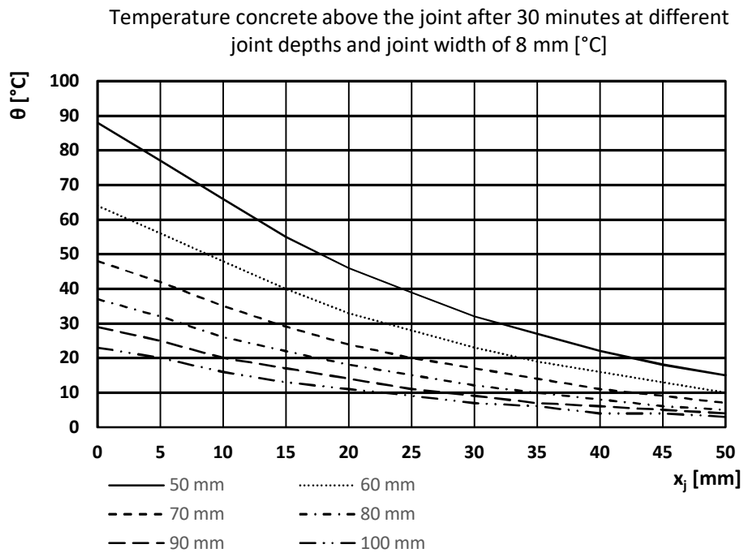

Temperature concrete above the joint after 60 minutes at different joint depts and joint width of 8 mm [°C]						
x_j [mm]	Joint depth [mm]					
	50	60	70	80	90	100
0	212	154	120	96	78	64
5	188	139	109	87	71	58
10	160	123	97	77	62	51
15	138	108	85	68	55	45
20	120	94	75	60	48	39
25	106	83	66	52	42	34
30	93	73	58	46	37	30
35	81	64	51	41	33	26
40	72	57	45	36	29	23
45	63	50	39	31	25	20
50	56	44	35	27	22	18

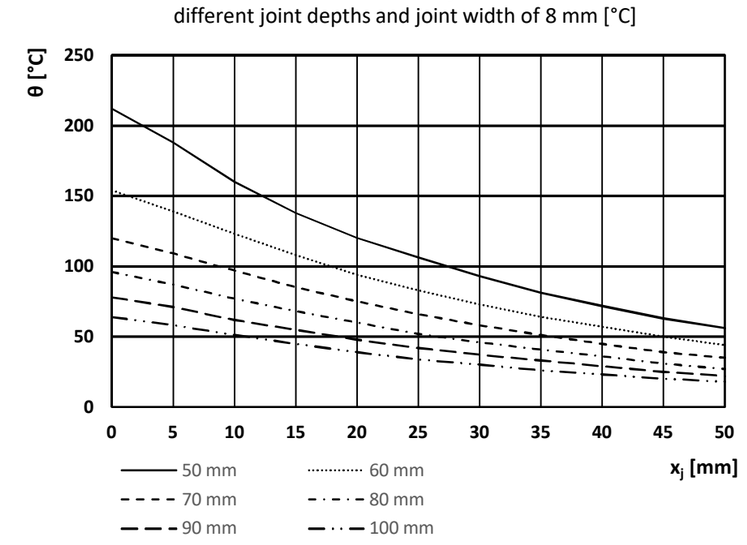

Temperature concrete above the joint after 90 minutes at different joint depts and joint width of 8 mm [°C]						
x_j [mm]	Joint depth [mm]					
	50	60	70	80	90	100
0	326	248	200	156	128	107
5	298	234	181	142	118	99
10	264	206	158	128	106	89
15	231	178	140	115	95	80
20	202	154	125	103	85	71
25	175	137	112	92	77	64
30	151	123	101	83	69	58
35	135	110	90	75	62	52
40	121	99	81	67	56	47
45	108	89	73	61	50	42
50	97	80	66	55	46	38

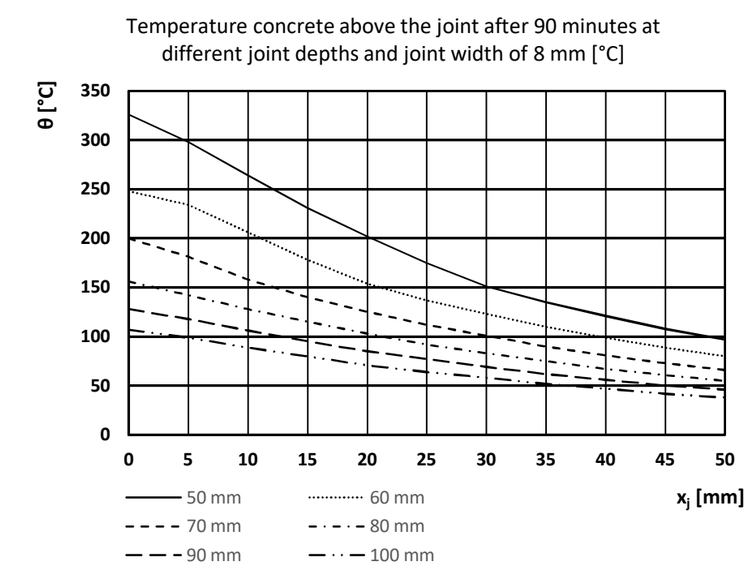

Temperature concrete above the joint after 120 minutes at different joint depts and joint width of 8 mm [°C]						
x_j [mm]	Joint depth [mm]					
	50	60	70	80	90	100
0	410	338	276	226	183	149
5	380	312	255	207	167	138
10	344	282	229	184	148	126
15	309	252	203	162	134	114
20	277	224	180	144	122	104
25	248	199	158	131	111	94
30	220	176	141	119	101	86
35	195	155	129	108	92	78
40	173	139	117	99	84	72
45	152	127	107	90	77	65
50	138	116	97	82	70	60

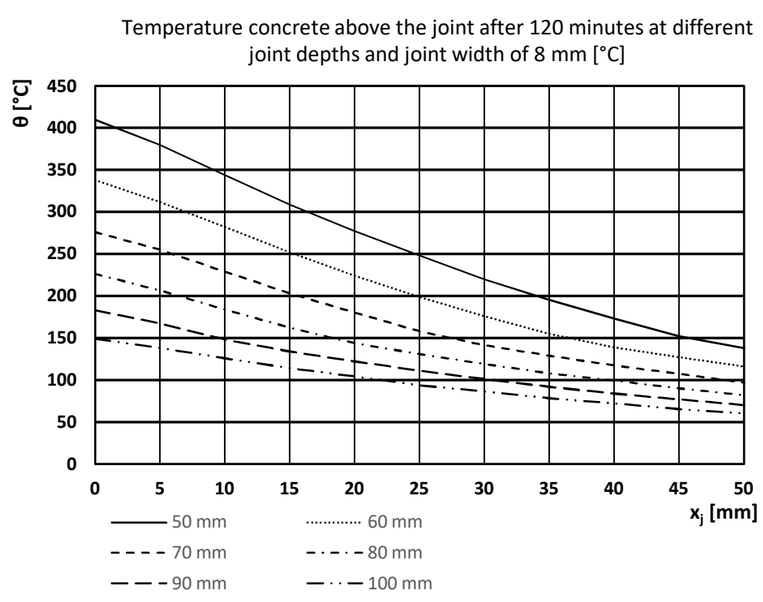

Temperatures above the joint, joint width 9 mm

Temperature concrete above the joint after 30 minutes at different joint depts and joint width of 9 mm [°C]						
x_j [mm]	**Joint depth [mm]**					
	50	60	70	80	90	100
0	87	66	49	38	30	24
5	77	58	43	32	25	20
10	66	49	36	27	21	16
15	55	41	30	22	17	13
20	46	34	25	18	14	11
25	39	28	21	15	11	9
30	32	23	17	12	9	7
35	27	19	14	10	7	6
40	22	16	11	8	6	5
45	18	13	9	7	5	4
50	15	11	7	5	4	3

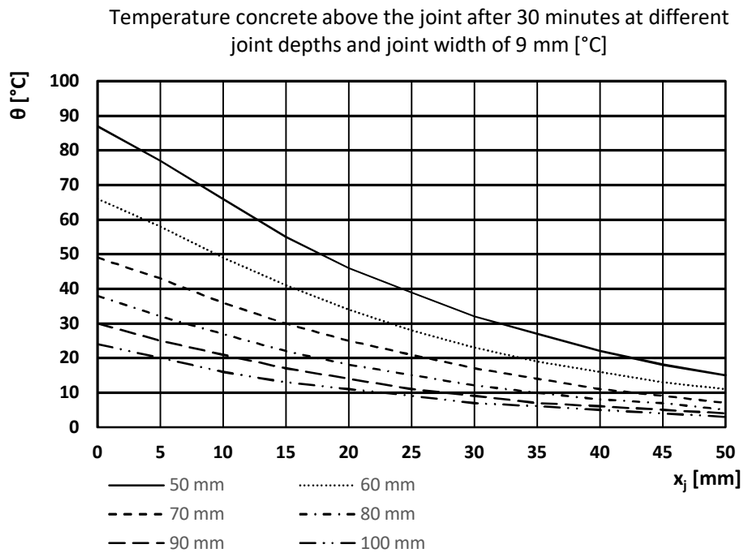

Temperature concrete above the joint after 60 minutes at different joint depts and joint width of 9 mm [°C]						
x_j [mm]	**Joint depth [mm]**					
	50	60	70	80	90	100
0	212	158	122	97	79	65
5	188	141	111	89	72	59
10	160	125	98	78	63	52
15	138	109	86	69	56	45
20	121	96	76	61	49	40
25	106	84	67	53	43	35
30	93	74	59	47	38	30
35	82	65	51	41	33	27
40	72	57	46	36	29	23
45	63	50	40	32	25	20
50	56	44	35	28	22	18

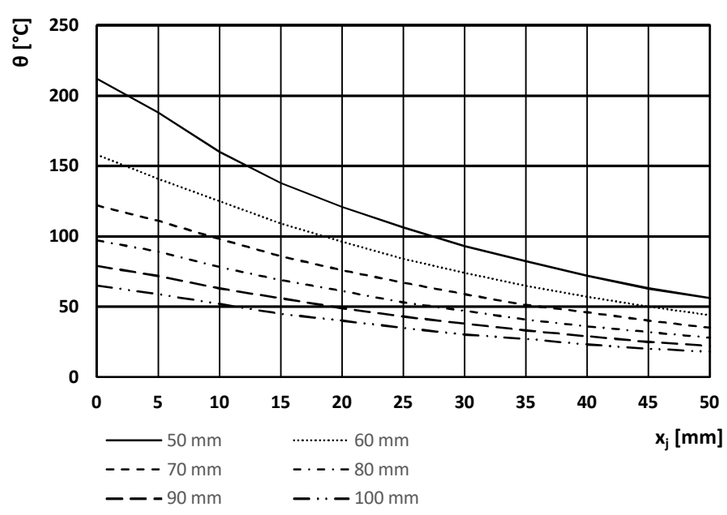

Temperature concrete above the joint after 90 minutes at different joint depts and joint width of 9 mm [°C]						
x_j [mm]	**Joint depth [mm]**					
	50	60	70	80	90	100
0	326	264	206	159	130	109
5	298	239	185	144	119	100
10	265	210	161	130	108	90
15	232	182	141	116	96	81
20	203	157	127	104	87	72
25	175	139	113	94	78	65
30	152	124	102	84	70	59
35	135	111	91	76	63	53
40	121	100	82	68	57	47
45	109	90	74	61	51	43
50	98	81	67	55	46	38

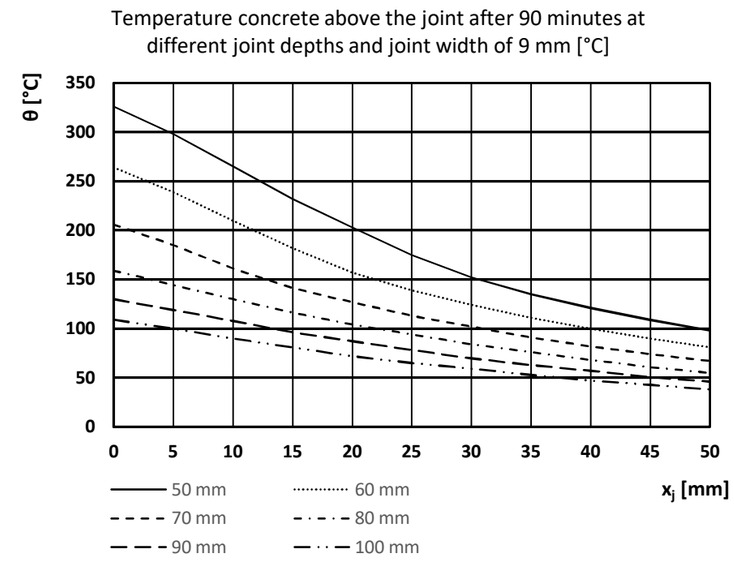

Temperature concrete above the joint after 120 minutes at different joint depts and joint width of 9 mm [°C]						
x_j [mm]	**Joint depth [mm]**					
	50	60	70	80	90	100
0	411	346	283	230	187	152
5	381	319	260	211	170	140
10	356	287	233	188	151	127
15	311	257	207	165	136	116
20	278	228	183	147	124	105
25	249	202	161	133	112	96
30	221	179	143	121	102	87
35	196	157	130	110	93	79
40	173	141	118	100	85	72
45	153	128	108	91	77	66
50	138	117	98	83	71	60

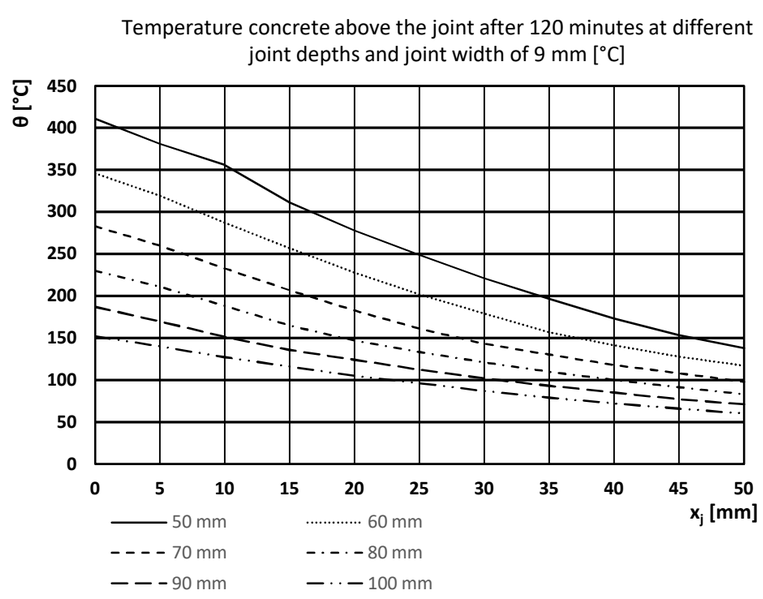

Temperatures above the joint, joint width 10 mm

Temperature concrete above the joint after 30 minutes at different joint depts and joint width of 10 mm [°C]						
x_j [mm]	**Joint depth [mm]**					
	50	60	70	80	90	100
0	90	67	51	39	31	25
5	79	59	44	34	26	21
10	67	50	37	28	22	17
15	56	41	31	23	18	14
20	47	34	26	19	14	11
25	39	29	21	16	12	9
30	33	24	17	13	10	7
35	27	20	14	10	8	6
40	23	16	12	8	6	5
45	19	13	9	7	5	4
50	15	11	8	5	4	3

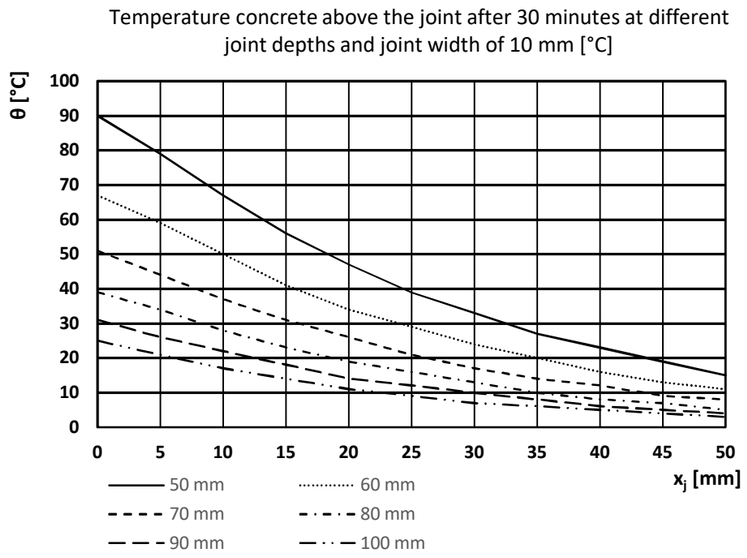

Temperature concrete above the joint after 60 minutes at different joint depts and joint width of 10 mm [°C]						
x_j [mm]	**Joint depth [mm]**					
	50	60	70	80	90	100
0	220	162	125	100	81	67
5	194	143	113	91	73	60
10	164	126	100	80	65	53
15	140	111	88	70	57	46
20	123	97	77	62	50	41
25	107	85	68	54	44	36
30	94	75	59	48	38	31
35	83	66	52	42	34	27
40	73	58	46	37	29	24
45	67	51	40	32	26	21
50	56	45	35	28	23	18

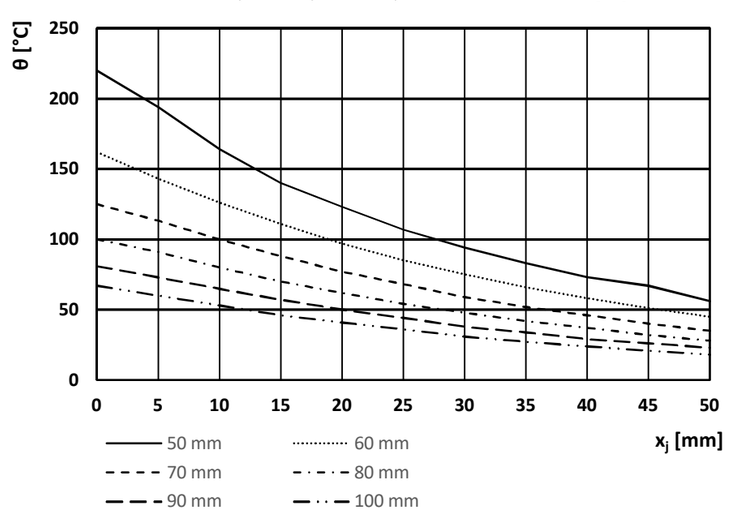

Temperature concrete above the joint after 90 minutes at different joint depts and joint width of 10 mm [°C]						
x_j [mm]	**Joint depth [mm]**					
	50	60	70	80	90	100
0	338	270	212	165	132	111
5	307	244	190	148	122	102
10	272	214	166	133	110	92
15	237	185	144	119	98	82
20	207	160	129	106	88	74
25	179	140	115	95	79	66
30	154	125	103	86	71	60
35	137	112	93	77	64	54
40	123	101	83	69	57	48
45	110	91	75	62	52	43
50	99	81	67	56	47	39

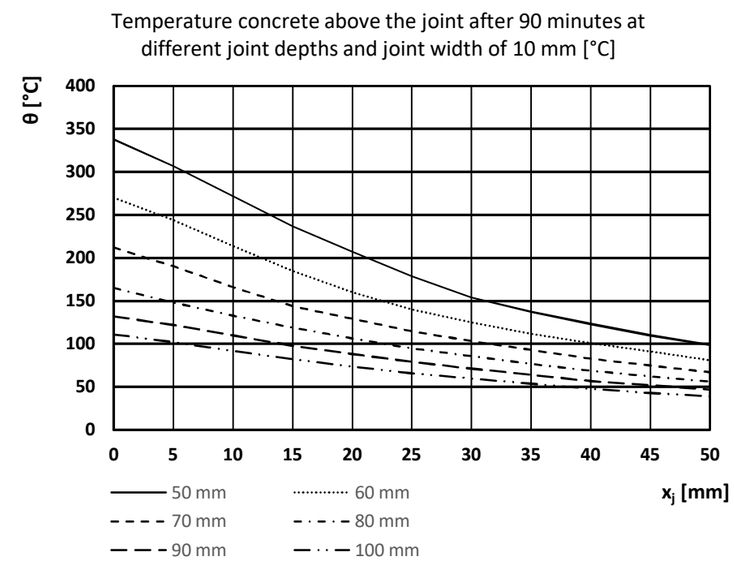

Temperature concrete above the joint after 120 minutes at different joint depts and joint width of 10 mm [°C]						
x_j [mm]	**Joint depth [mm]**					
	50	60	70	80	90	100
0	425	354	291	238	191	156
5	391	325	267	217	174	143
10	354	292	239	193	154	130
15	317	261	212	170	139	118
20	284	232	187	150	126	107
25	253	205	164	135	114	97
30	225	181	146	123	104	89
35	200	159	132	112	94	81
40	176	142	120	101	86	74
45	155	129	109	92	78	67
50	140	118	99	84	72	61

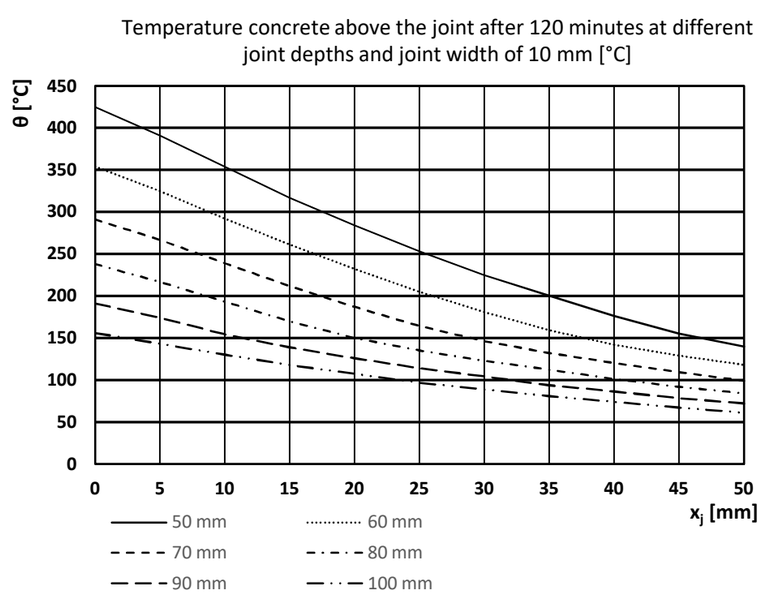

Temperatures above the joint, joint width 11 mm

Temperature concrete above the joint after 30 minutes at different joint depts and joint width of 11 mm [°C]						
x_j [mm]	**Joint depth [mm]**					
	50	60	70	80	90	100
0	89	66	51	38	31	25
5	78	58	44	33	26	21
10	67	49	37	28	22	17
15	56	41	31	23	18	14
20	47	34	26	19	15	12
25	39	29	21	16	12	9
30	33	24	17	13	10	8
35	27	20	14	10	8	6
40	22	16	12	8	6	5
45	18	13	9	7	5	4
50	15	11	8	5	4	3

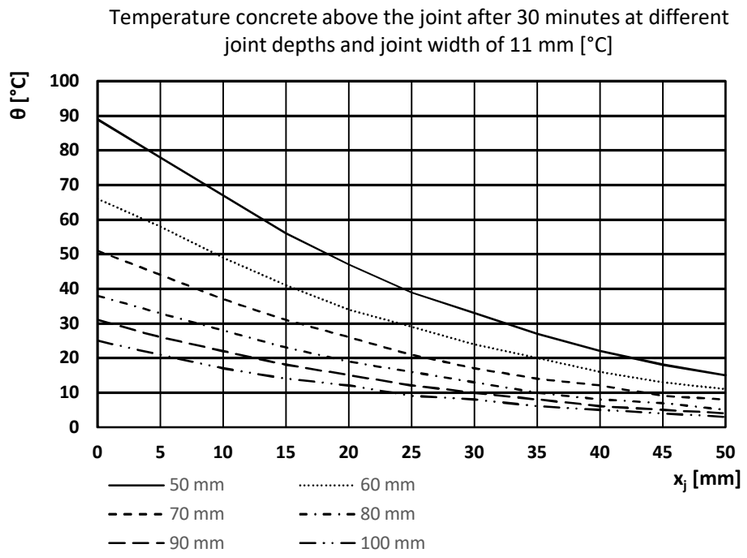

Temperature concrete above the joint after 60 minutes at different joint depts and joint width of 11 mm [°C]						
x_j [mm]	**Joint depth [mm]**					
	50	60	70	80	90	100
0	217	159	125	98	81	67
5	192	142	113	89	73	60
10	164	126	100	79	65	53
15	140	110	88	70	57	47
20	122	97	77	61	50	41
25	107	85	68	54	44	36
30	94	74	60	47	38	31
35	82	65	52	42	34	27
40	73	58	46	37	30	24
45	64	51	40	32	26	21
50	56	45	36	28	23	18

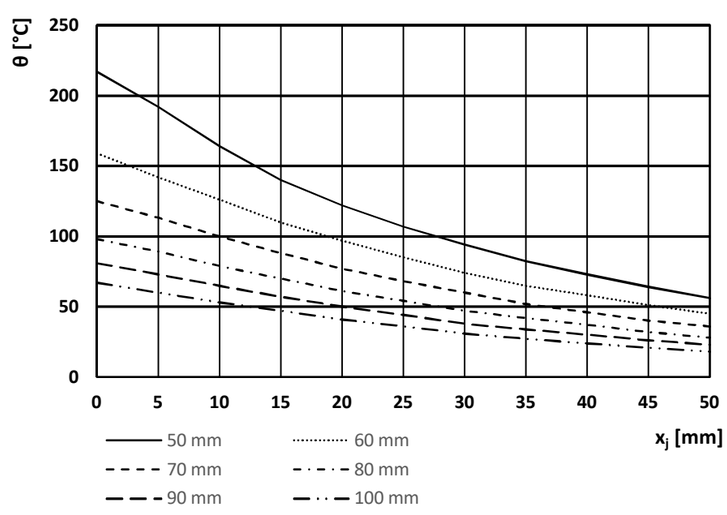

Temperature concrete above the joint after 90 minutes at different joint depts and joint width of 11 mm [°C]						
x_j [mm]	**Joint depth [mm]**					
	50	60	70	80	90	100
0	336	266	213	161	132	112
5	305	241	191	146	122	102
10	271	213	166	132	110	92
15	237	184	144	118	98	83
20	207	159	129	106	88	74
25	179	140	115	95	79	67
30	154	125	103	85	71	60
35	137	112	93	77	64	54
40	123	101	83	69	58	48
45	110	90	75	62	52	44
50	99	81	68	56	47	39

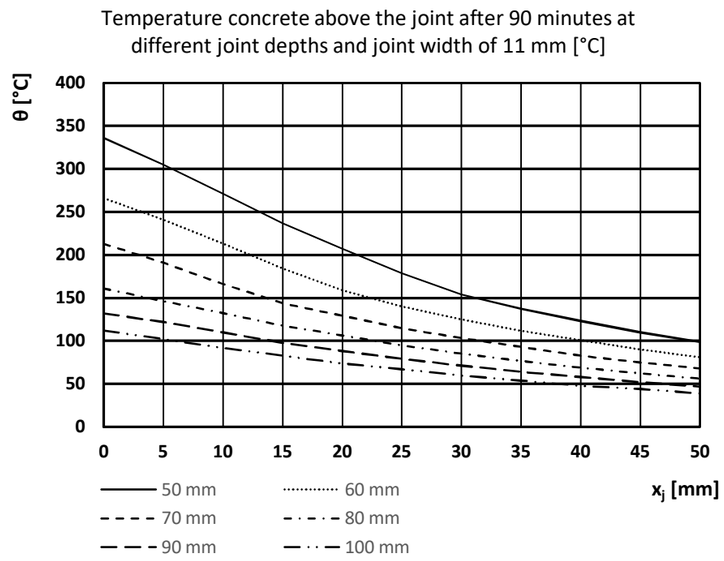

Temperature concrete above the joint after 120 minutes at different joint depts and joint width of 11 mm [°C]						
x_j [mm]	**Joint depth [mm]**					
	50	60	70	80	90	100
0	423	350	292	233	191	156
5	390	322	267	214	174	143
10	353	291	240	191	154	130
15	317	260	212	169	139	118
20	284	231	187	149	126	107
25	254	205	165	135	114	98
30	226	181	146	122	104	89
35	200	159	132	111	95	81
40	176	142	120	101	86	74
45	155	129	109	92	79	67
50	140	118	100	84	72	62

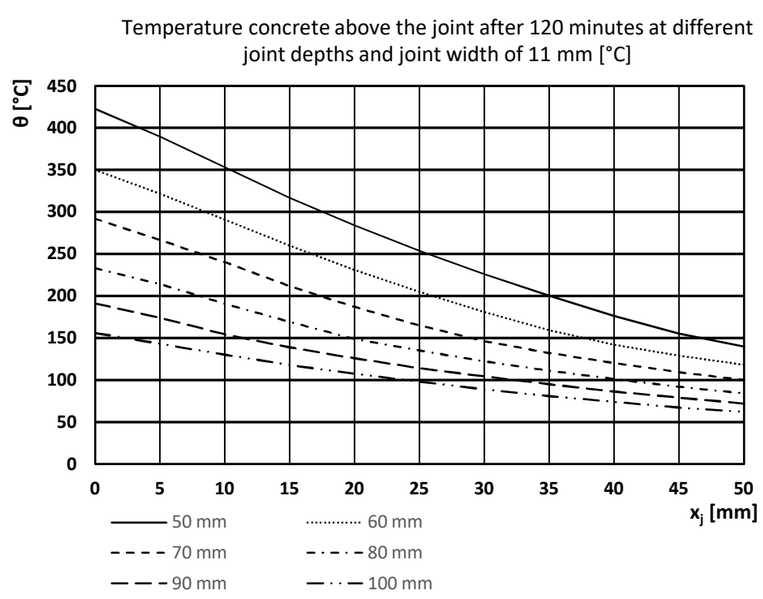

Temperatures above the joint, joint width 12 mm

Temperature concrete above the joint after 30 minutes at different joint depts and joint width of 12 mm [°C]						
x_j [mm]	**Joint depth [mm]**					
	50	60	70	80	90	100
0	90	66	51	40	31	26
5	79	58	44	34	27	22
10	67	49	37	29	22	18
15	57	41	31	24	18	15
20	47	35	26	20	15	12
25	40	29	21	16	12	10
30	33	24	18	13	10	8
35	27	20	14	11	8	6
40	23	16	12	9	6	5
45	19	13	10	7	5	4
50	15	11	8	6	4	3

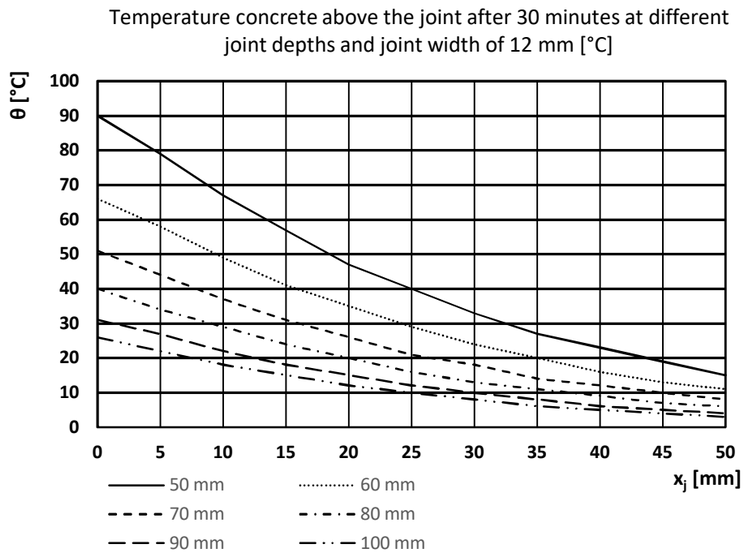

Temperature concrete above the joint after 60 minutes at different joint depts and joint width of 12 mm [°C]						
x_j [mm]	**Joint depth [mm]**					
	50	60	70	80	90	100
0	221	159	126	101	82	68
5	194	142	114	91	74	61
10	165	126	101	81	65	54
15	141	111	88	71	57	47
20	123	97	78	62	50	41
25	108	85	68	55	44	36
30	95	75	60	48	39	32
35	83	66	53	42	34	28
40	73	58	46	37	30	24
45	64	51	41	33	26	21
50	57	45	36	29	23	19

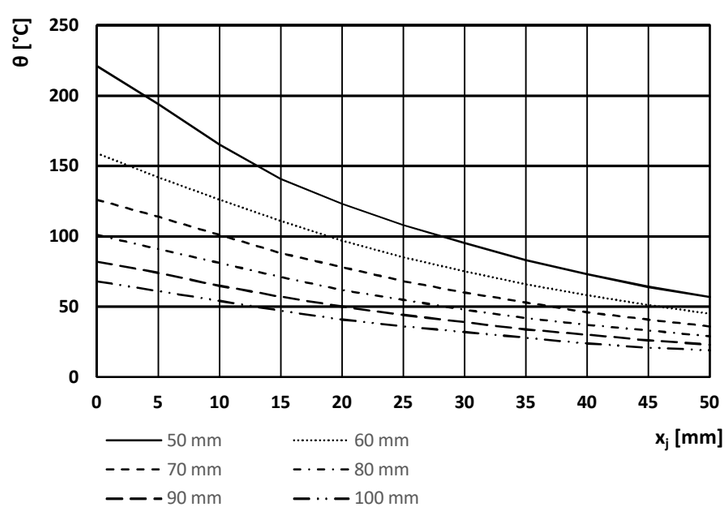

Temperature concrete above the joint after 90 minutes at different joint depts and joint width of 12 mm [°C]						
x_j [mm]	**Joint depth [mm]**					
	50	60	70	80	90	100
0	341	268	214	167	133	113
5	309	243	192	149	123	103
10	274	214	167	134	111	93
15	240	186	145	120	99	84
20	209	160	130	107	89	75
25	181	141	116	96	80	67
30	156	126	100	86	72	61
35	138	113	93	78	65	54
40	123	101	84	70	58	49
45	111	91	75	63	52	44
50	99	82	68	57	47	40

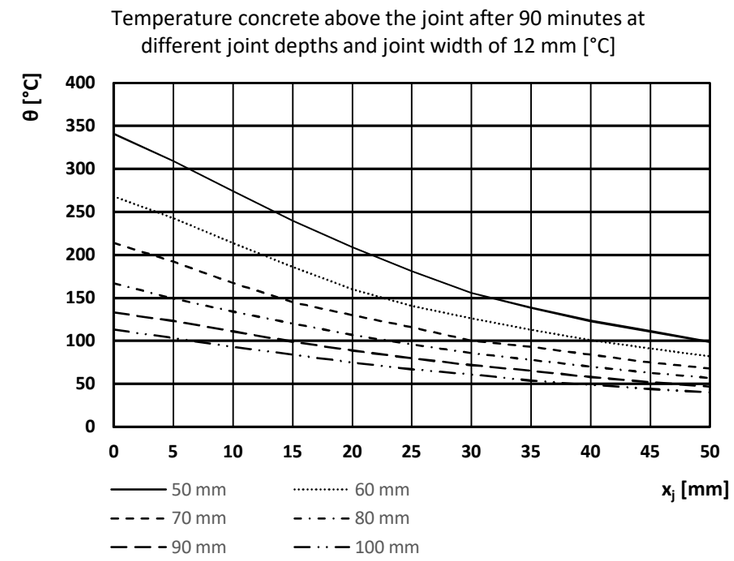

Temperature concrete above the joint after 120 minutes at different joint depts and joint width of 12 mm [°C]						
x_j [mm]	**Joint depth [mm]**					
	50	60	70	80	90	100
0	430	352	294	240	193	158
5	394	325	269	219	176	145
10	357	293	241	196	156	132
15	320	262	214	172	140	120
20	287	233	189	152	127	109
25	256	207	166	137	115	99
30	227	182	147	124	105	90
35	202	160	133	113	95	82
40	178	143	121	102	87	75
45	156	130	110	93	79	68
50	140	118	100	85	69	62

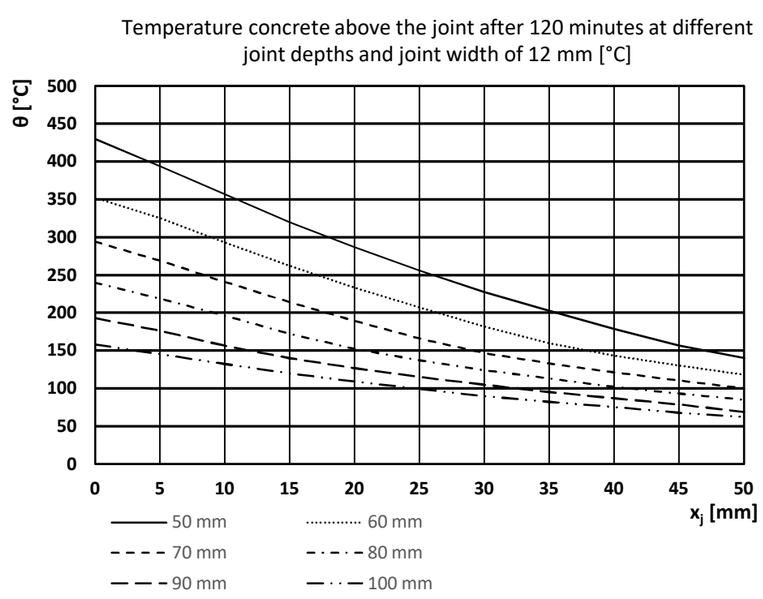

Temperatures above the joint, joint width 13 mm

Temperature concrete above the joint after 30 minutes at different joint depts and joint width of 13 mm [°C]						
x_j [mm]	Joint depth [mm]					
	50	60	70	80	90	100
0	91	68	52	40	33	27
5	80	59	45	35	28	22
10	68	50	38	29	23	18
15	57	42	32	24	19	15
20	48	35	26	20	15	12
25	40	29	22	16	13	10
30	33	24	18	13	10	8
35	28	20	15	11	8	6
40	23	16	12	9	7	5
45	19	13	10	7	5	4
50	15	11	8	6	4	3

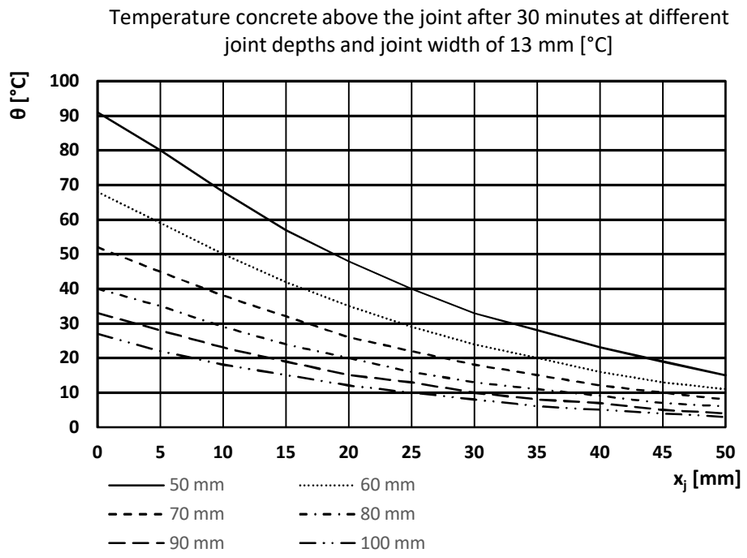

Temperature concrete above the joint after 60 minutes at different joint depts and joint width of 13 mm [°C]						
x_j [mm]	Joint depth [mm]					
	50	60	70	80	90	100
0	223	163	127	102	84	69
5	197	144	115	92	76	62
10	167	128	102	82	67	55
15	142	112	89	72	59	48
20	124	98	78	63	51	42
25	109	86	69	55	45	37
30	95	75	60	49	39	32
35	84	66	53	43	35	28
40	73	58	47	37	30	25
45	65	51	41	33	27	22
50	57	45	36	29	23	19

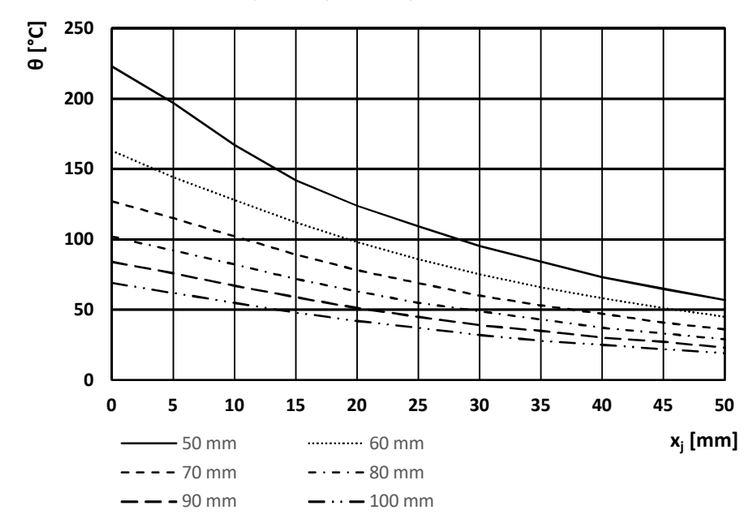

Temperature concrete above the joint after 90 minutes at different joint depts and joint width of 13 mm [°C]						
x_j [mm]	Joint depth [mm]					
	50	60	70	80	90	100
0	346	274	217	169	137	114
5	313	247	194	151	125	104
10	277	217	169	135	113	94
15	242	189	147	121	101	84
20	211	162	131	108	90	76
25	183	142	117	97	81	68
30	157	127	105	87	73	61
35	139	114	94	78	65	55
40	124	102	84	70	59	49
45	111	92	76	63	53	44
50	100	82	68	57	48	40

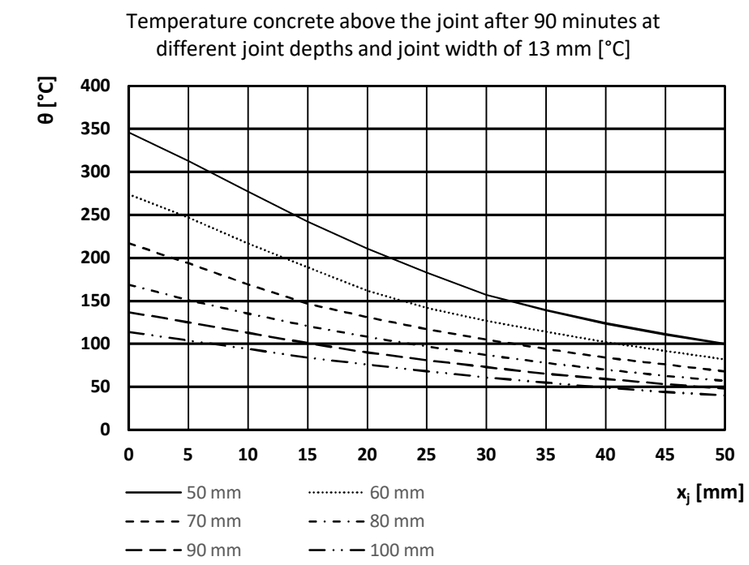

Temperature concrete above the joint after 120 minutes at different joint depts and joint width of 13 mm [°C]						
x_j [mm]	Joint depth [mm]					
	50	60	70	80	90	100
0	436	360	298	243	200	160
5	400	330	272	222	181	147
10	361	297	244	198	160	133
15	324	265	217	174	142	121
20	290	236	191	153	129	110
25	258	209	168	138	117	100
30	230	184	148	125	106	91
35	203	162	134	113	97	82
40	179	144	122	103	88	75
45	158	131	111	94	80	69
50	141	119	101	86	73	63

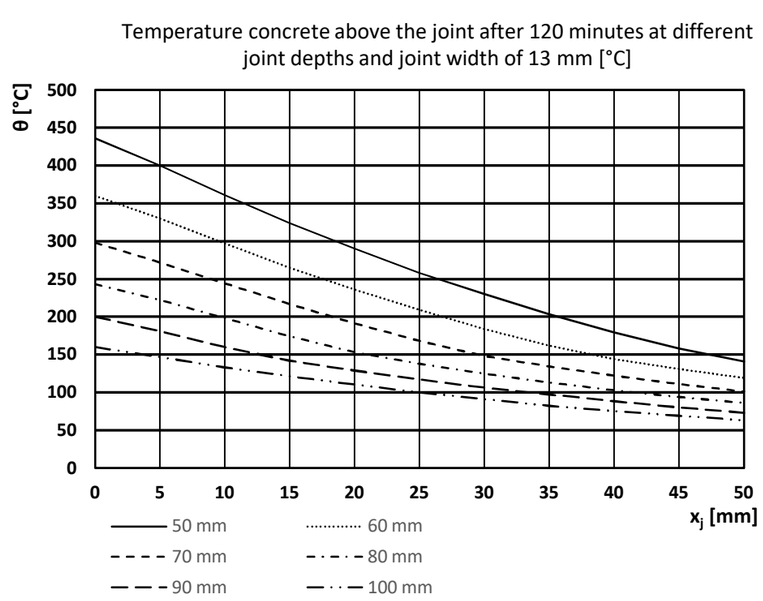

Temperatures above the joint, joint width 14 mm

Temperature concrete above the joint after 30 minutes at different joint depts and joint width of 14 mm [°C]						
x_j [mm]	**Joint depth [mm]**					
	50	60	70	80	90	100
0	90	70	53	42	34	27
5	79	61	46	36	28	23
10	68	51	39	30	24	19
15	57	43	32	25	19	15
20	48	36	27	20	16	13
25	40	30	22	17	13	10
30	33	25	18	14	11	8
35	28	20	15	11	9	7
40	23	17	12	9	7	5
45	19	14	10	7	6	4
50	15	11	8	6	4	3

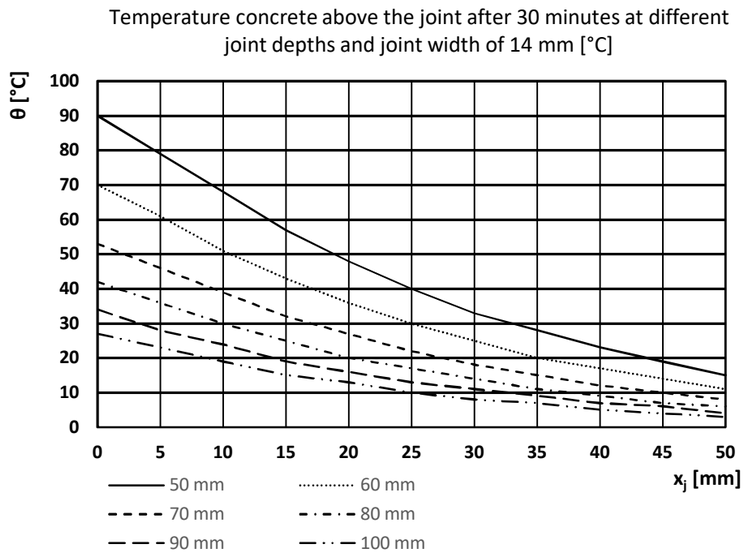

Temperature concrete above the joint after 60 minutes at different joint depts and joint width of 14 mm [°C]						
x_j [mm]	**Joint depth [mm]**					
	50	60	70	80	90	100
0	222	169	129	105	86	70
5	196	148	117	94	77	63
10	166	130	103	83	68	55
15	142	114	90	73	60	49
20	124	99	79	64	52	43
25	109	87	70	56	46	37
30	95	76	61	49	40	33
35	84	67	54	43	35	29
40	73	59	47	38	31	25
45	65	52	41	33	27	22
50	57	46	36	29	24	19

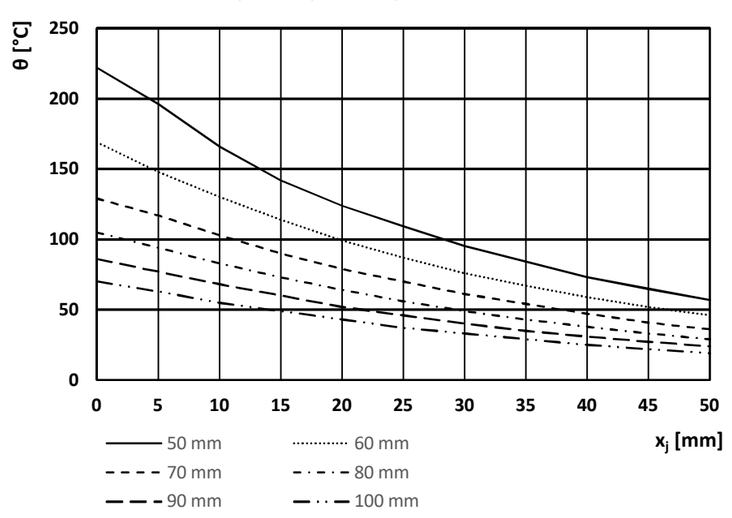

Temperature concrete above the joint after 90 minutes at different joint depts and joint width of 14 mm [°C]						
x_j [mm]	**Joint depth [mm]**					
	50	60	70	80	90	100
0	344	283	222	175	140	115
5	312	253	198	155	128	106
10	276	222	173	138	115	95
15	242	183	149	123	103	86
20	211	166	133	110	92	77
25	183	144	119	98	82	69
30	157	129	106	88	74	62
35	139	115	95	79	66	56
40	124	103	85	71	60	50
45	111	92	77	64	54	45
50	100	83	69	58	48	40

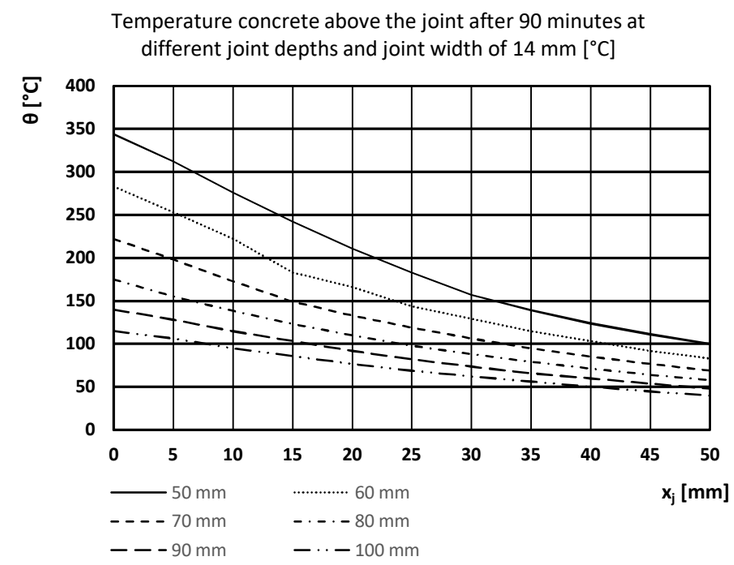

Temperature concrete above the joint after 120 minutes at different joint depts and joint width of 14 mm [°C]						
x_j [mm]	**Joint depth [mm]**					
	50	60	70	80	90	100
0	434	371	303	251	204	163
5	399	338	277	227	185	148
10	361	303	248	202	163	135
15	324	271	220	178	145	122
20	290	240	195	156	131	111
25	258	213	171	140	119	101
30	230	187	150	127	108	92
35	204	165	135	115	98	83
40	180	146	123	104	89	76
45	158	132	112	95	81	69
50	141	120	102	87	74	63

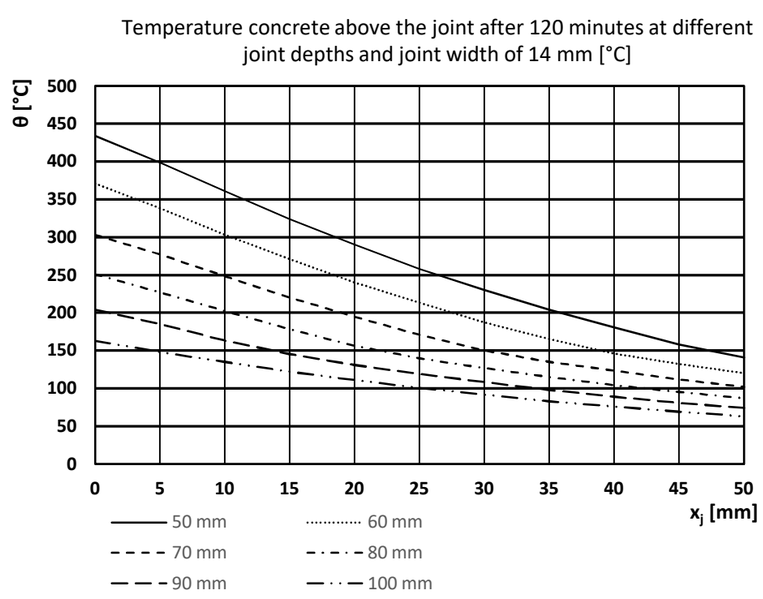

Temperatures above the joint, joint width 15 mm

Temperature concrete above the joint after 30 minutes at different joint depts and joint width of 15 mm [°C]						
x_j [mm]	Joint depth [mm]					
	50	60	70	80	90	100
0	94	72	53	43	36	31
5	81	62	46	37	30	26
10	69	53	39	31	25	22
15	58	44	32	25	20	18
20	49	37	27	21	17	15
25	41	31	22	17	14	12
30	34	26	18	14	11	10
35	28	21	15	11	9	8
40	23	18	12	9	7	7
45	19	14	10	8	6	5
50	16	12	8	6	5	4

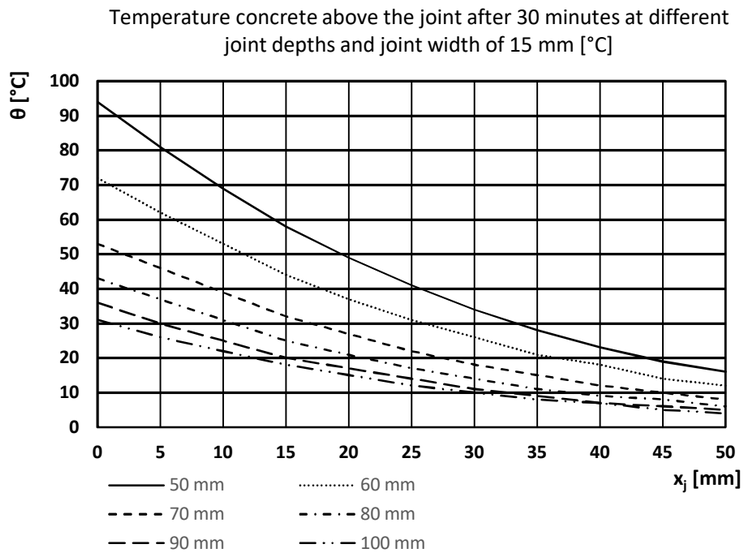

Temperature concrete above the joint after 60 minutes at different joint depts and joint width of 15 mm [°C]						
x_j [mm]	Joint depth [mm]					
	50	60	70	80	90	100
0	232	175	129	107	90	73
5	202	151	117	96	80	65
10	171	132	103	85	70	58
15	145	116	91	74	61	51
20	126	101	80	65	54	45
25	110	89	70	57	47	39
30	96	78	61	50	41	35
35	85	68	54	44	36	30
40	74	60	47	39	32	27
45	65	53	42	34	28	23
50	57	47	37	30	24	20

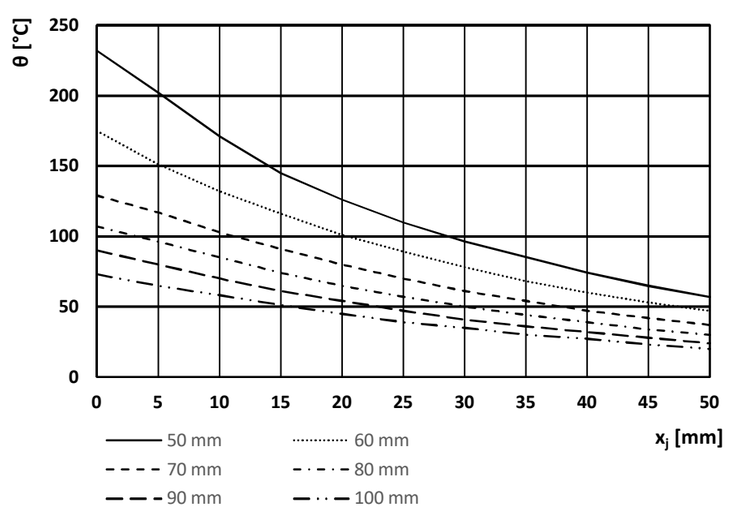

Temperature concrete above the joint after 90 minutes at different joint depts and joint width of 15 mm [°C]						
x_j [mm]	Joint depth [mm]					
	50	60	70	80	90	100
0	359	292	222	179	146	118
5	321	260	199	158	132	108
10	283	228	173	140	118	97
15	248	198	150	125	106	87
20	216	170	133	112	94	79
25	186	147	119	100	84	71
30	160	131	107	89	76	64
35	140	117	95	80	68	47
40	126	105	86	72	61	52
45	113	94	77	65	55	46
50	101	85	69	58	49	42

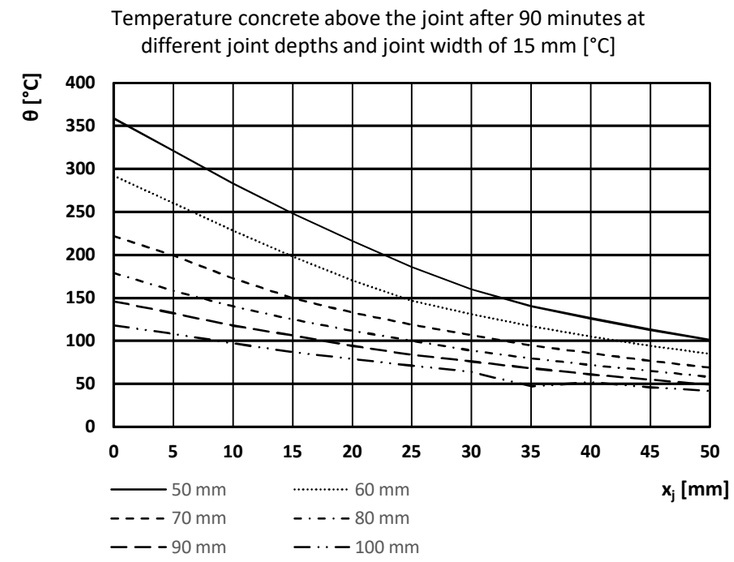

Temperature concrete above the joint after 120 minutes at different joint depts and joint width of 15 mm [°C]						
x_j [mm]	Joint depth [mm]					
	50	60	70	80	90	100
0	451	382	304	256	215	167
5	410	346	278	232	193	150
10	369	311	250	206	170	136
15	331	278	222	182	149	124
20	296	247	196	159	134	113
25	263	193	172	141	121	103
30	234	182	151	128	110	93
35	207	170	136	116	100	85
40	182	150	123	106	91	78
45	161	135	112	96	83	71
50	143	123	102	87	75	64

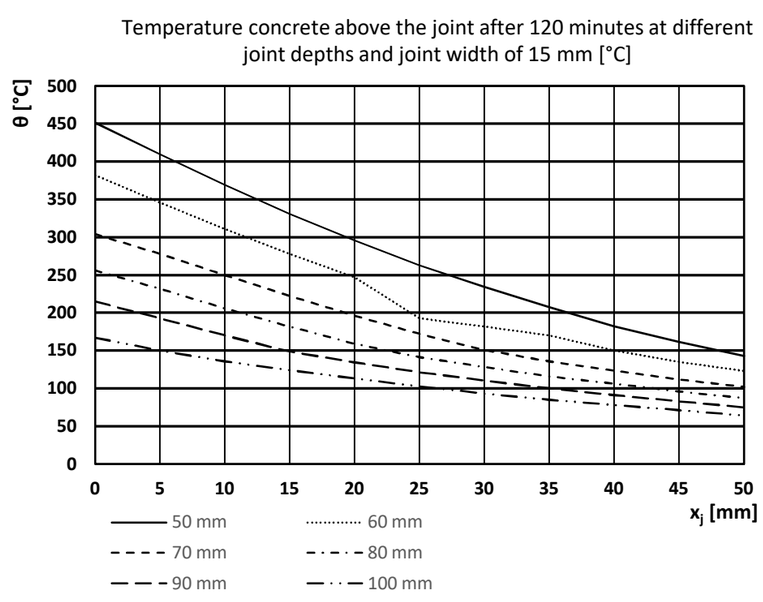

Temperatures above the joint, joint width 16 mm

Temperature concrete above the joint after 30 minutes at different joint depts and joint width of 16 mm [°C]						
x_j [mm]	Joint depth [mm]					
	50	60	70	80	90	100
0	92	71	55	43	36	30
5	80	61	47	37	30	25
10	69	52	40	31	25	20
15	58	43	33	26	21	17
20	48	36	27	21	17	14
25	40	30	23	17	14	11
30	34	25	19	14	11	9
35	28	21	15	12	9	7
40	23	17	13	9	7	6
45	19	14	10	8	6	5
50	16	11	8	6	5	4

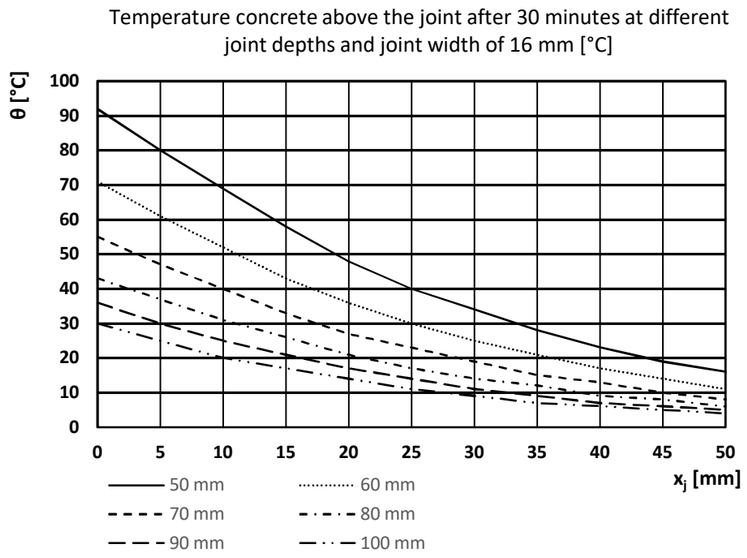

Temperature concrete above the joint after 60 minutes at different joint depts and joint width of 16 mm [°C]						
x_j [mm]	Joint depth [mm]					
	50	60	70	80	90	100
0	228	171	132	107	90	74
5	201	149	119	96	80	66
10	171	131	105	85	70	58
15	145	115	92	75	62	51
20	126	100	81	65	54	44
25	110	88	71	57	47	39
30	97	77	62	50	41	34
35	85	68	55	44	36	30
40	74	60	48	39	32	26
45	65	52	42	34	28	23
50	57	46	37	30	24	20

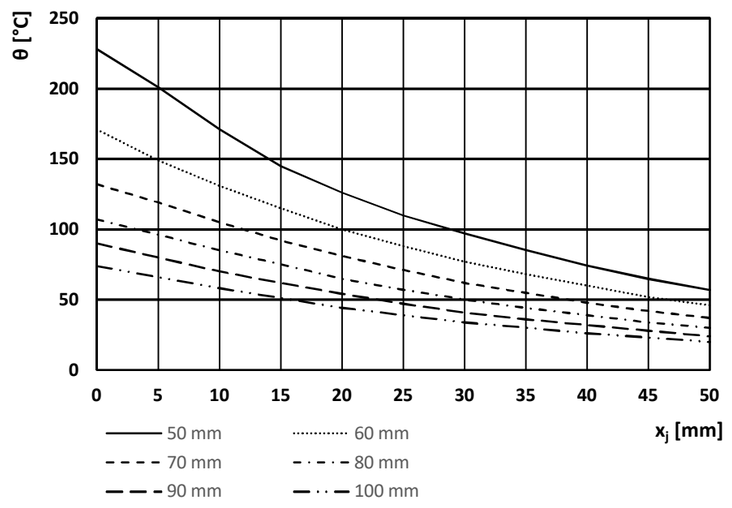

Temperature concrete above the joint after 90 minutes at different joint depts and joint width of 16 mm [°C]						
x_j [mm]	Joint depth [mm]					
	50	60	70	80	90	100
0	355	287	228	179	146	121
5	321	257	203	158	132	110
10	284	225	177	140	118	99
15	249	196	152	125	106	89
20	216	168	135	112	94	79
25	187	146	120	100	85	71
30	161	130	108	90	76	64
35	141	116	97	81	68	57
40	126	104	87	72	61	51
45	113	93	78	65	55	46
50	101	84	70	58	49	42

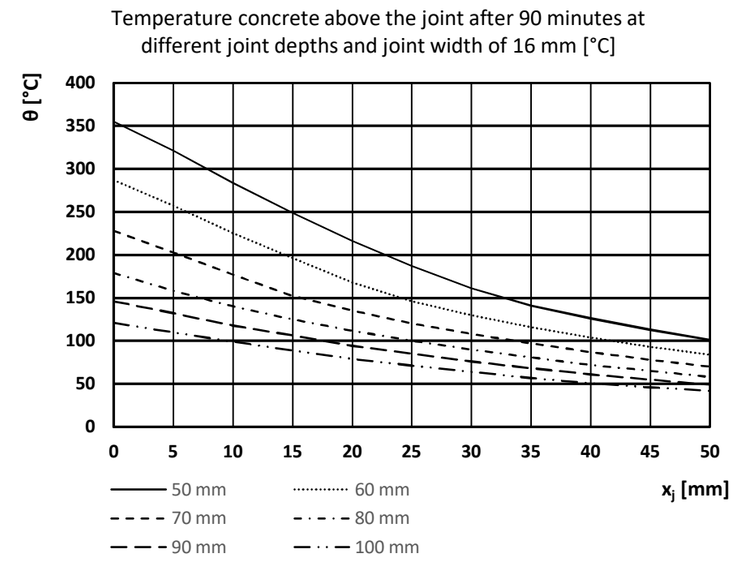

Temperature concrete above the joint after 120 minutes at different joint depts and joint width of 16 mm [°C]						
x_j [mm]	Joint depth [mm]					
	50	60	70	80	90	100
0	449	376	312	256	214	173
5	410	342	284	233	193	155
10	371	308	254	207	170	140
15	332	275	225	183	149	127
20	297	244	199	160	134	115
25	265	216	175	142	122	104
30	235	190	153	129	110	94
35	208	167	138	117	100	86
40	184	148	125	106	91	78
45	161	134	113	96	83	71
50	144	121	103	88	76	64

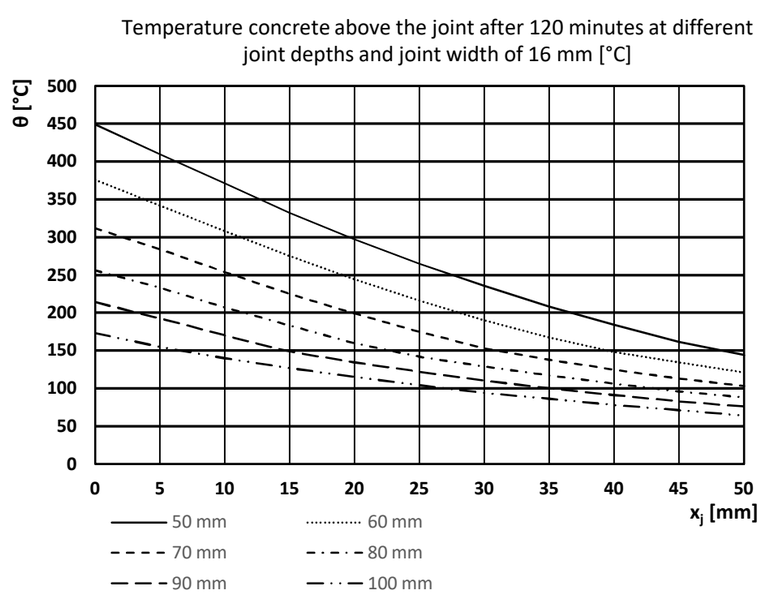

Temperatures above the joint, joint width 17 mm

Temperature concrete above the joint after 30 minutes at different joint depts and joint width of 17 mm [°C]						
x_j [mm]	**Joint depth [mm]**					
	50	60	70	80	90	100
0	95	71	56	44	37	27
5	82	61	48	37	31	22
10	70	52	40	31	26	19
15	59	44	34	26	21	15
20	49	36	28	22	17	13
25	41	30	22	18	14	10
30	34	25	19	15	12	8
35	28	21	16	12	9	7
40	24	17	13	10	8	6
45	19	14	10	8	6	5
50	16	11	8	6	5	4

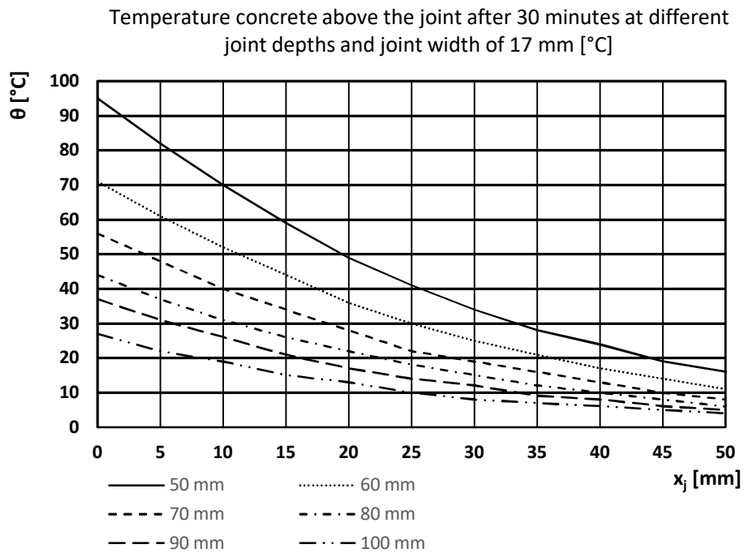

Temperature concrete above the joint after 60 minutes at different joint depts and joint width of 17 mm [°C]						
x_j [mm]	**Joint depth [mm]**					
	50	60	70	80	90	100
0	235	171	133	108	91	68
5	205	149	120	97	81	61
10	174	131	106	86	71	54
15	146	115	93	75	62	48
20	127	101	81	66	55	42
25	111	88	71	58	48	37
30	97	77	63	51	42	33
35	85	68	55	45	37	29
40	75	60	48	39	32	25
45	66	52	42	34	28	22
50	58	46	37	30	25	19

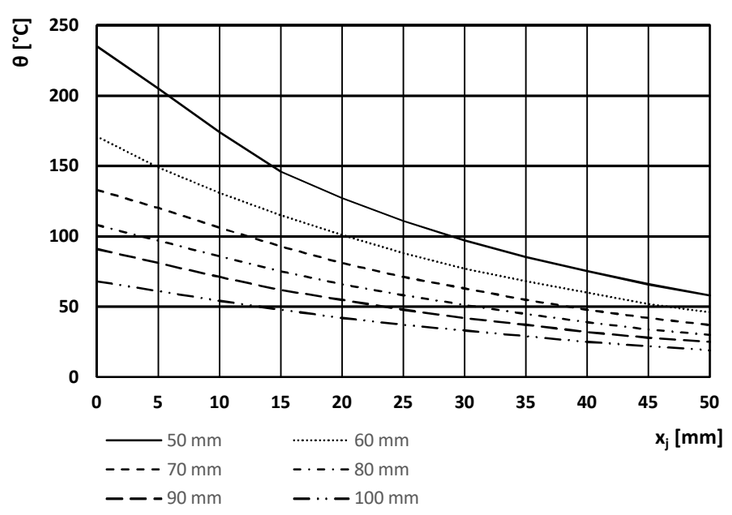

Temperature concrete above the joint after 90 minutes at different joint depts and joint width of 17 mm [°C]						
x_j [mm]	**Joint depth [mm]**					
	50	60	70	80	90	100
0	365	287	231	181	148	112
5	327	257	205	160	133	103
10	288	226	178	142	120	93
15	252	196	154	127	107	85
20	219	169	136	113	95	76
25	189	146	121	101	85	69
30	163	130	108	90	76	62
35	142	117	97	81	89	56
40	127	104	87	73	62	50
45	114	94	78	65	55	45
50	102	84	70	59	50	41

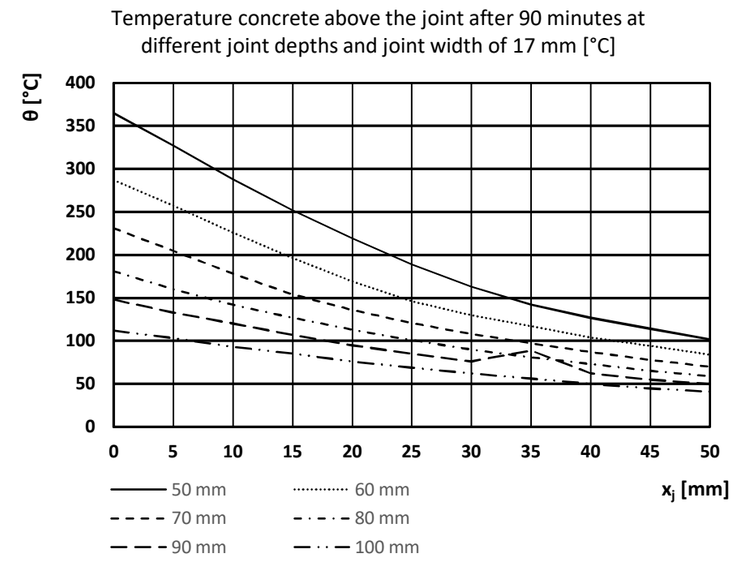

Temperature concrete above the joint after 120 minutes at different joint depts and joint width of 17 mm [°C]						
x_j [mm]	**Joint depth [mm]**					
	50	60	70	80	90	100
0	459	377	315	259	217	158
5	417	343	286	235	195	144
10	375	309	256	210	172	133
15	336	276	227	185	151	121
20	300	245	201	162	136	111
25	267	217	176	143	123	101
30	237	191	154	130	111	92
35	210	168	138	118	101	84
40	185	148	126	107	92	76
45	163	134	114	97	84	70
50	145	122	104	88	76	64

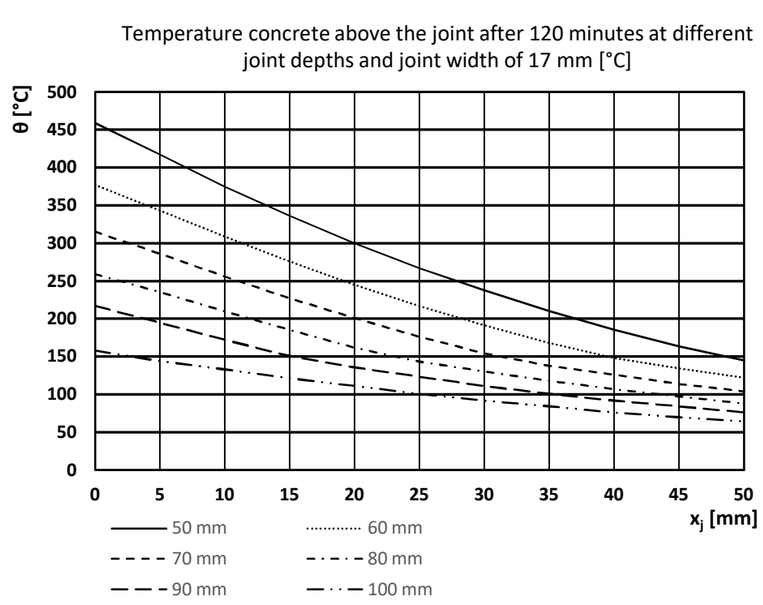

Temperatures above the joint, joint width 18 mm

Temperature concrete above the joint after 30 minutes at different joint depts and joint width of 18 mm [°C]						
x_j [mm]	Joint depth [mm]					
	50	60	70	80	90	100
0	98	74	58	45	29	32
5	84	63	50	38	23	26
10	74	54	42	32	19	22
15	60	45	35	26	15	18
20	50	37	29	22	12	15
25	42	31	24	18	10	12
30	35	26	20	15	8	10
35	29	21	16	12	7	8
40	24	18	13	10	5	7
45	20	14	11	8	4	6
50	16	12	9	6	3	5

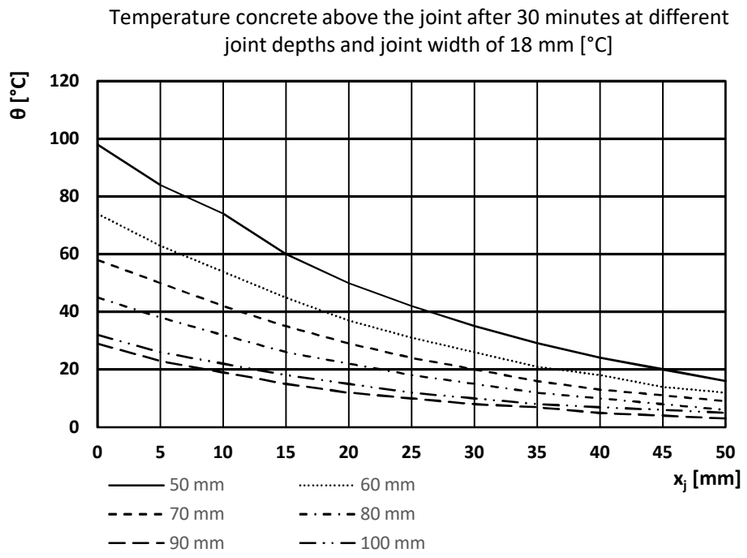

Temperature concrete above the joint after 60 minutes at different joint depts and joint width of 18 mm [°C]						
x_j [mm]	Joint depth [mm]					
	50	60	70	80	90	100
0	244	179	139	109	66	76
5	211	154	123	98	57	67
10	178	134	108	86	49	59
15	149	117	95	76	42	52
20	129	102	83	66	37	46
25	113	90	73	58	32	40
30	99	79	64	51	28	36
35	86	69	56	45	24	32
40	76	61	49	39	21	28
45	66	53	43	35	18	24
50	58	47	38	30	16	21

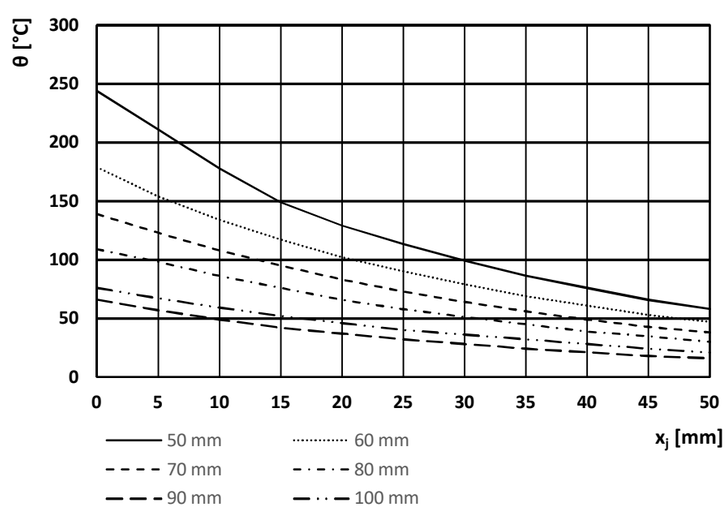

Temperature concrete above the joint after 90 minutes at different joint depts and joint width of 18 mm [°C]						
x_j [mm]	Joint depth [mm]					
	50	60	70	80	90	100
0	378	298	241	183	150	113
5	335	265	213	162	135	111
10	294	232	184	142	121	100
15	257	201	158	127	108	90
20	223	173	139	114	96	81
25	193	149	124	102	86	73
30	165	132	110	91	77	66
35	144	118	99	82	69	59
40	128	106	88	73	62	53
45	115	95	79	66	56	48
50	103	85	71	59	50	43

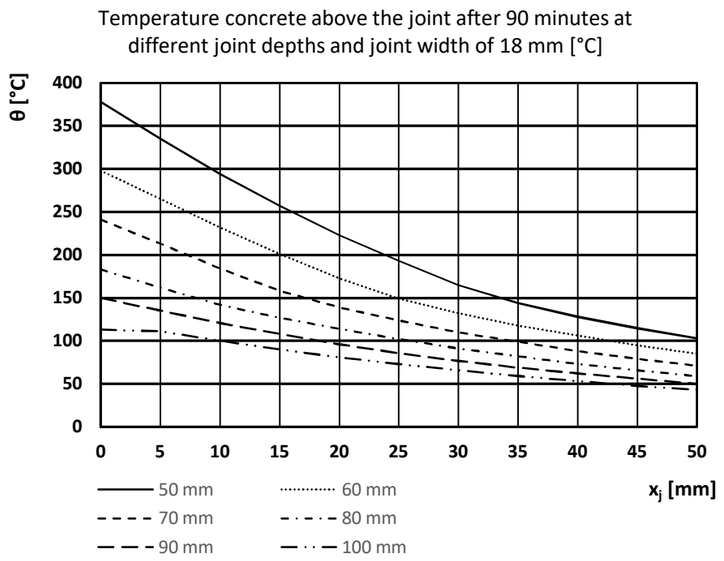

Temperature concrete above the joint after 120 minutes at different joint depts and joint width of 18 mm [°C]						
x_j [mm]	Joint depth [mm]					
	50	60	70	80	90	100
0	474	390	327	262	220	175
5	427	353	296	237	198	156
10	383	316	264	211	174	141
15	342	282	234	186	153	128
20	305	250	206	163	137	117
25	271	221	181	144	124	106
30	241	195	158	131	112	97
35	213	171	141	118	102	88
40	188	150	127	108	93	80
45	165	136	116	98	84	73
50	146	123	105	89	77	67

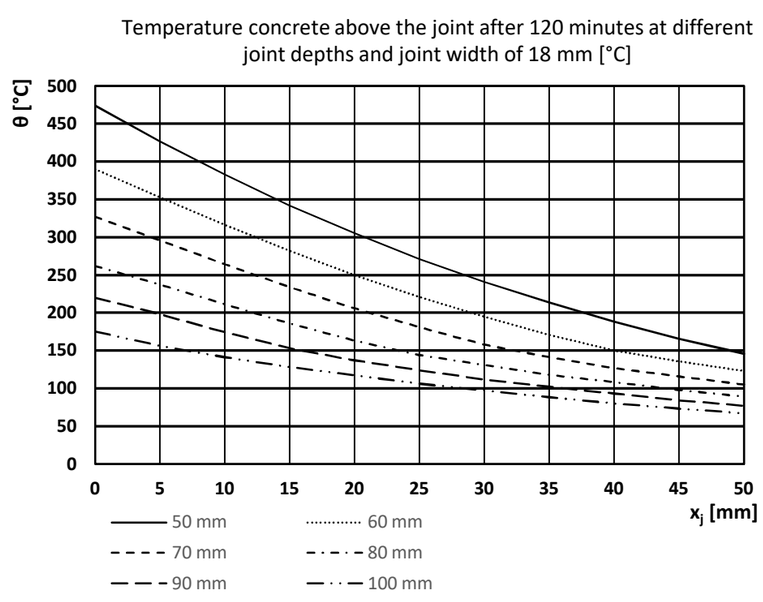

Temperatures above the joint, joint width 19 mm

Temperature concrete above the joint after 30 minutes at different joint depts and joint width of 19 mm [°C]						
x_j [mm]	Joint depth [mm]					
	50	60	70	80	90	100
0	106	69	60	47	39	33
5	91	60	51	40	33	27
10	76	52	42	33	27	23
15	64	43	35	28	22	18
20	53	36	29	23	18	15
25	44	30	24	19	15	12
30	37	25	20	15	12	10
35	30	21	16	13	10	8
40	25	17	13	10	8	7
45	21	14	11	8	7	5
50	17	12	9	7	5	4

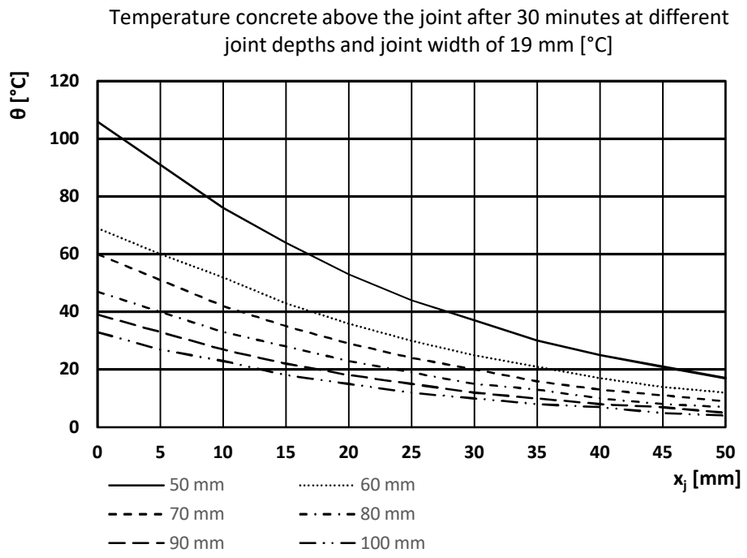

Temperature concrete above the joint after 60 minutes at different joint depts and joint width of 19 mm [°C]						
x_j [mm]	Joint depth [mm]					
	50	60	70	80	90	100
0	264	166	141	113	94	80
5	227	147	125	101	84	70
10	191	130	110	89	73	62
15	159	115	96	78	64	54
20	135	101	84	68	56	47
25	118	88	74	60	49	41
30	103	77	64	52	43	36
35	90	68	56	46	38	32
40	79	60	50	40	33	28
45	69	53	43	35	29	24
50	61	46	38	31	26	21

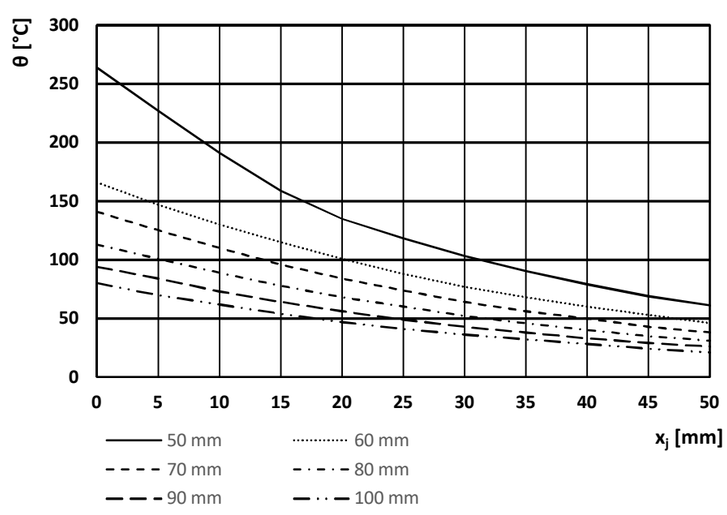

Temperature concrete above the joint after 90 minutes at different joint depts and joint width of 19 mm [°C]						
x_j [mm]	Joint depth [mm]					
	50	60	70	80	90	100
0	403	281	246	193	153	130
5	356	254	216	169	138	117
10	311	224	187	147	123	104
15	271	196	161	131	110	93
20	235	169	140	117	98	83
25	202	146	125	104	88	75
30	174	131	111	93	79	67
35	150	117	100	84	71	60
40	133	105	89	75	63	54
45	119	94	80	67	57	49
50	106	84	72	61	51	44

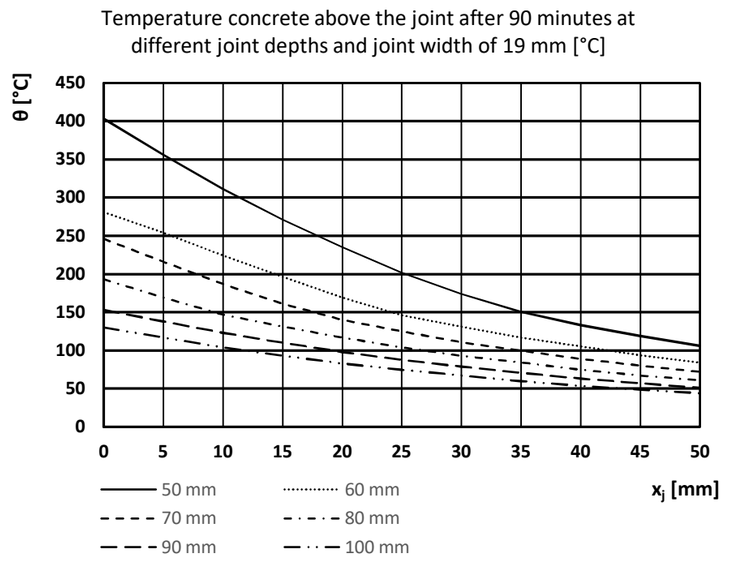

Temperature concrete above the joint after 120 minutes at different joint depts and joint width of 19 mm [°C]						
x_j [mm]	Joint depth [mm]					
	50	60	70	80	90	100
0	502	370	333	273	226	187
5	451	340	300	247	203	166
10	403	307	268	219	179	147
15	359	275	237	193	156	133
20	319	245	209	169	140	120
25	284	217	183	148	126	109
30	251	192	160	134	114	99
35	222	168	142	121	104	90
40	196	149	129	110	94	81
45	172	134	117	100	86	74
50	152	122	106	91	78	68

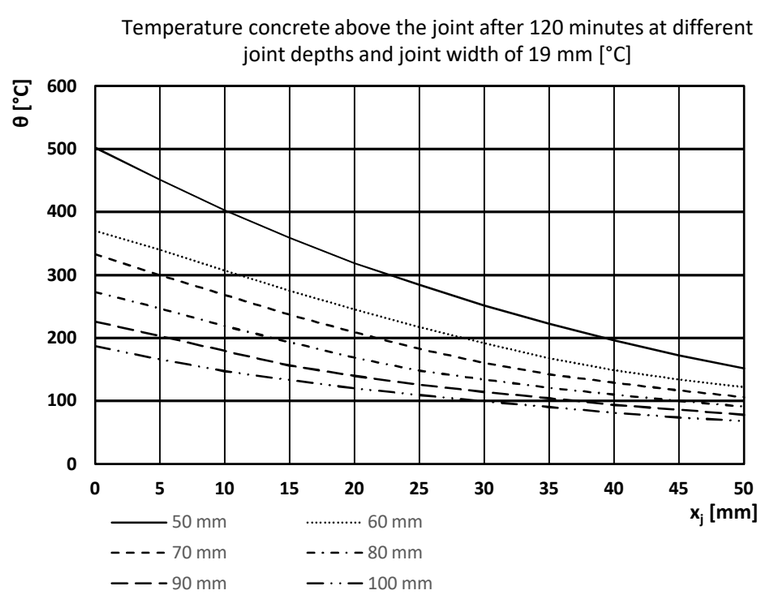

Temperatures above the joint, joint depth 50 mm

Temperature concrete above the joint after 30 minutes at different joint widths and joint depth of 50 mm [°C																			
x_j [mm]	Joint width [mm]																		
	1	2	3	4	5	6	7	8	9	10	11	12	13	14	15	16	17	18	19
0	93	92	90	84	89	83	82	88	87	90	89	90	91	90	94	92	95	98	106
5	78	78	77	74	78	74	73	77	77	79	78	79	80	79	81	80	82	84	91
10	65	65	65	62	66	62	62	66	66	67	67	67	68	68	69	69	70	74	76
15	54	54	54	52	55	52	52	55	55	56	56	57	57	57	58	58	59	60	64
20	45	45	45	44	46	44	44	46	46	47	47	47	48	48	49	48	49	50	53
25	38	38	38	36	38	37	37	39	39	39	39	40	40	40	41	40	41	42	44
30	31	32	32	30	32	30	31	32	32	33	33	33	33	33	34	34	34	35	37
35	26	26	26	25	27	25	25	27	27	27	27	27	28	28	28	28	28	29	30
40	22	22	22	21	22	21	21	22	22	23	22	23	23	23	23	23	24	24	25
45	18	18	18	17	18	17	17	18	18	19	18	19	19	19	19	19	19	20	21
50	15	15	15	14	15	14	14	15	15	15	15	15	15	15	16	16	16	16	17

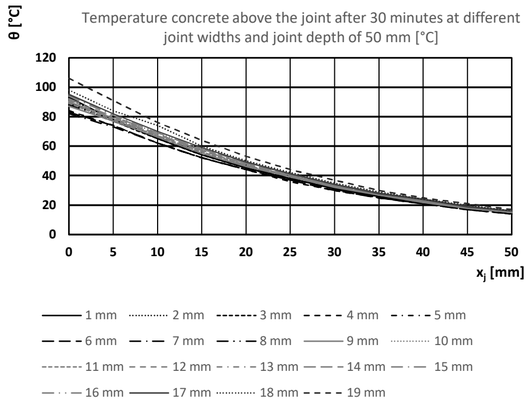

Temperature concrete above the joint after 60 minutes at different joint widths and joint depth of 50 mm [°C]																			
x_j [mm]	Joint width [mm]																		
	1	2	3	4	5	6	7	8	9	10	11	12	13	14	15	16	17	18	19
0	220	218	213	214	214	215	213	212	212	220	217	221	223	222	232	228	235	244	264
5	187	187	186	180	189	181	181	188	188	194	192	194	197	196	202	201	205	211	227
10	156	157	156	152	159	153	153	160	160	164	164	165	167	166	171	171	174	178	191
15	135	135	135	132	137	133	133	138	138	140	140	141	142	142	145	145	146	149	159
20	118	118	118	116	120	117	117	120	121	123	122	123	124	124	126	126	127	129	135
25	104	104	104	102	105	102	103	106	106	107	107	108	109	109	110	110	111	113	118
30	91	91	91	89	92	90	90	93	93	94	94	95	95	95	96	97	97	99	103
35	80	80	80	79	81	79	79	81	82	83	82	83	84	84	85	85	85	86	90
40	70	71	71	69	71	70	70	72	72	73	73	73	73	73	74	74	75	76	79
45	62	62	62	61	63	61	62	63	63	67	64	64	65	65	65	65	66	66	69
50	55	55	55	54	56	54	54	56	56	56	56	57	57	57	57	57	58	58	61

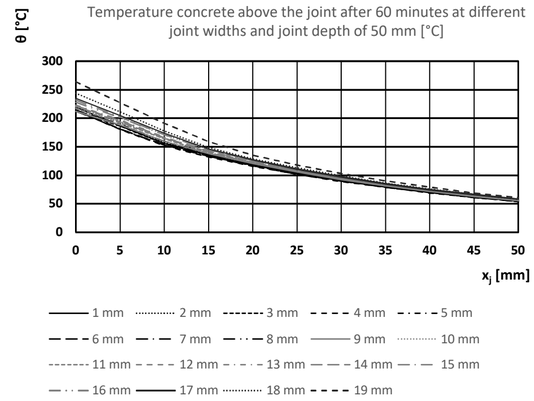

Temperature concrete above the joint after 90 minutes at different joint widths and joint depth of 50 mm [°C]																			
x_j [mm]	Joint width [mm]																		
	1	2	3	4	5	6	7	8	9	10	11	12	13	14	15	16	17	18	19
0	327	325	321	313	325	316	315	326	326	338	336	341	346	344	359	355	365	378	403
5	290	291	291	285	296	288	289	298	298	307	305	309	313	312	321	321	327	335	356
10	255	257	256	251	261	255	255	264	265	272	271	274	277	276	283	284	288	294	311
15	224	225	225	221	229	223	224	231	232	237	237	240	242	242	248	249	252	257	271
20	195	196	196	192	200	195	195	202	203	207	207	209	211	211	216	216	219	223	235
25	169	170	170	167	173	169	169	175	175	179	179	181	183	183	186	187	189	193	202
30	147	148	148	146	150	147	147	151	152	154	154	156	157	157	160	161	163	165	174
35	132	132	132	131	134	132	132	135	135	137	137	138	139	139	140	141	142	144	150
40	118	119	119	117	120	118	118	121	121	123	123	123	124	124	126	126	127	128	133
45	106	107	107	106	108	106	106	108	109	110	110	111	111	111	113	113	114	115	119
50	96	96	96	95	97	96	96	97	98	99	99	99	100	100	101	101	102	103	106

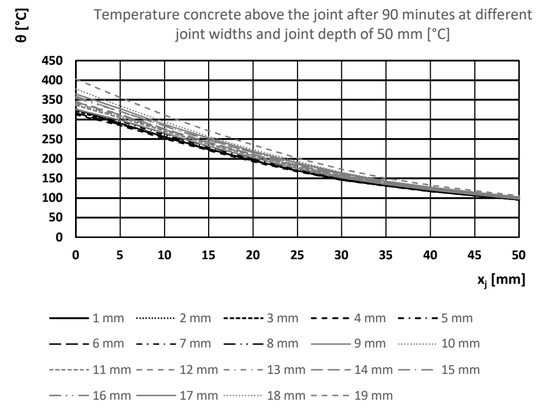

Temperature concrete above the joint after 120 minutes at different joint widths and joint depth of 50 mm [°C]																			
x_j [mm]	Joint width [mm]																		
	1	2	3	4	5	6	7	8	9	10	11	12	13	14	15	16	17	18	19
0	405	404	400	394	407	399	399	410	411	425	423	430	436	434	451	449	459	474	502
5	368	369	369	364	376	369	370	380	381	391	390	394	400	399	410	410	417	427	451
10	331	333	333	329	340	333	334	344	356	354	353	357	361	361	369	371	375	383	403
15	298	300	300	296	306	300	301	309	311	317	317	320	324	324	331	332	336	342	359
20	267	269	269	266	274	269	270	277	278	284	284	287	290	290	296	297	300	305	319
25	239	241	241	238	245	241	242	248	249	253	254	256	258	258	263	265	267	271	284
30	213	214	215	212	218	214	215	220	221	225	226	227	230	230	234	235	237	241	251
35	189	190	191	188	194	190	191	195	196	200	200	202	203	204	207	208	210	213	222
40	167	168	169	166	171	168	169	173	173	176	176	178	179	180	182	184	185	188	196
45	148	149	150	148	151	149	149	152	153	155	155	156	158	158	161	161	163	165	172
50	135	136	136	134	137	135	135	138	138	140	140	140	141	141	143	144	145	146	152

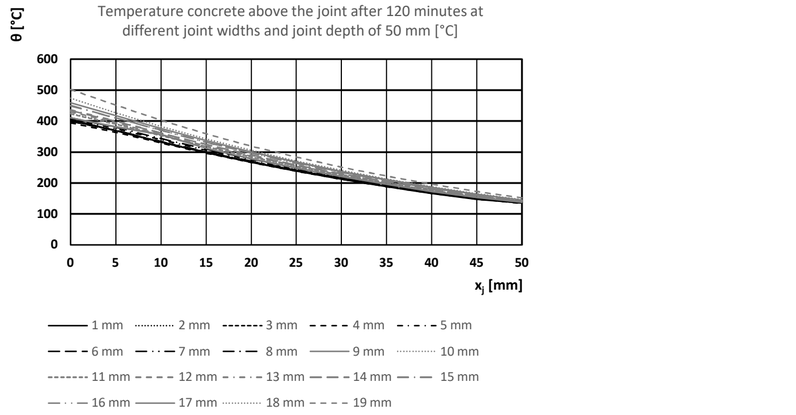

Temperatures above the joint, joint depth 60 mm

Temperature concrete above the joint after 30 minutes at different joint widths and joint depth of 60 mm [°C																		
x_j [mm]	Joint width [mm]																	
	1	2	3	4	5	6	7	8	9	10	11	12	13	14	15	16	17	18	19
0	67	66	64	65	65	65	65	64	66	67	66	66	68	70	72	71	71	74	69
5	56	56	55	56	57	57	57	56	58	59	58	58	59	61	62	61	61	63	60
10	47	47	47	47	47	47	48	48	49	50	49	49	50	51	53	52	52	54	52
15	39	39	39	39	40	40	40	40	41	41	41	41	42	43	44	43	44	45	43
20	32	32	32	33	33	33	33	33	34	34	34	35	35	36	37	36	36	37	36
25	27	27	27	27	27	27	28	28	28	29	29	29	29	30	31	30	30	31	30
30	22	23	23	22	23	23	23	23	23	24	24	24	24	25	26	25	25	26	25
35	18	18	18	19	19	19	18	19	19	20	20	20	20	20	21	21	21	21	21
40	15	15	15	15	15	15	15	16	16	16	16	16	16	17	18	17	17	18	17
45	12	12	12	12	12	13	13	13	13	13	13	13	13	14	14	14	14	14	14
50	10	10	10	10	10	10	10	10	11	11	11	11	11	11	12	11	11	12	12

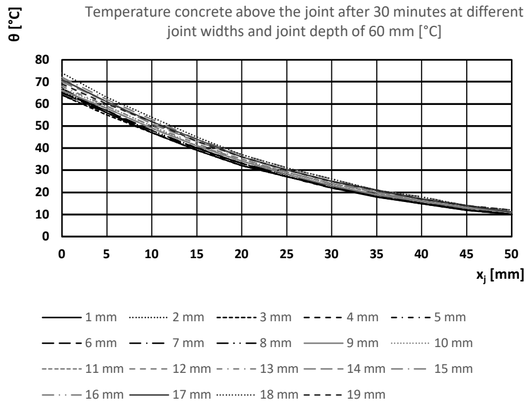

Temperature concrete above the joint after 60 minutes at different joint widths and joint depth of 60 mm [°C]																		
x_j [mm]	Joint width [mm]																	
	1	2	3	4	5	6	7	8	9	10	11	12	13	14	15	16	17	18	19
0	159	157	152	156	156	155	156	154	158	162	159	159	163	169	175	171	171	179	166
5	137	137	136	138	139	139	140	139	141	143	142	142	144	148	151	149	149	154	147
10	120	121	120	121	122	122	122	123	125	126	126	126	128	130	132	131	131	134	130
15	105	105	105	106	107	107	107	108	109	111	110	111	112	114	116	115	115	117	115
20	92	92	92	93	93	94	94	94	96	97	97	97	98	99	101	100	101	102	101
25	81	81	81	82	82	82	83	83	84	85	85	85	86	87	89	88	88	90	88
30	71	71	71	72	72	72	73	73	74	75	74	75	75	76	78	77	77	79	77
35	63	63	63	63	64	64	64	64	65	66	65	66	66	67	68	68	68	69	68
40	55	56	56	56	56	56	56	57	57	58	58	58	58	59	60	60	60	61	60
45	49	49	49	49	49	49	50	50	50	51	51	51	51	52	53	52	52	53	53
50	43	43	43	43	43	43	44	44	44	45	45	45	45	46	47	46	46	47	46

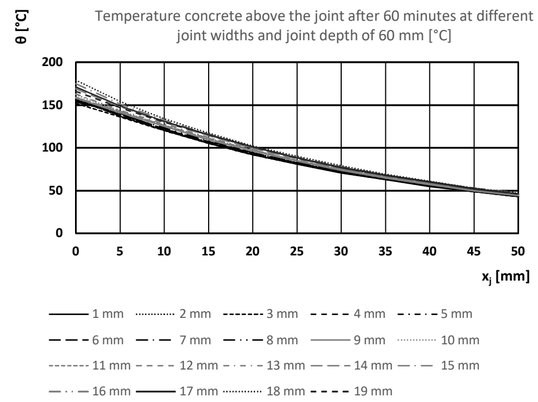

Temperature concrete above the joint after 90 minutes at different joint widths and joint depth of 60 mm [°C]																		
x_j [mm]	Joint width [mm]																	
	1	2	3	4	5	6	7	8	9	10	11	12	13	14	15	16	17	18	19
0	258	256	252	256	257	257	258	248	264	270	266	268	274	283	292	287	287	298	281
5	227	228	228	230	232	232	234	234	239	244	241	243	247	253	260	257	257	265	254
10	198	200	199	201	202	203	205	206	210	214	213	214	217	222	228	225	226	232	224
15	171	172	172	174	175	176	177	178	182	185	184	186	189	183	198	196	196	201	196
20	149	150	151	151	152	152	153	154	157	160	159	160	162	166	170	168	169	173	169
25	133	134	134	134	135	135	136	137	139	140	140	141	142	144	147	146	146	149	146
30	119	120	120	120	121	121	122	123	124	125	125	126	127	129	131	130	130	132	131
35	107	107	107	108	109	109	110	110	111	112	112	113	114	115	117	116	117	118	117
40	96	97	97	97	98	98	98	99	100	101	101	101	102	103	105	104	104	106	105
45	87	88	88	88	88	88	89	89	90	91	90	91	92	92	94	93	94	95	94
50	78	78	78	79	79	79	80	80	81	81	81	82	82	83	85	84	84	85	84

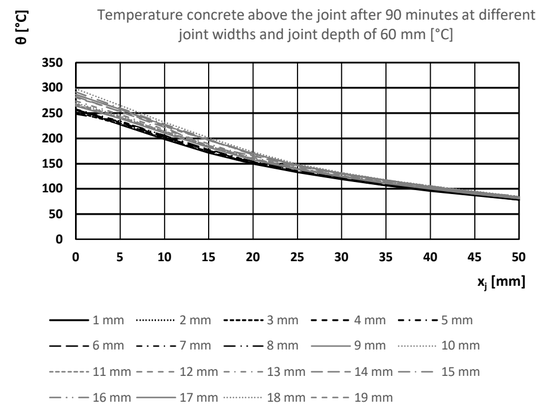

Temperature concrete above the joint after 120 minutes at different joint widths and joint depth of 60 mm [°C]																			
x_j [mm]	Joint width [mm]																		
	1	2	3	4	5	6	7	8	9	10	11	12	13	14	15	16	17	18	19
0	334	333	329	334	336	336	338	338	346	354	350	352	360	371	382	376	377	390	370
5	301	302	302	306	309	310	312	312	319	325	322	325	330	338	346	342	343	353	340
10	270	272	272	275	277	278	280	282	287	292	291	293	297	303	311	308	309	316	307
15	241	243	243	246	248	249	251	252	257	261	260	262	265	271	278	275	276	282	275
20	215	217	217	219	220	221	223	224	228	232	231	233	236	240	247	244	245	250	245
25	191	193	193	194	195	196	198	199	202	205	205	207	209	213	193	216	217	221	217
30	169	170	171	171	173	173	175	176	179	181	181	182	184	187	219	190	191	195	192
35	149	150	151	151	152	153	154	155	157	159	159	160	162	165	170	167	168	171	168
40	135	136	137	137	138	138	139	139	141	142	142	143	144	146	150	148	148	150	149
45	123	124	125	125	125	126	126	127	128	129	129	130	131	132	135	134	134	136	134
50	113	114	114	114	114	115	115	116	117	118	118	118	119	120	123	121	122	123	122

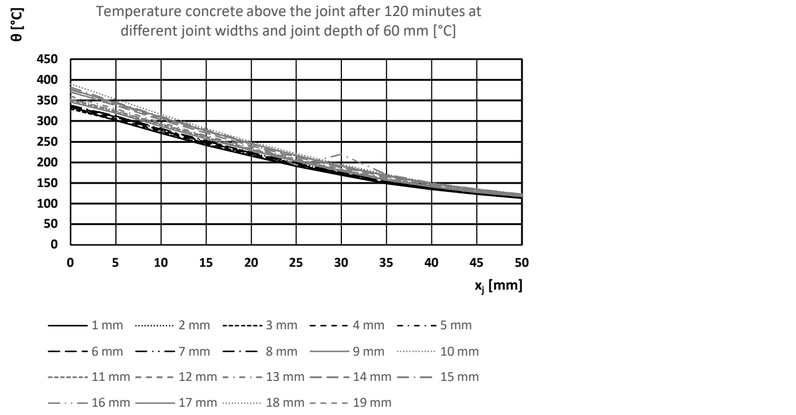

Temperatures above the joint, joint depth 70 mm

Temperature concrete above the joint after 30 minutes at different joint widths and joint depth of 70 mm [°C																		
x_j [mm]	Joint width [mm]																	
	1	2	3	4	5	6	7	8	9	10	11	12	13	14	15	16	17	18	19
0	49	48	46	48	49	48	48	48	49	51	51	51	52	53	53	55	56	58	60
5	41	41	40	41	42	42	42	42	43	44	44	44	45	46	46	47	48	50	51
10	34	34	34	34	35	35	35	35	36	37	37	37	38	39	39	40	40	42	42
15	28	28	28	28	29	29	29	29	30	31	31	31	32	32	32	33	34	35	35
20	23	23	23	24	24	24	24	24	25	26	26	26	26	27	27	27	28	29	29
25	19	19	19	19	20	20	20	20	21	21	21	21	22	22	22	23	22	24	24
30	16	17	17	16	16	16	16	17	17	17	17	18	18	18	18	19	19	20	20
35	13	13	13	13	13	13	13	14	14	14	14	14	15	15	15	15	16	16	16
40	10	10	10	11	11	11	11	11	11	12	12	12	12	12	12	13	13	13	13
45	8	8	8	9	9	9	9	9	9	9	9	10	10	10	10	10	10	11	11
50	7	7	7	7	7	7	7	7	7	8	8	8	8	8	8	8	8	9	9

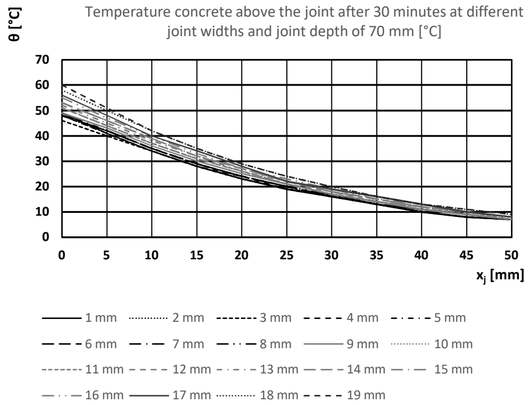

Temperature concrete above the joint after 60 minutes at different joint widths and joint depth of 70 mm [°C]																			
x_j [mm]	Joint width [mm]																		
	1	2	3	4	5	6	7	8	9	10	11	12	13	14	15	16	17	18	19
0	122	120	115	120	122	121	120	120	122	125	125	126	127	129	129	132	133	139	141
5	107	107	106	108	109	109	109	109	111	113	113	114	115	117	117	119	120	123	125
10	94	93	94	95	96	96	96	97	98	100	100	101	102	103	103	105	106	108	110
15	82	82	82	83	84	84	84	85	86	88	88	88	89	90	91	92	93	95	96
20	72	72	72	73	74	74	74	75	76	77	77	78	78	79	80	81	81	83	84
25	64	64	64	64	65	65	65	66	67	68	68	68	69	70	70	71	71	73	74
30	56	56	56	57	57	57	57	58	59	59	60	60	60	61	61	62	63	64	64
35	49	49	49	50	50	50	51	51	51	52	52	53	53	54	54	55	55	56	56
40	43	44	44	44	44	44	44	45	46	46	46	46	47	47	47	48	48	49	50
45	38	38	38	39	39	39	39	39	40	40	40	41	41	41	42	42	42	43	43
50	34	34	34	34	34	34	34	35	35	35	36	36	36	36	37	37	37	38	38

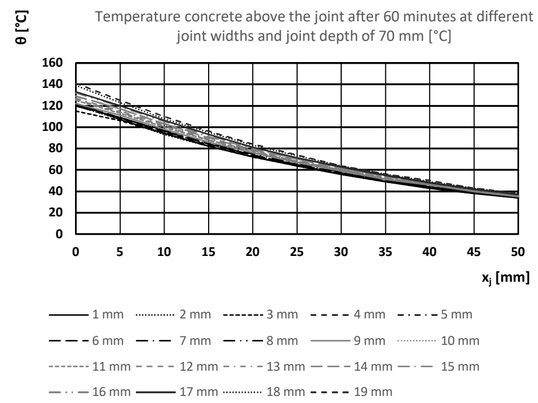

Temperature concrete above the joint after 90 minutes at different joint widths and joint depth of 70 mm [°C]																			
x_j [mm]	Joint width [mm]																		
	1	2	3	4	5	6	7	8	9	10	11	12	13	14	15	16	17	18	19
0	201	199	195	199	203	201	201	200	206	212	213	214	217	222	222	228	231	241	246
5	175	176	176	177	181	180	181	181	185	190	191	192	194	198	199	203	205	213	216
10	151	153	152	153	156	156	156	158	161	166	166	167	169	173	173	177	178	184	187
15	135	136	136	136	138	138	138	140	141	144	144	145	147	149	150	152	154	158	161
20	121	122	122	122	123	124	124	125	127	129	129	130	131	133	133	135	136	139	140
25	108	109	109	110	111	111	111	112	113	115	115	116	117	119	119	120	121	124	125
30	97	98	98	98	99	100	100	101	102	103	103	100	105	106	107	108	108	110	111
35	88	88	88	89	89	90	90	90	91	93	93	93	94	95	95	97	97	99	100
40	79	80	80	80	80	81	81	81	82	83	83	84	84	85	86	87	87	88	89
45	71	72	72	72	72	73	73	73	74	75	75	75	76	77	77	78	78	79	80
50	64	64	64	65	65	65	66	66	67	67	68	68	68	69	69	70	70	71	72

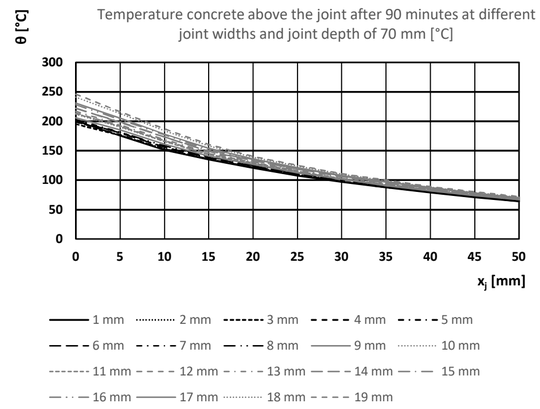

Temperature concrete above the joint after 120 minutes at different joint widths and joint depth of 70 mm [°C]																			
x_j [mm]	Joint width [mm]																		
	1	2	3	4	5	6	7	8	9	10	11	12	13	14	15	16	17	18	19
0	274	273	269	273	277	276	276	276	283	291	292	294	298	303	304	312	315	327	333
5	245	246	246	249	253	253	254	255	260	267	267	269	272	277	278	284	286	296	300
10	218	220	220	222	225	226	227	229	233	239	240	241	244	248	250	254	256	264	268
15	193	195	195	197	200	200	201	203	207	212	212	214	217	220	222	225	227	234	237
20	171	173	173	174	176	177	178	180	183	187	187	189	191	195	196	199	201	206	209
25	151	152	152	153	155	165	156	158	161	164	165	166	168	171	172	175	176	181	183
30	136	137	138	138	140	140	140	141	143	146	146	147	148	150	151	153	154	158	160
35	124	125	126	126	127	127	128	129	130	132	132	133	134	135	136	138	138	141	142
40	113	114	115	115	116	116	116	117	118	120	120	121	122	123	123	125	126	127	129
45	103	104	105	105	105	106	106	107	108	109	109	110	111	112	112	113	114	116	117
50	95	96	96	95	96	96	97	97	98	99	100	100	101	102	102	103	104	105	106

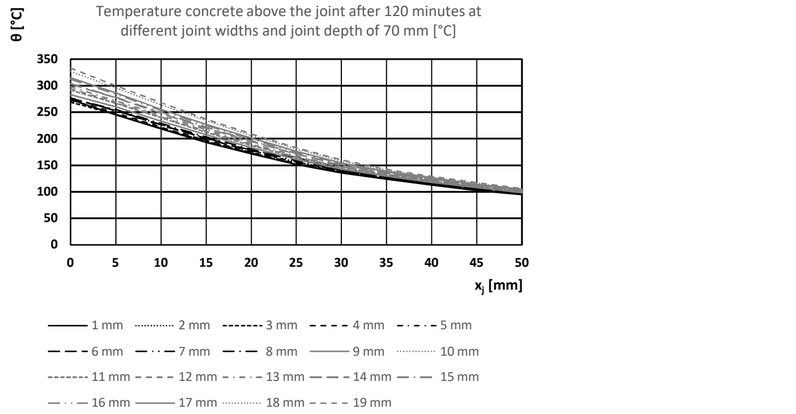

Temperatures above the joint, joint depth 80 mm

Temperature concrete above the joint after 30 minutes at different joint widths and joint depth of 80 mm [°C																			
x_j [mm]	Joint width [mm]																		
	1	2	3	4	5	6	7	8	9	10	11	12	13	14	15	16	17	18	19
0	37	36	34	36	37	36	37	37	38	39	38	40	40	42	43	43	44	45	47
5	30	30	29	30	31	31	32	32	32	34	33	34	35	36	37	37	37	38	40
10	25	25	25	25	26	26	26	26	27	28	28	29	29	30	31	31	31	32	33
15	20	20	20	21	21	21	22	22	22	23	23	24	24	25	25	26	26	26	28
20	17	17	17	17	17	18	18	18	18	19	19	20	20	20	21	21	22	22	23
25	14	14	14	14	14	14	15	15	15	16	16	16	16	17	17	17	18	18	19
30	11	12	12	11	12	12	12	12	12	13	13	13	13	14	14	14	15	15	15
35	9	9	9	9	9	9	10	10	10	10	10	11	11	11	11	12	12	12	13
40	7	7	7	7	8	8	8	8	8	8	8	9	9	9	9	9	10	10	10
45	6	6	6	6	6	6	6	6	7	7	7	7	7	7	8	8	8	8	8
50	5	5	5	5	5	5	5	5	5	5	5	6	6	6	6	6	6	6	7

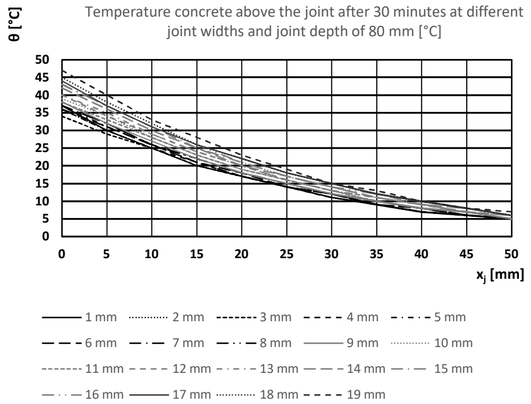

Temperature concrete above the joint after 60 minutes at different joint widths and joint depth of 80 mm [°C]																			
x_j [mm]	Joint width [mm]																		
	1	2	3	4	5	6	7	8	9	10	11	12	13	14	15	16	17	18	19
0	97	95	90	95	96	96	96	96	97	100	98	101	102	105	107	107	108	109	113
5	85	85	84	85	87	87	87	87	89	91	89	91	92	94	96	96	97	98	101
10	74	75	74	75	76	76	77	77	78	80	79	81	82	83	85	85	86	86	89
15	65	65	65	66	67	67	67	68	69	70	70	71	72	73	74	75	75	76	78
20	57	57	57	58	59	59	59	60	61	62	61	62	63	64	65	65	66	66	68
25	50	50	50	51	52	52	52	52	53	54	54	55	55	56	57	57	58	58	60
30	44	44	44	45	45	46	46	46	47	48	47	48	49	49	50	50	51	51	52
35	39	39	39	39	40	40	40	41	41	42	42	42	43	43	44	44	45	45	46
40	34	35	35	35	35	35	35	36	36	37	37	37	37	38	39	39	39	39	40
45	30	30	30	30	31	31	31	31	32	32	32	33	33	33	34	34	34	35	35
50	26	26	26	27	27	27	27	27	28	28	28	29	29	29	30	30	30	30	31

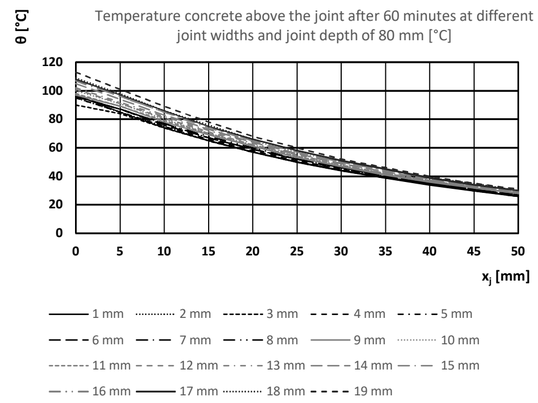

Temperature concrete above the joint after 90 minutes at different joint widths and joint depth of 80 mm [°C]																			
x_j [mm]	Joint width [mm]																		
	1	2	3	4	5	6	7	8	9	10	11	12	13	14	15	16	17	18	19
0	155	153	149	153	156	155	156	156	159	165	161	167	169	175	179	179	181	183	193
5	137	138	138	139	141	141	142	142	144	148	146	149	151	155	158	158	160	162	169
10	123	125	125	124	126	126	127	128	130	133	132	134	135	138	140	140	142	142	147
15	110	111	111	112	113	113	114	115	116	119	118	120	121	123	125	125	127	127	131
20	99	100	100	100	101	102	102	103	104	106	106	107	108	110	112	112	113	114	117
25	89	90	90	90	91	91	92	92	94	95	95	96	97	98	100	100	101	102	104
30	80	81	81	81	82	82	82	83	84	86	85	86	87	88	89	90	90	91	93
35	72	72	72	73	74	74	74	75	76	77	77	78	78	79	80	81	81	82	84
40	65	66	66	66	66	67	67	67	68	69	69	70	70	71	72	72	73	73	75
45	59	60	60	59	60	60	60	61	61	62	62	63	63	64	65	65	65	66	67
50	53	53	53	54	54	54	54	55	55	56	56	57	57	58	58	58	59	59	61

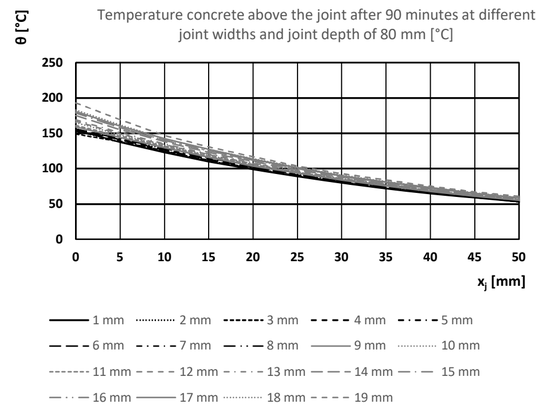

Temperature concrete above the joint after 120 minutes at different joint widths and joint depth of 80 mm [°C																			
x_j [mm]	Joint width [mm]																		
	1	2	3	4	5	6	7	8	9	10	11	12	13	14	15	16	17	18	19
0	222	221	217	221	225	224	226	226	230	238	233	240	243	251	256	256	259	262	273
5	197	198	198	200	205	205	206	207	211	217	214	219	222	227	232	233	235	237	247
10	174	176	176	177	181	181	182	184	188	193	191	196	198	202	206	207	210	211	219
15	153	155	155	156	159	159	161	162	165	170	169	172	174	178	182	183	185	186	193
20	138	140	140	140	142	142	143	144	147	150	149	152	153	156	159	160	162	163	169
25	126	128	128	127	129	129	130	131	133	135	135	137	138	140	141	142	143	144	148
30	115	116	117	116	117	118	118	119	121	123	122	124	125	127	128	129	130	131	134
35	104	105	106	106	107	108	108	108	110	112	111	113	113	115	116	117	118	118	121
40	95	96	97	96	98	98	98	99	100	101	101	102	103	104	106	106	107	108	110
45	87	88	89	88	89	89	90	90	91	92	92	93	94	95	96	96	97	98	100
50	80	81	81	81	81	82	82	82	83	84	84	85	86	87	87	88	88	89	91

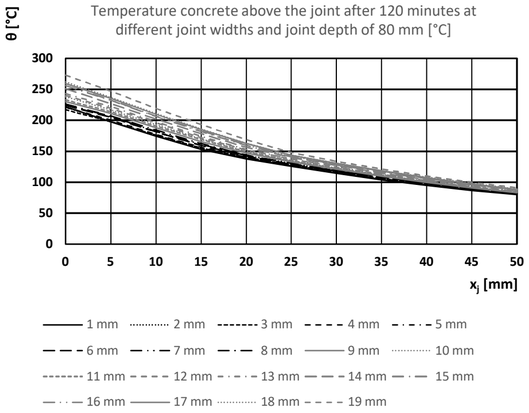

Temperatures above the joint, joint depth 90 mm

Temperature concrete above the joint after 30 minutes at different joint widths and joint depth of 90 mm [°C																		
x_j [mm]	Joint width [mm]																	
	1	2	3	4	5	6	7	8	9	10	11	12	13	14	15	16	17	18	19
0	29	28	26	20	28	28	29	29	30	31	31	31	33	34	36	36	37	29	39
5	21	21	20	17	24	24	24	25	25	26	26	27	28	28	30	30	31	23	33
10	17	17	17	14	19	20	20	20	21	22	22	22	23	24	25	25	26	19	27
15	14	14	14	12	16	16	16	17	17	18	18	18	19	19	20	21	21	15	22
20	10	10	10	9	13	13	13	14	14	14	15	15	15	16	17	17	17	12	18
25	9	9	9	7	11	11	11	11	11	12	12	12	13	13	14	14	14	10	15
30	7	8	8	6	8	9	9	9	9	10	10	10	10	11	11	11	12	8	12
35	6	6	6	5	7	7	7	7	7	8	8	8	8	9	9	9	9	7	10
40	5	5	5	4	5	6	6	6	6	6	6	6	7	7	7	7	8	5	8
45	4	4	4	3	4	4	5	5	5	5	5	5	5	6	6	6	6	4	7
50	3	3	3	2	3	4	4	4	4	4	4	4	4	4	5	5	5	3	5

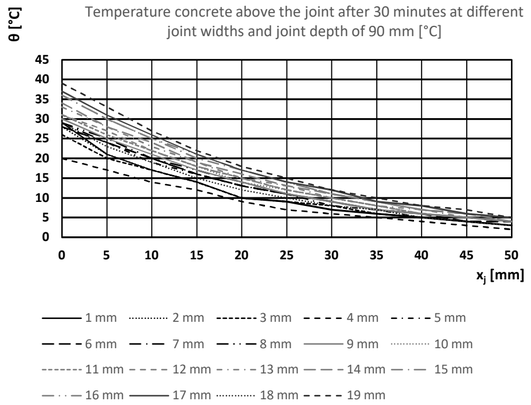

Temperature concrete above the joint after 60 minutes at different joint widths and joint depth of 90 mm [°C]																		
x_j [mm]	Joint width [mm]																	
	1	2	3	4	5	6	7	8	9	10	11	12	13	14	15	16	17	18	19
0	72	70	65	66	78	78	78	78	79	81	81	82	84	86	90	90	91	66	94
5	68	68	67	61	70	70	70	71	72	73	73	74	76	77	80	80	81	57	84
10	59	59	58	54	61	61	62	62	63	65	65	65	67	68	70	70	71	49	73
15	50	50	50	47	54	54	54	55	56	57	57	57	59	60	61	62	62	42	64
20	44	44	44	42	47	47	48	48	49	50	50	50	51	52	54	54	55	37	56
25	39	39	39	37	41	42	42	42	43	44	44	44	45	46	47	47	48	32	49
30	34	34	34	32	36	37	37	37	38	38	38	39	39	40	41	41	42	28	43
35	29	29	29	28	32	32	32	33	33	34	34	34	35	35	36	36	37	24	38
40	26	27	27	25	28	28	28	29	29	29	30	30	30	31	32	32	32	21	33
45	23	23	23	22	24	25	25	25	25	26	26	26	27	27	28	28	28	18	29
50	20	20	20	19	21	22	22	22	22	23	23	23	23	24	24	24	25	16	26

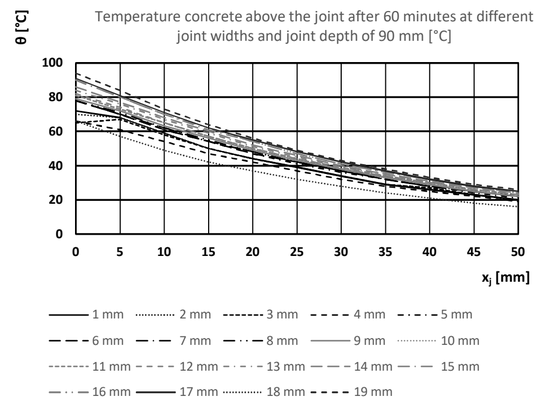

Temperature concrete above the joint after 90 minutes at different joint widths and joint depth of 90 mm [°C]																		
x_j [mm]	Joint width [mm]																	
	1	2	3	4	5	6	7	8	9	10	11	12	13	14	15	16	17	18	19
0	127	125	121	113	127	127	128	128	130	132	132	133	137	140	146	146	148	150	153
5	110	111	111	105	116	117	118	118	119	122	122	123	125	128	132	132	133	135	138
10	98	100	99	95	104	105	105	106	108	110	110	111	113	115	118	118	120	121	123
15	88	89	89	85	93	94	95	95	96	98	98	99	101	103	106	106	107	108	110
20	80	81	81	77	84	84	85	85	87	88	88	89	90	92	94	94	95	96	98
25	72	73	73	70	75	76	76	77	78	79	79	80	81	82	84	85	85	86	88
30	64	65	65	63	68	68	69	69	70	71	71	72	73	74	76	76	76	77	79
35	58	58	58	57	61	61	62	62	63	64	64	65	65	66	68	68	69	69	71
40	52	53	53	51	55	55	56	56	57	57	58	58	59	60	61	61	62	62	63
45	46	47	47	46	50	50	50	50	51	52	52	52	53	54	55	55	55	56	57
50	43	43	43	42	45	45	45	46	46	47	47	47	48	48	49	49	50	50	51

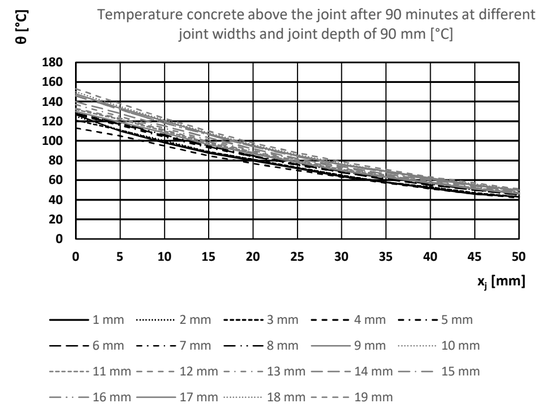

Temperature concrete above the joint after 120 minutes at different joint widths and joint depth of 90 mm [°C]																			
x_j [mm]	Joint width [mm]																		
	1	2	3	4	5	6	7	8	9	10	11	12	13	14	15	16	17	18	19
0	170	169	165	159	182	182	183	183	187	191	191	193	200	204	215	214	217	220	226
5	151	152	152	147	164	165	166	167	170	174	174	176	181	185	193	193	195	198	203
10	136	138	138	134	145	146	147	148	151	154	154	156	160	163	170	170	172	174	179
15	124	126	126	122	132	132	133	134	136	139	139	140	142	145	149	149	151	153	156
20	113	114	114	111	120	120	121	122	124	126	126	127	129	131	134	134	136	137	140
25	103	105	105	102	109	109	110	111	112	114	114	115	117	119	121	122	123	124	126
30	94	95	96	93	100	100	100	101	102	104	104	105	106	108	110	110	111	112	114
35	86	87	88	85	90	91	91	92	93	94	95	95	97	98	100	100	101	102	104
40	79	80	81	78	83	83	83	84	85	86	86	87	88	89	91	91	92	93	94
45	71	72	73	71	75	76	74	77	77	78	79	79	80	81	83	83	84	84	86
50	62	63	63	65	69	69	70	70	71	72	72	69	73	74	75	76	76	77	78

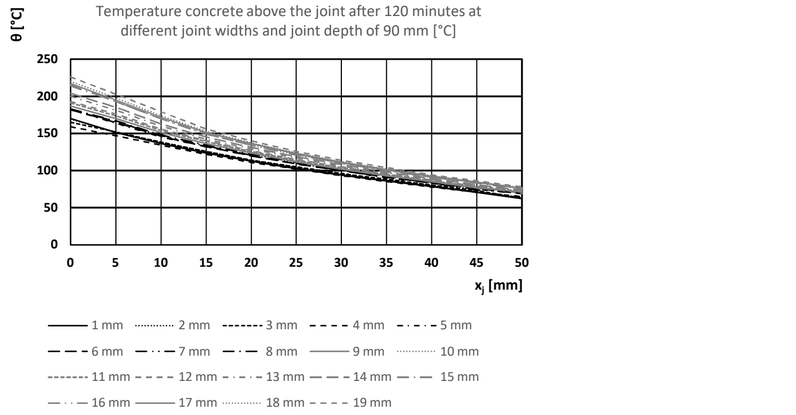

Temperatures above the joint, joint depth 100 mm

Temperature concrete above the joint after 30 minutes at different joint widths and joint depth of 100 mm [°C																			
x_j [mm]	Joint width [mm]																		
	1	2	3	4	5	6	7	8	9	10	11	12	13	14	15	16	17	18	19
0	22	21	19	22	22	22	23	23	24	25	25	26	27	27	31	30	27	32	33
5	17	17	16	18	18	19	19	20	20	21	21	22	22	23	26	25	22	26	27
10	14	14	14	14	15	15	16	16	16	17	17	18	18	19	22	20	19	22	23
15	11	11	11	12	12	12	13	13	13	14	14	15	15	15	18	17	15	18	18
20	9	9	9	9	10	10	10	11	11	11	12	12	12	13	15	14	13	15	15
25	7	7	7	8	8	8	8	9	9	9	9	10	10	10	12	11	10	12	12
30	6	7	7	6	6	6	7	7	7	7	8	8	8	8	10	9	8	10	10
35	5	5	5	5	5	5	5	6	6	6	6	6	6	7	8	7	7	8	8
40	4	4	4	4	4	4	4	4	5	5	5	5	5	5	7	6	6	7	7
45	3	3	3	3	3	3	3	4	4	4	4	4	4	4	5	5	5	6	5
50	2	2	2	3	3	3	3	3	3	3	3	3	3	3	4	4	4	5	4

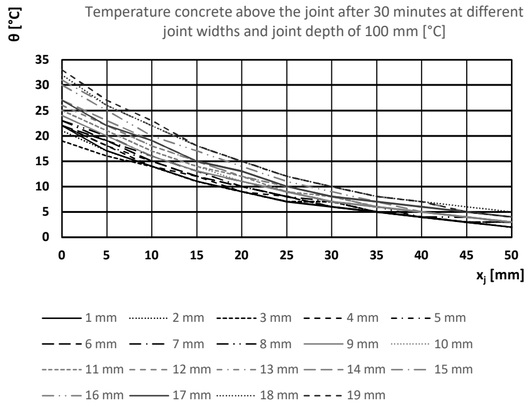

Temperature concrete above the joint after 60 minutes at different joint widths and joint depth of 100 mm [°C]																			
x_j [mm]	Joint width [mm]																		
	1	2	3	4	5	6	7	8	9	10	11	12	13	14	15	16	17	18	19
0	63	61	56	62	63	63	64	64	65	67	67	68	69	70	73	74	68	76	80
5	55	55	56	55	56	57	57	58	59	60	60	61	62	63	65	66	61	67	70
10	48	49	48	48	49	50	50	51	52	53	53	54	55	55	58	58	54	59	62
15	42	42	42	42	43	44	44	45	45	46	47	47	48	49	51	51	48	52	54
20	37	37	37	37	38	38	39	39	40	41	41	41	42	43	45	44	42	46	47
25	32	32	32	32	33	33	34	34	35	36	36	36	37	37	39	39	37	40	41
30	28	28	28	29	29	29	30	30	30	31	31	32	32	33	35	34	33	36	36
35	25	25	25	25	26	26	26	26	27	27	27	28	28	29	30	30	29	32	32
40	22	23	23	22	22	22	23	23	23	24	24	24	25	25	27	26	25	28	28
45	19	19	19	19	19	20	20	20	20	21	21	21	22	22	23	23	22	24	24
50	16	16	16	17	17	17	17	18	18	18	18	19	19	19	20	20	19	21	21

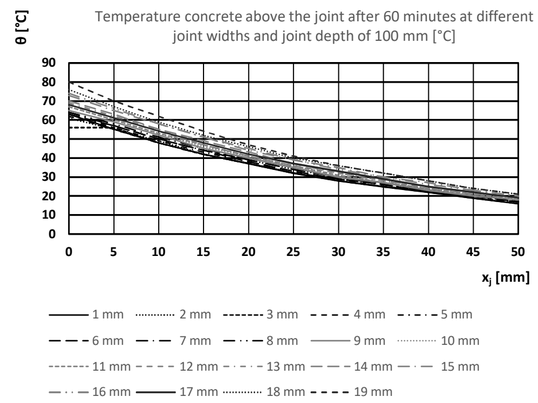

Temperature concrete above the joint after 90 minutes at different joint widths and joint depth of 100 mm [°C]																			
x_j [mm]	Joint width [mm]																		
	1	2	3	4	5	6	7	8	9	10	11	12	13	14	15	16	17	18	19
0	105	103	99	104	106	106	106	107	109	111	112	113	114	115	118	121	112	113	130
5	94	95	95	95	97	97	98	99	100	102	102	103	104	106	108	110	103	111	117
10	84	86	85	85	87	87	88	89	90	92	92	93	94	95	97	99	93	100	104
15	75	76	76	76	78	78	79	80	81	82	83	84	84	86	87	89	85	90	93
20	68	69	69	69	70	70	71	71	72	74	74	75	76	77	79	79	76	81	83
25	61	62	62	62	73	63	64	64	65	66	67	67	68	69	71	71	69	73	75
30	55	56	56	56	57	57	57	58	59	60	60	61	61	62	64	64	62	66	67
35	49	49	49	50	51	51	52	52	53	54	54	54	55	56	47	57	56	59	60
40	45	46	46	45	46	46	46	47	47	48	48	49	49	50	52	51	50	53	54
45	40	41	41	41	41	41	42	42	43	43	44	44	44	45	46	46	45	48	49
50	36	36	36	37	37	37	38	38	38	39	39	40	40	40	42	42	41	43	44

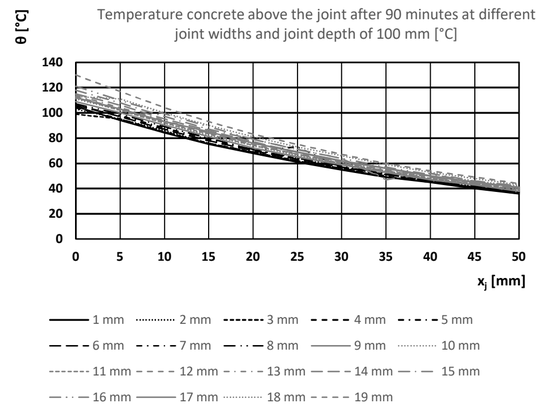

Temperature concrete above the joint after 120 minutes at different joint widths and joint depth of 100 mm [°C]																			
x_j [mm]	Joint width [mm]																		
	1	2	3	4	5	6	7	8	9	10	11	12	13	14	15	16	17	18	19
0	145	144	140	144	147	147	148	149	152	156	156	158	160	163	167	173	158	175	187
5	131	132	132	133	135	136	137	138	140	143	143	145	147	148	150	155	144	156	166
10	119	121	121	121	123	123	124	126	127	130	130	132	133	135	136	140	133	141	147
15	108	110	110	110	111	112	113	114	116	118	118	120	121	122	124	127	121	128	133
20	98	100	100	100	101	102	103	104	105	107	107	109	110	111	113	115	111	117	120
25	90	92	92	91	92	93	93	94	96	97	98	99	100	101	103	104	101	106	109
30	82	83	84	83	84	84	78	86	87	89	89	90	91	92	93	94	92	97	99
35	75	76	77	76	77	77	71	78	79	81	81	82	82	83	85	86	84	88	90
40	68	69	70	69	70	70	65	72	72	74	74	75	75	76	78	78	76	80	81
45	63	64	65	63	64	64	59	65	66	67	67	68	69	69	71	71	70	73	74
50	57	58	58	58	59	59	54	60	60	61	62	62	63	63	64	64	64	67	68

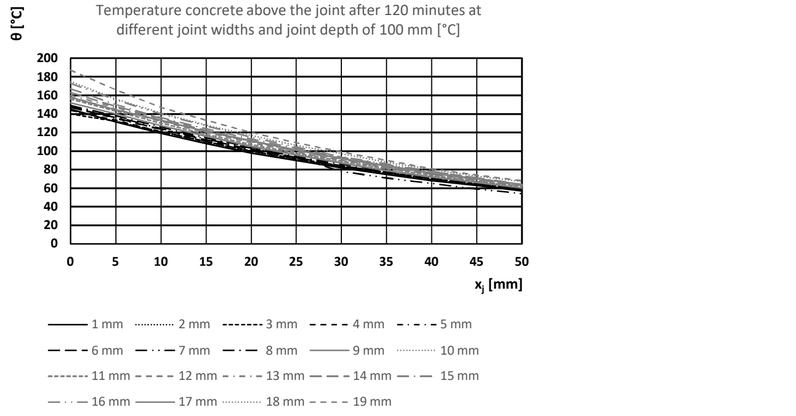

Comparison temperatures in normative situation joint width 19 mm and joint depth 50 mm

Temperatures at different locations in the composite floor											
Analytical analyses ABAQUS Surface Critical Detail [°C]				Analytical analyses ABAQUS 50 mm next to Critical Detail [°C]				Joint 19 mm [°C]			
30 min.	60 min.	90 min.	120 min.	30 min.	60 min.	90 min.	120 min.	30min	60min	90min	120min
818	896	973	997	878	890	967	993				
584	782	878	921	509	696	795	849				
432	661	782	844	342	541	652	723				
304	538	674	753	221	415	532	612				
199	416	557	647	140	314	430	514				
116	282	416	511	96	232	344	427	106	264	403	502
77	192	310	400	68	165	270	352	76	191	311	403
53	135	233	318	47	124	208	286	53	135	235	319
37	102	173	250	33	96	157	229	37	103	174	251
25	78	132	195	23	74	125	181	25	79	133	196
17	60	106	151	16	58	101	143	17	61	106	152

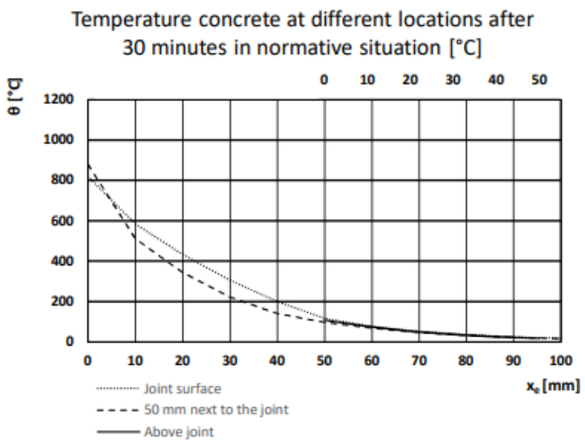

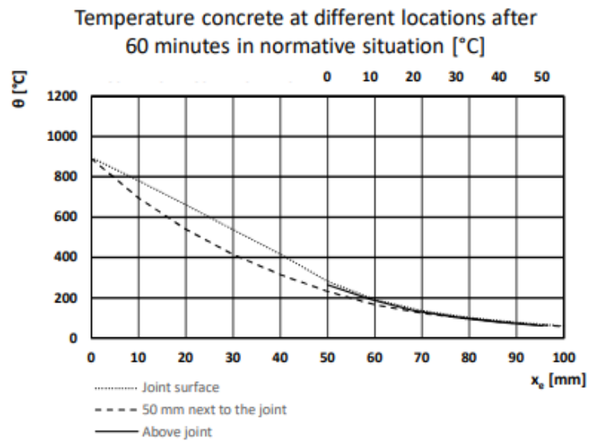

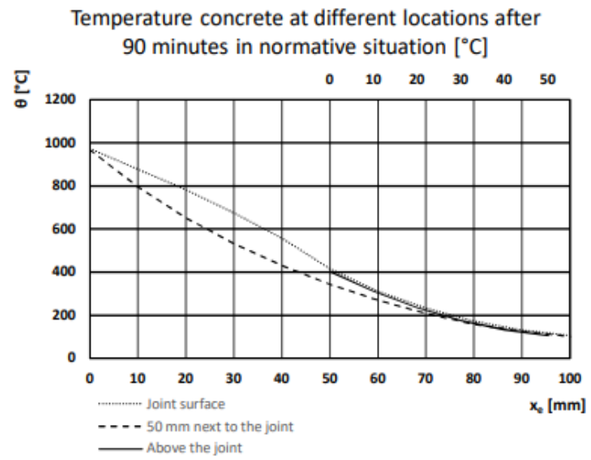

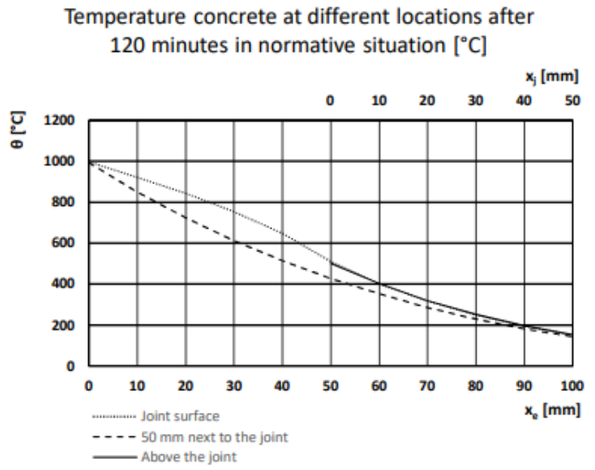

Excel file Reduction moment capacity composite floor

Momentcapacity above joint without fire at distance in the precast plate measured from exposed surface

Diameter reinforcement	Distance in the precast plate measured from exposed surface			Distance in the precast plate measured from exposed surface			Distance in the precast plate measured from exposed surface			Distance in the precast plate measured from exposed surface			Distance in the precast plate measured from exposed surface			Distance in the precast plate measured from exposed surface		
	0 mm			5 mm			10 mm			15 mm			20 mm			25 mm		
	A [mm²]	d [mm]	Mrd [kNm]	A [mm²]	d [mm]	Mrd [kNm]	A [mm²]	d [mm]	Mrd [kNm]	A [mm²]	d [mm]	Mrd [kNm]	A [mm²]	d [mm]	Mrd [kNm]	A [mm²]	d [mm]	Mrd [kNm]
Ø8 h.o.h. 100	503	158	31.1	503	153	30.1	503	148	29.1	503	143	28.2	503	138	27.2	503	133	26.2
Ø8 h.o.h. 125	402	158	24.9	402	153	24.1	402	148	23.3	402	143	22.5	402	138	21.7	402	133	20.9
Ø8 h.o.h. 150	335	158	20.7	335	153	20.1	335	148	19.4	335	143	18.8	335	138	18.1	335	133	17.4
Ø10 h.o.h. 100	785	155	47.6	785	150	46.1	785	145	44.6	785	140	43.0	785	135	41.5	785	130	40.0
Ø10 h.o.h. 125	628	155	38.1	628	150	36.9	628	145	35.6	628	140	34.4	628	135	33.2	628	130	32.0
Ø10 h.o.h. 150	524	155	31.8	524	150	30.8	524	145	29.7	524	140	28.7	524	135	27.7	524	130	26.7
Ø12 h.o.h. 100	1131	152	67.3	1131	147	65.1	1131	142	62.9	1131	137	60.7	1131	132	58.4	1131	127	56.2
Ø12 h.o.h. 125	905	152	53.9	905	147	52.1	905	142	50.3	905	137	48.5	905	132	46.8	905	127	45.0
Ø12 h.o.h. 150	754	152	44.9	754	147	43.4	754	142	41.9	754	137	40.4	754	132	39.0	754	127	37.5
Ø16 h.o.h. 100	2011	146	114.9	2011	141	111.0	2011	136	107.1	2011	131	103.1	2011	126	99.2	2011	121	95.3
Ø16 h.o.h. 125	1608	146	91.9	1608	141	88.8	1608	136	85.6	1608	131	82.5	1608	126	79.3	1608	121	76.2
Ø16 h.o.h. 150	1340	146	76.6	1340	141	74.0	1340	136	71.3	1340	131	68.7	1340	126	66.1	1340	121	63.5
Ø20 h.o.h. 100	3142	140	172.2	3142	135	166.1	3142	130	159.9	3142	125	153.8	3142	120	147.6	3142	115	141.5
Ø20 h.o.h. 125	2513	140	137.7	2513	135	132.8	2513	130	127.9	2513	125	123.0	2513	120	118.1	2513	115	113.1
Ø20 h.o.h. 150	2094	140	114.8	2094	135	110.7	2094	130	106.6	2094	125	102.5	2094	120	98.4	2094	115	94.3

Distance in the precast plate measured from exposed surface			Distance in the precast plate measured from exposed surface			Distance in the precast plate measured from exposed surface			Distance in the precast plate measured from exposed surface			Distance in the precast plate measured from exposed surface		
30 mm			35 mm			40 mm			45 mm			50 mm		
A [mm²]	d [mm]	Mrd [kNm]	A [mm²]	d [mm]	Mrd [kNm]	A [mm²]	d [mm]	Mrd [kNm]	A [mm²]	d [mm]	Mrd [kNm]	A [mm²]	d [mm]	Mrd [kNm]
503	128	25.2	503	123	24.2	503	118	23.2	503	113	22.3	503	108	21.3
402	128	20.1	402	123	19.4	402	118	18.6	402	113	17.8	402	108	17.0
335	128	16.8	335	123	16.1	335	118	15.5	335	113	14.8	335	108	14.2
785	125	38.4	785	120	36.9	785	115	35.3	785	110	33.8	785	105	32.3
628	125	30.7	628	120	29.5	628	115	28.3	628	110	27.0	628	105	25.8
524	125	25.6	524	120	24.6	524	115	23.6	524	110	22.6	524	105	21.5
1131	122	54.0	1131	117	51.8	1131	112	49.6	1131	107	47.4	1131	102	45.2
905	122	43.2	905	117	41.5	905	112	39.7	905	107	37.9	905	102	36.1
754	122	36.0	754	117	34.5	754	112	33.1	754	107	31.6	754	102	30.1
2011	116	91.3	2011	111	87.4	2011	106	83.5	2011	101	79.5	2011	96	75.6
1608	116	73.0	1608	111	69.9	1608	106	66.7	1608	101	63.6	1608	96	60.4
1340	116	60.9	1340	111	58.2	1340	106	55.6	1340	101	53.0	1340	96	50.4
3142	110	135.3	3142	105	129.2	3142	100	123.0	3142	95	116.9	3142	90	110.7
2513	110	108.2	2513	105	103.3	2513	100	98.4	2513	95	93.5	2513	90	88.5
2094	110	90.2	2094	105	86.1	2094	100	82.0	2094	95	77.9	2094	90	73.8

Reduced momentcapacity precast plate after fire at distance in the precast plate measured from exposed surface

Reduced momentcapacity precast without fire at distance in the precast plate measured from exposed surface Ø8 h.o.h. 100																					
Depth x_j in the floor above joint	30 minutes					60 minutes					90 minutes					120 minutes				
	Temperature above the joint	Reduction reinforce-ment strength	Reduction concrete	Reduced moment capacity	Reduction moment capacity	Temperature above the joint	Reduction reinforce-ment strength	Reduction concrete	Reduced moment capacity	Reduction moment capacity	Temperature above the joint	Reduction reinforce-ment strength	Reduction concrete	Reduced moment capacity	Reduction moment capacity	Temperature above the joint	Reduction reinforce-ment strength	Reduction concrete	Reduced moment capacity	Reduction moment capacity
	[°C]	[%]	[mm]	[kNm]	[%]	[°C]	[%]	[mm]	[kNm]	[%]	[°C]	[%]	[mm]	[kNm]	[%]	[°C]	[%]	[mm]	[kNm]	[%]
0 mm	106	0	15	28.2	9.5	264	0	35	24.2	22.2	403	12.5	45	19.5	37.4	502	40	50	12.8	59.0
5 mm	91	0	15	27.2	9.8	227	0	35	23.2	22.9	356	1	45	21.1	30.1	451	25	50	15.2	49.5
10 mm	76	0	15	26.2	10.1	191	0	35	22.3	23.6	311	0	45	20.3	30.4	403	12.5	50	16.9	42.1
15 mm	64	0	15	25.2	10.5	159	0	35	21.3	24.5	271	0	45	19.3	31.5	359	1	50	18.1	35.6
20 mm	53	0	15	24.2	10.9	135	0	35	20.3	25.4	235	0	45	18.3	32.6	319	0	50	17.3	36.2
25 mm	44	0	15	23.2	11.3	118	0	35	19.3	26.3	202	0	45	17.3	33.8	284	0	50	16.3	37.6
30 mm	37	0	15	22.3	11.7	103	0	35	18.3	27.3	174	0	45	16.3	35.2	251	0	50	15.4	39.1
35 mm	30	0	15	21.3	12.2	90	0	35	17.3	28.5	150	0	45	15.4	36.6	222	0	50	14.4	40.7
40 mm	25	0	15	20.3	12.7	79	0	35	16.3	29.7	133	0	45	14.4	38.1	196	0	50	13.4	42.4
45 mm	21	0	15	19.3	13.3	69	0	35	15.4	31.0	119	0	45	13.4	39.8	172	0	50	12.4	44.2
50 mm	17	0	15	18.3	13.9	61	0	35	14.4	32.4	106	0	45	12.4	41.7	152	0	50	11.4	46.3

Reduced momentcapacity precast without fire at distance in the precast plate measured from exposed surface Ø8 h.o.h. 125																					
Depth x_j in the floor above joint	30 minutes					60 minutes					90 minutes					120 minutes				
	Temperature above the joint	Reduction reinforce-ment strength	Reduction concrete	Reduced moment capacity	Reduction moment capacity	Temperature above the joint	Reduction reinforce-ment strength	Reduction concrete	Reduced moment capacity	Reduction moment capacity	Temperature above the joint	Reduction reinforce-ment strength	Reduction concrete	Reduced moment capacity	Reduction moment capacity	Temperature above the joint	Reduction reinforce-ment strength	Reduction concrete	Reduced moment capacity	Reduction moment capacity
	[°C]	[%]	[mm]	[kNm]	[%]	[°C]	[%]	[mm]	[kNm]	[%]	[°C]	[%]	[mm]	[kNm]	[%]	[°C]	[%]	[mm]	[kNm]	[%]
0 mm	106	0	15	22.5	9.5	264	0	35	19.4	22.2	403	12.5	45	15.6	37.4	502	40	50	10.2	59.0
5 mm	91	0	15	21.7	9.8	227	0	35	18.6	22.9	356	1	45	16.8	30.1	451	25	50	12.2	49.5
10 mm	76	0	15	20.9	10.1	191	0	35	17.8	23.6	311	0	45	16.2	30.4	403	12.5	50	13.5	42.1
15 mm	64	0	15	20.1	10.5	159	0	35	17.0	24.5	271	0	45	15.4	31.5	359	1	50	14.5	35.6
20 mm	53	0	15	19.4	10.9	135	0	35	16.2	25.4	235	0	45	14.6	32.6	319	0	50	13.8	36.2
25 mm	44	0	15	18.6	11.3	118	0	35	15.4	26.3	202	0	45	13.8	33.8	284	0	50	13.1	37.6
30 mm	37	0	15	17.8	11.7	103	0	35	14.6	27.3	174	0	45	13.1	35.2	251	0	50	12.3	39.1
35 mm	30	0	15	17.0	12.2	90	0	35	13.8	28.5	150	0	45	12.3	36.6	222	0	50	11.5	40.7
40 mm	25	0	15	16.2	12.7	79	0	35	13.1	29.7	133	0	45	11.5	38.1	196	0	50	10.7	42.4
45 mm	21	0	15	15.4	13.3	69	0	35	12.3	31.0	119	0	45	10.7	39.8	172	0	50	9.9	44.2
50 mm	17	0	15	14.6	13.9	61	0	35	11.5	32.4	106	0	45	9.9	41.7	152	0	50	9.1	46.3

Reduced momentcapacity precast without fire at distance in the precast plate measured from exposed surface Ø8 h.o.h. 150																					
Depth x_j in the floor above joint	30 minutes					60 minutes					90 minutes					120 minutes				
	Temperature above the joint	Reduction reinforce-ment strength	Reduction concrete	Reduced moment capacity	Reduction moment capacity	Temperature above the joint	Reduction reinforce-ment strength	Reduction concrete	Reduced moment capacity	Reduction moment capacity	Temperature above the joint	Reduction reinforce-ment strength	Reduction concrete	Reduced moment capacity	Reduction moment capacity	Temperature above the joint	Reduction reinforce-ment strength	Reduction concrete	Reduced moment capacity	Reduction moment capacity
	[°C]	[%]	[mm]	[kNm]	[%]	[°C]	[%]	[mm]	[kNm]	[%]	[°C]	[%]	[mm]	[kNm]	[%]	[°C]	[%]	[mm]	[kNm]	[%]
0 mm	106	0	15	18.8	9.5	264	0	35	16.1	22.2	403	12.5	45	13.0	37.4	502	40	50	8.5	59.0
5 mm	91	0	15	18.1	9.8	227	0	35	15.5	22.9	356	1	45	14.0	30.1	451	25	50	10.1	49.5
10 mm	76	0	15	17.4	10.1	191	0	35	14.8	23.6	311	0	45	13.5	30.4	403	12.5	50	11.2	42.1
15 mm	64	0	15	16.8	10.5	159	0	35	14.2	24.5	271	0	45	12.9	31.5	359	1	50	12.1	35.6
20 mm	53	0	15	16.1	10.9	135	0	35	13.5	25.4	235	0	45	12.2	32.6	319	0	50	11.5	36.2
25 mm	44	0	15	15.5	11.3	118	0	35	12.9	26.3	202	0	45	11.5	33.8	284	0	50	10.9	37.6
30 mm	37	0	15	14.8	11.7	103	0	35	12.2	27.3	174	0	45	10.9	35.2	251	0	50	10.2	39.1
35 mm	30	0	15	14.2	12.2	90	0	35	11.5	28.5	150	0	45	10.2	36.6	222	0	50	9.6	40.7
40 mm	25	0	15	13.5	12.7	79	0	35	10.9	29.7	133	0	45	9.6	38.1	196	0	50	8.9	42.4
45 mm	21	0	15	12.9	13.3	69	0	35	10.2	31.0	119	0	45	8.9	39.8	172	0	50	8.3	44.2
50 mm	17	0	15	12.2	13.9	61	0	35	9.6	32.4	106	0	45	8.3	41.7	152	0	50	7.6	46.3

Reduced momentcapacity precast without fire at distance in the precast plate measured from exposed surface Ø10 h.o.h. 100																				
Depth x_j in the floor above joint	30 minutes					60 minutes					90 minutes					120 minutes				
	Temperature above the joint	Reduction reinforce-ment strength	Reduction concrete	Reduced moment capacity	Reduction moment capacity	Temperature above the joint	Reduction reinforce-ment strength	Reduction concrete	Reduced moment capacity	Reduction moment capacity	Temperature above the joint	Reduction reinforce-ment strength	Reduction concrete	Reduced moment capacity	Reduction moment capacity	Temperature above the joint	Reduction reinforce-ment strength	Reduction concrete	Reduced moment capacity	Reduction moment capacity
	[°C]	[%]	[mm]	[kNm]	[%]	[°C]	[%]	[mm]	[kNm]	[%]	[°C]	[%]	[mm]	[kNm]	[%]	[°C]	[%]	[mm]	[kNm]	[%]
0 mm	106	0	15	43.0	9.7	264	0	35	36.9	22.6	403	12.5	45	29.6	37.9	502	40	50	19.4	59.4
5 mm	91	0	15	41.5	10.0	227	0	35	35.3	23.3	356	1	45	31.9	30.7	451	25	50	23.0	50.0
10 mm	76	0	15	40.0	10.3	191	0	35	33.8	24.1	311	0	45	30.7	31.0	403	12.5	50	25.5	42.7
15 mm	64	0	15	38.4	10.7	159	0	35	32.3	25.0	271	0	45	29.2	32.1	359	1	50	27.4	36.4
20 mm	53	0	15	36.9	11.1	135	0	35	30.7	25.9	235	0	45	27.7	33.3	319	0	50	26.1	37.0
25 mm	44	0	15	35.3	11.5	118	0	35	29.2	26.9	202	0	45	26.1	34.6	284	0	50	24.6	38.5
30 mm	37	0	15	33.8	12.0	103	0	35	27.7	28.0	174	0	45	24.6	36.0	251	0	50	23.0	40.0
35 mm	30	0	15	35.3	4.2	90	0	35	29.2	20.8	150	0	45	26.1	29.2	222	0	50	24.6	33.3
40 mm	25	0	15	30.7	13.0	79	0	35	24.6	30.4	133	0	45	21.5	39.1	196	0	50	20.0	43.5
45 mm	21	0	15	29.2	13.6	69	0	35	23.0	31.8	119	0	45	20.0	40.9	172	0	50	18.4	45.5
50 mm	17	0	15	27.7	14.3	61	0	35	21.5	33.3	106	0	45	18.4	42.9	152	0	50	16.9	47.6

Reduced momentcapacity precast without fire at distance in the precast plate measured from exposed surface Ø10 h.o.h. 125																				
Depth x_j in the floor above joint	30 minutes					60 minutes					90 minutes					120 minutes				
	Temperature above the joint	Reduction reinforce-ment strength	Reduction concrete	Reduced moment capacity	Reduction moment capacity	Temperature above the joint	Reduction reinforce-ment strength	Reduction concrete	Reduced moment capacity	Reduction moment capacity	Temperature above the joint	Reduction reinforce-ment strength	Reduction concrete	Reduced moment capacity	Reduction moment capacity	Temperature above the joint	Reduction reinforce-ment strength	Reduction concrete	Reduced moment capacity	Reduction moment capacity
	[°C]	[%]	[mm]	[kNm]	[%]	[°C]	[%]	[mm]	[kNm]	[%]	[°C]	[%]	[mm]	[kNm]	[%]	[°C]	[%]	[mm]	[kNm]	[%]
0 mm	106	0	15	34.4	9.7	264	0	35	29.5	22.6	403	12.5	45	23.7	37.9	502	40	50	15.5	59.4
5 mm	91	0	15	33.2	10.0	227	0	35	28.3	23.3	356	1	45	25.6	30.7	451	25	50	18.4	50.0
10 mm	76	0	15	32.0	10.3	191	0	35	27.0	24.1	311	0	45	24.6	31.0	403	12.5	50	20.4	42.7
15 mm	64	0	15	30.7	10.7	159	0	35	25.8	25.0	271	0	45	23.4	32.1	359	1	50	21.9	36.4
20 mm	53	0	15	29.5	11.1	135	0	35	24.6	25.9	235	0	45	22.1	33.3	319	0	50	20.9	37.0
25 mm	44	0	15	28.3	11.5	118	0	35	23.4	26.9	202	0	45	20.9	34.6	284	0	50	19.7	38.5
30 mm	37	0	15	27.0	12.0	103	0	35	22.1	28.0	174	0	45	19.7	36.0	251	0	50	18.4	40.0
35 mm	30	0	15	25.8	12.5	90	0	35	20.9	29.2	150	0	45	18.4	37.5	222	0	50	17.2	41.7
40 mm	25	0	15	24.6	13.0	79	0	35	19.7	30.4	133	0	45	17.2	39.1	196	0	50	16.0	43.5
45 mm	21	0	15	23.4	13.6	69	0	35	18.4	31.8	119	0	45	16.0	40.9	172	0	50	14.8	45.5
50 mm	17	0	15	22.1	14.3	61	0	35	17.2	33.3	106	0	45	14.8	42.9	152	0	50	13.5	47.6

Reduced momentcapacity precast without fire at distance in the precast plate measured from exposed surface Ø10 h.o.h. 150																				
Depth x_j in the floor above joint	30 minutes					60 minutes					90 minutes					120 minutes				
	Temperature above the joint	Reduction reinforce-ment strength	Reduction concrete	Reduced moment capacity	Reduction moment capacity	Temperature above the joint	Reduction reinforce-ment strength	Reduction concrete	Reduced moment capacity	Reduction moment capacity	Temperature above the joint	Reduction reinforce-ment strength	Reduction concrete	Reduced moment capacity	Reduction moment capacity	Temperature above the joint	Reduction reinforce-ment strength	Reduction concrete	Reduced moment capacity	Reduction moment capacity
	[°C]	[%]	[mm]	[kNm]	[%]	[°C]	[%]	[mm]	[kNm]	[%]	[°C]	[%]	[mm]	[kNm]	[%]	[°C]	[%]	[mm]	[kNm]	[%]
0 mm	106	0	15	28.7	9.7	264	0	35	24.6	22.6	403	12.5	45	19.7	37.9	502	40	50	12.9	59.4
5 mm	91	0	15	27.7	10.0	227	0	35	23.6	23.3	356	1	45	22.3	27.4	451	25	50	15.4	50.0
10 mm	76	0	15	26.7	10.3	191	0	35	22.6	24.1	311	0	45	22.6	24.1	403	12.5	50	17.1	42.7
15 mm	64	0	15	25.6	10.7	159	0	35	21.5	25.0	271	0	45	22.6	21.4	359	1	50	18.3	36.4
20 mm	53	0	15	24.6	11.1	135	0	35	20.5	25.9	235	0	45	22.6	18.5	319	0	50	17.4	37.0
25 mm	44	0	15	23.6	11.5	118	0	35	19.5	26.9	202	0	45	22.6	15.4	284	0	50	16.4	38.5
30 mm	37	0	15	22.6	12.0	103	0	35	18.5	28.0	174	0	45	22.6	12.0	251	0	50	15.4	40.0
35 mm	30	0	15	21.5	12.5	90	0	35	17.4	29.2	150	0	45	22.6	8.3	222	0	50	14.4	41.7
40 mm	25	0	15	20.5	13.0	79	0	35	16.4	30.4	133	0	45	22.6	4.3	196	0	50	13.3	43.5
45 mm	21	0	15	19.5	13.6	69	0	35	15.4	31.8	119	0	45	22.6	0.0	172	0	50	12.3	45.5
50 mm	17	0	15	18.5	14.3	61	0	35	14.4	33.3	106	0	45	22.6	-4.8	152	0	50	11.3	47.6

Reduced momentcapacity precast without fire at distance in the precast plate measured from exposed surface Ø12 h.o.h. 100

Depth x_j in the floor above joint	30 minutes					60 minutes					90 minutes					120 minutes				
	Temperature above the joint	Reduction reinforce-ment strength	Reduction concrete	Reduced moment capacity	Reduction moment capacity	Temperature above the joint	Reduction reinforce-ment strength	Reduction concrete	Reduced moment capacity	Reduction moment capacity	Temperature above the joint	Reduction reinforce-ment strength	Reduction concrete	Reduced moment capacity	Reduction moment capacity	Temperature above the joint	Reduction reinforce-ment strength	Reduction concrete	Reduced moment capacity	Reduction moment capacity
	[°C]	[%]	[mm]	[kNm]	[%]	[°C]	[%]	[mm]	[kNm]	[%]	[°C]	[%]	[mm]	[kNm]	[%]	[°C]	[%]	[mm]	[kNm]	[%]
0 mm	106	0	15	60.7	9.9	264	0	35	51.8	23.0	403	12.5	45	41.5	38.4	502	40	50	27.1	59.7
5 mm	91	0	15	58.4	10.2	227	0	35	49.6	23.8	356	1	45	44.7	31.3	451	25	50	32.2	50.5
10 mm	76	0	15	56.2	10.6	191	0	35	47.4	24.6	311	0	45	43.0	31.7	403	12.5	50	35.6	43.3
15 mm	64	0	15	54.0	10.9	159	0	35	45.2	25.5	271	0	45	40.7	32.8	359	1	50	38.1	37.1
20 mm	53	0	15	51.8	11.4	135	0	35	43.0	26.5	235	0	45	38.5	34.1	319	0	50	36.3	37.9
25 mm	44	0	15	49.6	11.8	118	0	35	40.7	27.6	202	0	45	36.3	35.4	284	0	50	34.1	39.4
30 mm	37	0	15	47.4	12.3	103	0	35	38.5	28.7	174	0	45	34.1	36.9	251	0	50	31.9	41.0
35 mm	30	0	15	45.2	12.8	90	0	35	36.3	29.9	150	0	45	31.9	38.5	222	0	50	29.7	42.7
40 mm	25	0	15	43.0	13.4	79	0	35	34.1	31.3	133	0	45	29.7	40.2	196	0	50	27.5	44.6
45 mm	21	0	15	40.7	14.0	69	0	35	31.9	32.7	119	0	45	27.5	42.1	172	0	50	25.2	46.7
50 mm	17	0	15	38.5	14.7	61	0	35	29.7	34.3	106	0	45	25.2	44.1	152	0	50	23.0	49.0

Reduced momentcapacity precast without fire at distance in the precast plate measured from exposed surface Ø12 h.o.h. 125																				
Depth x_j in the floor above joint	30 minutes					60 minutes					90 minutes					120 minutes				
	Temperature above the joint	Reduction reinforce-ment strength	Reduction concrete	Reduced moment capacity	Reduction moment capacity	Temperature above the joint	Reduction reinforce-ment strength	Reduction concrete	Reduced moment capacity	Reduction moment capacity	Temperature above the joint	Reduction reinforce-ment strength	Reduction concrete	Reduced moment capacity	Reduction moment capacity	Temperature above the joint	Reduction reinforce-ment strength	Reduction concrete	Reduced moment capacity	Reduction moment capacity
	[°C]	[%]	[mm]	[kNm]	[%]	[°C]	[%]	[mm]	[kNm]	[%]	[°C]	[%]	[mm]	[kNm]	[%]	[°C]	[%]	[mm]	[kNm]	[%]
0 mm	106	0	15	48.5	9.9	264	0	35	41.5	23.0	403	12.5	45	33.2	38.4	502	40	50	21.7	59.7
5 mm	91	0	15	46.8	10.2	227	0	35	39.7	23.8	356	1	45	35.8	31.3	451	25	50	25.8	50.5
10 mm	76	0	15	45.0	10.6	191	0	35	37.9	24.6	311	0	45	34.4	31.7	403	12.5	50	28.5	43.3
15 mm	64	0	15	43.2	10.9	159	0	35	36.1	25.5	271	0	45	32.6	32.8	359	1	50	30.5	37.1
20 mm	53	0	15	41.5	11.4	135	0	35	34.4	26.5	235	0	45	30.8	34.1	319	0	50	29.1	37.9
25 mm	44	0	15	39.7	11.8	118	0	35	32.6	27.6	202	0	45	29.1	35.4	284	0	50	27.3	39.4
30 mm	37	0	15	37.9	12.3	103	0	35	30.8	28.7	174	0	45	27.3	36.9	251	0	50	25.5	41.0
35 mm	30	0	15	36.1	12.8	90	0	35	29.1	29.9	150	0	45	25.5	38.5	222	0	50	23.7	42.7
40 mm	25	0	15	34.4	13.4	79	0	35	27.3	31.3	133	0	45	23.7	40.2	196	0	50	22.0	44.6
45 mm	21	0	15	32.6	14.0	69	0	35	25.5	32.7	119	0	45	22.0	42.1	172	0	50	20.2	46.7
50 mm	17	0	15	30.8	14.7	61	0	35	23.7	34.3	106	0	45	20.2	44.1	152	0	50	18.4	49.0

Reduced momentcapacity precast without fire at distance in the precast plate measured from exposed surface Ø12 h.o.h. 150																				
Depth x_j in the floor above joint	30 minutes					60 minutes					90 minutes					120 minutes				
	Temperature above the joint	Reduction reinforce-ment strength	Reduction concrete	Reduced moment capacity	Reduction moment capacity	Temperature above the joint	Reduction reinforce-ment strength	Reduction concrete	Reduced moment capacity	Reduction moment capacity	Temperature above the joint	Reduction reinforce-ment strength	Reduction concrete	Reduced moment capacity	Reduction moment capacity	Temperature above the joint	Reduction reinforce-ment strength	Reduction concrete	Reduced moment capacity	Reduction moment capacity
	[°C]	[%]	[mm]	[kNm]	[%]	[°C]	[%]	[mm]	[kNm]	[%]	[°C]	[%]	[mm]	[kNm]	[%]	[°C]	[%]	[mm]	[kNm]	[%]
0 mm	106	0	15	40.4	9.9	264	0	35	34.5	23.0	403	12.5	45	27.6	38.4	502	40	50	18.1	59.7
5 mm	91	0	15	39.0	10.2	227	0	35	33.1	23.8	356	1	45	29.8	31.3	451	25	50	21.5	50.5
10 mm	76	0	15	37.5	10.6	191	0	35	31.6	24.6	311	0	45	28.6	31.7	403	12.5	50	23.8	43.3
15 mm	64	0	15	36.0	10.9	159	0	35	30.1	25.5	271	0	45	27.2	32.8	359	1	50	25.4	37.1
20 mm	53	0	15	34.5	11.4	135	0	35	28.6	26.5	235	0	45	25.7	34.1	319	0	50	24.2	37.9
25 mm	44	0	15	33.1	11.8	118	0	35	27.2	27.6	202	0	45	24.2	35.4	284	0	50	22.7	39.4
30 mm	37	0	15	31.6	12.3	103	0	35	25.7	28.7	174	0	45	22.7	36.9	251	0	50	21.3	41.0
35 mm	30	0	15	30.1	12.8	90	0	35	24.2	29.9	150	0	45	21.3	38.5	222	0	50	19.8	42.7
40 mm	25	0	15	28.6	13.4	79	0	35	22.7	31.3	133	0	45	19.8	40.2	196	0	50	18.3	44.6
45 mm	21	0	15	27.2	14.0	69	0	35	21.3	32.7	119	0	45	18.3	42.1	172	0	50	16.8	46.7
50 mm	17	0	15	25.7	14.7	61	0	35	34.5	-14.7	106	0	45	16.8	44.1	152	0	50	15.3	49.0

Reduced momentcapacity precast without fire at distance in the precast plate measured from exposed surface Ø16 h.o.h. 100				
Depth x_j in the floor above joint	30 minutes	60 minutes	90 minutes	120 minutes

	Temperature above the joint	Reduction reinforce-ment strength	Reduction concrete	Reduced moment capacity	Reduction moment capacity	Temperature above the joint	Reduction reinforce-ment strength	Reduction concrete	Reduced moment capacity	Reduction moment capacity	Temperature above the joint	Reduction reinforce-ment strength	Reduction concrete	Reduced moment capacity	Reduction moment capacity	Temperature above the joint	Reduction reinforce-ment strength	Reduction concrete	Reduced moment capacity	Reduction moment capacity
	[°C]	[%]	[mm]	[kNm]	[%]	[°C]	[%]	[mm]	[kNm]	[%]	[°C]	[%]	[mm]	[kNm]	[%]	[°C]	[%]	[mm]	[kNm]	[%]
0 mm	106	0	15	103.1	10.3	264	0	35	87.4	24.0	403	12.5	45	69.6	39.5	502	40	50	45.3	60.5
5 mm	91	0	15	99.2	10.6	227	0	35	83.5	24.8	356	1	45	74.8	32.6	451	25	50	53.7	51.6
10 mm	76	0	15	95.3	11.0	191	0	35	79.5	25.7	311	0	45	71.6	33.1	403	12.5	50	59.2	44.7
15 mm	64	0	15	91.3	11.5	159	0	35	75.6	26.7	271	0	45	67.7	34.4	359	1	50	63.1	38.8
20 mm	53	0	15	87.4	35.1	135	0	35	71.6	46.8	235	0	45	63.8	52.6	319	0	50	59.8	55.6
25 mm	44	0	15	83.5	12.4	118	0	35	67.7	28.9	202	0	45	59.8	37.2	284	0	50	55.9	41.3
30 mm	37	0	15	79.5	12.9	103	0	35	63.8	30.2	174	0	45	55.9	38.8	251	0	50	52.0	43.1
35 mm	30	0	15	75.6	13.5	90	0	35	59.8	31.5	150	0	45	52.0	40.5	222	0	50	48.0	45.0
40 mm	25	0	15	71.6	14.2	79	0	35	55.9	33.0	133	0	45	48.0	42.5	196	0	50	44.1	47.2
45 mm	21	0	15	67.7	14.9	69	0	35	52.0	34.7	119	0	45	44.1	44.6	172	0	50	40.2	49.5
50 mm	17	0	15	63.8	15.6	61	0	35	48.0	36.5	106	0	45	40.2	46.9	152	0	50	36.2	52.1

Reduced momentcapacity precast without fire at distance in the precast plate measured from exposed surface Ø16 h.o.h. 125																				
Depth x_j in the floor above joint	30 minutes					60 minutes					90 minutes					120 minutes				
	Temperature above the joint	Reduction reinforce-ment strength	Reduction concrete	Reduced moment capacity	Reduction moment capacity	Temperature above the joint	Reduction reinforce-ment strength	Reduction concrete	Reduced moment capacity	Reduction moment capacity	Temperature above the joint	Reduction reinforce-ment strength	Reduction concrete	Reduced moment capacity	Reduction moment capacity	Temperature above the joint	Reduction reinforce-ment strength	Reduction concrete	Reduced moment capacity	Reduction moment capacity
	[°C]	[%]	[mm]	[kNm]	[%]	[°C]	[%]	[mm]	[kNm]	[%]	[°C]	[%]	[mm]	[kNm]	[%]	[°C]	[%]	[mm]	[kNm]	[%]
0 mm	106	0	15	82.5	10.3	264	0	35	69.9	24.0	403	12.5	45	55.6	39.5	502	40	50	36.3	60.5
5 mm	91	0	15	79.3	10.6	227	0	35	66.7	24.8	356	1	45	59.8	32.6	451	25	50	43.0	51.6
10 mm	76	0	15	76.2	11.0	191	0	35	63.6	25.7	311	0	45	57.3	33.1	403	12.5	50	47.4	44.7
15 mm	64	0	15	73.0	11.5	159	0	35	60.4	26.7	271	0	45	54.1	34.4	359	1	50	50.5	38.8
20 mm	53	0	15	69.9	11.9	135	0	35	57.3	27.8	235	0	45	51.0	35.7	319	0	50	47.8	39.7
25 mm	44	0	15	66.7	12.4	118	0	35	54.1	28.9	202	0	45	47.8	37.2	284	0	50	44.7	41.3
30 mm	37	0	15	63.6	12.9	103	0	35	51.0	30.2	174	0	45	44.7	38.8	251	0	50	41.5	43.1
35 mm	30	0	15	60.4	13.5	90	0	35	47.8	31.5	150	0	45	41.5	40.5	222	0	50	38.4	45.0
40 mm	25	0	15	57.3	14.2	79	0	35	44.7	33.0	133	0	45	38.4	42.5	196	0	50	35.3	47.2
45 mm	21	0	15	54.1	14.9	69	0	35	41.5	34.7	119	0	45	35.3	44.6	172	0	50	32.1	49.5
50 mm	17	0	15	51.0	15.6	61	0	35	38.4	36.5	106	0	45	32.1	46.9	152	0	50	29.0	52.1

Reduced momentcapacity precast without fire at distance in the precast plate measured from exposed surface Ø16 h.o.h. 150																				
Depth x_j in the floor above joint	30 minutes					60 minutes					90 minutes					120 minutes				
	Temperature above the joint	Reduction reinforce-ment strength	Reduction concrete	Reduced moment capacity	Reduction moment capacity	Temperature above the joint	Reduction reinforce-ment strength	Reduction concrete	Reduced moment capacity	Reduction moment capacity	Temperature above the joint	Reduction reinforce-ment strength	Reduction concrete	Reduced moment capacity	Reduction moment capacity	Temperature above the joint	Reduction reinforce-ment strength	Reduction concrete	Reduced moment capacity	Reduction moment capacity
	[°C]	[%]	[mm]	[kNm]	[%]	[°C]	[%]	[mm]	[kNm]	[%]	[°C]	[%]	[mm]	[kNm]	[%]	[°C]	[%]	[mm]	[kNm]	[%]
0 mm	106	0	15	68.7	10.3	264	0	35	58.2	24.0	403	12.5	45	46.4	39.5	502	40	50	30.2	60.5
5 mm	91	0	15	66.1	10.6	227	0	35	55.6	24.8	356	1	45	49.9	32.6	451	25	50	35.8	51.6
10 mm	76	0	15	63.5	11.0	191	0	35	53.0	25.7	311	0	45	47.7	33.1	403	12.5	50	39.5	44.7
15 mm	64	0	15	60.9	11.5	159	0	35	50.4	26.7	271	0	45	45.1	34.4	359	1	50	42.1	38.8
20 mm	53	0	15	58.2	11.9	135	0	35	47.7	27.8	235	0	45	42.5	35.7	319	0	50	39.9	39.7
25 mm	44	0	15	55.6	12.4	118	0	35	45.1	28.9	202	0	45	39.9	37.2	284	0	50	37.2	41.3
30 mm	37	0	15	53.0	12.9	103	0	35	42.5	30.2	174	0	45	37.2	38.8	251	0	50	34.6	43.1
35 mm	30	0	15	50.4	13.5	90	0	35	39.9	31.5	150	0	45	34.6	40.5	222	0	50	32.0	45.0
40 mm	25	0	15	47.7	14.2	79	0	35	37.2	33.0	133	0	45	32.0	42.5	196	0	50	29.4	47.2
45 mm	21	0	15	45.1	14.9	69	0	35	34.6	34.7	119	0	45	29.4	44.6	172	0	50	26.8	49.5
50 mm	17	0	15	42.5	15.6	61	0	35	32.0	36.5	106	0	45	26.8	46.9	152	0	50	24.1	52.1

Reduced momentcapacity precast without fire at distance in the precast plate measured from exposed surface Ø20 h.o.h. 100				
Depth x_j in the floor above joint	30 minutes	60 minutes	90 minutes	120 minutes

	Temperature above the joint	Reduction reinforce-ment strength	Reduction concrete	Reduced moment capacity	Reduction moment capacity	Temperature above the joint	Reduction reinforce-ment strength	Reduction concrete	Reduced moment capacity	Reduction moment capacity	Temperature above the joint	Reduction reinforce-ment strength	Reduction concrete	Reduced moment capacity	Reduction moment capacity	Temperature above the joint	Reduction reinforce-ment strength	Reduction concrete	Reduced moment capacity	Reduction moment capacity
	[°C]	[%]	[mm]	[kNm]	[%]	[°C]	[%]	[mm]	[kNm]	[%]	[°C]	[%]	[mm]	[kNm]	[%]	[°C]	[%]	[mm]	[kNm]	[%]
0 mm	106	0	15	153.8	10.7	264	0	35	129.2	25.0	403	12.5	45	102.3	40.6	502	40	50	66.4	61.4
5 mm	91	0	15	147.6	11.1	227	0	35	123.0	25.9	356	1	45	109.6	34.0	451	25	50	78.4	52.8
10 mm	76	0	15	141.5	11.5	191	0	35	116.9	26.9	311	0	45	104.6	34.6	403	12.5	50	86.1	46.2
15 mm	64	0	15	135.3	12.0	159	0	35	110.7	28.0	271	0	45	98.4	36.0	359	1	50	91.3	40.6
20 mm	53	0	15	129.2	12.5	135	0	35	104.6	29.2	235	0	45	92.3	37.5	319	0	50	86.1	41.7
25 mm	44	0	15	123.0	13.0	118	0	35	98.4	30.4	202	0	45	86.1	39.1	284	0	50	80.0	43.5
30 mm	37	0	15	116.9	13.6	103	0	35	92.3	31.8	174	0	45	80.0	40.9	251	0	50	73.8	45.5
35 mm	30	0	15	110.7	14.3	90	0	35	86.1	33.3	150	0	45	73.8	42.9	222	0	50	67.7	47.6
40 mm	25	0	15	104.6	15.0	79	0	35	80.0	35.0	133	0	45	67.7	45.0	196	0	50	61.5	50.0
45 mm	21	0	15	98.4	15.8	69	0	35	73.8	36.8	119	0	45	61.5	47.4	172	0	50	55.4	52.6
50 mm	17	0	15	92.3	16.7	61	0	35	67.7	38.9	106	0	45	55.4	50.0	152	0	50	49.2	55.6

Reduced momentcapacity precast without fire at distance in the precast plate measured from exposed surface Ø16 h.o.h. 125																				
Depth x_j in the floor above joint	30 minutes					60 minutes					90 minutes					120 minutes				
	Temperature above the joint	Reduction reinforce-ment strength	Reduction concrete	Reduced moment capacity	Reduction moment capacity	Temperature above the joint	Reduction reinforce-ment strength	Reduction concrete	Reduced moment capacity	Reduction moment capacity	Temperature above the joint	Reduction reinforce-ment strength	Reduction concrete	Reduced moment capacity	Reduction moment capacity	Temperature above the joint	Reduction reinforce-ment strength	Reduction concrete	Reduced moment capacity	Reduction moment capacity
	[°C]	[%]	[mm]	[kNm]	[%]	[°C]	[%]	[mm]	[kNm]	[%]	[°C]	[%]	[mm]	[kNm]	[%]	[°C]	[%]	[mm]	[kNm]	[%]
0 mm	106	0	15	123.0	10.7	264	0	35	103.3	25.0	403	12.5	45	81.8	40.6	502	40	50	53.1	61.4
5 mm	91	0	15	118.1	11.1	227	0	35	98.4	25.9	356	1	45	87.7	34.0	451	25	50	62.7	52.8
10 mm	76	0	15	113.1	11.5	191	0	35	93.5	26.9	311	0	45	83.6	34.6	403	12.5	50	68.9	46.2
15 mm	64	0	15	108.2	12.0	159	0	35	88.5	28.0	271	0	45	78.7	36.0	359	1	50	73.1	40.6
20 mm	53	0	15	103.3	12.5	135	0	35	83.6	29.2	235	0	45	73.8	37.5	319	0	50	68.9	41.7
25 mm	44	0	15	98.4	13.0	118	0	35	78.7	30.4	202	0	45	68.9	39.1	284	0	50	63.9	43.5
30 mm	37	0	15	93.5	13.6	103	0	35	73.8	31.8	174	0	45	63.9	40.9	251	0	50	59.0	45.5
35 mm	30	0	15	88.5	14.3	90	0	35	68.9	33.3	150	0	45	59.0	42.9	222	0	50	54.1	47.6
40 mm	25	0	15	83.6	15.0	79	0	35	63.9	35.0	133	0	45	54.1	45.0	196	0	50	49.2	50.0
45 mm	21	0	15	78.7	15.8	69	0	35	59.0	36.8	119	0	45	49.2	47.4	172	0	50	44.3	52.6
50 mm	17	0	15	73.8	16.7	61	0	35	54.1	38.9	106	0	45	44.3	50.0	152	0	50	39.4	55.6

Reduced momentcapacity precast without fire at distance in the precast plate measured from exposed surface Ø16 h.o.h. 150																				
Depth x_j in the floor above joint	30 minutes					60 minutes					90 minutes					120 minutes				
	Temperature above the joint	Reduction reinforce-ment strength	Reduction concrete	Reduced moment capacity	Reduction moment capacity	Temperature above the joint	Reduction reinforce-ment strength	Reduction concrete	Reduced moment capacity	Reduction moment capacity	Temperature above the joint	Reduction reinforce-ment strength	Reduction concrete	Reduced moment capacity	Reduction moment capacity	Temperature above the joint	Reduction reinforce-ment strength	Reduction concrete	Reduced moment capacity	Reduction moment capacity
	[°C]	[%]	[mm]	[kNm]	[%]	[°C]	[%]	[mm]	[kNm]	[%]	[°C]	[%]	[mm]	[kNm]	[%]	[°C]	[%]	[mm]	[kNm]	[%]
0 mm	106	0	15	102.5	10.7	264	0	35	86.1	25.0	403	12.5	45	68.1	40.6	502	40	50	44.3	61.4
5 mm	91	0	15	98.4	11.1	227	0	35	82.0	25.9	356	1	45	73.0	34.0	451	25	50	52.3	52.8
10 mm	76	0	15	94.3	11.5	191	0	35	77.9	26.9	311	0	45	69.7	34.6	403	12.5	50	57.4	46.2
15 mm	64	0	15	90.2	12.0	159	0	35	73.8	28.0	271	0	45	65.6	36.0	359	1	50	60.9	40.6
20 mm	53	0	15	86.1	12.5	135	0	35	69.7	29.2	235	0	45	61.5	37.5	319	0	50	57.4	41.7
25 mm	44	0	15	82.0	13.0	118	0	35	65.6	30.4	202	0	45	57.4	39.1	284	0	50	53.3	43.5
30 mm	37	0	15	77.9	13.6	103	0	35	61.5	31.8	174	0	45	53.3	40.9	251	0	50	49.2	45.5
35 mm	30	0	15	73.8	14.3	90	0	35	57.4	33.3	150	0	45	49.2	42.9	222	0	50	45.1	47.6
40 mm	25	0	15	69.7	15.0	79	0	35	53.3	35.0	133	0	45	45.1	45.0	196	0	50	41.0	50.0
45 mm	21	0	15	65.6	15.8	69	0	35	49.2	36.8	119	0	45	41.0	47.4	172	0	50	36.9	52.6
50 mm	17	0	15	61.5	16.7	61	0	35	45.1	38.9	106	0	45	36.9	50.0	152	0	50	32.8	55.6

Measures for momentcapacity												
		0 mm	10 mm	20 mm	30 mm	40 mm	50 mm	60 mm	70 mm	80 mm	90 mm	100 mm
Reinforcement	A [mm²]	d [mm]	d [mm]	d [mm]	d [mm]	d [mm]	d [mm]	d [mm]	d [mm]	d [mm]	d [mm]	d [mm]
Ø8 h.o.h. 100	503	158	153	148	143	138	133	128	123	118	113	108
Ø8 h.o.h. 125	402	158	153	148	143	138	133	128	123	118	113	108
Ø8 h.o.h. 150	335	158	153	148	143	138	133	128	123	118	113	108
Ø10 h.o.h. 100	785	155	150	145	140	135	130	125	120	115	110	105
Ø10 h.o.h. 125	628	155	150	145	140	135	130	125	120	115	110	105
Ø10 h.o.h. 150	524	155	150	145	140	135	130	125	120	115	110	105
Ø12 h.o.h. 100	1131	152	147	142	137	132	127	122	117	112	107	102
Ø12 h.o.h. 125	905	152	147	142	137	132	127	122	117	112	107	102
Ø12 h.o.h. 150	754	152	147	142	137	132	127	122	117	112	107	102
Ø16 h.o.h. 100	2011	146	141	136	131	126	121	116	111	106	101	96
Ø16 h.o.h. 125	1608	146	141	136	131	126	121	116	111	106	101	96
Ø16 h.o.h. 150	1340	146	141	136	131	126	121	116	111	106	101	96
Ø20 h.o.h. 100	3142	140	135	130	125	120	115	110	105	100	95	90
Ø20 h.o.h. 125	2513	140	135	130	125	120	115	110	105	100	95	90
Ø20 h.o.h. 150	2094	140	135	130	125	120	115	110	105	100	95	90

Momentcapacity precast plate without fire at distance in the precast plate measured from exposed surface

Diameter reinforcement	Distance in the precast plate measured from exposed surface			Distance in the precast plate measured from exposed surface			Distance in the precast plate measured from exposed surface			Distance in the precast plate measured from exposed surface			Distance in the precast plate measured from exposed surface			Distance in the precast plate measured from exposed surface		
	0 mm			10 mm			20 mm			30 mm			40 mm			50 mm		
	A [mm²]	d [mm]	Mrd [kNm]	A [mm²]	d [mm]	Mrd [kNm]	A [mm²]	d [mm]	Mrd [kNm]	A [mm²]	d [mm]	Mrd [kNm]	A [mm²]	d [mm]	Mrd [kNm]	A [mm²]	d [mm]	Mrd [kNm]
Ø8 h.o.h. 100	503	143	28.2	503	153	30.1	503	163	32.1	503	173	34.1	503	183	36.0	503	193	38.0
Ø8 h.o.h. 125	402	143	22.5	402	153	24.1	402	163	25.7	402	173	27.2	402	183	28.8	402	193	30.4
Ø8 h.o.h. 150	335	143	18.8	335	153	20.1	335	163	21.4	335	173	22.7	335	183	24.0	335	193	25.3
Ø10 h.o.h. 100	785	140	43.0	785	150	46.1	785	160	49.2	785	170	52.2	785	180	55.3	785	190	58.4
Ø10 h.o.h. 125	628	140	34.4	628	150	36.9	628	160	39.3	628	170	41.8	628	180	44.3	628	190	46.7
Ø10 h.o.h. 150	524	140	28.7	524	150	30.8	524	160	32.8	524	170	34.9	524	180	36.9	524	190	39.0
Ø12 h.o.h. 100	1131	137	60.7	1131	147	65.1	1131	157	69.5	1131	167	73.9	1131	177	78.4	1131	187	82.8
Ø12 h.o.h. 125	905	137	48.5	905	147	52.1	905	157	55.6	905	167	59.2	905	177	62.7	905	187	66.3
Ø12 h.o.h. 150	754	137	40.4	754	147	43.4	754	157	46.3	754	167	49.3	754	177	52.2	754	187	55.2
Ø16 h.o.h. 100	2011	131	103.1	2011	141	111.0	2011	151	118.9	2011	161	126.8	2011	171	134.6	2011	181	142.5
Ø16 h.o.h. 125	1608	131	82.5	1608	141	88.8	1608	151	95.1	1608	161	101.4	1608	171	107.6	1608	181	113.9
Ø16 h.o.h. 150	1340	131	68.7	1340	141	74.0	1340	151	79.2	1340	161	84.5	1340	171	89.7	1340	181	95.0
Ø20 h.o.h. 100	3142	125	153.8	3142	135	166.1	3142	145	178.4	3142	155	190.7	3142	165	203.0	3142	175	215.3
Ø20 h.o.h. 125	2513	125	123.0	2513	135	132.8	2513	145	142.7	2513	155	152.5	2513	165	162.3	2513	175	172.2
Ø20 h.o.h. 150	2094	125	102.5	2094	135	110.7	2094	145	118.9	2094	155	127.1	2094	165	135.3	2094	175	143.5

Distance in the precast plate measured from exposed surface			Distance in the precast plate measured from exposed surface			Distance in the precast plate measured from exposed surface			Distance in the precast plate measured from exposed surface			Distance in the precast plate measured from exposed surface		
60 mm			70 mm			80 mm			90 mm			100 mm		
A [mm²]	d [mm]	Mrd [kNm]	A [mm²]	d [mm]	Mrd [kNm]	A [mm²]	d [mm]	Mrd [kNm]	A [mm²]	d [mm]	Mrd [kNm]	A [mm²]	d [mm]	Mrd [kNm]
503	203	40.0	503	213	41.9	503	223	43.9	503	233	45.9	503	243	47.9
402	203	31.9	402	213	33.5	402	223	35.1	402	233	36.7	402	243	38.2
335	203	26.6	335	213	27.9	335	223	29.2	335	233	30.6	335	243	31.9
785	200	61.5	785	210	64.5	785	220	67.6	785	230	70.7	785	240	73.8
628	200	49.2	628	210	51.6	628	220	54.1	628	230	56.5	628	240	59.0
524	200	41.0	524	210	43.1	524	220	45.1	524	230	47.2	524	240	49.2
1131	197	87.2	1131	207	91.7	1131	217	96.1	1131	227	100.5	1131	237	104.9
905	197	69.8	905	207	73.3	905	217	76.9	905	227	80.4	905	237	84.0
754	197	58.2	754	207	61.1	754	217	64.1	754	227	67.0	754	237	70.0
2011	191	150.4	2011	201	158.2	2011	211	166.1	2011	221	174.0	2011	231	181.9
1608	191	120.2	1608	201	126.5	1608	211	132.8	1608	221	139.1	1608	231	145.4
1340	191	100.2	1340	201	105.4	1340	211	110.7	1340	221	115.9	1340	231	121.2
3142	185	227.6	3142	195	239.9	3142	205	252.2	3142	215	264.5	3142	225	276.8
2513	185	182.0	2513	195	191.8	2513	205	201.7	2513	215	211.5	2513	225	221.4
2094	185	151.7	2094	195	159.9	2094	205	168.1	2094	215	176.3	2094	225	184.5

Reduced momentcapacity precast plate after fire at distance in the precast plate measured from exposed surface

x

Reduced momentcapacity precast without fire at distance in the precast plate measured from exposed surface Ø8 h.o.h. 100																				
Depth x_j in the floor above joint	30 minutes					60 minutes					90 minutes					120 minutes				
	Temperature above the joint	Reduction reinforce-ment strength	Reduction concrete	Reduced moment capacity	Reduction moment capacity	Temperature above the joint	Reduction reinforce-ment strength	Reduction concrete	Reduced moment capacity	Reduction moment capacity	Temperature above the joint	Reduction reinforce-ment strength	Reduction concrete	Reduced moment capacity	Reduction moment capacity	Temperature above the joint	Reduction reinforce-ment strength	Reduction concrete	Reduced moment capacity	Reduction moment capacity
	[°C]	[%]	[mm]	[kNm]	[%]	[°C]	[%]	[mm]	[kNm]	[%]	[°C]	[%]	[mm]	[kNm]	[%]	[°C]	[%]	[mm]	[kNm]	[%]
0 mm	818	92	15	2.0	92.8	896	95	35	1.1	96.2	973	97	45	0.6	97.9	997	97	50	0.5	98.0
10 mm	584	61	15	10.6	64.8	782	91	35	2.1	93.1	878	95	45	1.1	96.5	921	96	50	0.8	97.3
20 mm	432	15	15	24.8	22.8	661	80	35	5.0	84.3	782	91	45	2.1	93.5	844	95	50	1.1	96.5
30 mm	304	0	15	31.1	8.7	538	45	35	14.9	56.1	674	85	45	3.8	88.9	753	91	50	2.2	93.6
40 mm	199	0	15	33.1	8.2	416	18	35	23.9	33.7	557	45	45	14.9	58.5	647	75	50	6.5	81.8
50 mm	116	0	15	35.1	7.8	282	0	35	31.1	18.1	416	18	45	23.9	37.1	511	40	50	16.9	55.5
60 mm	77	0	15	37.0	7.4	192	0	35	33.1	17.2	310	0	45	31.1	22.2	400	12	50	26.5	33.7
70 mm	53	0	15	39.0	7.0	135	0	35	35.1	16.4	233	0	45	33.1	21.1	318	0	50	32.1	23.5
80 mm	37	0	15	41.0	6.7	102	0	35	37.0	15.7	173	0	45	35.1	20.2	250	0	50	34.1	22.4
90 mm	25	0	15	42.9	6.4	78	0	35	39.0	15.0	132	0	45	37.0	19.3	195	0	50	36.0	21.5
100 mm	17	0	15	44.9	6.2	60	0	35	41.0	14.4	106	0	45	39.0	18.5	151	0	50	38.0	20.6

Reduced momentcapacity precast without fire at distance in the precast plate measured from exposed surface Ø8 h.o.h. 125																				
Depth x_j in the floor above joint	30 minutes					60 minutes					90 minutes					120 minutes				
	Temperature above the joint	Reduction reinforce-ment strength	Reduction concrete	Reduced moment capacity	Reduction moment capacity	Temperature above the joint	Reduction reinforce-ment strength	Reduction concrete	Reduced moment capacity	Reduction moment capacity	Temperature above the joint	Reduction reinforce-ment strength	Reduction concrete	Reduced moment capacity	Reduction moment capacity	Temperature above the joint	Reduction reinforce-ment strength	Reduction concrete	Reduced moment capacity	Reduction moment capacity
	[°C]	[%]	[mm]	[kNm]	[%]	[°C]	[%]	[mm]	[kNm]	[%]	[°C]	[%]	[mm]	[kNm]	[%]	[°C]	[%]	[mm]	[kNm]	[%]
0 mm	818	92	15	1.6	92.8	896	95	35	0.8	96.2	973	97	45	0.5	97.9	997	97	50	0.4	98.0
10 mm	584	61	15	8.5	64.8	782	91	35	1.7	93.1	878	95	45	0.8	96.5	921	96	50	0.6	97.3
20 mm	432	15	15	19.8	22.8	661	80	35	4.0	84.3	782	91	45	1.7	93.5	844	95	50	0.9	96.5
30 mm	304	0	15	24.9	8.7	538	45	35	11.9	56.1	674	85	45	3.0	88.9	753	91	50	1.7	93.6
40 mm	199	0	15	26.4	8.2	416	18	35	19.1	33.7	557	45	45	11.9	58.5	647	75	50	5.2	81.8
50 mm	116	0	15	28.0	7.8	282	0	35	24.9	18.1	416	18	45	19.1	37.1	511	40	50	13.5	55.5
60 mm	77	0	15	29.6	7.4	192	0	35	26.4	17.2	310	0	45	24.9	22.2	400	12	50	21.2	33.7
70 mm	53	0	15	31.2	7.0	135	0	35	28.0	16.4	233	0	45	26.4	21.1	318	0	50	25.7	23.5
80 mm	37	0	15	32.7	6.7	102	0	35	29.6	15.7	173	0	45	28.0	20.2	250	0	50	27.2	22.4
90 mm	25	0	15	34.3	6.4	78	0	35	31.2	15.0	132	0	45	29.6	19.3	195	0	50	28.8	21.5
100 mm	17	0	15	35.9	6.2	60	0	35	32.7	14.4	106	0	45	31.2	18.5	151	0	50	30.4	20.6

Reduced momentcapacity precast without fire at distance in the precast plate measured from exposed surface Ø8 h.o.h. 150																				
Depth x_j in the floor above joint	30 minutes					60 minutes					90 minutes					120 minutes				
	Temperature above the joint	Reduction reinforce-ment strength	Reduction concrete	Reduced moment capacity	Reduction moment capacity	Temperature above the joint	Reduction reinforce-ment strength	Reduction concrete	Reduced moment capacity	Reduction moment capacity	Temperature above the joint	Reduction reinforce-ment strength	Reduction concrete	Reduced moment capacity	Reduction moment capacity	Temperature above the joint	Reduction reinforce-ment strength	Reduction concrete	Reduced moment capacity	Reduction moment capacity
	[°C]	[%]	[mm]	[kNm]	[%]	[°C]	[%]	[mm]	[kNm]	[%]	[°C]	[%]	[mm]	[kNm]	[%]	[°C]	[%]	[mm]	[kNm]	[%]
0 mm	818	92	15	1.3	92.8	896	95	35	0.7	96.2	973	97	45	0.4	97.9	997	97	50	0.4	98.0
10 mm	584	61	15	7.1	64.8	782	91	35	1.4	93.1	878	95	45	0.7	96.5	921	96	50	0.5	97.3
20 mm	432	15	15	16.5	22.8	661	80	35	3.4	84.3	782	91	45	1.4	93.5	844	95	50	0.7	96.5
30 mm	304	0	15	20.7	8.7	538	45	35	10.0	56.1	674	85	45	2.5	88.9	753	91	50	1.5	93.6
40 mm	199	0	15	22.0	8.2	416	18	35	15.9	33.7	557	45	45	10.0	58.5	647	75	50	4.4	81.8
50 mm	116	0	15	23.3	7.8	282	0	35	20.7	18.1	416	18	45	15.9	37.1	511	40	50	11.3	55.5
60 mm	77	0	15	24.7	7.4	192	0	35	22.0	17.2	310	0	45	20.7	22.2	400	12	50	17.7	33.7
70 mm	53	0	15	26.0	7.0	135	0	35	23.3	16.4	233	0	45	22.0	21.1	318	0	50	21.4	23.5
80 mm	37	0	15	27.3	6.7	102	0	35	24.7	15.7	173	0	45	23.3	20.2	250	0	50	22.7	22.4
90 mm	25	0	15	28.6	6.4	78	0	35	26.0	15.0	132	0	45	24.7	19.3	195	0	50	24.0	21.5
100 mm	17	0	15	29.9	6.2	60	0	35	27.3	14.4	106	0	45	26.0	18.5	151	0	50	25.3	20.6

Reduced momentcapacity precast without fire at distance in the precast plate measured from exposed surface Ø10 h.o.h. 100																				
Depth x_j in the floor above joint	30 minutes					60 minutes					90 minutes					120 minutes				
	Temperature above the joint	Reduction reinforce-ment strength	Reduction concrete	Reduced moment capacity	Reduction moment capacity	Temperature above the joint	Reduction reinforce-ment strength	Reduction concrete	Reduced moment capacity	Reduction moment capacity	Temperature above the joint	Reduction reinforce-ment strength	Reduction concrete	Reduced moment capacity	Reduction moment capacity	Temperature above the joint	Reduction reinforce-ment strength	Reduction concrete	Reduced moment capacity	Reduction moment capacity
	[°C]	[%]	[mm]	[kNm]	[%]	[°C]	[%]	[mm]	[kNm]	[%]	[°C]	[%]	[mm]	[kNm]	[%]	[°C]	[%]	[mm]	[kNm]	[%]
0 mm	818	92	15	3.1	92.9	896	95	35	1.6	96.3	973	97	45	0.9	98.0	997	97	50	0.8	98.1
10 mm	584	61	15	16.2	64.9	782	91	35	3.2	93.1	878	95	45	1.6	96.5	921	96	50	1.2	97.3
20 mm	432	15	15	37.9	23.0	661	80	35	7.7	84.4	782	91	45	3.2	93.5	844	95	50	1.7	96.6
30 mm	304	0	15	47.6	8.8	538	45	35	22.8	56.3	674	85	45	5.8	89.0	753	91	50	3.3	93.6
40 mm	199	0	15	50.7	8.3	416	18	35	36.5	33.9	557	45	45	22.8	58.8	647	75	50	10.0	81.9
50 mm	116	0	15	53.8	7.9	282	0	35	47.6	18.4	416	18	45	36.5	37.4	511	40	50	25.8	55.8
60 mm	77	0	15	56.9	7.5	192	0	35	50.7	17.5	310	0	45	47.6	22.5	400	12	50	40.6	34.0
70 mm	53	0	15	53.8	16.7	135	0	35	47.6	26.2	233	0	45	44.6	31.0	318	0	50	43.0	33.3
80 mm	37	0	15	63.0	6.8	102	0	35	56.9	15.9	173	0	45	53.8	20.5	250	0	50	52.2	22.7
90 mm	25	0	15	66.1	6.5	78	0	35	59.9	15.2	132	0	45	56.9	19.6	195	0	50	55.3	21.7
100 mm	17	0	15	69.1	6.3	60	0	35	63.0	14.6	106	0	45	59.9	18.8	151	0	50	58.4	20.8

Reduced momentcapacity precast without fire at distance in the precast plate measured from exposed surface Ø10 h.o.h. 125																				
Depth x_j in the floor above joint	30 minutes					60 minutes					90 minutes					120 minutes				
	Temperature above the joint	Reduction reinforce-ment strength	Reduction concrete	Reduced moment capacity	Reduction moment capacity	Temperature above the joint	Reduction reinforce-ment strength	Reduction concrete	Reduced moment capacity	Reduction moment capacity	Temperature above the joint	Reduction reinforce-ment strength	Reduction concrete	Reduced moment capacity	Reduction moment capacity	Temperature above the joint	Reduction reinforce-ment strength	Reduction concrete	Reduced moment capacity	Reduction moment capacity
	[°C]	[%]	[mm]	[kNm]	[%]	[°C]	[%]	[mm]	[kNm]	[%]	[°C]	[%]	[mm]	[kNm]	[%]	[°C]	[%]	[mm]	[kNm]	[%]
0 mm	818	92	15	2.5	92.9	896	95	35	1.3	96.3	973	97	45	0.7	98.0	997	97	50	0.7	98.1
10 mm	584	61	15	12.9	64.9	782	91	35	2.5	93.1	878	95	45	1.3	96.5	921	96	50	1.0	97.3
20 mm	432	15	15	30.3	23.0	661	80	35	6.1	84.4	782	91	45	2.5	93.5	844	95	50	1.4	96.6
30 mm	304	0	15	38.1	8.8	538	45	35	18.3	56.3	674	85	45	4.6	89.0	753	91	50	2.7	93.6
40 mm	199	0	15	40.6	8.3	416	18	35	29.2	33.9	557	45	45	18.3	58.8	647	75	50	8.0	81.9
50 mm	116	0	15	43.0	7.9	282	0	35	38.1	18.4	416	18	45	29.2	37.4	511	40	50	20.7	55.8
60 mm	77	0	15	45.5	7.5	192	0	35	40.6	17.5	310	0	45	38.1	22.5	400	12	50	32.5	34.0
70 mm	53	0	15	47.9	7.1	135	0	35	43.0	16.7	233	0	45	40.6	21.4	318	0	50	39.3	23.8
80 mm	37	0	15	50.4	6.8	102	0	35	45.5	15.9	173	0	45	43.0	20.5	250	0	50	41.8	22.7
90 mm	25	0	15	52.9	6.5	78	0	35	47.9	15.2	132	0	45	45.5	19.6	195	0	50	44.3	21.7
100 mm	17	0	15	55.3	6.3	60	0	35	50.4	14.6	106	0	45	47.9	18.8	151	0	50	46.7	20.8

Reduced momentcapacity precast without fire at distance in the precast plate measured from exposed surface Ø10 h.o.h. 150																				
Depth x_j in the floor above joint	30 minutes					60 minutes					90 minutes					120 minutes				
	Temperature above the joint	Reduction reinforce-ment strength	Reduction concrete	Reduced moment capacity	Reduction moment capacity	Temperature above the joint	Reduction reinforce-ment strength	Reduction concrete	Reduced moment capacity	Reduction moment capacity	Temperature above the joint	Reduction reinforce-ment strength	Reduction concrete	Reduced moment capacity	Reduction moment capacity	Temperature above the joint	Reduction reinforce-ment strength	Reduction concrete	Reduced moment capacity	Reduction moment capacity
	[°C]	[%]	[mm]	[kNm]	[%]	[°C]	[%]	[mm]	[kNm]	[%]	[°C]	[%]	[mm]	[kNm]	[%]	[°C]	[%]	[mm]	[kNm]	[%]
0 mm	818	92	15	2.1	92.9	896	95	35	1.1	96.3	973	97	45	0.6	15.7	997	97	50	0.6	98.1
10 mm	584	61	15	10.8	64.9	782	91	35	2.1	93.1	878	95	45	1.0	16.8	921	96	50	0.8	97.3
20 mm	432	15	15	25.3	23.0	661	80	35	5.1	84.4	782	91	45	1.8	17.9	844	95	50	1.1	96.6
30 mm	304	0	15	31.8	8.8	538	45	35	15.2	56.3	674	85	45	2.9	18.9	753	91	50	2.2	93.6
40 mm	199	0	15	33.8	8.3	416	18	35	24.4	33.9	557	45	45	10.7	19.1	647	75	50	6.7	81.9
50 mm	116	0	15	35.9	7.9	282	0	35	31.8	18.4	416	18	45	16.0	19.6	511	40	50	17.2	55.8
60 mm	77	0	15	38.0	7.5	192	0	35	33.8	17.5	310	0	45	19.5	20.4	400	12	50	27.1	34.0
70 mm	53	0	15	40.0	7.1	135	0	35	35.9	16.7	233	0	45	19.5	21.5	318	0	50	32.8	23.8
80 mm	37	0	15	42.1	6.8	102	0	35	38.0	15.9	173	0	45	19.5	22.6	250	0	50	34.9	22.7
90 mm	25	0	15	44.1	6.5	78	0	35	40.0	15.2	132	0	45	19.5	23.8	195	0	50	36.9	21.7
100 mm	17	0	15	46.2	6.2	60	0	35	42.1	14.6	106	0	45	19.5	24.9	151	0	50	39.0	20.8

Reduced momentcapacity precast without fire at distance in the precast plate measured from exposed surface Ø12 h.o.h. 100

Depth x_j in the floor above joint	30 minutes					60 minutes					90 minutes					120 minutes				
	Temperature above the joint	Reduction reinforce-ment strength	Reduction concrete	Reduced moment capacity	Reduction moment capacity	Temperature above the joint	Reduction reinforce-ment strength	Reduction concrete	Reduced moment capacity	Reduction moment capacity	Temperature above the joint	Reduction reinforce-ment strength	Reduction concrete	Reduced moment capacity	Reduction moment capacity	Temperature above the joint	Reduction reinforce-ment strength	Reduction concrete	Reduced moment capacity	Reduction moment capacity
	[°C]	[%]	[mm]	[kNm]	[%]	[°C]	[%]	[mm]	[kNm]	[%]	[°C]	[%]	[mm]	[kNm]	[%]	[°C]	[%]	[mm]	[kNm]	[%]
0 mm	818	92	15	4.3	92.9	896	95	35	2.3	96.3	973	97	45	1.2	98.0	997	97	50	1.2	98.1
10 mm	584	61	15	22.8	65.0	782	91	35	4.5	93.1	878	95	45	2.3	96.5	921	96	50	1.7	97.4
20 mm	432	15	15	53.4	23.1	661	80	35	10.8	84.5	782	91	45	4.5	93.6	844	95	50	2.4	96.6
30 mm	304	0	15	67.3	9.0	538	45	35	32.1	56.5	674	85	45	8.1	89.0	753	91	50	4.7	93.7
40 mm	199	0	15	71.7	8.5	416	18	35	51.6	34.2	557	45	45	32.1	59.0	647	75	50	14.1	82.1
50 mm	116	0	15	76.2	8.0	282	0	35	67.3	18.7	416	18	45	51.6	37.7	511	40	50	36.4	56.0
60 mm	77	0	15	80.6	7.6	192	0	35	71.7	17.8	310	0	45	67.3	22.8	400	12	50	57.3	34.3
70 mm	53	0	15	85.0	7.2	135	0	35	76.2	16.9	233	0	45	71.7	21.7	318	0	50	69.5	24.2
80 mm	37	0	15	89.4	6.9	102	0	35	80.6	16.1	173	0	45	76.2	20.7	250	0	50	73.9	23.0
90 mm	25	0	15	93.9	6.6	78	0	35	85.0	15.4	132	0	45	80.6	19.8	195	0	50	78.4	22.0
100 mm	17	0	15	98.3	6.3	60	0	35	89.4	14.8	106	0	45	85.0	19.0	151	0	50	82.8	21.1

Reduced momentcapacity precast without fire at distance in the precast plate measured from exposed surface Ø12 h.o.h. 125																				
Depth x_j in the floor above joint	30 minutes					60 minutes					90 minutes					120 minutes				
	Temperature above the joint	Reduction reinforce-ment strength	Reduction concrete	Reduced moment capacity	Reduction moment capacity	Temperature above the joint	Reduction reinforce-ment strength	Reduction concrete	Reduced moment capacity	Reduction moment capacity	Temperature above the joint	Reduction reinforce-ment strength	Reduction concrete	Reduced moment capacity	Reduction moment capacity	Temperature above the joint	Reduction reinforce-ment strength	Reduction concrete	Reduced moment capacity	Reduction moment capacity
	[°C]	[%]	[mm]	[kNm]	[%]	[°C]	[%]	[mm]	[kNm]	[%]	[°C]	[%]	[mm]	[kNm]	[%]	[°C]	[%]	[mm]	[kNm]	[%]
0 mm	818	92	15	3.5	92.9	896	95	35	1.8	96.3	973	97	45	1.0	98.0	997	97	50	0.9	98.1
10 mm	584	61	15	18.2	65.0	782	91	35	3.6	93.1	878	95	45	1.8	96.5	921	96	50	1.4	97.4
20 mm	432	15	15	42.8	23.1	661	80	35	8.6	84.5	782	91	45	3.6	93.6	844	95	50	1.9	96.6
30 mm	304	0	15	53.9	9.0	538	45	35	25.7	56.5	674	85	45	6.5	89.0	753	91	50	3.7	93.7
40 mm	199	0	15	57.4	8.5	416	18	35	41.3	34.2	557	45	45	25.7	59.0	647	75	50	11.2	82.1
50 mm	116	0	15	60.9	8.0	282	0	35	53.9	18.7	416	18	45	41.3	37.7	511	40	50	29.1	56.0
60 mm	77	0	15	64.5	7.6	192	0	35	57.4	17.8	310	0	45	53.9	22.8	400	12	50	45.8	34.3
70 mm	53	0	15	68.0	7.2	135	0	35	60.9	16.9	233	0	45	57.4	21.7	318	0	50	55.6	24.2
80 mm	37	0	15	71.6	6.9	102	0	35	64.5	16.1	173	0	45	60.9	20.7	250	0	50	59.2	23.0
90 mm	25	0	15	75.1	6.6	78	0	35	68.0	15.4	132	0	45	64.5	19.8	195	0	50	62.7	22.0
100 mm	17	0	15	78.7	6.3	60	0	35	71.6	14.8	106	0	45	68.0	19.0	151	0	50	66.3	21.1

Reduced momentcapacity precast without fire at distance in the precast plate measured from exposed surface Ø12 h.o.h. 150																				
Depth x_j in the floor above joint	30 minutes					60 minutes					90 minutes					120 minutes				
	Temperature above the joint	Reduction reinforce-ment strength	Reduction concrete	Reduced moment capacity	Reduction moment capacity	Temperature above the joint	Reduction reinforce-ment strength	Reduction concrete	Reduced moment capacity	Reduction moment capacity	Temperature above the joint	Reduction reinforce-ment strength	Reduction concrete	Reduced moment capacity	Reduction moment capacity	Temperature above the joint	Reduction reinforce-ment strength	Reduction concrete	Reduced moment capacity	Reduction moment capacity
	[°C]	[%]	[mm]	[kNm]	[%]	[°C]	[%]	[mm]	[kNm]	[%]	[°C]	[%]	[mm]	[kNm]	[%]	[°C]	[%]	[mm]	[kNm]	[%]
0 mm	818	92	15	2.9	92.9	896	95	35	1.5	96.3	973	97	45	0.8	98.0	997	97	50	0.8	98.1
10 mm	584	61	15	15.2	65.0	782	91	35	3.0	93.1	878	95	45	1.5	96.5	921	96	50	1.1	97.4
20 mm	432	15	15	35.6	23.1	661	80	35	7.2	84.5	782	91	45	3.0	93.6	844	95	50	1.6	96.6
30 mm	304	0	15	44.9	9.0	538	45	35	21.4	56.5	674	85	45	5.4	89.0	753	91	50	3.1	93.7
40 mm	199	0	15	47.8	8.5	416	18	35	34.4	34.2	557	45	45	21.4	59.0	647	75	50	9.4	82.1
50 mm	116	0	15	50.8	8.0	282	0	35	44.9	18.7	416	18	45	34.4	37.7	511	40	50	24.3	56.0
60 mm	77	0	15	53.7	7.6	192	0	35	47.8	17.8	310	0	45	44.9	22.8	400	12	50	38.2	34.3
70 mm	53	0	15	56.7	7.2	135	0	35	50.8	16.9	233	0	45	47.8	21.7	318	0	50	46.3	24.2
80 mm	37	0	15	59.6	6.9	102	0	35	53.7	16.1	173	0	45	50.8	20.7	250	0	50	49.3	23.0
90 mm	25	0	15	62.6	6.6	78	0	35	56.7	15.4	132	0	45	53.7	19.8	195	0	50	52.2	22.0
100 mm	17	0	15	65.5	6.3	60	0	35	30.1	57.0	106	0	45	27.2	61.2	151	0	50	55.2	21.1

Reduced momentcapacity precast without fire at distance in the precast plate measured from exposed surface Ø16 h.o.h. 100				
Depth x_j in the floor above joint	30 minutes	60 minutes	90 minutes	120 minutes

	Temperature above the joint	Reduction reinforce-ment strength	Reduction concrete	Reduced moment capacity	Reduction moment capacity	Temperature above the joint	Reduction reinforce-ment strength	Reduction concrete	Reduced moment capacity	Reduction moment capacity	Temperature above the joint	Reduction reinforce-ment strength	Reduction concrete	Reduced moment capacity	Reduction moment capacity	Temperature above the joint	Reduction reinforce-ment strength	Reduction concrete	Reduced moment capacity	Reduction moment capacity
	[°C]	[%]	[mm]	[kNm]	[%]	[°C]	[%]	[mm]	[kNm]	[%]	[°C]	[%]	[mm]	[kNm]	[%]	[°C]	[%]	[mm]	[kNm]	[%]
0 mm	818	92	15	7.3	92.9	896	95	35	3.8	96.3	973	97	45	2.0	98.0	997	97	50	1.9	98.1
10 mm	584	61	15	38.7	65.1	782	91	35	7.5	93.2	878	95	45	3.8	96.6	921	96	50	2.9	97.4
20 mm	432	15	15	91.0	23.4	661	80	35	18.3	84.6	782	91	45	7.5	93.7	844	95	50	4.0	96.7
30 mm	304	0	15	114.9	9.3	538	45	35	54.6	57.0	674	85	45	13.7	89.2	753	91	50	7.9	93.8
40 mm	199	0	15	122.8	8.8	416	18	35	87.8	34.8	557	45	45	54.6	59.5	647	75	50	23.8	82.3
50 mm	116	0	15	130.7	8.3	282	0	35	114.9	19.3	416	18	45	87.8	38.4	511	40	50	61.9	56.6
60 mm	77	0	15	138.6	7.9	192	0	35	122.8	18.3	310	0	45	114.9	23.6	400	12	50	97.7	35.0
70 mm	53	0	15	146.4	7.5	135	0	35	130.7	17.4	233	0	45	122.8	22.4	318	0	50	118.9	24.9
80 mm	37	0	15	154.3	7.1	102	0	35	138.6	16.6	173	0	45	130.7	21.3	250	0	50	126.8	23.7
90 mm	25	0	15	162.2	6.8	78	0	35	146.4	15.8	132	0	45	138.6	20.4	195	0	50	134.6	22.6
100 mm	17	0	15	170.1	6.5	60	0	35	154.3	15.2	106	0	45	146.4	19.5	151	0	50	142.5	21.6

Reduced momentcapacity precast without fire at distance in the precast plate measured from exposed surface Ø16 h.o.h. 125																				
Depth x_j in the floor above joint	30 minutes					60 minutes					90 minutes					120 minutes				
	Temperature above the joint	Reduction reinforce-ment strength	Reduction concrete	Reduced moment capacity	Reduction moment capacity	Temperature above the joint	Reduction reinforce-ment strength	Reduction concrete	Reduced moment capacity	Reduction moment capacity	Temperature above the joint	Reduction reinforce-ment strength	Reduction concrete	Reduced moment capacity	Reduction moment capacity	Temperature above the joint	Reduction reinforce-ment strength	Reduction concrete	Reduced moment capacity	Reduction moment capacity
	[°C]	[%]	[mm]	[kNm]	[%]	[°C]	[%]	[mm]	[kNm]	[%]	[°C]	[%]	[mm]	[kNm]	[%]	[°C]	[%]	[mm]	[kNm]	[%]
0 mm	818	92	15	5.8	92.9	896	95	35	3.0	96.3	973	97	45	1.6	98.0	997	97	50	1.5	98.1
10 mm	584	61	15	30.9	65.1	782	91	35	6.0	93.2	878	95	45	3.0	96.6	921	96	50	2.3	97.4
20 mm	432	15	15	72.8	23.4	661	80	35	14.6	84.6	782	91	45	6.0	93.7	844	95	50	3.2	96.7
30 mm	304	0	15	91.9	9.3	538	45	35	43.6	57.0	674	85	45	11.0	89.2	753	91	50	6.3	93.8
40 mm	199	0	15	98.2	8.8	416	18	35	70.2	34.8	557	45	45	43.6	59.5	647	75	50	19.0	82.3
50 mm	116	0	15	104.5	8.3	282	0	35	91.9	19.3	416	18	45	70.2	38.4	511	40	50	49.5	56.6
60 mm	77	0	15	110.8	7.9	192	0	35	98.2	18.3	310	0	45	91.9	23.6	400	12	50	78.1	35.0
70 mm	53	0	15	117.1	7.5	135	0	35	104.5	17.4	233	0	45	98.2	22.4	318	0	50	95.1	24.9
80 mm	37	0	15	123.4	7.1	102	0	35	110.8	16.6	173	0	45	104.5	21.3	250	0	50	101.4	23.7
90 mm	25	0	15	129.7	6.8	78	0	35	117.1	15.8	132	0	45	110.8	20.4	195	0	50	107.6	22.6
100 mm	17	0	15	136.0	6.5	60	0	35	123.4	15.2	106	0	45	117.1	19.5	151	0	50	113.9	21.6

Reduced momentcapacity precast without fire at distance in the precast plate measured from exposed surface Ø16 h.o.h. 150																				
Depth x_j in the floor above joint	30 minutes					60 minutes					90 minutes					120 minutes				
	Temperature above the joint	Reduction reinforce-ment strength	Reduction concrete	Reduced moment capacity	Reduction moment capacity	Temperature above the joint	Reduction reinforce-ment strength	Reduction concrete	Reduced moment capacity	Reduction moment capacity	Temperature above the joint	Reduction reinforce-ment strength	Reduction concrete	Reduced moment capacity	Reduction moment capacity	Temperature above the joint	Reduction reinforce-ment strength	Reduction concrete	Reduced moment capacity	Reduction moment capacity
	[°C]	[%]	[mm]	[kNm]	[%]	[°C]	[%]	[mm]	[kNm]	[%]	[°C]	[%]	[mm]	[kNm]	[%]	[°C]	[%]	[mm]	[kNm]	[%]
0 mm	818	92	15	4.9	92.9	896	95	35	2.5	96.3	973	97	45	1.4	98.0	997	97	50	1.3	98.1
10 mm	584	61	15	25.8	65.1	782	91	35	5.0	93.2	878	95	45	2.5	96.6	921	96	50	1.9	97.4
20 mm	432	15	15	60.6	23.4	661	80	35	12.2	84.6	782	91	45	5.0	93.7	844	95	50	2.6	96.7
30 mm	304	0	15	76.6	9.3	538	45	35	36.4	57.0	674	85	45	9.1	89.2	753	91	50	5.2	93.8
40 mm	199	0	15	81.8	8.8	416	18	35	58.5	34.8	557	45	45	36.4	59.5	647	75	50	15.9	82.3
50 mm	116	0	15	87.1	8.3	282	0	35	76.6	19.3	416	18	45	58.5	38.4	511	40	50	41.2	56.6
60 mm	77	0	15	92.3	7.9	192	0	35	81.8	18.3	310	0	45	76.6	23.6	400	12	50	65.1	35.0
70 mm	53	0	15	97.6	7.5	135	0	35	87.1	17.4	233	0	45	81.8	22.4	318	0	50	79.2	24.9
80 mm	37	0	15	102.8	7.1	102	0	35	92.3	16.6	173	0	45	87.1	21.3	250	0	50	84.5	23.7
90 mm	25	0	15	108.1	6.8	78	0	35	97.6	15.8	132	0	45	92.3	20.4	195	0	50	89.7	22.6
100 mm	17	0	15	113.3	6.5	60	0	35	102.8	15.2	106	0	45	97.6	19.5	151	0	50	95.0	21.6

Reduced momentcapacity precast without fire at distance in the precast plate measured from exposed surface Ø20 h.o.h. 100				
Depth x_j in the floor above joint	30 minutes	60 minutes	90 minutes	120 minutes

	Temperature above the joint	Reduction reinforce-ment strength	Reduction concrete	Reduced moment capacity	Reduction moment capacity	Temperature above the joint	Reduction reinforce-ment strength	Reduction concrete	Reduced moment capacity	Reduction moment capacity	Temperature above the joint	Reduction reinforce-ment strength	Reduction concrete	Reduced moment capacity	Reduction moment capacity	Temperature above the joint	Reduction reinforce-ment strength	Reduction concrete	Reduced moment capacity	Reduction moment capacity
	[°C]	[%]	[mm]	[kNm]	[%]	[°C]	[%]	[mm]	[kNm]	[%]	[°C]	[%]	[mm]	[kNm]	[%]	[°C]	[%]	[mm]	[kNm]	[%]
0 mm	818	92	15	10.8	93.0	896	95	35	5.5	96.4	973	97	45	3.0	98.1	997	97	50	2.8	98.2
10 mm	584	61	15	57.6	65.3	782	91	35	11.1	93.3	878	95	45	5.5	96.7	921	96	50	4.2	97.5
20 mm	432	15	15	135.9	23.8	661	80	35	27.1	84.8	782	91	45	11.1	93.8	844	95	50	5.8	96.7
30 mm	304	0	15	172.2	9.7	538	45	35	81.2	57.4	674	85	45	20.3	89.4	753	91	50	11.6	93.9
40 mm	199	0	15	184.5	9.1	416	18	35	131.1	35.4	557	45	45	81.2	60.0	647	75	50	35.4	82.6
50 mm	116	0	15	196.8	8.6	282	0	35	172.2	20.0	416	18	45	131.1	39.1	511	40	50	92.3	57.1
60 mm	77	0	15	209.1	8.1	192	0	35	184.5	18.9	310	0	45	172.2	24.3	400	12	50	146.1	35.8
70 mm	53	0	15	221.4	7.7	135	0	35	196.8	17.9	233	0	45	184.5	23.1	318	0	50	178.4	25.6
80 mm	37	0	15	233.7	7.3	102	0	35	209.1	17.1	173	0	45	196.8	22.0	250	0	50	190.7	24.4
90 mm	25	0	15	246.0	7.0	78	0	35	221.4	16.3	132	0	45	209.1	20.9	195	0	50	203.0	23.3
100 mm	17	0	15	258.3	6.7	60	0	35	233.7	15.6	106	0	45	221.4	20.0	151	0	50	215.3	22.2

Reduced momentcapacity precast without fire at distance in the precast plate measured from exposed surface Ø16 h.o.h. 125																				
Depth x_j in the floor above joint	30 minutes					60 minutes					90 minutes					120 minutes				
	Temperature above the joint	Reduction reinforce-ment strength	Reduction concrete	Reduced moment capacity	Reduction moment capacity	Temperature above the joint	Reduction reinforce-ment strength	Reduction concrete	Reduced moment capacity	Reduction moment capacity	Temperature above the joint	Reduction reinforce-ment strength	Reduction concrete	Reduced moment capacity	Reduction moment capacity	Temperature above the joint	Reduction reinforce-ment strength	Reduction concrete	Reduced moment capacity	Reduction moment capacity
	[°C]	[%]	[mm]	[kNm]	[%]	[°C]	[%]	[mm]	[kNm]	[%]	[°C]	[%]	[mm]	[kNm]	[%]	[°C]	[%]	[mm]	[kNm]	[%]
0 mm	818	92	15	8.7	93.0	896	95	35	4.4	96.4	973	97	45	2.4	98.1	997	97	50	2.2	98.2
10 mm	584	61	15	46.0	65.3	782	91	35	8.9	93.3	878	95	45	4.4	96.7	921	96	50	3.3	97.5
20 mm	432	15	15	108.7	23.8	661	80	35	21.6	84.8	782	91	45	8.9	93.8	844	95	50	4.7	96.7
30 mm	304	0	15	137.7	9.7	538	45	35	64.9	57.4	674	85	45	16.2	89.4	753	91	50	9.3	93.9
40 mm	199	0	15	147.6	9.1	416	18	35	104.9	35.4	557	45	45	64.9	60.0	647	75	50	28.3	82.6
50 mm	116	0	15	157.4	8.6	282	0	35	137.7	20.0	416	18	45	104.9	39.1	511	40	50	73.8	57.1
60 mm	77	0	15	167.3	8.1	192	0	35	147.6	18.9	310	0	45	137.7	24.3	400	12	50	116.9	35.8
70 mm	53	0	15	177.1	7.7	135	0	35	157.4	17.9	233	0	45	147.6	23.1	318	0	50	142.7	25.6
80 mm	37	0	15	186.9	7.3	102	0	35	167.3	17.1	173	0	45	157.4	22.0	250	0	50	152.5	24.4
90 mm	25	0	15	196.8	7.0	78	0	35	177.1	16.3	132	0	45	167.3	20.9	195	0	50	162.3	23.3
100 mm	17	0	15	206.6	6.7	60	0	35	186.9	15.6	106	0	45	177.1	20.0	151	0	50	172.2	22.2

Reduced momentcapacity precast without fire at distance in the precast plate measured from exposed surface Ø16 h.o.h. 150																				
Depth x_j in the floor above joint	30 minutes					60 minutes					90 minutes					120 minutes				
	Temperature above the joint	Reduction reinforce-ment strength	Reduction concrete	Reduced moment capacity	Reduction moment capacity	Temperature above the joint	Reduction reinforce-ment strength	Reduction concrete	Reduced moment capacity	Reduction moment capacity	Temperature above the joint	Reduction reinforce-ment strength	Reduction concrete	Reduced moment capacity	Reduction moment capacity	Temperature above the joint	Reduction reinforce-ment strength	Reduction concrete	Reduced moment capacity	Reduction moment capacity
	[°C]	[%]	[mm]	[kNm]	[%]	[°C]	[%]	[mm]	[kNm]	[%]	[°C]	[%]	[mm]	[kNm]	[%]	[°C]	[%]	[mm]	[kNm]	[%]
0 mm	818	92	15	7.2	93.0	896	95	35	3.7	96.4	973	97	45	2.0	98.1	997	97	50	1.8	98.2
10 mm	584	61	15	38.4	65.3	782	91	35	7.4	93.3	878	95	45	3.7	96.7	921	96	50	2.8	97.5
20 mm	432	15	15	90.6	23.8	661	80	35	18.0	84.8	782	91	45	7.4	93.8	844	95	50	3.9	96.7
30 mm	304	0	15	114.8	9.7	538	45	35	54.1	57.4	674	85	45	13.5	89.4	753	91	50	7.7	93.9
40 mm	199	0	15	123.0	9.1	416	18	35	87.4	35.4	557	45	45	54.1	60.0	647	75	50	23.6	82.6
50 mm	116	0	15	131.2	8.6	282	0	35	114.8	20.0	416	18	45	87.4	39.1	511	40	50	61.5	57.1
60 mm	77	0	15	139.4	8.1	192	0	35	123.0	18.9	310	0	45	114.8	24.3	400	12	50	97.4	35.8
70 mm	53	0	15	147.6	7.7	135	0	35	131.2	17.9	233	0	45	123.0	23.1	318	0	50	118.9	25.6
80 mm	37	0	15	155.8	7.3	102	0	35	139.4	17.1	173	0	45	131.2	22.0	250	0	50	127.1	24.4
90 mm	25	0	15	164.0	7.0	78	0	35	147.6	16.3	132	0	45	139.4	20.9	195	0	50	135.3	23.3
100 mm	17	0	15	172.2	6.7	60	0	35	155.8	15.6	106	0	45	147.6	20.0	151	0	50	143.5	22.2

Measures for momentcapacity												
		0 mm	10 mm	20 mm	30 mm	40 mm	50 mm	60 mm	70 mm	80 mm	90 mm	100 mm
Reinforcement	A [mm²]	d [mm]	d [mm]	d [mm]	d [mm]	d [mm]	d [mm]	d [mm]	d [mm]	d [mm]	d [mm]	d [mm]
Ø8 h.o.h. 100	503	143	153	163	173	183	193	203	213	223	233	243
Ø8 h.o.h. 125	402	143	153	163	173	183	193	203	213	223	233	243
Ø8 h.o.h. 150	335	143	153	163	173	183	193	203	213	223	233	243
Ø10 h.o.h. 100	785	140	150	160	170	180	190	200	210	220	230	240
Ø10 h.o.h. 125	628	140	150	160	170	180	190	200	210	220	230	240
Ø10 h.o.h. 150	524	140	150	160	170	180	190	200	210	220	230	240
Ø12 h.o.h. 100	1131	137	147	157	167	177	187	197	207	217	227	237
Ø12 h.o.h. 125	905	137	147	157	167	177	187	197	207	217	227	237
Ø12 h.o.h. 150	754	137	147	157	167	177	187	197	207	217	227	237
Ø16 h.o.h. 100	2011	131	141	151	161	171	181	191	201	211	221	231
Ø16 h.o.h. 125	1608	131	141	151	161	171	181	191	201	211	221	231
Ø16 h.o.h. 150	1340	131	141	151	161	171	181	191	201	211	221	231
Ø20 h.o.h. 100	3142	125	135	145	155	165	175	185	195	205	215	225
Ø20 h.o.h. 125	2513	125	135	145	155	165	175	185	195	205	215	225
Ø20 h.o.h. 150	2094	125	135	145	155	165	175	185	195	205	215	225